NASA TECHNICAL TRANSLATION

NASA TT F-81

C. 1

NASA TT F-81

LOAN COPY: RETURN TO
AFSWC (SWOIL)
KIRTLAND AFB, NMEX

TECH LIBRARY KAFB, NM
0068631

AEROELASTICITY SYMPOSIUM

Göttingen, April 16-17, 1957

Published by the *Max-Planck-Institut für Strömungsforschung und Aerodynamische Versuchsanstalt,*
No. 18, 1958

NATIONAL AERONAUTICS AND SPACE ADMINISTRATION • WASHINGTON, D. C. • SEPTEMBER 1963

TECH LIBRARY KAFB, NM
0068631

TECHNICAL TRANSLATION F-81

AEROELASTICITY SYMPOSIUM*

Göttingen, April 16-17, 1957

Published by the Max-Planck-Institut für Strömungsforschung
und Aerodynamische Versuchsanstalt
No. 18, 1958

*Translation of "Aeroelastisches Kolloquim in Göttingen
am 16. und 17. April 1957"

NATIONAL AERONAUTICS AND SPACE ADMINISTRATION

INTRODUCTION

The plan for an aeroelastic symposium in Göttingen originated after Germany was permitted to engage again in aeronautics and the restrictions against aircraft construction and aviation research had been removed. Aeroelastics has acquired a steadily increasing importance in modern aircraft construction. It seemed therefore desirable to acquaint the collaborators of aircraft construction plants and aviation research institutes through lectures and discussion with progress made since the end of the war and to discuss still unsolved problems.

The field of aeroelastics is so large that only a few themata could be selected. The lectures of the first section treat of the theoretical methods for demonstrating resistance to flutter of aircraft, i.e., recently developed mathematical computation methods for the determination of the critical velocity of flutter. The second section is concerned with experimental procedures for obtaining parameters for the calculation of flutter. They include wind-tunnel measurement of aerodynamic forces on vibrating wings, measurements in the electric-potential tank as a means of analogy in the determination of theoretical aerodynamic forces, and the static-vibration test on the actual aircraft as a means for the determination of elastic and mass parameters.

The discussions were recorded on magnetic tape and their evaluation required a considerable amount of time to supplement the inferences of verbal delivery. We are particularly obligated to Dr. Krumhaar for preparing the final form of the lectures and discussions in collaboration with the participants of the symposium.

Göttingen, 15 October 1957 H. G. Küssner

TABLE OF CONTENTS

Welcoming Address (A. Betz). 3

Calculating Methods for the Solution of Aeroelastic Problems Concerning Plate Wings and Entire Aircraft (H. G. Küssner) . . . 4

Flutter Calculation with Many Degrees of Freedom for Modern Aircraft (A. I. van de Vooren) 51

Rational Use in Flutter Calculation of Values Found by Static-Vibration Test (G. de Vries). 78

Different Calculations of Flutter for Ailerons with Hydraulic Servo-Control (E. Gruschwitz). 99

Experimental Determination of Aerodynamic Coefficients of Vibrating Wings (H. Bergh) 106

Determination of Non-Steady Aerodynamic Forces at M = 0 by Electric Analogy (Potential Tank) (H. Merbt, S. Hansson) 132

Part I: Basic Theory and Method of Solution for Two-Dimensional Cases (H. Merbt) 133

Part II: Execution of Measurements in the Three-Dimensional Potential Tank and Results for a Rectangular Wing (S. Hansson). 138

Static-Vibration Test with Electronic Measuring Instruments on a Glider (J. Schoen). 167

Motion Pictures Shown. 190

List of Participants at Symposium. 191

WELCOMING ADDRESS OF PROFESSOR DR. ALBERT BETZ

I am happy to be able to welcome here today so many well-known experts. I regard this as a sign that the reconstruction of the completely destroyed Aerodynamic Experimentation Institute is making itself already felt in spite of all the difficulties arising out of many circumstances. I myself am to a large extent a layman in your specific field, that of the problem of flutter. I have always been satisfied to know this task is in the capable hands of Dr. Küssner. Moreover, I have the impression that the findings produced by Dr. Küssner and several others in the past have since proved their value. We hear today much less frequently of flutter as a cause of airplane crashes. However, in my opinion, the theoretical principles are extremely complicated and require considerable mathematical training. Because I do not possess the latter myself, I personally would prefer that these matters could be made comprehensive in simpler and less abstract fashion. The important point, however, is that we are able to treat these matters at all. From the fact that so many of you have taken the trouble to come here, I conclude that there still remains much to be done, in spite of the large knowledge already adduced in this field. I should like to express my hope that this conference also will be a further contribution to these very important findings and wish all of you in this sense a very successful meeting.

A CALCULATION METHOD FOR SOLVING AEROELASTIC PROBLEMS FOR STUB WINGS AND ENTIRE AIRCRAFT

by H. G. Küssner

SUMMARY

The different types of aeroelastic action are described. They can be investigated experimentally with the aid of dynamically analogous aircraft models or may be examined mathematically where certain simplifying assumptions are made. The thin and short wing is treated as a flat plate. The continuous load is replaced by a system of n individual forces at n points, causing corresponding deflections at these points. The equations of motion for these n points in response to aerodynamic and mass forces are stated in the form of matrices. A review on the theory of aerodynamic forces is given. Calculation of pressure through collocation of the downwash at the n points is treated by numerical examples. The integral-equation method for the entire aircraft and the equations of Rayleigh-Ritz and of Galerkin are derived. A semi-experimental method is indicated for determining the deformation tensor by means of the static vibration test.

ARRANGEMENT:

		Page
1.	Introduction.	5
	1.1 Different Types of Aeroelastic Action.	5
	1.2 Method for Solving Aeroelastic Problems.	7
2.	Simplifying Assumptions	9
3.	Matrix Method for Level Elastic Plates.	9
4.	Integral-Equation Method for the Entire Aircraft.	13
5.	Semi-Experimental Method for Determining Deformation Tensor . .	15
6.	Calculation of Approximate Solutions of Integral Equations. . .	17
7.	Theory of Aerodynamic Pressure Distribution	22
8.	Collocation Method of Pressure Calculation.	25
9.	Literature References	27
	Appendix 1 - Derivation of Formula for Generalized Mass	28
	Appendix 2 - Theory of Static Vibration Test.	30
	Illustrations	37
	Discussion.	47

1. INTRODUCTION

1.1 Different Types of Aeroelastic Action

If all aircraft were completely rigid, there would be no aeroelastic problems. Deformations of the flying aircraft produce variations of aerodynamic pressure on the surface which produce in turn further deformations. In general, this leads to a new stable condition of equilibrium. This condition may have undesirable factors which interfere with flying stability or may even make control of the aircraft impossible. At critical flying speeds, certain aircraft do not have any stable condition of equilibrium at all. In such cases, deformations increase until the respective structural aggregate breaks.

Such aeroelastic action is generally counteracted by reducing rigidity and increasing flying speed. Both are development tendencies of modern aircraft construction. In order to reduce resistance, relatively thin wings and empennages of correspondingly low rigidity are built. The latest supersonic aircraft have, for instance, a wing thickness of 4% of the wing chord.

The prevention of damaging aeroelastic action is therefore a more difficult problem today than it was twenty years ago. The leading aircraft builders of America today employ about as many engineers in their aeroelastic divisions as in the static divisions. Aeroelastic instability did occur, although infrequently, already in the first engine-powered aircraft. Langley's monoplane in 1903 probably crashed by reason of torsional instability of the wing. The D-8 monoplane of Fokker produced several crashes in 1917 for the same reason which initially was unexplained. In 1915, the 0/400 biplane of Handley-Page developed empennage flutter.

Aeroelastic action is caused by the joint effect of aerodynamic and elastomechanic forces. During rapid variations in time, forces of mass are added to these. This results in a great number of eventual aeroelastic problems which are here illustrated by means of a triangle of forces (Fig. 1).

The aerodynamic force A, the elastic force E, and the mass force M is entered in the angles of the triangle. Below the triangle are located the normal mechanical vibrations not involving aerodynamic forces (V). Above the summit of the triangle is located the static flying stability G and the aircraft is here assumed as rigid and not possessing mass. On the right side of the triangle is the dynamic flying stability H and the aircraft is here assumed as rigid. These three factors do not actually belong to aeroelastics but form its basis.

Action to the left of the triangle takes place so slowly that the forces of mass are negligibly small. If the wing distorts in flight, the wing ends may be subjected to greater lift than in a rigid aircraft L. This increases the torsional moments of the wing. Such variations of aerodynamic load distribution also create moments of

torque around the transverse axis of the aircraft and so change the static flying stability GE. When the pilot actuates the aileron, an additional aerodynamic load distribution is created in the wing. This load attempts to change the position of the aircraft in space but simultaneously produces an asymmetrical distortion of the wing which results in turn in new aerodynamic forces. These aerodynamic forces may counteract the change of position of the aircraft intended by the pilot (C). At critical flying speeds, the aerodynamic moments around the longitudinal axis produced by the deflection of the aileron and the resulting torsion of the wing may just about cancel themselves out (R). The aircraft is then no longer controllable. At further increases of speed, the action of the aileron even becomes reversed.

The neutral axis of the wing connects the points at quarter chord (Fig. 2). The resultant of the aerodynamic forces acts here under changes in angle of incidence when each cross-section of the wing is considered separately. If the elastic axis of the wing lies back of the neutral axis, then there does not exist any stable equilibrium above critical flying speeds. The wing attached rigidly to the fuselage becomes increasingly distorted under the effect of the self-produced aerodynamic forces until it finally breaks. This action is designated as static pitch (D) or static torsional instability.

We now come to the processes within the triangle. A self-produced vibration of the entire aircraft or its parts at constant amplitude is designated as flutter (F). The energy required for overcoming the (structural) inner damping and bearing friction is here taken aerodynamically from the air stream. If the flying speed changes, amplitude of vibration may increase to fracture.

There are several types of flutter. We shall first consider flutter from streamline flow. Depending on whether the wing, the empennage or the rudder and auxiliary control surfaces have the highest amplitudes, we speak of wing, empennage, or rudder flutter. In point of fact, flutter affects the entire aircraft. At supersonic speeds, the skin of the wing and of the fuselage may flutter on their framing members assumed as rigid, especially if it expands under heat. This type of flutter first occurred in V-2 rockets. In given cases, flutter from steady flow may take place with only one degree of freedom but more often several degrees of freedom participate in it.

The blades of air-screws, rotors, turbines and compressors can flutter in the same manner as aircraft wings. When a helicopter rotor is running without thrust while standing, its blades may flutter because of passing through their own slipstream. Even a minor vertical flow through the rotor causes this type of flutter to disappear.

Under burble flow, e.g. at a wide angle of attack of the wing, burble flutter may occur. The absorption of energy from the air stream is here based on the hysteresis of the aerodynamic forces under small variations of angle of attack which is already possible with one degree of freedom.

This type of flutter may occur on elongated bodies of any given cross-section because of the Karman vortex. The flutter of condenser pipes, roller weirs, sending towers and suspension bridges is well known. The destruction of the Takoma suspension bridge through flutter will be remembered, particularly because it was filmed by chance and shown in newsreels at the time.

Flutter is a homogeneous dynamic problem of stability in which extraneous forces are absent. It is of basic importance for all other aeroelastic processes. The dynamic flying stability of an elastic aircraft HE is differentiated from flutter essentially only by the fact that the frequency of oscillation is lower and that the automatic pilot enters into this. In the borderline case of zero frequency, the phenomenon of flutter deteriorates into the aeroelasto-static processes D and R. If we introduce gust forces into the start of flutter, we then obtain a basis of formulation for the "dynamic response" Z. The same is true when we introduce arbitrary movements of the rudder by the pilot as disturbances of the homogeneous problem.

Irregular oscillations created by aerodynamic forces are called "shaking" or "buffeting" B. These may originate in the wing through burbling of the flow as well as at the empennage if it is encountered by vortices of the wing or the power plant. The aerodynamic forces are here therefore either not at all or negligibly influenced by the deformations of the aircraft. The shock fronts travelling back and forth on the wing surface in flight closely below supersonic speed have similar effects.

1.2 Method for Solving Aeroelastic Problems

There are two main methods for solving aeroelastic problems, i.e. theoretical calculation and the investigation of dynamically analogous aircraft models. However, the problem is much too complicated to permit exact solution. Large aircraft builders consequently very often employ both methods simultaneously in the hope that they will mutually correct each other. Finally, the airworthiness of the completed aircraft must be proved in flight tests. Here a matter of particular concern are the manufacturing tolerances. Very slight deviations in one part, the installation of a bail edge at the rudder or a new coat of paint may lead to flutter. In one aircraft, the point of transition from laminary to turbulent boundary layer lay by chance closely ahead of the rudder gap. The rudder fluttered even though careful previous examination excluded this. The disturbance was removed by roughening the wing surface ahead of the rudder.

The method of investigation by models will be shown later in a film which was made during the war in the former Institute for Non-Steady Processes of the Aerodynamic Experimental Institute (AVA). By dynamically analogous model is understood a model geometrically analogous on the exterior and with the same specific weight, the same distribution of mass and the same natural oscillations as the life-size construction.

All natural frequencies are multiplied, however, by a constant factor k. At Mach numbers below 0.7, the influence of the compressibility of air on aeroelastic processes can generally be neglected. If an incompressible fluid is assumed, the factor k can be selected so that flutter can be easily observed in a given wind tunnel. In order to reduce the oscillation frequency of the wing and to make possible at the same time large deflections of the wing without rupture, the spars are often constructed as flat ribs whose thickness is only about 20% of the wing thickness. When selecting such a design, it is possible to obtain only the lowest natural oscillations approximately correctly. However, these are generally decisive for flutter.

As soon as it is desired to consider the influence of the compressibility of air, the construction of models becomes more difficult. We are then no longer able to select the factor k freely. The model must be investigated at the actual Mach number and also has to be in part geometrically analogous in the interior. The ratio of supersonic speeds of the flow medium and of the structural materials must be the same in the model and in the large-scale construction. If the investigation is to be made in air, we are therefore forced to employ aluminum as structural material for the model. The Americans utilize for this purpose thin aluminum sheets as well as miniature rollers for producing profiles from these sheets which are assembled by adhesive materials. If the wind tunnel is filled with a gas of a lower supersonic speed, e.g. Freon-12 (CF_2Cl_2), certain plastics can be used for constructing the models.

Such a model of the same or like Mach number and its investigation in a large wind tunnel at actual flying speeds is very expensive. It is less expensive to investigate it in the open on towing tracks which exist in California, for instance. If power plants, measuring instruments and radio senders are incorporated in the model, it can then also be investigated in free flight which has many advantages.

If we are only concerned with testing certain assumptions of an aeroelastic theory, this can be done with small and highly simplified models. In the supersonic range, wing models are used for this purpose, among others, which consist of a light foam substance which is covered on the outside by aluminum foil. If such a model breaks during flutter, the wind tunnel cannot be damaged.

A purely experimental treatment of aeroelastic problems would be defeated merely by the great number of parameter variations required, even if we disregard other difficulties. The most general and at the same time least expensive method of investigation consequently remains the theoretical method. The closer we come to the limits of technology, the more we need a mathematical, theoretical examination of the problems, even with highly simplifying assumptions. Anyone unaccustomed to this at first fails to find this treatment illustrative. However, illustration here means after all nothing else than an understanding of the

inner relations. Engineers who have occupied themselves intensively with aeroelastic processes therefore find such a mathematical formula as the complex flutter determinant as adequately illustrative.

2. Simplifying Assumptions

As far as aeroelastic problems are problems of stability, we can restrict ourselves to infinitely small disturbances because we intend to prevent even the start of any non-stable process. Through this assumption, the basis of formulation is linearized and can only now be treated mathematically. In any linearized physical theory, finite or infinite systems of linear equations play an important role. These are best solved with the aid of matrix algebra.

A long slender aircraft wing can be represented elastomechanically approximately by a straight beam with rigid ribs. Most of the calculations of flutter effected so far are based on this assumption. However, modern high-speed aircraft have short and thin wings which can no longer be treated as beams. For these wings, we want to communicate methods and results of calculations as well as some simple bases of formulation which are valid for the whole craft as a dynamic unit and can be applied to details as desired.

3. Matrix Methods for a Level Elastic Plate

Let us take a plate-like wing in the plane xy which is rigidly fixed in its plane of symmetry $y = 0$ (cf. Fig. 3). This plate shall be divided into n slabs and the centers of gravity or stations (point) shall be $P_i = P(x_i, y_i)$. At slab i, let aerodynamic mass-forces attack, the sum of which is the force Q_i. These forces Q_i attack vertically to the plate at the point P_i and produce vertical elastic displacement at all points P_k. In accordance with the theory of elasticity, there then become valid, for infinitely small displacements, the matrix equations

$$Q_i = a_{ik}\, u_k \quad ; \quad a_{ik} = a_{ki} \quad ; \tag{1}$$

$$u_k = b_{k\ell}\, Q_\ell \quad ; \quad b_{k\ell} = b_{\ell k} \quad ; \quad i, k, \ell = 1, 2, \ldots, n. \tag{2}$$

All indices of a product occurring several times must be summed up from 1 to n unless they are shown in parenthesis. This is a convention eliminating "pen pushing" as useful as the invention of the integral. Matrices are nothing more than stenograms for systems of linear equations which occur nearly everywhere in physics and technology. Q_i and u_k are

single-row matrices with n members; a_{ik} and $b_{k\ell}$ are quadratic matrices with n^2 members. a_{ik} is called the rigidity matrix. $b_{k\ell}$ is called the deformation matrix; both are symmetrical and their product is

$$a_{ik} \cdot b_{k\ell} = \delta_{i\ell} = \begin{cases} 0, & \text{when } i \neq \ell \\ 1, & \text{when } i = \ell \end{cases} \tag{3}$$

If the rigidity matrix a_{ik} is known, we obtain the deformation matrix $b_{k\ell}$ by solving the linear equation system (1) according to u_k. In order to abbreviate, we write

$$b_{ki} = \left[a_{ik}\right]^{-1} \quad ; \qquad a_{ik} = \left[b_{ki}\right]^{-1} . \tag{4}$$

It is therefore necessary to determine only one of these matrices experimentally or theoretically. If the wing is loaded at all points P_ℓ successively by a unit load $Q_\ell = 1$ and if we measure the small deflections at all points P_k, we then obtain the deformation matrix $b_{k\ell}$. The symmetry condition $b_{k\ell} = b_{\ell k}$ serves as control in this.

During recent years, several theoretical methods have been developed for the determination of the elastic properties of short and thin wings (cf. 1, 2). They are

1) Subdivision of the wing into a finite number of easily calculable partial bodies, e.g. bars, plates, or boxes. The forces (acting) on them are the unknown factors. These are calculated by utilizing the principle of the smallest potential energy;

2) The same subdivision into partial bodies but the unknown factors are the deformations of the partial bodies;

3) Development of deformation in a series of predetermined functions. The coefficients are calculated by utilizing the principle of the smallest potential energy.

We cannot further enter into these methods here.

Let us assume as given a mass distribution $m(x, y)$ and a distribution of aerodynamic pressures $p(x, y)$ on the plate. If the plate were subdivided in many slabs, we could then be satisfied with the integrals of these magnitudes over the individual slabs. For obvious reasons, however, an attempt is made to restrict the total n of the points P_i. A more accurate determination of the masses and forces to be applied at the individual points P_i is therefore desired. This is necessary, especially if the points are not arranged in a regular pattern as in

Fig. 3. In order to calculate the aerodynamic pressures, we also need the derivation of the deformations of the plate along the coordinate x. These deformations can be formed, however, only if we represent the deformation of the plate with the aid of certain point functions as a constant function in x and y.

For this purpose, let us assume a class of functions F (x, y; r, s) which are, in the area of the plate, regular, i.e. finite, constant and differentiable; let r, s be whole-number parameters 0, 1, 2, ...

We develop the deflection u (x, y) of the plate according to a series of functions F by means of the basic formulation

$$u(x,y) = F(x,y;\ r_i, s_i)\ g_{ik}\ u_k \quad ; \quad 0 \leq r_i + s_i < m \ . \tag{5}$$

r_i and s_i are current whole numbers herein, m is a fixed predetermined whole number and u_k are the given deflections of the plate in the $n = \binom{m+1}{2}$ points P_k. The functions F and/or the points $P_k = P(x_k, y_k)$ must be selected so that their determinant is

$$\det \left| F(x_k, y_k\ ;\ r_i, s_i) \right| \neq 0$$

Very small finite values of this determinant should also be avoided. From equation 5 follows, by introducing the coordinates $x = x_\ell$, $y = y_\ell$, the equation

$$F(x_\ell, y_\ell\ ;\ r_i, s_i)\ g_{ik} = \delta_{\ell k}$$

and, with the designations established in equations 3 and 4, the matrix

$$g_{ik} = \left[F(x_k, y_k\ ;\ r_i, s_i) \right]^{-1} \ . \tag{6}$$

The representation of equation 5 is exact if the function u(x, y) belongs to the class of functions F(x, y; r, s) and is, in the case of a polynomial, of a lower than degree m; otherwise it is valid approximately. If the deformation u(x, y) has a non-steadiness because of a rudder discontinuity, two separate basic formulations must be made and joined along the rudder axis. This can be done in the most simple manner if an adequate total of points is placed along the rudder axis.

If we integrate equation 5 over the plate (a), we obtain the well-known formula of the numerical integration

$$\iint_{(a)} u(x, y)\, dx\, dy = \alpha_k\, u_k \tag{7}$$

with the weight factors

$$\alpha_k = g_{ik} \iint_{(a)} F(x, y;\ r_i, s_i)\, dx\, dy \quad . \tag{8}$$

If the function $u(x, y)$ belongs to class $F(x, y; r, s)$ and is lower than the m^{th} order, then equation 7 is valid exactly and otherwise approximately and the error can here be estimated (cf. 3). For numerical integrations, the polynomials

$$F(x, y;\ r, s) = x^r y^s \quad ; \quad 0 \leq r + s < m \tag{9}$$

are utilized generally. For the circular and for the elliptical plate, there exist octagonal polynomials, i.e. the coordinated polynomials of Legendre and of Lame which are more advantageous in these cases.

Let us assume a given integrable distribution of mass $m(x, y)$ on the plate. This we want to replace by n individual masses M_k at n points P_k in such manner that the total masses, the static and inertial moments, etc. of both distributions agree. This condition is fulfilled if

$$M_k\, F(x_k, y_k;\ r_i, s_i) = \iint_{(a)} F(x, y;\ r_i, s_i)\, m(x, y)\, dx\, dy\ ; \tag{10}$$

$$M_k = g_{ik} \iint_{(a)} F(x, y;\ r_i, s_i)\, m(x, y)\, dx\, dy \quad . \tag{11}$$

The function $m(x, y)$ may also contain integrable singularities and individual masses. The integrals 10 and 11 must then be replaced by Stieltjes integrals with the differentials $dm(x, y)$. The forces of mass are

$$Q_k^{(m)} = - M_{(k)}\, \ddot{u}_k(t) \quad , \tag{12}$$

in which the upper index (m) points to the force of mass. Entirely in correspondence with this, there follow, from the aerodynamic pressure distribution $p(x, y, t)$, the individual forces $Q_k^{(\alpha)}$ at points P_k

$$Q_k^{(\alpha)} = -2\, g_{ik} \iint_{(a)} F(x, y;\, r_i, s_i)\; p(x, y, t)\, dx\, dy \quad , \qquad (13)$$

in which the upper index (α) points to the aerodynamic force. The factor 2 is justified because the pressures on both sides of the wing are uniformly opposed. We can now state the total forces Q_k at points P_k. The deflections $u_k = u_k(t)$ are functions of time t. If we enter equations 12 and 13 in equation 1, we then obtain the equation of motion of the n points P_k

$$a_{ik}\, u_i(t) + M_{(k)}\, \ddot{u}_k(t) + 2\, g_{ik} \iint_{(a)} F(x, y;\, r_i, s_i)\; p(x, y, t)\, dx\, dy = 0 \quad . \qquad (14)$$

In order to solve these equations, we now need only the data of the aerodynamic pressures to which I will return later. When $p = 0$, then equation 14 represents the static vibrations of an elastic plate.

So that we can determine approximately correctly the first m natural vibrations of the plate with this method, there are needed at least m^2 points. The natural values $\lambda^{(s)} = 1/\omega^2_{(s)}$ are best determined by iteration (cf. 2). Here we must use the orthogonality relation of the natural-vibration forms

$$u_k^{(r)}\, u_k^{(s)}\, M_k = \mu_r\, \delta_{rs} \quad ; \quad k, r, s = 1, 2, \ldots, n \qquad (15)$$

in order to prevent converging of the solution to the 1st natural value. This relation follows from the symmetry of the deformation matrix.

4. Integral-Equation Method for Entire Aircraft

We now let the total of the surface elements of the wing become infinite and write in abbreviation

$$x, y = P \quad ; \quad x', y' = P' \quad ; \quad dx'\, dy' = dP' \quad .$$

The matrix equation 2 then becomes transformed into integral equation 16:

$$u(P) = \iint_{(a)} G(P, P')\, Q(P')\, dP' \quad . \qquad (16)$$

The double integral is to be extended over the entire wing surface (a). P is now any given point of the wing, Q(P) the force per surface unit and u(P) the elastic displacement in it. The Green function G(P, P') is a so-called two-point function. We immediately see the close relation of the matrix equation 2 and of the integral equation 16. In aeroelastics, both forms are utilized interchangeably. In numerical calculation, we generally arrive at matrix equations.

So far we have investigated only the fixed level plate. We now want to treat the aircraft as dynamic unit in free flight. If the aircraft were a rigid body, then the coordinate system based in its center of gravity $P = 0$ would undergo the following normal and angular accelerations:

$$\ddot{u}_k(0, t) = \frac{1}{M_{(k)}} \iiint_{(v)} Q_k(P', t)\, dP' \quad ; \quad i \neq j \neq k = 1, 2, 3 \quad , \tag{17}$$

$$\ddot{\vartheta}_k(0, t) = \frac{1}{J_k} \iiint_{(v)} \left[x_i\, Q_j(P', t) - x_j\, Q_i(P', t) \right] dP' \tag{18}$$

$$+ \frac{1}{J_k} \left[D_i\ \dot{\vartheta}_j(0, t) - D_j\ \dot{\vartheta}_i(0, t) \right]$$

In this, $P = P(x_1, x_2, x_3)$ = point in space; dP = element of volume; Q_k = intensity of force; M_k = mass; J_k = inertial moment around axis x_k; and D_i = free drift (spin) of the aircraft. The integration should extend over the volume (v) of the aircraft. The Kelvin impulses can be taken into account in the most simple manner by making certain additions to M_k and J_k for the entrained masses of air or by experimentally determining these magnitudes through static vibration tests with the aircraft in air. Then the mass M_k also depends on the direction of motion.

The equations 17 and 18 are the Euler equations of motion of the rigid body. To this is added the deformation of the elastic aircraft in relation to the coordinate system fixed in the center of gravity. If we transpose equation 16 into the space, then the deformation becomes

$$\bar{u}_k(P, t) = \iiint_{(v)} T_{ik}(P, P')\, Q_i(P', t)\, dP' \quad ; \quad i, k = 1, 2, 3 \quad . \tag{19}$$

This equation can be inverted into

$$Q_i(P, t) = \iiint_{(v)} S_{ik}(P, P')\ \bar{u}_k(P', t)\ dP' \quad . \tag{20}$$

In accordance with the classic theory of elasticity, the deformation tensor T_{ik} and the rigidity tensor S_{ik} are independent of time. However, if we want to take the elastic after-effect and the inner damping into account accurately, then these tensors are dependent also on time and equations 19, and 20 would also have to be integrated over time. Furthermore, both tensors are symmetrical; there are applicable the equations

$$T_{ik}(P, P') = T_{ki}(P', P) \; ; \; S_{ik}(P, P') = S_{ki}(P', P) \quad .$$

In addition to the force of intensity Q_k, there are also created individual moments due to the gyratory effect of the individual power plants

$$\bar{M}_k(P, t) = -D_i(P, t)\ \dot{\vartheta}_j(P, t) + D_j(P, t)\ \dot{\vartheta}_i(P, t) \quad . \tag{21}$$

In this, $D_i(P, t)$ = torque of rotating parts of a power plant and $\dot{\vartheta}_i(P, t)$ = angular velocity of power-plant housing in space. If the torque axes of the power plants are approximately parallel to the plane of the wing, then the deformations of the aircraft so created are very small because the wing is in general very rigid against deformation in its plane. These small deformations are consequently not taken into account in the following. During a static vibration test with a dynamically analogous model of an He-219 aircraft, the influence of torque on the natural vibrations was shown to be immeasurably small.

The entire infinitely small displacement of a point P against a coordinate system moving uniformly in a straight line then is

$$u_k(P, t) = u_k(0, t) + x_i\ \vartheta_j(0, t) - x_j\ \vartheta_i(0, t) + \bar{u}_k(P, t) \quad . \tag{22}$$

5. Semi-Experimental Method for Determination of Deformation Tensor

The equations 17 to 22 are the most general linearized basic formulation of aeroelastic processes. The accuracy of solution depends initially on the accuracy of approximation of the deformation tensor T_{ik}.

We should like to communicate here a semi-experimental method frequently utilized. The basic formulation (19) becomes very much simpler when it is applied to the harmonic vibrations of a free-floating aircraft without incident flow. Let $\varrho_{kr}(P)$ be the density of mass of the aircraft at point P. Then the natural-vibration form r becomes

$$u_{ir}(P) = \omega_{(r)}^2 \iiint_{(v)} T_{ik}(P, P')\, u_{kr}(P')\, \varrho_{k(r)}(P')\, dP' \quad . \qquad (23)$$

ω_r is the corresponding natural frequency. These magnitudes can be determined on an actual aircraft by a static vibration test under roof. Here there also occur aerodynamic forces, the so-called Kelvin impulses. However, these act in essence as if certain added masses were rigidly connected with the surface elements of the aircraft which changes only the function $\varrho_{kr}(P)$ slightly. When taking into account the Kelvin impulses, the density of mass $\varrho_{kr}(P)$ then is dependent on the coordinate direction (k) and on the vibration form (r).

The individual natural-vibration forms u_{ir} are theoretically orthogonal to each other because the nucleus of the integral equation 23 is symmetrical, i.e. there is applicable, analogous to equation 15,

$$\iiint_{(v)} u_{kr}(P')\, u_{ks}(P')\, \varrho_{k(r)}(P')\, dP' = M_{(r)}\, \delta_{rs} \quad . \qquad (24)$$

In this, M_r = generalized mass of natural-vibration form r. There are several experimental methods for the determination of M_r which do not require exact data on the distribution of mass $\varrho_{kr}(P')$ of the aircraft. For instance, we can locate known added masses dM_ℓ at several points P_ℓ which are approximately proportional to the mass components existing in the vicinity of the aircraft and can measure the change $d\omega$ of the resonance frequency so brought about. There is then applicable for small added masses

$$M_r = -\frac{\omega_{(r)}}{2}\, u_{k(r)}^2(P_\ell)\, \frac{dM_\ell}{d\omega_r} \quad . \qquad (25)$$

According to the matrix rules, we need to totalize over all indices k and λ. From equations 23 and 24, there then follows the desired deformation tensor according to Mercer if all natural values ω_r^2 are positive,

$$T_{ik}(P, P') = \frac{u_{ir}(P)\, u_{kr}(P')}{\omega_r^2\, M_r} \quad ; \quad r = 1, 2, \ldots, \infty \; . \tag{26}$$

This series always converges under the assumption stated. We can determine theoretically or experimentally only a limited number n of natural-vibration forms. If we extend the sum of $r = 1$ as far as n, we then obtain an approximate expression of the deformation tensor.

The rigidity tensor S_{ik} can also be determined from the static vibrations:

$$S_{ik}(P, P') = \frac{\omega_r^2}{M_r}\, u_{ir}(P)\, \varrho_{(i)r}(P)\, u_{kr}(P')\, \varrho_{(k)r}(P') \; . \tag{27}$$

6. Calculation of Approximate Solutions of Integral Equations

In order to solve the integral equations 18 or 19 approximately, we can make a linear formulation for the deformation.

$$u_i(P, t) = f_{ir}(P)\, q_r(t) \quad ; \quad r = 1, 2, \ldots, n \; . \tag{28}$$

In this, $f_{ir}(P)$ are any given predetermined formulation functions which need to fulfill only certain boundary conditions; $q_r(t)$ are generalized coordinates which still need to be determined. The formulation function for the parallel displacement of the aircraft as a rigid body is

$$f_{ir}(P) = 1 \cdot \delta_{ir} \quad ; \quad r = 1, 2, 3 \; , \tag{29}$$

and for the displacements due to rotation of the aircraft as a rigid body

$$f_{kr}(P) = x_i\, \delta_{js} - x_j\, \delta_{is} \quad ; \quad s = r - 3 = 1, 2, 3 \; . \tag{30}$$

Corresponding formulations are also valid for the displacement due to rotation of a rigid control surface.

We decompose the intensity of force Q_i into the intensity of force of mass without Kelvin impulses and into the intensity of aerodynamic force which acts only on the exterior surface of the aircraft:

$$Q_i(P, t) = - f_{ir}(P)\, \varrho(P)\, \ddot{q}_r(t) - p_i \left\{ f_{\ell r}(P)\, q_r(t) \right\} \delta(\sigma) \ . \qquad (31)$$

p_i = component of aerodynamic force per surface unit acting in the coordinate direction i; $\delta(\sigma)$ = Dirac δ-function; σ = distance from surface of aircraft. In that case,

$$\delta(\sigma) = \begin{cases} 0, & \text{when } \sigma \neq 0 \\ \infty, & \text{when } \sigma = 0 \end{cases} \quad ; \quad \int_{-c}^{c} \delta(\sigma)\, d\sigma = 1 \ . \qquad (32)$$

Through this factor, the aerodynamic force per surface unit is changed into intensity of force. The pressure $p = \sqrt{p_i^2}$ is a functional $\{\ \}$ of the deformations of the aircraft and of the displacements of the coordinate system fixed in the aircraft, e.g. a function of the derivations of u_ℓ or an integral over such divisions. In equation 31, we need to totalize from 1 to 3 over ℓ and from 1 to n over r.

We obtain appropriate formulations for the calculation of approximate solutions when we introduce the formulations 28 and 31 in equations 20 or 19 and multiply these equations in addition with the integral operators

$$\iiint_{(v)} g_{is}(P)\, dP \quad \text{and/or} \quad \iiint_{(v)} g_{is}(P)\, \varrho(P)\, dP \qquad (33)$$

This process is called formation of median values or "weighting" with the weight functions $g_{is}(P)$ which must be selected appropriately. We then obtain the following systems of integral-differential equations for the determination of the generalized coordinates $q_r(t)$:

$$\ddot{q}_r(t)\, M_{rs} + q_r(t)\, K_{rs} + V_s \left\{ f_{\ell r}(P)\, q_r(t) \right\} = 0 \ \text{(Rayleigh-Ritz)}, \qquad (34)$$

$$q_r(t)\, M_{rs} + \ddot{q}_r(t)\, L_{rs} + W_s \left\{ f_{\ell r}(P)\, q_r(t) \right\} = 0 \ \text{(Galerkin)} \ . \qquad (35)$$

in which

$$M_{rs} = \iiint_{(v)} f_{ir}(P)\, g_{is}(P)\, \varrho(P)\, dP\,,$$

$$K_{rs} = \iiint_{(v)} \iiint_{(v)} S_{ik}(P, P')\, g_{is}(P)\, f_{kr}(P')\, dP\, dP',$$

$$L_{rs} = \iiint_{(v)} \iiint_{(v)} \Gamma_{ik}(P, P')\, g_{is}(P)\, \varrho(P)\, f_{kr}(P')\, \varrho(P')\, dP\, dP', \qquad (36)$$

$$V_s = \iint_{(a)} g_{is}(P)\, p_i \left\{ f_{\ell r}(P)\, q_r(t) \right\} dP,$$

$$W_s = \iiint_{(v)} \iint_{(a)} T_{ik}(P, P')\, g_{is}(P)\, \varrho(P)\, p_k \left\{ f_{\ell r}(P')\, q_r(t) \right\} dP\, dP'$$

These magnitudes are called the generalized masses, rigidities, deformations and forces. Equation 34 follows from equation 20 and is called the Rayleigh-Ritz equation; equation 35 follows from equation 19 and is called the Galerkin equation. We need obviously to decide on the utilization of one of these equations because they are dependent on each other.

There is a formal analogy between the two equations 34 and 14. The weight function is here

$$g_k(x, y) = g_{ik} F(x, y; r_i, s_i) \;; \quad i, k = 1, 2, \ldots, n\,.$$

Usually, the weight functions in equations 34 and 35 are stated as

$$g_{is}(P) = f_{is}(P) \qquad (37)$$

The results are then identical with the Lagrange equations of motion

$$\left[\frac{d}{dt} \frac{\partial}{\partial \dot{q}_s} - \frac{\partial}{\partial q_s} \right] (T - U) + V_s = 0$$

in which the kinetic energy is

$$T = \frac{1}{2} M_{rs} \dot{q}_r \dot{q}_s$$

and the potential energy

$$U = \frac{1}{2} K_{rs} q_r q_s \quad .$$

For harmonic vibrations, the weight functions may be determined analogous to equation 19:

$$g_{is}(P) = \iiint_{(v)} T_{ik}(P, P') Q_k \left\{ f_{\ell s}(P') \right\} dP' \quad . \tag{38}$$

This Grammel method therefore contains a partial iteration. Depending on the manner of weighting, there are also numerous approximation methods which may be advantageous for special problems and special formulations. When investigating the static torsional stability of a slender wing, the intensity $\varrho(P)$ is more suitably replaced in the integral operator (33) by

$$e(P)\ \ell(P) \quad ,$$

in which $e(P)$ represents the position of the elastic axis back of the neutral axis and $\ell(P)$ one-half of the wing chord.

We obtain a particularly simple result if we utilize as formulation functions the static-vibration forms:

$$u_i(P, t) = u_{ir}(P)\ q_r(t) \quad ; \quad r = 1, 2, \ldots, n \quad . \tag{39}$$

If we introduce this formulation and the tensor representations of equations 26 and/or 27 into the fundamental equations 20 and/or 19 with the weight function as $g_{is} = u_{is}$, we then obtain from both equations concurrently the same energy equation

$$\ddot{q}_r(t)\ M_r\ \delta_{rs} + q_r(t)\, \omega_r^2\ M_r\ \delta_{rs} +$$

$$+ \iint_{(a)} u_{is}(P)\ p_i \left\{ u_{\ell r}(P)\ q_r(t) \right\} dP = 0 \quad . \tag{40}$$

M_r = generalized mass and ω_r = natural frequency of static-vibration form r.

If we introduce in equation 34 or 35 or 40 successively s = 1, 2, ... , n, we then obtain a system of n linear integral-differential equations for the n generalized coordinates $q_r(t)$. If this concerns harmonic vibrations without external disturbance, i.e. flutter or dynamic stability, then the generalized coordinate is

$$q_r(t) = q_r \exp \omega t \quad . \tag{41}$$

All derivations and integrals of $q_r(t)$ are then proportional to $q_r(t)$ and we obtain a system of n homogeneous lineary algebraic equations in q_r.

Actual assemblies have an inner damping which is nearly independent of frequency and rises only slightly with amplitude because it is based on the close friction of riveted parts. In order to approximately take into account the inner damping of the aircraft, it is permissible to substitute, for the generalized rigidity in equation 40, the complex value

$$\omega_r^2 M_r \longrightarrow \omega_r^2 M_r \exp i g_r \tag{42}$$

where the damping phase angle g_r for each vibration form $u_{ir}(P)$ can be determined through the static vibration test; for aircraft, this is on the order of magnitude g_r = 0.01 to 0.10.

It is appropriate to multiply equation 40 with the so-called natural value $\lambda = 1/\omega^2$; this then becomes

$$(1 + \lambda \omega_r^2 \exp i g_r) M_r q_r \delta_{rs} + q_r F_{rs}(\beta, \omega^*) = 0 \quad , \tag{43}$$

in which the reduced frequency

$$\omega^* = \frac{\omega \ell}{v(1 - \beta^2)} \tag{44}$$

and the Mach number β are non-dimensional parameters of our problem. ℓ is a characteristic length, e.g. one-half of the largest wing chord. The function F_{rs} result after performing the integrations in equation 40. Their matrix is no longer symmetrical. This circumstance makes solution more difficult.

The equation system 43 possesses finite solutions q_r only when its nominator determinant disappears. This condition results in a complex algebraic equation of the nth degree for the natural value λ, the so-called secular equation. The latter has generally n complex solution surfaces $\lambda_s(\beta, \omega^*)$. In this multitude of mathematical solutions, however, only those correspond to an actual physical process whose argument is

$$\arg \lambda_s = -2 \arg \omega^* \pm 2k\pi \qquad (45)$$

For instance, if we insert the aerodynamic forces for a pure sine oscillation, then $\arg \omega^* = \pi/2$; $\arg \lambda = \pm \pi$. In this case, only pure real, negative values of λ_s therefore correspond to a physical process. If the complex parameter ω^* is selected so that its argument is

$$0 < \arg \omega^* < \pi/2$$

we obtain a physical flutter process with increasing amplitude. Although only a few points of the solution surfaces $\lambda_s(\beta, \omega^*)$ correspond to an actual physical process, it has been found appropriate to calculate all solution surfaces because this affords us a good comprehension of the influence of the individual parameters.

The result of such a calculation with four degrees of freedom is shown in Fig. 4. The critical speed v_s is entered as ordinate and the argument of λ_s as abscissa. Of the four roots λ_s , only the branch identified by III leads to flutter because only its natural values have an argument $\arg \lambda_s > \pi$. The broken line corresponds to a median inner damping $g_s = 0.10$. All points to the right of this line are nonstable and lead to flutter with increasing amplitude.

7. Theory of Aerodynamic Stress Distribution

We now come to the aerodynamic forces. The experimental determination of non-steady aerodynamic forces on oscillating models in the wind tunnel has recently been improved through the development of very small piezoelectrical and electrodynamic pressure gauges. With these and with other methods, the aerodynamic theory can be tested in individual cases and be eventually improved by adaptation factors. For the

large number of possible vibration forms and parameters, however, we remain restricted to theory.

The tenuity of the fluid can be considered by us in this theory only phenomenologically when we assume, by following Kutta, smooth downwash at the sharp trailing edge of the wing but otherwise calculate with a fluid not possessing friction. The calculation of stress distribution at any given wing movements is even then extremely difficult. In order to facilitate this, we shall assume that the wing is infinitely thin and that all disturbances are infinitely small. This simplified theory of sustentation surfaces does produce correct results within a certain order of magnitude but the variations through control-surface moments may amount to as much as 50%, depending on the Reynolds number. The influence of the wing thickness is always noticeable, especially at high Mach numbers. In certain cases, the influence of the thickness can be calculated at least in a first approximation, i.e. with smooth flow and $\beta = 0$, as well as generally with $\beta > 2$. For reasons of simplification, however, we generally calculate with zero wing thickness and will use this procedure in the following.

We are assuming that the wing is smooth except for infinitely small variations and lies in the plane $z = 0$ (Fig. 5). The wing shall move in the direction of the positive x-axis with the velocity $v = 1$ and shall cover the distance $s = vt$. In order to simplify, we also set the density of air as $\varrho = 1$. The linearized Euler equations:

$$\left(\frac{\partial}{\partial s} - \frac{\partial}{\partial x}\right) \Phi(s, x, y, z) + p(s, x, y, z) = 0 \quad , \tag{46}$$

$$\left[\frac{\partial^2}{\partial x^2} + \frac{\partial^2}{\partial y^2} + \frac{\partial^2}{\partial z^2} - \beta^2 \left(\frac{\partial}{\partial s} - \frac{\partial}{\partial x}\right)^2\right] \Phi(s, x, y, z) = 0 \quad . \tag{47}$$

in which Φ = velocity potential; p = pressure; and β = Mach number. We are seeking solutions of these differential equations under the following boundary conditions: the pressure $p(s', x', y', z')$ or the downwash

$$w(s', x', y', z') = \Phi_{z'}(s', x', y', z') \tag{48}$$

must have predetermined values at the wing, with the exception of the leading edge. Furthermore, the pressure at the trailing edge must be finite and remain integrable at the leading edge if it becomes infinite here.

At the wing, the downwash is determined either through the small deformations of the wing

$$w(s', x', y', z') = \left(\frac{\partial}{\partial s'} - \frac{\partial}{\partial x'}\right) u(s', x', y', z') \quad , \tag{49}$$

or through an atmospheric squall area. The solutions of this boundary-value problem can generally be represented as Stieltjes integrals over the given pressure distribution or over the given downwash:

$$w(s, x, y, z) = \iint_{(a)} dx'dy' \int_{s'=0}^{s'=s} dp(s', x', y', z')\, H(s-s', x-x', y-y', z-z'), \tag{50}$$

$$p(s, x, y, z) = \iint_{(a)} dx'dy' \int_{s'=0}^{s'=s} dw(s', x', y', z')\, K(s-s', x-x', y-y', z-z'). \tag{51}$$

The purpose of representation as Stieltjes integrals lies in the ability of integrating even over non-steady finite variations of the pressure $dp(s')$ or of the downwash $dw(s')$ on the wing. The integration variable s' here serves as parameter for the differentials stated. The Green functions H and K occurring in equations 50 and 51 are so-called difference nuclei. This property is important because it simplifies the theory. An immediate consequence of this property is the so-called "reverse flow theorem" which has become known only during the last few years. The nuclei H and K are easily calculable algebraic functions in those cases where they are independent from the edge conditions of the pressure. In the nucleus H, this is always the case because the edge conditions must already have been fulfilled in the predetermined pressure distribution p. In the nucleus K, this is the case only in pure supersonic areas of the wing because here the edge conditions are fulfilled a priori.

In Fig. 6, we show the leading Mach cones of a wing flying at supersonic speed. One-half of the opening angle of the cone is the Mach angle ϑ. The pure supersonic area of the wing is white. At point 1, the nucleus K is therefore a simple and known function. The flow at point 2 is influenced by the leading-edge condition of the right wing tip and the flow at point 3 through the trailing-edge condition.

In the shaded area, the underface of the wing influences the surface of the wing. In this area, it is more difficult to determine the nucleus K because in it the Kutta condition and the integrability condition of the pressure at the edges of the wing must be fulfilled. So far this has been possible only by means of orthogonal functions. With

smooth wings, however, these exist only for the elliptical surface of sustentation and its border cases, the ribbon and the circle.

In smooth two-dimensional flow, the nucleus K for all Mach numbers is known. For the calculation of the aerodynamic coefficients, we need only perform quadratures. For slender wings, it may be assumed as approximation that the flow is smooth in each section of wing. This is more valid as the wing is slender and vibrates more quickly.

At Mach numbers $\beta > 2$, it is possible to calculate as approximation with one-dimensional flow. According to this so-called piston theory, the pressure (at $v = \varrho = 1$) is

$$p(P,t) = \frac{1}{\beta} w(P,t) + \frac{\gamma+1}{4} w^2(P,t) + \frac{\gamma+1}{12} \beta w^3(P,t) + \ldots . \quad (52)$$

In this, $w(P,t)$ = given downwash at body surface calculable from equation 49; γ = ratio of specific heats of the fluid. This formula makes it possible to consider even the influence of the wing thickness as has already been stated.

8. The Collocation Method of Pressure Calculation

If the pressure p is desired when the nucleus K is unknown, we must invert the integral equation 50 whose nucleus H is always known. This can be done in general only numerically for a finite number of points. This procedure is called a collocation method.

Let us assume n points P_i on the wing, e.g. the centers of gravity of the n slabs in Fig. 3. In these, the vertical displacement u_i and the downwash w_i shall be assumed as known but the pressure p_i is desired. If all values of p_i were known, we could then from this interpolate a steady pressure distribution $p(x, y)$ which would suffice for the edge conditions. In a subsonic range (shaded in Fig. 6), the pressure then is:

$$p'(x,y) = \sqrt{\frac{x - x_h(y)}{x_v(y) - x}} \; F(x,y\,;\; r_i, s_i)\; g'_{ik}\; p_k \quad , \quad (53)$$

and in a supersonic range (white in Fig. 6)

$$p''(x,y) = F(x,y\,;\; r_i, s_i)\; g''_{ik}\; p_k \quad . \quad (54)$$

In this, $x_v(y)$ = coordinate of leading edge, $x_h(y)$ = coordinate of trailing edge of wing. At the boundary between the two ranges in Fig. 6, both pressure distributions must be uniform. This requirement

can be fulfilled with an interpolated pressure distribution only at some points. It is therefore appropriate to locate a sufficient number of points P_i along this boundary because in them this requirement is fulfilled a priori. From equations 53 and 54, we then obtain directly the matrices g'_{ik} and g''_{ik} by insertion of the coordinates of all the points.

The steady pressure distributions 53 and 54 must now be introduced into the integral equation 50 and be numerically integrated. From this follows the matrix equation

$$w_i = H_{ik}\, p_k \tag{55}$$

and its inversion

$$p_k = \left[H_{ik}\right]^{-1} w_i \quad , \tag{56}$$

which is obtained by solving the lineary equation system 55. From the steady pressure distribution according to equations 53, 54 and 56, we can calculate the individual aerodynamic forces $Q_k^{(\alpha)}$ at the n stations according to equation 14. This pressure distribution may also be introduced into the integrals 36 or 40 and the latter can then be calculated.

Such numerical problems have been solved by Zartarian, Hsu and Voss (4) and by Hsu, Martucelli and Ashley (5) for short wings in the subsonic range. An approximation method was utilized for this which did not employ any of the interpolation formulas given here but used only integrals over sufficiently small rectangular slabs which can be performed as approximation analytically. The wing is here divided, without regard to its actual contour, in a sufficiently large number of rectangular slabs as well as possible. For each of these slabs, a special exponential series of the pressure is developed in which the development coefficients are determined in such manner that the pressure distribution at the slab boundaries is steady, with the exception of the free boundaries.

We now show the results for a vibrating quadratic surface of sustentation which is divided into 36 quadratic slabs. The parameters are

$$\beta = 0 \quad ; \qquad \omega^* = 0.238 \quad .$$

In Fig. 7 and 8, the pressure distributions of one-half of the wing are entered for oscillatory and torsional vibrations. The curves are the theoretical values and the individual points are the experimental values.

The strong fluctuation of the individual pressure values is typical for the collocation method. In Fig. 9 and 10, the total lift and the moment are entered as function of the reduced frequency. Two other theoretical approximation methods and the experimental values serve as comparison. The concordance of the theoretical value (▲) with the measurements is satisfactory in regard to the absolute amounts of the complex numbers whereas some arguments deviate to a greater extent.

The same procedure was carried out for a 60°-delta wing. The sub-division of the latter into quadratic slabs is shown in Fig. 11. A dynamically analagous model of this wing was subjected to a static vibration test. Calculation of flutter according to the energy equation 40 was carried out with the first four static-vibration forms. The critical velocity of the flutter in the wind tunnel was also measured. For reasons of security, numerical results were not communicated but only the following qualitative findings:

1) The collocation method produces satisfactory numerical values for the critical velocity of the flutter. However, the predictions of critical frequency are less exact.
2) The investigated approximation theories for wings of very low aspect ratio do not produce satisfactory numerical values.

In view of the relatively small number of stations ($n = 15$) and, for a delta wing, of the rather arbitrary subdivision into quadratic slabs, these favorable findings seem to us more a matter of chance. By utilization of the interpolation method described above, consideration of the actual wing contour and increase of the number of points, the collocation method is capable of being improved.

LITERATURE REFERENCES

1. R. L. Bisplinghoff, H. Ashley, R. L. Halfman, Aeroelasticity. Addison-Wesley, Cambridge, 1955, p. 49-66.
2. D. Williams, Recent Developments in the Structural Approach to Aeroelastic Problems. Journ. Roy. Aeron. Soc. 58 (1954), p. 403-428.
3. R. v. Mises, Numerische Berechnung mehrdimensionaler Integrale (Numerical Calculation of Multidimensional Integrals). Z. Angew. Math. Mech. (J. Appl. Math. Mech.) 34 (1954), p. 201-210.
4. G. Zartarian, P. T. Hsu, H. M. Voss, Application of Numerical Integration Techniques to the Low-Aspect-Ratio Flutter Problem in Subsonic and Supersonic Flows. Aeroelastic and Structures Research Laboratory, Massachusetts Institute of Technology. Techn. Rep. 52-3, October 1954.
5. P. T. Hsu, J. R. Martucelli, H. Ashley, Oscillatory Aerodynamic Loads on Low-Aspect-Ratio Wings in Subsonic Flow. Aeroelastic and Structures Research Laboratory, Massachusetts Institute of Technology. Techn. Rep. 52-4, December 1955.

APPENDIX 1

Derivation of a Formula for the Generalized Mass*

The following is a demonstration of the formula, indicated in the article, for the determination of the generalized mass of any given spatial vibration system for any given very small added masses. For a system containing only elastic forces and forces of mass, the intensity of force according to equation 20 of the article is

$$Q_i(P,t) = \ddot{u}_i(P,t)\,\varrho(P) + \iiint_{(v)} S_{ik}(P,P')\,u_k(P',t)\,dP' = 0 \quad . \qquad (1)$$

We can replace this integral equation arbitrarily by a system of N point masses μ_i^{ℓ} at the points P_ℓ and by the rigidity coefficients

$$S_{ik}(P_\ell, P_n') = S_{ik}^{\ell n} = S_{ki}^{n\ell}$$

if $N \longrightarrow \infty$. Under harmonic vibrations, the displacement of the point P_ℓ in the coordinate direction i is

$$u_i(P_\ell, t) = A_i^{\ell} \exp\,(t\sqrt{\lambda}) \quad .$$

If we introduce these expressions in equation 1, we then obtain this system of the $3N$ linear equations in matrix form

$$\lambda \mu_{(i)}^{(\ell)} A_i^{\ell} + S_{ik}^{\ell n} A_k^{n} = 0 \; ; \quad i, k = 1, 2, 3 \; ; \; \ell, n = 1, 2, \ldots, N \; . \qquad (2)$$

If aerodynamic forces are absent, $\mu_1^{\ell} = \mu_2^{\ell} = \mu_3^{\ell}$. In each product, summation must be performed over factors with the same indices if the indices are not shown in parenthesis.

The determinant of the coefficient matrix of this equation system, is, in the case of resonance,

$$D = \det \left| \lambda \mu_i^{\ell} + S_{ik}^{\ell n} \right| = 0 \quad . \qquad (3)$$

---

* Added subsequent to printing of article.

The minor of this determinant to the coefficient $S_{ik}^{\ell n}$ shall be $D_{ik}^{\ell n}$. Because D is symmetrical, there are valid for the vibration amplitudes A_i^{ℓ} the equations

$$A_i^{\ell} = C\sqrt{D_{ii}^{\ell\ell}} \quad ; \quad i, \ell \text{ arbitrary}; \quad C = \text{const} . \tag{4}$$

By differentiation of equation 3 after λ, we obtain

$$\left(\mu_i^{\ell} + \lambda \frac{d\mu_i^{\ell}}{d\lambda}\right) D_{ii}^{\ell\ell} = 0 \quad . \tag{5}$$

From equation 4 and 5 follows

$$\left(\mu_i^{\ell} + \lambda \frac{d\mu_i^{\ell}}{d\lambda}\right) (A_i^{\ell})^2 = 0 \quad , \tag{6}$$

in which summation must be performed over i and ℓ. According to equation 24 of the article, the generalized mass of the r^{th} natural vibration form with the natural frequency $\omega_r = \sqrt{-\lambda_r}$ defined by

$$M_r = (A_i^{\ell})^2 \mu_i^{\ell} \Big| \lambda = \lambda_r \quad . \tag{7}$$

From equation 6 and 7 follows the formula of the generalized mass

$$M_r = -\lambda_r \sum_{\ell=1}^{N} \sum_{i=1}^{3} (A_i^{\ell})^2 \frac{d\mu_i^{\ell}}{d\lambda} \Big| \lambda = \lambda_r \quad . \tag{8}$$

which agrees with equation 25 of the article. For greater clarity, the sum signs are here written out. In practice, the added masses $d\mu_i^{\ell}$ are selected at only a few points P_{ℓ}, e.g. at the excitation points, different from zero. It should be particularly noted that all three displacement components must be considered because the individual points of a vibrating aircraft may have any given directions of movement in space.

The static vibration tests of aircraft take place in air at atmospheric pressure. The additional forces due to the resonance vibration of the air masses here act in essence like forces of mass. We therefore have in general

$$\mu_1^{\ell} + \mu_2^{\ell} + \mu_3^{\ell} \quad .$$

The magnitude of the mass components depends on the density of the air and the given natural vibration form. The added masses $d\mu_i^{\ell}$, however, are compact metal blocks in the test and therefore practically independent of the density of the air;

$$d\mu_1^{\ell} = d\mu_2^{\ell} = d\mu_3^{\ell} \quad .$$

It is desirable that no further changes of mass take place except for these accurately known changes of mass. The resonating air mass does not change in such a test only then when the natural-vibration form $u_{ir}(P)$ does not change. This is the case only then when the added masses $d\mu_i^{\ell}$ are distributed proportionally to the existing masses. Under this assumption, we obtain by differentiation of equation 23 of the article, after λ and the introduction of equation 24 and 26 the generalized mass

$$M_r = \iiint u_{k(r)}^2(P')\varrho_{kr}(P')\,dP' = -\lambda \iiint u_{k(r)}^2(P') \frac{d\varrho_{kr}(P')}{d\lambda}\,dP' \Bigg|_{\lambda = \lambda_r} . \quad (9)$$

If the participation of the resonant air mass in the total mass is only small, we are able to neglect, even at a distribution of the added masses only roughly proportional to the existing mass distribution, the change of the resonant air masses due to frequency changes.

We therefore obtain with the aid of such a test and by means of equation 8 an approximation of the generalized mass of the aircraft increased by the Kelvin impulses. Consequently, in the basic formulation of the aerodynamic forces for the calculation of flutter, the Kelvin impulses must be subtracted and/or be recalculated for another density of air when the flight takes place at a greater height than the altitude of the static vibration test.

APPENDIX 2

Theory of Static Vibration Test*

By using the basic formulations given above, it is fairly easy to state a linearized theory of the enforced vibrations of an elastic body with damping. This theory answers the questions at what points and to

---

* Added subsequent to printing of article.

what extent we should locate excitation forces on the elastically suspended aircraft in order to obtain its natural-vibration forms as unaltered as possible.

We consider first a free-floating elastic body without damping in which oscillation is induced with the angular velocity ω by excitation forces. $Q_i(P)$ shall be the intensity of force at the point P of the body in the coordinate direction i. According to equation 20 and by disregarding the factor $\exp j\omega t$ ($j = \sqrt{-1}$) is

$$Q_i(P) = -\omega^2 \varrho_i(P,\omega)\, u_i(P) + \sum_{k=1}^{3} \iiint S_{ik}(P,P')\, u_k(P')\, dP' \quad ; \qquad (1)$$

$$i = 1,\ 2,\ 3 \ .$$

Here and hereafter, all sum signs are written out for greater clarity. In consideration of the resonant air masses, the density of mass ϱ depends on the coordinate direction i and on the vibration form and therefore also on ω. A natural vibration of this body is characterized through $Q_i = 0$, $\omega = \omega_r$, $u_i(P) = u_{ir}(P)$. $u_{ir}(P)$ is the r^{th} natural-vibration form. There then follows from equation 1

$$0 = -\omega_r^2 \varrho_{ir}(P)\, u_{ir}(P) + \sum_{k=1}^{3} \iiint S_{ik}(P,P')\, u_{kr}(P')\, dP' \ .$$

Here and hereafter, $i,k = 1, 2, 3$ and $r,s = 1, 2, \ldots \infty$.

If we consider the resonant air masses, the generalized mass then becomes

$$M_r\, \delta_{rs} = \sum_{k=1}^{3} \iiint u_{kr}(P)\, u_{ks}(P)\, \varrho_{ks}(P)\, dP \ . \qquad (2)$$

This is the orthogonality relation of the natural-vibration forms. Within the body, the density is $\varrho_{ks}(P) = \varrho(P)$. On the surface of the body, $\varrho_{ks}(P)$ indicates a wing loading with mass which must be integrated over the surface.

In a gas not possessing friction, the mass loading of any given oscillation form replacing the aerodynamic forces is

$$\varrho_{ks}(P) = C_s(\varkappa)\, \varrho_k(P) \ .$$

In this, $\varrho_k(P)$ is a localized function depending only on the body shape which we calculated for the ellipsoid.* $C_s(\varkappa)$ is a complex function depending on the oscillation form and the wave number

$$\varkappa = \frac{\omega \ell_o}{c}$$

$C_s(0)$ is real. ℓ_o is a characteristic length of the body and c the speed of sound of the air. Because $C_s(\varkappa)$ is complex, acoustic effort is radiated out and the natural-vibration forms $u_{ks}(P)$ have an imaginary, although small, share. In order to simplify calculation, we neglect this imaginary share in the following and take acoustic damping into account through an addition to the inner damping. Both dampings are determined in any event as sum in the static vibration test and their separation is difficult. In the following, M_r, ϱ_{ks} and u_{ks} are therefore assumed as real.

In order to consider both the inner damping as well as the acoustic damping approximately, the rigidity tensor is enlarged according to equation 27 by the addition of a damping factor $\exp j\gamma_r$.

$$S_{ik}(P, P') = \sum_{r=1}^{\infty} \frac{\omega_r^2}{M_r} u_{ir}(P)\, \varrho_{ir}(P)\, u_{kr}(P')\, \varrho_{kr}(P')\, \exp j\gamma_r \quad . \quad (3)$$

In this, γ_r is the damping phase angle which is obtained for each natural-vibration form u_{ir} by oscillation-decay tests. This is usually $\gamma_r = 0.01$ to 0.10. Actually, the angle of damping depends not only on the vibration form, but also on the locality. The basic formulations become very complicated, however, and it is also very difficult to determine this localized function experimentally.

Any given change of shape of the body can be developed from natural-vibration forms:

$$u_i(P) = \sum_{r=1}^{\infty} a_r\, u_{ir}(P) \quad . \quad (4)$$

---

* Let u, v, w be orthogonal elliptical coordinates; let u = const. be the surface of the ellipsoid; let P be a point on the surface with the Cartesian coordinates x_1, x_2, x_3. The function is then

$$\varrho_k(P) = \left| \frac{\partial}{\partial u} x_k(u, v, w) \right| \quad .$$

If we insert equations 2 to 4 in equation 1, we then obtain the intensity of excitation force

$$Q_i(P) = \sum_{r=1}^{\infty} a_r \, u_{ir}(P) \; \varrho_{ir}(P) \; (\omega_r^2 \exp j \, \gamma_r - \omega^2) \quad . \tag{5}$$

A pure natural-vibration form $u_{is}(P)$ is obtained only under very definite conditions, i.e.

$$a_r = \begin{cases} 0 \, , & \text{when} \quad r \neq s \, , \\ 1 \, , & \text{when} \quad r = s \, . \end{cases} \tag{6}$$

Through separation of the real and imaginary share, there then follows from equations 5 and 6 the natural frequency and the density of excitation force

$$\omega^2 = \omega_s^2 \cos \gamma_s \, ,$$

$$Q_i(P) = u_{is}(P) \; \varrho_{is}(P) \; \omega_s^2 \; j \sin \gamma_s \quad . \tag{7}$$

The factor $j = \sqrt{-1}$ means that the excitation force has the phase angle $\frac{\pi}{2}$ to the change of shape. Because $\omega_s^2 \sin \gamma_s = \text{const.}$, the excitation force Q_i becomes proportional at any point P to the product from the change of shape u_{is} and the density of mass ϱ_{is}. E. Schultze* has obtained a corresponding result for smooth plates.

Such excitation can experimentally not be realized. We therefore investigate to what extent we can approach the ideal of a real natural-vibration form by a finite number of discrete excitation forces $K_k(P_\ell)$ at L points P_ℓ. We also take into consideration the elastic suspension of the aircraft at N points P_n' with the spring constants $c_k(P_n')$ and the resonant masses of the suspension $m_k(P_n')$. For an excitation frequency ω, the following discrete forces act on the aircraft:

---

* E. Schultze, The Induction of Real Natural Vibrations of Aircraft Wings, ZAMP 6 (1955), pp. 126-135.

Points P_ℓ : $K_k(P_\ell)$, $\ell = 1, \ldots, L$,

Points P'_n : $\left[\omega^2 m_k(P'_n) - c_k(P'_n)\right] u_k(P'_n)$, $n = 1, \ldots, N$.

For the treatment of discrete forces, the basic formulation 19 is more suitable. According to this, through excitation with a frequency ω and elimination of the factor $\exp j\omega t$, the resultant deformation $u_i(P)$ is

$$u_i(P) = \omega^2 \sum_{k=1}^{3} \iiint T_{ik}(P, P')\, u_k(P')\, \varrho_k(P', \omega)\, dP' \qquad (8)$$

$$+ \sum_{k=1}^{3} \sum_{\ell=1}^{L} T_{ik}(P, P_\ell)\, K_k(P_\ell) + \sum_{k=1}^{3} \sum_{n=1}^{N} T_{ik}(P, P'_n)\, u_k(P'_n) \left[\omega^2 m_k(P'_n) - c_k(P'_n)\right] .$$

The deformation tensor T_{ik} with damping is analagous to equation 26

$$T_{ik}(P, P') = \sum_{r=1}^{\infty} \frac{1}{\omega_r^2 M_r}\, u_{ir}(P)\, u_{kr}(P')\, \exp(-j\gamma_r) \quad . \qquad (9)$$

From equations 2, 4, 8, 9 follows the condition

$$\sum_{r=1}^{\infty} \frac{1}{\omega_r^2 M_r}\, u_{ir}(P)\, \exp(-j\gamma_r) \left\{ a_r M_r (\omega^2 - \omega_r^2 \exp j\gamma_r) \right. \qquad (10)$$

$$\left. + \sum_{k=1}^{3} \sum_{\ell=1}^{L} u_{kr}(P_\ell) K_k(P_\ell) + \sum_{k=1}^{3} \sum_{n=1}^{N} u_{kr}(P'_n) \left[\omega^2 m_k(P'_n) - c_k(P'_n)\right] \sum_{r'=1}^{\infty} a_{r'}\, u_{kr'}(P'_n) \right\} = 0 .$$

In order to comply with equation 10 for all points P, the brackets $\{\ \}$ must disappear for all values of r. This consequently produces a system of an infinite number of linear equations for the unknown factor a_r which determines the actual form of oscillation according to equation 4.

We see from equation 10 that equation 6 cannot be solved for all values of r. With this type of excitation, any real natural-vibration form is consequently not possible. However, by suitable selection of L excitation forces K_k and their points of attack P_ℓ ,

we can initially exclude $L - 1$ natural-vibration forms from the excitation. It is of particular importance to exclude the natural-vibration forms adjoining on either side of the desired natural-vibration form $r = s$. We therefore require that

$$a_r = \begin{cases} 0 \text{ , when } r = r_1, r_2, \ldots, r_L \neq s \text{ ,} \\ 1 \text{ , when } r = s \text{ .} \end{cases} \tag{11}$$

In order to be able to solve equation 10 iteratively, we start by initially considering only the number $r' = s$ in the last sum. We then obtain for $r = s$, after separation into the real and the imaginary components, the two equations

$$(\omega_s^2 \cos \gamma_s - \omega^2) M_s = \mathfrak{Re} \sum_{k=1}^{3} \sum_{l=1}^{L} u_{ks}(P_l)\, K_k(P_l) + \tag{12}$$

$$+ \sum_{k=1}^{3} \sum_{n=1}^{N} \left[u_{ks}(P_n')\right]^2 \left[\omega^2 m_k(P_n') - c_k(P_n')\right] \text{ ,}$$

$$\omega_s^2 M_s \sin \gamma_s = \mathfrak{Im} \sum_{k=1}^{3} \sum_{l=1}^{L} u_{ks}(P_l)\, K_k(P_l) \text{ .} \tag{13}$$

In order to cancel out the influence of the elastic suspension, i.e. to reduce both sides of equation 12 to zero, we can employ two methods. We can either determine the real components of the excitation forces K_k in such manner that the right side of equation 12 disappears or we can state $\mathfrak{Re}\, K_k(P_l) = 0$ and attune the elastic suspension again to resonance for each resonance frequency by changing either $m_k(P_n')$ or $c_k(P_n')$. Let this be

$$\omega^2 m_k(P_n') - c_k(P_n') = 0 \text{ .}$$

Then the right side of equation 12 also disappears and all excitation forces have the same phase angles of modulus π. Both methods may be combined. For example, we can attach an additional excitation force $K_k(P_1')$ at point P_1' of the suspension which carries the largest part of the aircraft weight and automatically control this force so that

$$K_k(P_1') + u_k(P_1') \left[\omega^2 m_k(P_1') - c_k(P_1')\right] = 0$$

The other points of suspension which need to absorb only minor forces can be made near the given nodal lines and can moreover be attuned to resonance.

From equation 10 and 11, there also follows for $r \neq s$

$$\sum_{k=1}^{J} \sum_{\ell=1}^{L} u_{kr}(P_\ell)\, K_k(P_\ell) = 0 \quad ; \quad r = r_1, r_2, \ldots, r_L \neq s \,. \qquad (14)$$

During the vibration test, the resonance frequency ω is measured at which all points vibrate with the same phase angle as far as possible. By means of equation 12, we can calculate from this the ideal resonance frequency of a free-floating body which is being excited according to equation 7. The equation 13 and 14 form a system of L linear equations for the calculation of L excitation forces K_k. In principle, the points P_ℓ and the direction of attack of the excitation forces can be selected at will. However, the researcher will select them as far as possible so that excitation forces K_k are produced from equation 13 and 14 which most efficiently utilize the existing electrodynamic exciters, i.e. are neither too large nor too small.

Certain guide lines for this are obtained when equation 7 is integrated over respective parts of the aircraft.

When the excitation forces have been calculated, we can then calculate the other coefficients a_r from equation 10, initially without consideration of the elastic suspension. Then the entire calculation is repeated as a second approximation in consideration of the elastic suspension. With the aid of equation 14, we can initially cancel out L - 1 natural-vibration forms. If we know the nodal lines of a further vibration form u_{ir}, and permits all excitation forces to act along these nodal lines, this vibration form also is not excited because $a_{r'} = 0$ follows out of equation 10.

The knowledge of the natural-vibration forms $u_{ir}(P)$ which this method presupposes, can be obtained experimentally only in successive steps. We initially determine one set of natural-vibration forms as well as possible as a first approximation, i.e. only with the phase-resonance condition. These forms are then utilized for calculation of the excitation forces and for subsequent experimental determination of the natural-vibration forms as a second approximation. This procedure must be repeated often enough until the results no longer change. Higher natural vibrations can be obtained relatively pure only when we utilize an adequate number of exciters. In general, the natural-vibration forms will be as much purer as the attenuation γ_r is smaller.

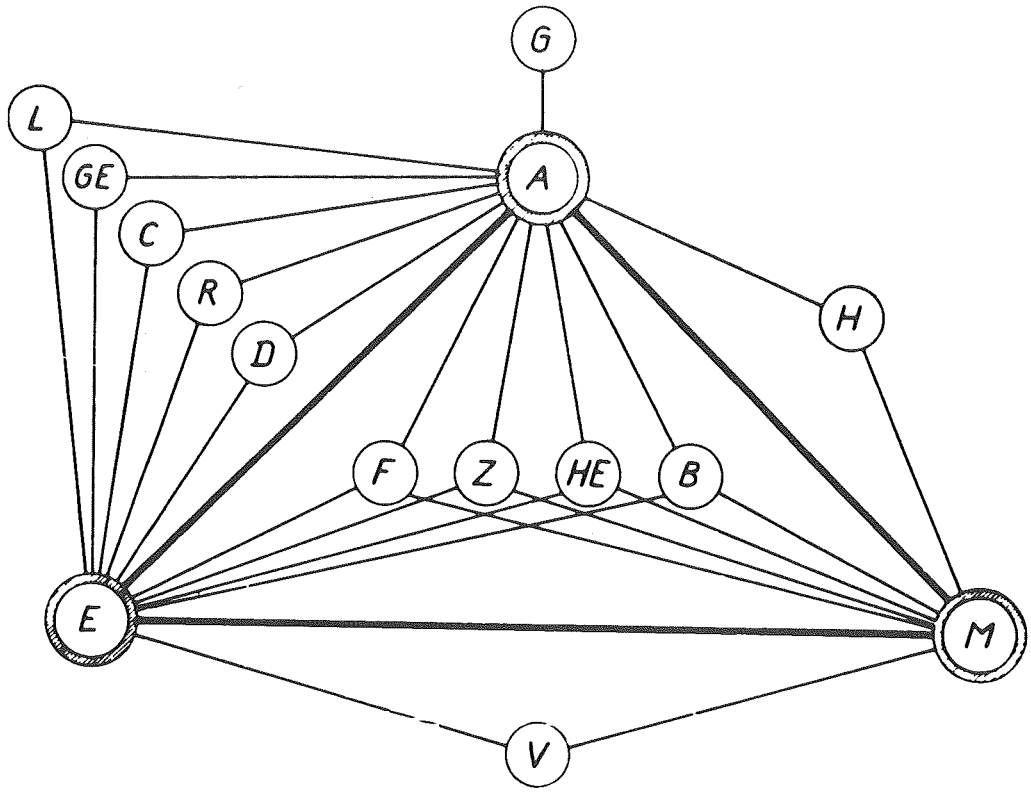

Fig. 1. Aeroelastic-Force Triangle

A - Aerodynamic force.
E - Elastic force.
M - Force of mass.
V - Mechanical vibration.
G - Static flight stability.
H - Dynamic flight stability.
B - Shaking (buffeting).

L - Aerodynamic load distribution.
GE - Static flight stability of elastic aircraft.
C - Control-surface effectiveness.
R - Inversion of control-surface action.
D - Static pitching of wing.
F - Flutter.
Z - Dynamic response.
HE - Dynamic flight stability of elastic aircraft.

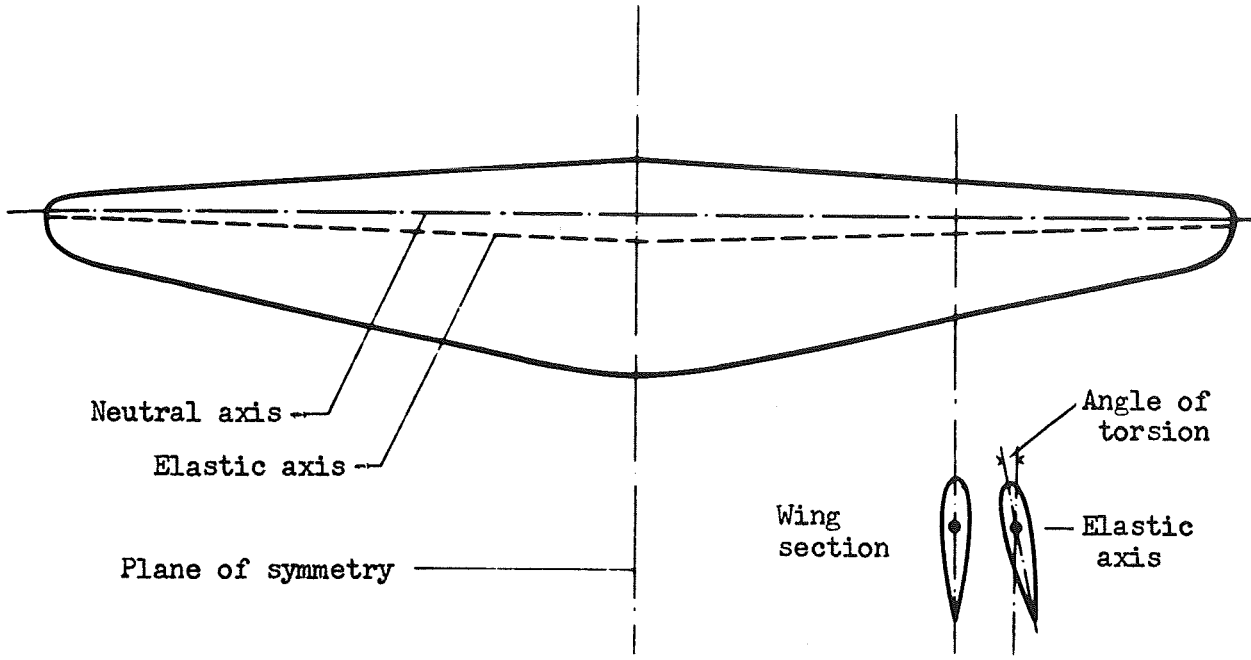

Fig. 2. Wing with Neutral Axis and Elastic Axis.

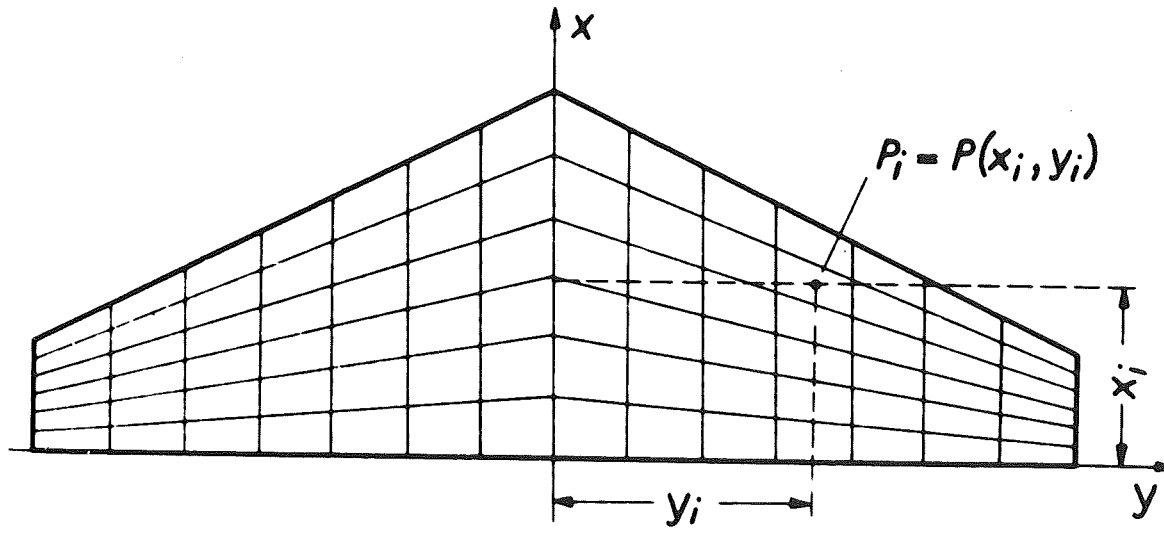

Fig. 3. Wing Subdivided as Elastic Plate in n Slabs

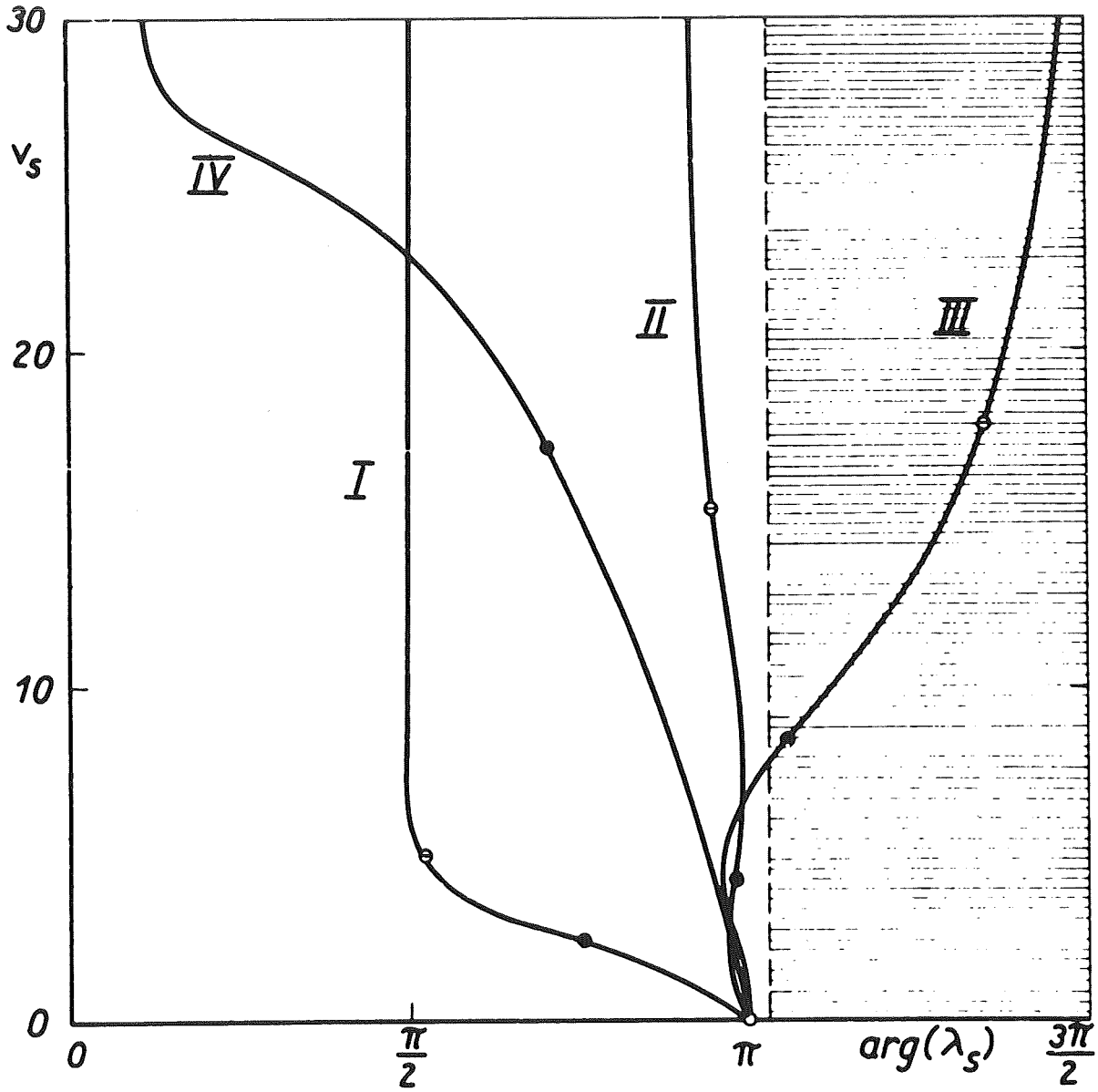

Fig. 4. Complex Natural Values of Flutter with 4 Degrees of Freedom.
Non-compressible Fluid $\beta = 0$.

$\omega^* = 0.1$: Point ●
$= 0.4$: Point ●
$= \infty$: Point ○

Non-stable range for $g_s = 0.1$.

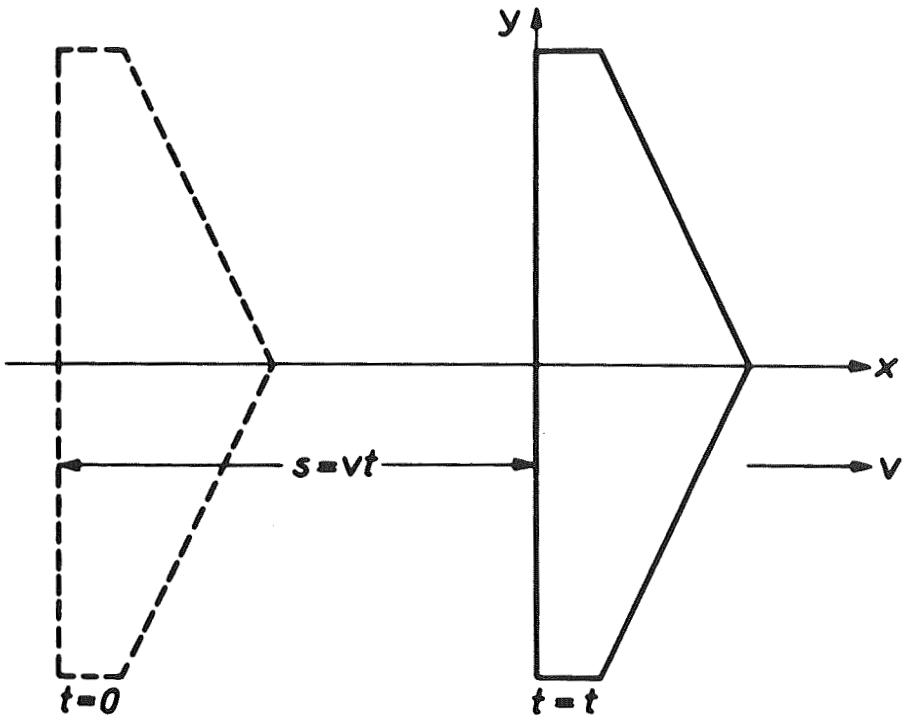

Fig. 5. Wing Surface Actuated in Plane z = 0.

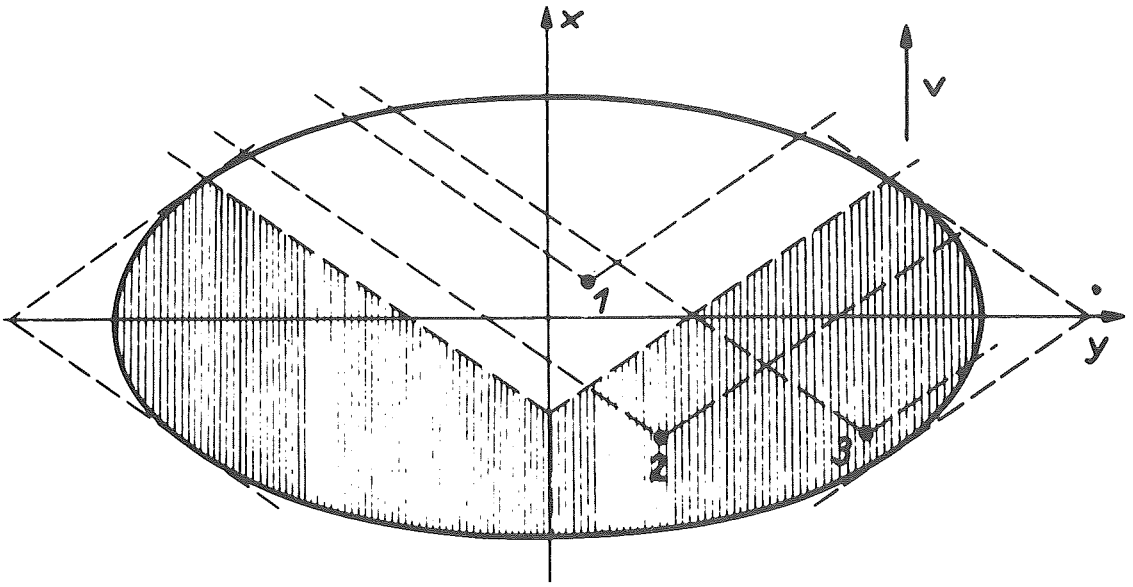

Fig. 6. Wing Surface Actuated with Supersonic Speed.

Mach number $\beta = 1.2$

Mach angle $\vartheta = \arcsin \frac{1}{\beta} = 56^{\circ}$.

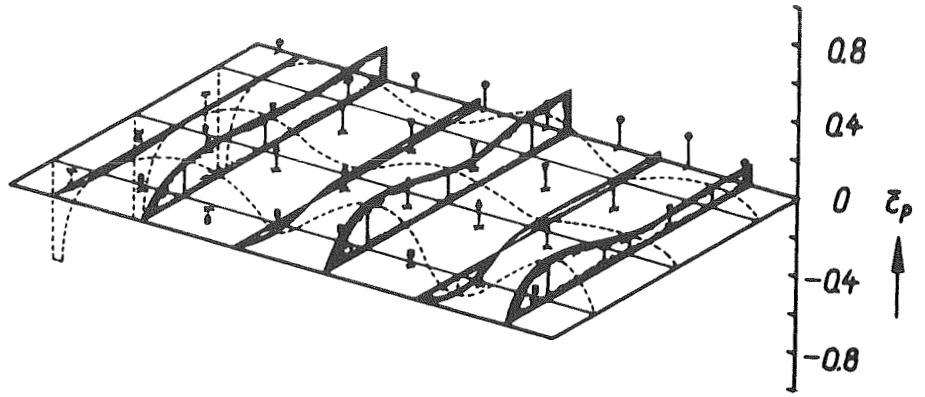

Real Component

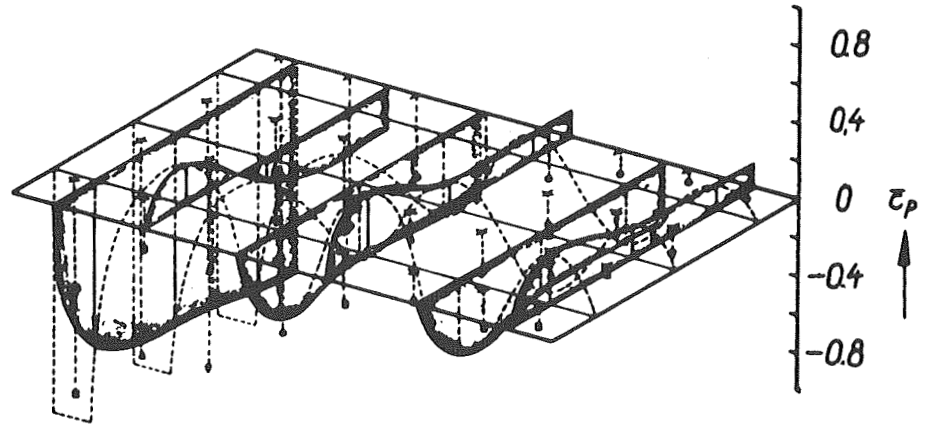

Imaginary Component

Fig. 7. Motion of Vertical Translation.

Distribution of the Real and Imaginary Components of the Coefficients $\bar{c}_p$ of the pressure over the left half of the Quadratic Wing Surface.
Above: Real Component. Below: Imaginary Component.
The experimental values of Laidlaw are entered as points ↕ above this. Reduced frequency of theoretical calculation $\omega^* = 0.238$. (Taken from Lit. Ref. 5 where the symbol ω^* is represented by k.)

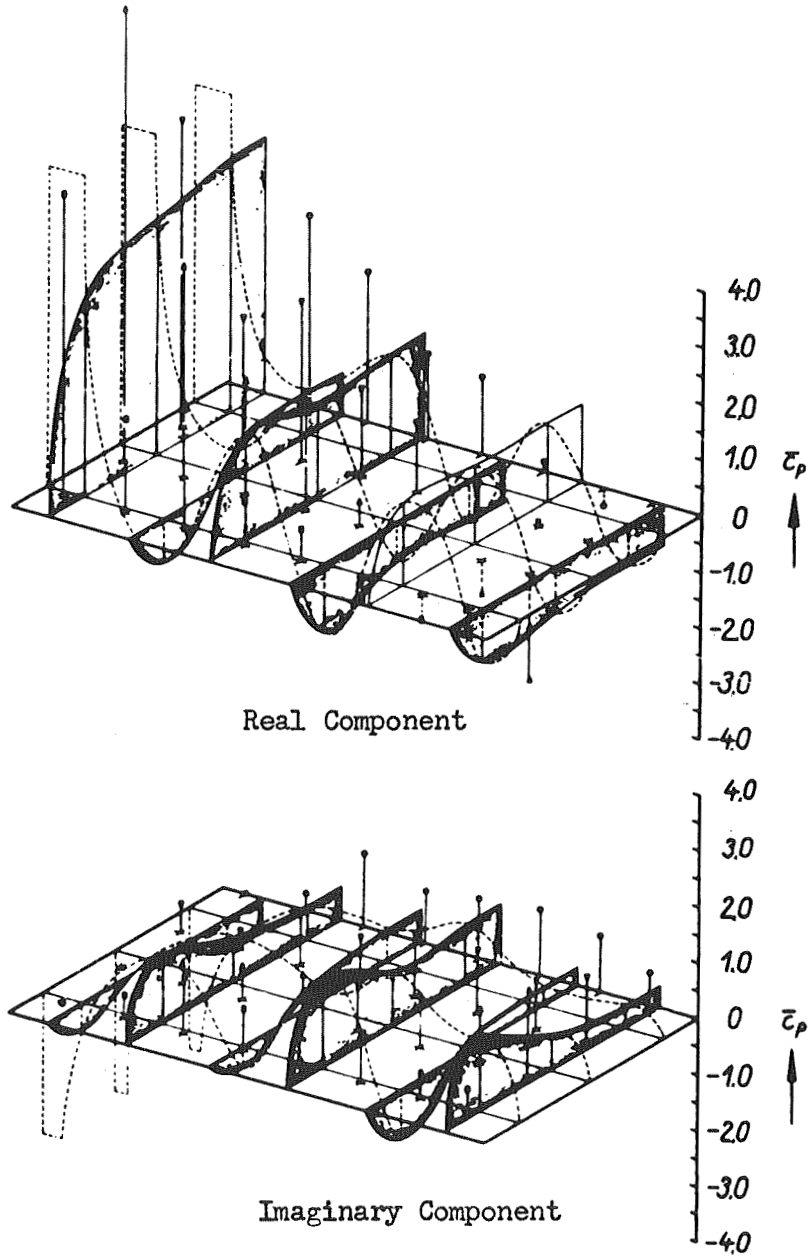

Fig. 8. Motion of Rotation Around Transverse Axis.
Distribution of real and imaginary components of the coefficients $\bar{c}_p$ of the pressure over the left half of the quadratic wing surface. Above: Real Component. Below: Imaginary Component. The experimental values of Laidlaw are entered as points ↕ above this. Reduced frequency of theoretical calculation $\omega^* = 0.238$. (Taken from Lit. Ref. 5 where the symbol ω^* is represented by k.)

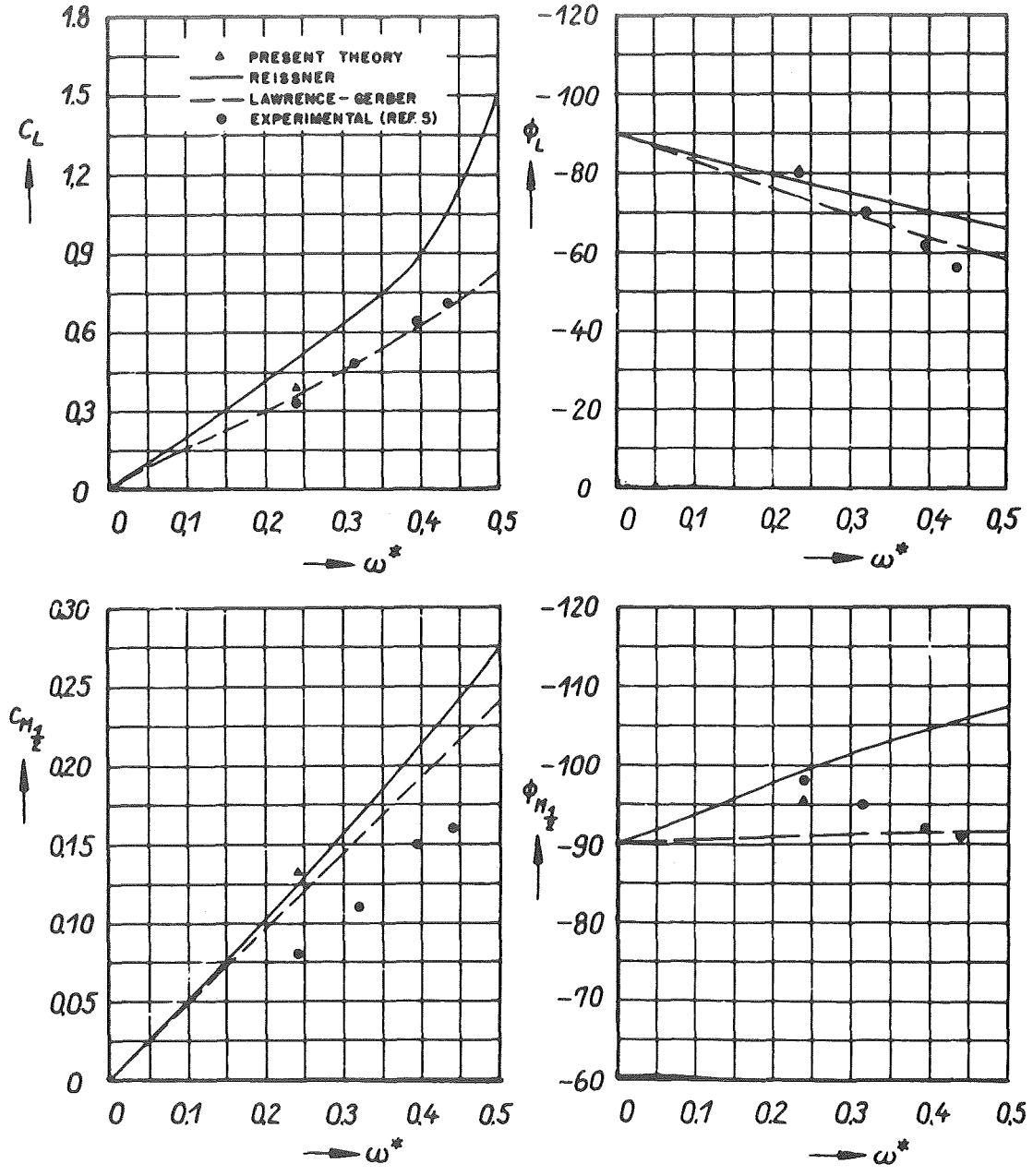

Fig. 9. Comparison of the Theoretical and Experimental Values of Lift and Moment in Motion of Vertical Translation for a Quadratic Wing Surface as a Function of Reduced Frequency ω^*. In theoretical calculation, $\omega^* = 0.238$. The Kelvin impulses (aerodynamic forces at flight-speed zero) have here been subtracted. - On the left, absolute amounts; on the right, arguments (phase angle in degree). (Taken from Lit. Ref. 5 where the symbol ω^* is represented by k.)

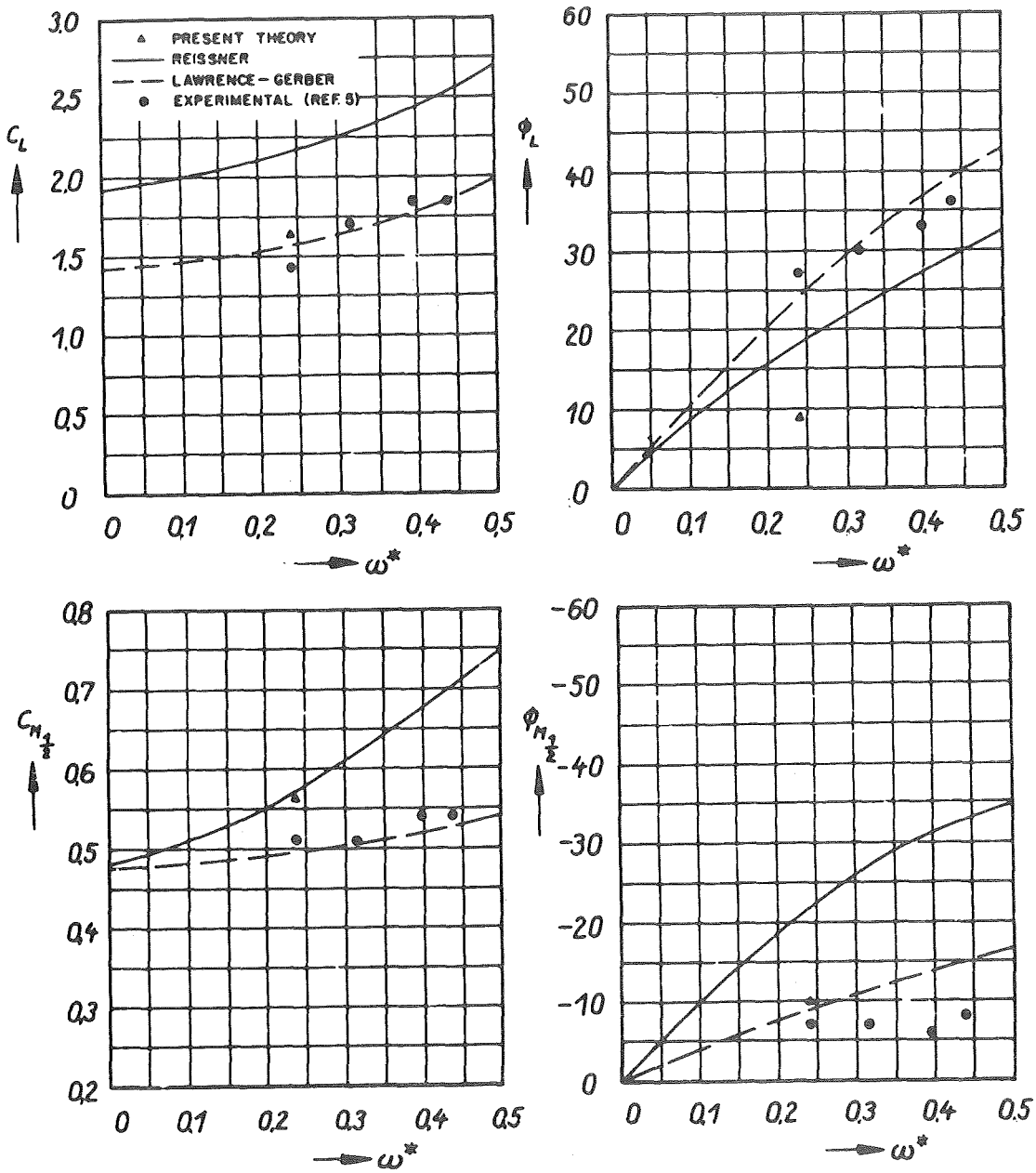

Fig. 10. Comparison of the Theoretical and Experimental Values of Lift and Moment in Motion of Rotation of a Quadratic Wing Surface Around its Transverse Axis as a Function of Reduced Frequency ω^*. In theoretical calculation, $\omega^* = 0.238$. The Kelvin impulses (aerodynamic forces at flight-speed zero) have here been subtracted. – On the left, absolute amounts; on the right, arguments (phase angle in degree). (Taken from Lit. Ref. 5 where the symbol ω^* is represented by k.)

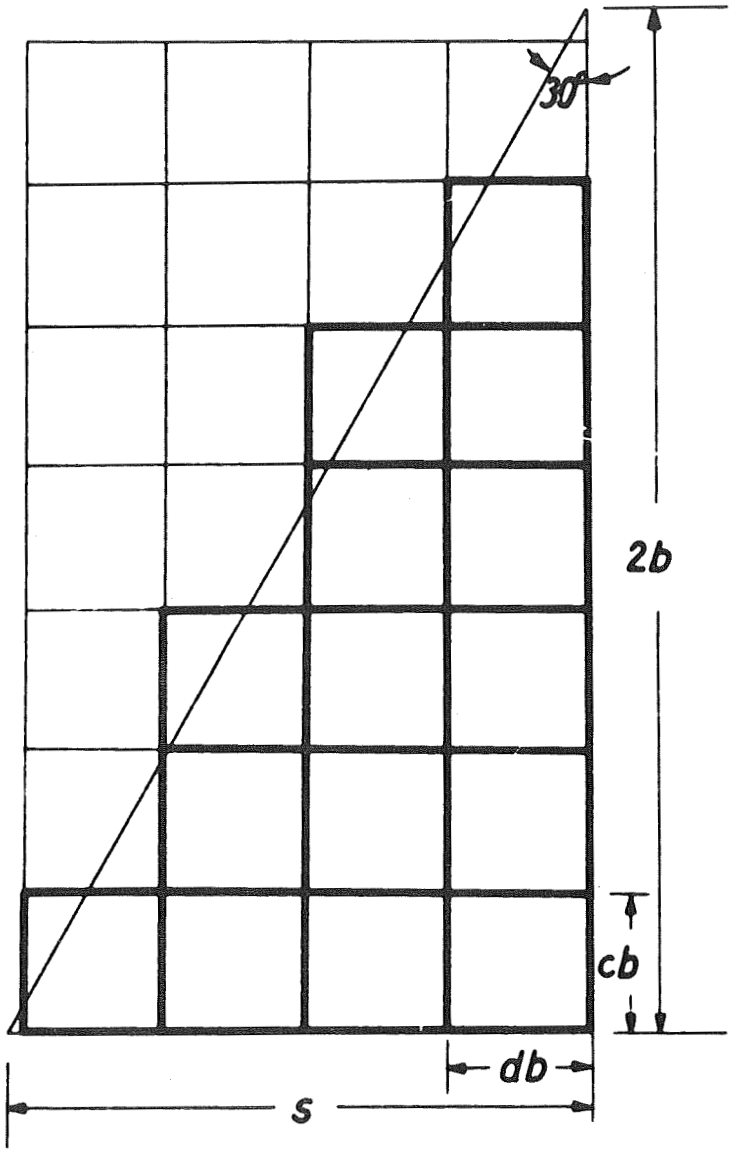

Fig. 11. Arrangement of Quadratic Slabs on a 60°-Delta wing.

DISCUSSION:

Ebner: You stated at the beginning that, in general, the method of the smallest potential energy is employed. Is this necessary? In my opinion, the principle of virtual displacement is more illustrative than the perhaps more general but somewhat more abstract energy principle. Do you always work with the principle of the smallest potential energy?

Küssner: Yes. This results in itself from the Lagrange equations of motion in which kinetic and potential energy occur. Previously, a system of beams was substituted for the aircraft (this is called "beamology" in the U.S.). We then obtain a system of total lineary differential equations which can be solved very simply and convincingly by multiple integration, i.e. by quadrature. If we abandon this primitive beamology and treat the aircraft as a given elastic body, we then arrive nearly forcibly at the tensor and matrix symbolism. The latter is shortest and automatically eliminates many sources of error.

Van de Vooren: I have one question: Professor Kussner has indicated an experimental method for measuring the generalized mass. Was this actually used in this manner? Did it concord well with the calculations?

De Vries: Shortly after the war, when we utilized the natural-vibration forms for calculation of flutter at the suggestion of Dr. Dorr, we ran into considerable difficulty by not knowing the generalized masses. We then investigated experimental procedures and employed two methods: the first is based in essence on measuring the energy introduced into the aircraft and determining from this the generalized mass by damping coefficients, also obtained by measurement (cf. G. de Vries "Experimental Determination of Generalized Masses," La Recherche Aeronautique No. 18, 1950). The second method was precisely that of the added masses (cf. idem, "Soundings of Vibrating Systems by Added Masses," ibid, No. 30, 1952). Experience has shown in hundreds of experiments that the second method is far more reliable, even if we assume the distribution of the added masses as not very exact. For example, it is sufficient to attach two or four individual masses at a wing or an empennage, on the assumption that these masses are small. This obviously results in the fact that the frequency displacements are extraordinarily small. The entire measuring installation must therefore be very exact. It must be possible to measure frequency with 10^{-4}. This presupposes that the frequency constant of excitation is at least 10^{-5}. We must also have available instruments capable of measuring the small frequency displacements, i.e. the small phase angles created, accurately. On this assumption, we obtain very reliable values. The theory also shows that the methods become very exact for any desired distribution of the added masses if we let the masses be very small.

Two publications (J. Leclerc "Modification of the Inherent Forms of a Structure by the Addition of Small Masses," Ibid, No. 50, 1956; H. Gauzy "The Displacement of the Inherent Frequencies of an

Overloaded System," Ibid, No. 59, 1957) treat the terms with which the added mass must comply in order for the errors in the determination of the generalized mass to be small. The detailed report of H. Gauzy shows that the error approaches zero, even for an individual mass located at will, if the mass becomes very small.

Van de Vooren: Does this not demand the requirement that the added masses may not cause any change of the vibration form?

De Vries: This is a secondary condition resulting automatically. If the masses are very small, then the changes of the vibration form are small of the second order (cf. H. Gauzy "The Displacement of the Inherent Frequencies of an Overloaded System," Ibid, above).

Van de Vooren: If the mass distribution is made so that it is proportional to the already existing mass distribution of the aircraft, then it is possible to select larger added masses.

De Vries: But then the existing mass distribution must be known or must have been approximated in some manner. However, between such a time-consuming procedure and a well developed measuring technique, a middle way should be sought because, if the measuring technique is developed too far, we find that the so-called lineary systems are all no longer lineary. In the last two years, I have found no static-vibration form which displayed actually a lineary characteristic.

Küssner: Is the cause of non-linearity only the inner damping?

De Vries: As you already stated, damping is created through the friction occurring between the rivets. This brings about not only energy consumption but also a change of rigidity of the wing with amplitude. Moreover, an aircraft is unfortunately not a simple beam but consists of a great number of structural parts which we do not see. There is the fuel tank, the control cables, more recently the jet engines which are suspended elastically in some manner and frequently by means of non-linear spring elements. The whole is a system which bears little resemblance to the ideal system assumed for the purposes of calculation.

Van de Vooren: I have a question in regard to the pressure distribution and coefficients of aerodynamic forces of the quadratic plate such as they are shown in Fig. 7 to 10. It is here demonstrated that the collocation method leads to very fluctuating pressure distributions. This is a rather peculiar result because theoretically a fluctuating pressure distribution is not to be anticipated for the non-compressible flow under consideration here. Although therefore pressure distribution is unreliable, Fig. 9 and 10 show that the coefficients of aerodynamic forces concord well with other results when the plate vibrates as a rigid whole. However, I believe that it is rather questionable if we will obtain such a concordance also during flutter. It will then probably be necessary to have a better pressure distribution.

Küssner: Yes, this is true! However, for the delta-wings, the first four natural-vibration forms as well as the corresponding pressure

distributions have been inserted in the calculation of flutter. This contains not only the coefficients for oscillatory and torsional vibration but also for deformation, at any event in the example for the delta-wing. Numerical values are unfortunately not yet stated in the report.

Merbt: Professor Kussner mentioned that calculation of flutter for delta-wings has produced good results with the aid of the aerodynamic forces calculated according to the box method. This may be due to the fact that the calculation of flutter for the respective wing was in general very little sensitive in regard to the choice of aerodynamic forces. In Sweden, we carried out flutter calculation for a delta-wing with a number of vibration forms of the whole wing by using aerodynamic forces calculated in the first case on the theory of low aspect ratio and in the second case by the strip theory (large aspect ratio). Both types of calculation produce almost the same flutter results. However, as soon as control-surface vibration forms and similar factors are included, differences may result.

De Vries: The quadratic procedure last indicated was applicable to subsonic speeds, was it not? A similar procedure is also employed for supersonics, except that we must then extend the integration range beyond the wing by considering all the quadrates but those lying on the wing itself in different manner than those outside on the wing contour.

Küssner: Formulas for this exist which can be found in the MIT reports mentioned in my article.

De Vries: Depending on the Mach number, the ranges are quite different. As soon as we find ourselves either in the outer or in the inner part of the cone, correspondingly different coefficients must be inserted.

Küssner: For this reason, I prefer the method with the constant basic formulation and interpolation. The method of integration by small slabs is complicated and requires extensive calculations. We have not yet carried out such calculations. However, if we should do so, we would then start by using the method with the interpolated functions, then go with these into the integrals of equation 50 and integrate them through the Mach conus, according to some appropriate numerical method.

Ebner: I have one question: the subdivision into quadrates all exactly alike is very bad at the edge. Would it not be possible to further subdivide in such manner that we carry out a less detailed division in the interior and a more detailed division at the edge?

Küssner: Yes, this can be done. We then have instead of fifteen equations with fifteen unknown factors, for instance, thirty equations with thirty unknown factors. The subdivision into quadrates shown earlier really appeared to be rather improper. It becomes better already when we select, instead of the quadratic fields, rectangular fields which are similar to the rectangle described by one-half of the wing.

Van de Vooren: I would like to make one statement. In the case of a delta-wing with a supersonic leading edge, pressure distribution can be calculated by simple integration over the wing. This result could then be compared with the result of the collocation method which employs quadrates.

Küssner: In actual supersonic flow, the nucleus K is known. The calculations mentioned were all carried out for subsonics in which the nucleus K is unknown.

Van de Vooren: In this way, we might judge the reliability of the collocation method in one case, i.e. that of the delta-wing with supersonic leading edge. A similar comparison would be possible in principle also for the delta-wing with subsonic leading edge because it is not only possible to solve the problems of the elliptical and the circular surface of sustentation with the aid of generalized coordinates but also the problem of the delta-wing with subsonic leading edge in supersonic flow. As far as I know, no attempt has been made as yet to arrive at numerical results for this problem by an analytical procedure.

Merbt: Instead of utilizing an arbitrary network of quadratic and/or rectangular boxes for $M > 1$, it would seem more appropriate to employ a network of congruent rectangles whose diagonals lie parallel to the Mach lines (cf. The Report of Ta Li, J. Aer. Sci., Vol. 23, No. 7, pp. 613/622, 1956).

FLUTTER CALCULATION WITH MANY DEGREES OF FREEDOM FOR MODERN AIRCRAFT*

by A. I. van de Vooren

SUMMARY

The report describes the manner in which calculation of flutter should be carried out for a large transport aircraft involving many degrees of freedom. The advantage is shown of letting the elimination of fuselage motion take place in such a manner that an equation system for the deformations is obtained instead of for the entire amplitudes. The static-vibration forms are utilized as normal coordinates for the flutter vibrations. The iteration method for the determination of natural values and natural vectors of an algebraic matrix can be appreciably shortened in the case of adjoining natural values, by solving a quadratic equation. The report terminates with some remarks on the comparison of calculation and measurement of static vibration. All computations can be made easily with the aid of an electronic computer.

ARRANGEMENT:

		Page
1.	Introduction.	52
2.	The Calculation of Static-Vibration Forms	53
	2.1 The Equation System.	53
	2.2 The Iteration Method	57
3.	The Calculation of Flutter Vibrations	60
	3.1 Introduction of Normal Coordinates	60
	3.2 The Iteration Method for Different Natural Values.	62
	3.3 Calculation of Interference.	66
4.	Comparison Between Calculated and Measured Static Vibrations. .	67
5.	Literature References	69
6.	Appendix: The Elimination of Fuselage Motion	70
	Discussion.	73

* The lecture was published as Report MP 146 of the Dutch National Aviation Laboratory in March 1957.

1. INTRODUCTION

At the present time, flutter calculations in the design of a new aircraft require an even greater expenditure of effort than has already been the case previously. This is a consequence both of the larger dimensions of the aircraft as well as of the higher flying speeds. The larger dimensions are the reason that the natural frequencies of the elastic system constituted by the aircraft assume lower values than in the past so that a greater number of the natural frequencies and vibration forms must be included in flutter calculation. In addition to the larger dimensions, fuel tanks at the wing ends also are a cause of lower natural frequencies. The higher speed of the aircraft is responsible, on the one hand, for the fact that the compressibility of air can no longer be neglected and, on the other hand, that eventual flutter vibrations can take place with greater frequency.

Because the engines and fuel tanks no longer permit us to consider the weight of the wing as small in comparison to the weight of the fuselage, we must also take into account fuselage motion. We know that the degrees of freedom of the fuselage may play an essential role in the flutter characteristics of swept-back and delta wings. For the straight wing, the question is frequently whether the mass and inertial moments of the fuselage should be included entirely or only partially in the calculation. Theoretically, it would obviously be best if the entire aircraft could be regarded as a unit but this method would lead to very large equation systems. If it is therefore at all possible, flutter calculation for the wing will be treated separately. It is necessary to very carefully consider the schematization of the fuselage in the calculation of wing flutter because the fuselage will no longer resonate as a rigid body when the natural frequencies of wing and fuselage closely adjoin. It may then be necessary to include also the respective degree of freedom of the fuselage in the system. Through the fuselage motion, the resonating horizontal or vertical empennage may introduce an additional aerodynamic attenuation.

It will almost always be necessary to consider fuselage motion and deformation in calculation of flutter for the empennage. The movements of the empennage are greatly influenced by fuselage torsion and the various fuselage resonances such as vertical or horizontal fuselage deflection and/or torsion. In general, the tendency will be to substitute an equivalent mass for the wing although we should keep in sight here also any possible adjoining frequencies.

The above considerations will have made it clear that it is often inescapable to base calculation of flutter on a relatively complicated mechanical system in which a great number of degrees of freedom will have been introduced. It is an almost impossible task to carry out these calculations if no modern computers are available. However, consideration of the results of completed calculations means an appreciably increased safety of flight in regard to flutter.

The following is a description of the manner of executing these calculations. The methods have in major part been indicated by the author in his dissertation (1) and have since been utilized in practice by the Flutter Group of the "N. V. Koninklijke Nederlandse Vliegtuigenfabriek Fokker" under the direction of Dr. J. H. Greidanus and Chief Engineer G. G. Piepers.

By way of introduction, we might briefly mention some points in regard to the investigation of flutter during the first stages of aircraft design. We can confine ourselves here to approximate calculations or to the criteria widely employed especially in Great Britain. The result of these criteria will give a guide for the required rigidity of sustentation surfaces and fuselage. These criteria will be found in the specifications of airworthiness of ICAO (2). The result of the criteria may give a rigidity either too high or too low. In orthodox construction, too high a rigidity may be derived because the criterion obviously cannot take into consideration all parameters and therefore necessarily produces an excessively safe value. Too low a rigidity may be obtained if the criterion is applied to a case for which it was not really intended or if a different vibration form occurs for some reason. With the exception of the simplest cases, the final design will therefore always be checked through complete calculations of flutter.

2. CALCULATION OF STATIC-VIBRATION FORMS

2.1 The Equation System

If the design has been settled in major part, calculation of static-vibration forms will be begun. In explanation of this procedure, we intend to discuss here as example a case of symmetrical wing vibrations.

It is assumed that the cross-sections of the wing remain undistorted spanwise. This assumption is not valid for cross-sections with wing engines where the engine nacelle very easily may have an additional distortion in relation to the wing chord. Moreover, the aileron may have a deflection. The deformations of the wing are then determined by a deflection function $z(y)$ measured in the elastic axis, a distortion function $\varphi(y)$, the distortion angle $\theta(y_i)$ of the engines assumed to be concentrated in the cross-sections $y_i (k = 1,2)$ and the angle of the aileron γ. All these magnitudes are measured in relation to the neutral position of the wing and indicate the entire vibration amplitudes. Here, as in many practical cases, it is assumed that the torsional rigidity of the aileron is infinitely large. This means that, with the definition employed, γ becomes independent of the y-coordinate. The bending rigidity of the aileron is neglected in relation to the bending rigidity of the wing.

The deformations referred to above can be determined with the aid of the elastic influence coefficients. In general, it will be possible to write for symmetrical vibrations:

$$
\left.
\begin{aligned}
z(y) - z(o) &= \int_o^b K_{11}(y,\eta)\, F(\eta)\, d\eta \quad , \\
\varphi(y) - \varphi(o) &= \int_o^b K_{22}(y,\eta)\, M(\eta)\, d\eta + K_{22}(y, b_r) \int_{b_1}^{b_2} N(\eta)\, d\eta + \\
&\quad + \sum_{i=1,2} \int_o^b K_{22}(y,\eta)\, P(\eta)\, \delta(\eta - \eta_i)\, d\eta \quad , \\
\gamma - \varphi(b_r) &= K_{33} \int_{b_1}^{b_2} N(\eta)\, d\eta \quad , \\
\theta(y_i) - \varphi(y_i) &= \int_o^b K_{44}(y_i,\eta)\, P(\eta)\, \delta(\eta - \eta_i)\, d\eta \, , \qquad i = 1, 2 \quad .
\end{aligned}
\right\} \qquad (2.1)
$$

in which:

$F(\eta)$ = the entire inertia of wing + aileron + engine in the cross-section η per unit of width;

$M(\eta)$ = moment of inertia of the wing + moment of inertia of the rudder assumed as concentrated in the rudder-pivot axis + moment of inertia of the engine assumed as concentrated in the engine linkage (?) and these moments are referred to the elastic axis in the cross-section η per unit of width;

$N(\eta)$ = moment of inertia of the rudder around the rudder-pivot axis in the cross-section η per unit of width;

$P(y_i)$ = moment of inertia of the engine around the motor hinge in one of the two cross-sections y_i assumed as concentrated spanwise;

$y = b_r$ = the cross-section in which the aileron is actuated;

$K_{11}(y, \eta)$ = the influence function of wing deflection;

$K_{22}(y, \eta)$ = influence function of wing torsion;

K_{33} = influence function of aileron deflection;

$K_{44}(y_i, \eta_i)$ = the influence function of engine torque.

The wing stretches from $y = 0$ to $y = b$; the aileron from $y = b_1$ to $y = b_2$.

$z(o)$ and $\varphi(o)$ determine the fuselage movements.

The δ-function is the Dirac function, i.e.

$$\delta(\eta-\eta_i) = 0 \quad \text{for} \quad \eta \neq \eta_i \quad , \qquad \int_{\eta_i^-}^{\eta_i^+} \delta(\eta-\eta_i)\, d\eta = 1 \quad .$$

We might mention that the assumption of an elastic axis is not essential; if no elastic axis exists, we need merely introduce another influence function $K_{12}(y, \eta)$.

The forces and moments of inertia are completely determined by the mass distribution and by the vibration amplitudes $z(y)$, $\varphi(y)$, γ and $\theta(y_i)$. There is applicable:

$$\begin{aligned}
F(y) &= \left\{ m_{11} z + m_{12}\varphi + m_{13}\gamma + m_{14}\,\theta\,\delta(y-y_i) \right\} \nu^2 \quad , \\
M(y) &= \left\{ m_{12} z + m_{22}\varphi + m_{23}\gamma + m_{24}\,\theta\,\delta(y-y_i) \right\} \nu^2 \quad , \\
N(y) &= \left\{ m_{13} z + m_{23}\varphi + m_{33}\gamma \right\} \nu^2 \quad , \\
P(y)\,\delta(y-y_i) &= \left[\left\{ m_{14} z + m_{24}\varphi + m_{44}\,\theta \right\} \delta(y-y_i) \right] \nu^2 \quad .
\end{aligned} \tag{2.2}$$

The magnitudes m_{11} to m_{44} can be calculated when the mass distribution is known. It should be noted that m_{11}, m_{12} and m_{22} contain a member with a δ-function.

When the expressions 2.2 are substituted in the equations 2.1 and if, in addition, the magnitudes $\varphi(b_r)$ and $\varphi(y_i)$ are eliminated in the third and fourth equation 2.1 with the aid of the second equation 2.1, we then obtain a system which can be written as a matrix equation

$$\underline{f}_d(y) = \int_o^b \underline{K}\,(y,\eta)\,\underline{\underline{m}}(\eta)\,\underline{f}(\eta)\, d\eta \quad , \tag{2.3}$$

in which

$$\underline{f}_d(y) = \begin{Vmatrix} z(y) - z(o) \\ \varphi(y) - \varphi(o) \\ \gamma - \varphi(o) \\ \theta(y_i) - \varphi(o) \end{Vmatrix}, \qquad \underline{f}(y) = \begin{Vmatrix} z(y) \\ \varphi(y) \\ \gamma \\ \theta(y_i) \end{Vmatrix},$$

(2.4)

$$\underline{K}(y,\eta) = \begin{Vmatrix} K_{11}(y,\eta) & 0 & 0 & 0 \\ 0 & K_{22}(y,\eta) & K_{22}(y,b_r) & K_{22}(y,\eta_i) \\ 0 & K_{22}(b_r,\eta) & K_{22}(b_r,b_r) + K_{33} & K_{22}(b_r,\eta_i) \\ 0 & K_{22}(y_i,\eta) & K_{22}(y_i,b_r) & K_{22}(y_i,\eta_i) + K_{44}(y_i,\eta_i) \end{Vmatrix},$$

$$\underline{m}(\eta) = \begin{Vmatrix} m_{11}(\eta) & m_{12}(\eta) & m_{13}(\eta) & m_{14}(\eta)\ \delta(\eta-\eta_i) \\ m_{12}(\eta) & m_{22}(\eta) & m_{23}(\eta) & m_{24}(\eta)\ \delta(\eta-\eta_i) \\ m_{13}(\eta) & m_{23}(\eta) & m_{33}(\eta) & 0 \\ m_{14}(\eta)\ \delta(\eta-\eta_i) & m_{24}(\eta)\ \delta(\eta-\eta_i) & 0 & m_{44}(\eta)\ \delta(\eta-\eta_i) \end{Vmatrix}.$$

The equation 2.3 has special symmetry properties, i.e. $\underline{K}(y,\eta)$ and $\underline{m}(\eta)$ are symmetrical matrices which means in regard to $\underline{K}(y,\eta)$ that

$$\underline{K}(y,\eta) = \underline{K}'(\eta,y)$$

where the underline points to the transposition of the matrix.

The integrals in the right member of the equation can be approximated with the trapezoidal rule or with the Simpson rule. For this, a subdivision into about 8 to 12 intervals spanwise is assumed. The integrations are then replaced by sums. The integrations are thereby transformed into a system of lineary algebraic equations for the magnitudes γ and $\theta(y_i)$ as well as for the values of the functions $z(y)$ and $\varphi(y)$ at the interval boundaries. However, the number of the unknowns is higher by two than the number of the equation. This is a consequence of the fuselage movements. Two additional equations, so-called first integrals, can be indicated which state that the entire inertia as well as the entire moment of all forces of inertia around the elastic axis shall disappear if no external forces act on the system. These equations are therefore

$$\int_o^b F(\eta)\, d\eta = 0, \qquad \int_o^b \left\{ M(\eta) + N(\eta) + P(\eta)\,\delta(\eta-\eta_i) \right\} d\eta = 0, \qquad (2.5)$$

in which also half the contributions of the fuselage must be included. It is possible, with the aid of these equations, to eliminate the fuselage motion $z(o)$ and $\varphi(o)$.

This elimination can be carried out in two different ways. We can either recalculate the deformations of the left member of 2.3 into absolute vibration amplitudes and also utilize $z(y)$, $\varphi(y)$, γ and $\theta(y_i)$ as unknowns or we can reduce the vibration amplitudes of the right member of 2.3 to deformations and introduce $z(y) - z(o)$, $\varphi(y) - \varphi(o)$, $\gamma - \varphi(o)$ and $\theta(y_i) - \varphi(o)$ as unknowns. The first method has been described in (1). This changes the matrix $\underline{K}$ of the influence functions and produces the disadvantage that this matrix does not remain symmetrical. As will become clear further on, this is an appreciable disadvantage.

The other method is described in the appendix for the case of a deflecting and distorting wing. Because the deformations are utilized here as new variables, the mass forces, i.e. the matrix $\underline{m}$, change. However, this matrix remains symmetrical. The matrix $\underline{K}$ does not change with this method.

The system of algebraic equations obtained by the second method has the form

$$\underline{f}_d = \nu^2 \, \underline{D} \, \underline{f}_d \quad \text{with} \quad \underline{D} = \underline{K} \cdot \underline{m}^* \,, \tag{2.6}$$

where $\underline{K}$ and $\underline{m}^*$ are symmetrical matrices and $\underline{m}^*$ represents the mass matrix after elimination of the fuselage movements. The calculation of the static-vibration forms is thus transformed into the calculation of the natural values and natural vectors of an algebraic matrix.

2.2 The Iteration Method

The problem of the calculation of natural values and natural vectors of an algebraic matrix can be solved by iteration and is then very suitable for computations with the aid of an electronic computer. Without this modern tool, it would be practically an almost impossible task to determine a few natural values and natural vectors of a matrix of the 20th or 24th degree, for example.

For the determination of the lowest natural value ν_1^2 with the respective natural vector $\underline{f}_1$, we estimate $\underline{f}_1$ as well as possible and normalizes the estimate by making the largest element of the vector equal to one, for example. The standardized vector is then multiplied from the left with the matrix $\underline{D}$. The vector resulting from this after normalization will be a better approximation of $\underline{f}_1$ than the initial estimate. This process can be repeated until the vector no longer changes and this gives us $\underline{f}_1$. The natural value ν_1^2 follows from the

factor which we need for the normalization. The convergence of the method is based on the fact that the starting vector

$$\underline{f}^{(o)} = a_1 \underline{f}_1 + a_2 \underline{f}_2 + a_3 \underline{f}_3 + \ldots \qquad (2.7)$$

after one step of iteration furnishes the vector

$$\underline{f}^{(1)} = \frac{a_1}{\nu_1^2} \underline{f}_1 + \frac{a_2}{\nu_2^2} \underline{f}_2 + \frac{a_3}{\nu_3^2} \underline{f}_3 + \ldots .$$

In this, the natural values ν_1^2 and the natural vectors $\underline{f}_i$ are numerated in the sequence of increasing natural values. We consequently see that, with each step of iteration, the share of the first natural vector is augmented relative to other natural vectors.

In order to determine the higher natural values and natural vectors, a new matrix $\underline{D}^{(2)}$ must be derived through transformation of the matrix $\underline{D}$ so that it will produce convergence after ν_2^2 and $\underline{f}_2$ with the same iteration method. Although several transformations are possible (1), the method of "deflation" (3) has proved to be the most appropriate. In order to utilize it, it is necessary to know not only the vector $\underline{f}_1$ but also the respective vector $\underline{g}_1$ of the transposed matrix $\underline{D}'$. The matrix $\underline{D}'$ is created from $\underline{D}$ through reflection (inversion?) at the main diagonal. It is therefore possible to determine, with the help of the iteration method mentioned above, the natural vector $\underline{g}_1$ of the matrix $\underline{D}'$. Since the characteristic equations of the matrices $\underline{D}$ and $\underline{D}'$ are identical, all natural values are also equal to each other.

Between the natural vectors $\underline{f}_i$ of the matrix $\underline{D}$ and the natural vectors $\underline{g}_j$ of the matrix $\underline{D}^{\dagger}$, there exists a bi-orthogonality, i.e. by definition, we have

$$\underline{f}_i = \nu_i^2 \underline{D} \underline{f}_i \quad \text{and} \quad \underline{g}_j = \nu_j^2 \underline{D}' \underline{g}_j \; . \qquad (2.8)$$

from which follows that

$$\nu_i^2 = \frac{\underline{g}_j' \underline{f}_i}{\underline{g}_j' \underline{D} \underline{f}_i} \; , \text{ but also } \quad \nu_j^2 = \frac{\underline{f}_i' \underline{g}_j}{\underline{f}_i' \underline{D}' \underline{g}_j} \; , \qquad (2.9)$$

where the underline indicates a line vector.

It follows from the identity of the two numerators and also of both denominators that ν_i^2 and ν_1^2 should be equal to each other if

not all numerators and denominators are equal to zero. For different natural values, the latter is applicable and we then have

$$\underline{g}_j' \underline{f}_i = \underline{g}_j' \underline{D} \underline{f}_i = 0 \text{ , when } i \neq j \text{ .} \qquad (2.10)$$

This is called a bi-orthogonality relation, because it describes the orthogonality of vectors of the $\underline{f}$-family with vectors from the g-family.

The formulas 2.9 cannot be used for calculation of the natural values if we take $i \neq j$. However, for $i = j$, we obtain the very useful formula

$$\nu_i^2 = \frac{\underline{g}_i' \underline{f}_i}{\underline{g}_i' \underline{D} \underline{f}_i} \text{ .} \qquad (2.11)$$

For $i = 1$, 2.11 furnishes a more accurate value for ν_1^2 than the normalization of the iteration method produces. By reason of the bi-orthogonality relation, the error in the natural value becomes small of the second order when the errors in the natural vectors are small of the first order. This means that the number of the exact figures in ν_1^2 is equal to the sum of the numbers of the exact figures in $\underline{f}_1$ and $\underline{g}_1$. In order to obtain a certain accuracy in ν_1^2, the iteration after $\underline{f}_1$ needs to be continued only half as far if $\underline{g}_1$ is also determined then when we confine ourselves to the determination of $\underline{f}_1$.

Here it is an advantage when the matrix $\underline{D}$ is available as product of two symmetrical matrices $\underline{K}$ and $\underline{m}^*$. It is then no longer necessary, for the determination of the natural vectors $\underline{g}_i$, to carry out new iterations and there is instead a simple relation between the natural vectors $\underline{f}_i$ and $\underline{g}_i$. If $\underline{K}$ and $\underline{m}^*$ are symmetrical matrices, there follows directly from $\underline{D} = \underline{K} \times \underline{m}^*$ that $\underline{D}' = \underline{m}^* \times \underline{K}$.

There consequently exist the following relations

$$\underline{g}_i = \nu_i^2 \underline{m}^* \underline{f}_i \quad \text{and} \quad \underline{f}_i = \underline{K} \underline{g}_i \text{ ,} \qquad (2.12)$$

of which we can convince ourselves by insertion in equation 2.8 for $\underline{g}_i$. With the help of this relation, we can also write, instead of equation 2.11,

$$\nu_i^2 = \frac{\underline{g}_i' \underline{K} \underline{g}_i}{\underline{f}_i' \underline{m}^* \underline{f}_i} \text{ .} \qquad (2.13)$$

After determination of $\underline{f}_1$ and $\underline{g}_1$, the transformation of the matrix $\underline{D}$ can be performed into a matrix $\underline{D}^{(2)}$ which produces, after iteration, the natural value ν_2^2 with the natural vectors $\underline{f}_2$ and $\underline{g}_2$.

$$\underline{D}^{(2)} = \underline{D} - \frac{1}{\nu_1^2} \frac{\underline{f}_1 \underline{g}_1'}{\underline{g}_1' \underline{f}_1} \quad . \tag{2.14}$$

The numerator of the fraction contains a quadratic matrix whereas the denominator contains a single number. If we again carry out the formula 2.7 for the starting vector, we then obtain, after the first step of iteration,

$$\underline{D}^{(2)} \underline{f}^{(o)} = \underline{D} \sum_{i=1}^{n} a_i \underline{f}_i - \frac{1}{\nu_1^2} \frac{\underline{f}_1 \underline{g}_1'}{\underline{g}_1' \underline{f}_1} \sum_{i=1}^{n} a_i \underline{f}_i = \sum_{i=1}^{n} \frac{a_i}{\nu_i^2} \underline{f}_i - \frac{a_1}{\nu_1^2} \underline{f}_1 = \sum_{i=2}^{n} \frac{a_i}{\nu_i^2} \underline{f}_i \quad .$$

We therefore see that, by reason of the bi-orthogonality relation, the second term in the expression for $\underline{D}^{(2)}$ directly eliminates the part of $\underline{f}_1$ in the starting vector. The part of $\underline{f}_2$ is moreover relatively reduced and we therefore obtain, with the normal iteration method, convergence to the natural vector $\underline{f}_2$.

In the same way, $\underline{D}^{(2)}$ can be further reduced to a matrix $\underline{D}^{(3)}$ which will show convergence to $\underline{f}_3$. It is therefore possible to calculate with this method an arbitrary number of natural values and natural vectors although we must expect that accuracy decreases for the higher natural values and natural vectors because of errors due to rounding-off.

3. THE CALCULATION OF FLUTTER VIBRATIONS

3.1 Introduction of Normal Coordinates

The difference between the fundamental equations for flutter vibrations and those for static vibrations is that the members for aerodynamic forces must be added to the first case. The integral equations 2.1 are therefore also valid for the flutter vibrations on the supposition that the magnitudes $F(\eta)$, $M(\eta)$, $N(\eta)$ and $P(\eta)$ now represent the entire stresses by forces of inertia and aerodynamic forces. From the equations 2.1 we can again derive, by elimination of fuselage motion, an equation of the type 2.6 for the deformations. Then

$$\underline{D} = \underline{K} \, (\underline{m}^* + \underline{a}^*) \quad .$$

in which $\underline{a}^*$ is the matrix of the aerodynamic coefficients after elimination of fuselage motion.

The elements of $\underline{a}^*$ are in general complex. The matrix $\underline{a}^*$ is neither a symmetrical nor a "Hermit" matrix (we speak of a Hermit matrix when the reflected /inverted?/ matrix is identical with the complex conjugated matrix). This means that the natural vectors of $\underline{D}$ and $\underline{D}'$ cannot be derived from each other but must be determined through separate iterations.

It is possible to write the complex matrix $\underline{D}$ of nth degree as a real matrix of $2n^{th}$ degree. We must then merely replace each complex element $D'_{jk} + iD''_{jk}$ by the submatrix

$$\begin{Vmatrix} D'_{jk} & -D''_{jk} \\ D''_{jk} & D'_{jk} \end{Vmatrix}$$

The natural vectors of this real matrix have $2n$ elements but these elements should be considered as n complex elements in the sense that all successive elements must be regarded as the real and imaginary component of a complex number. This must be taken into account especially in normalization.

Because the degree of the matrix $\underline{D}$ written as real matrix, is twice as high in the case of flutter as in the case of static vibration and we need to determine, moreover, the natural value and natural vectors for a series of matrices $\underline{D}$ depending on the value of the reduced frequency, this would be a very voluminous task even for an electronic computer. The number of degrees of freedom is therefore reduced here by the introduction of normal coordinates. These normal coordinates are indicated through the elements of the vector $\underline{q}$. This is then

$$\underline{f}_d = \underline{F}\,\underline{q}\ , \tag{3.1}$$

in which $\underline{F}$ is a rectangular matrix where the p-columns are equal to the natural vectors $\underline{f}_1, \underline{f}_2, \ldots, \underline{f}_p$ which belong to the lowest p natural values of matrix $\underline{D}$ in the case of static vibration.

If we further multiply equation 2.6 from the left with matrix $\underline{G}$ where the p lines of $\underline{G}'$ are equal to the natural vectors $\underline{g}'_1, \underline{g}'_2, \ldots, \underline{g}'_p$ of matrix $\underline{D}'$ in the case of static vibration, we then obtain, after substitution of 3.1,

$$\underline{G}'\underline{F}\,\underline{q} = \nu^2\, \underline{G}'\underline{D}\underline{F}\,\underline{q}\ . \tag{3.2}$$

On the basis of the bi-orthogonality relation 2.10, both the matrix $\underline{G}'\,\underline{F}$ and the matrix $\underline{C} = \underline{G}'\,\underline{D}\,\underline{F}$ becomes a diagonal matrix.

If we introduce a normalization of the natural-vector pairs $\underline{f}_i$, $\underline{g}_i$ by demanding

$$\underline{g}_i' \, \underline{f}_i = 1 \quad ,$$

then the diagonal matrix of the left side becomes identical with the unit matrix $\underline{I}$. The diagonal elements of matrix $\underline{C}$ then become equal to $1/\nu_i^2$. The natural vectors $\underline{q}$ are vectors in which all elements except one disappear. These elements can therefore be regarded as normal coordinates.

In the case of flutter, the matrix $\underline{C}$ becomes a quadratic matrix of p^{th} degree with complex elements in which generally none of the elements disappear. In principle, p is appreciably smaller than n, e.g., p will be about 6 to 8 as against n with 20 to 24.

The introduction of the normal coordinates means that we develop the unknown flutter-vibration forms by the system of the orthogonal static-vibration forms and restrict this development to the first p static-vibration forms. We know (4) that we can very well approximate the flutter-vibration forms with the aid of normal coordinates for static vibration. In general, fewer degrees of freedom are needed then when we select arbitrary deformations. We should always include in the calculation all static-vibration forms with frequencies below the flutter frequency to be anticipated and preferably also those which have an only slightly higher frequency.

The multiplication of the matrix $\underline{C} = \underline{G}' \, \underline{D} \, \underline{F}$ is again very suitable for calculation by means of an electronic computer.

3.2 Iteration Method for Two Only Slightly Different Natural Values

Iteration of a flutter matrix may become complicated by the fact that two natural values may have approximately the same modulus, although the real and imaginary components and consequently frequency and attenuation of the respective flutter-vibration forms show considerable differences. The convergence of the iteration method will then be much slower as follows directly from the starting vector given in equation 2.7 and the respective iterated vector. If ν_1^2 and ν_2^2 have about the same moduli but the modulus of ν_3^2 is appreciably greater, then the share of the vibration form $\underline{q}_3$ as well as the shares of the higher vibration forms $\underline{q}_4$, etc. will have disappeared, after a given number of steps of iteration. The vector then consists only of a lineary combination of $\underline{q}_1$ and $\underline{q}_2$. When this stage has been reached, it is possible to determine the natural vectors $\underline{q}_1$ and $\underline{q}_2$, by solving a quadratic equation, through three successive steps of iteration. Without normalization, we have

$$\underline{q}^{(k-2)} = b_1 \underline{q}_1 + b_2 \underline{q}_2 \quad ,$$

$$\underline{q}^{(k-1)} = \frac{b_1}{\nu_1^2} \underline{q}_1 + \frac{b_2}{\nu_2^2} \underline{q}_2 \quad , \qquad (3.3)$$

$$\underline{q}^{(k)} = \frac{b_1}{\nu_1^4} \underline{q}_1 + \frac{b_2}{\nu_2^4} \underline{q}_2 \quad .$$

It follows from the two first equations

$$b_1 \underline{q}_1 = \frac{\underline{q}^{(k-2)} - \nu_2^2 \underline{q}^{(k-1)}}{1 - \frac{\nu_2^2}{\nu_1^2}} \quad , \quad b_2 \underline{q}_2 = \frac{\underline{q}^{(k-2)} - \nu_1^2 \underline{q}^{(k-1)}}{1 - \frac{\nu_1^2}{\nu_2^2}} \quad . \qquad (3.4)$$

If ν_1^2 and ν_2^2 were known, then the last equation 3.3 would be superfluous. Since this is not the case, ν_1^2 and ν_2^2 can also be determined with the aid of the third equation. In the same manner, there follows from the second and third equations

$$b_1 \underline{q}_1 = \frac{\underline{q}^{(k-1)} - \nu_2^2 \underline{q}^{(k)}}{\frac{1}{\nu_1^2}(1 - \frac{\nu_2^2}{\nu_1^2})} \quad , \quad b_2 \underline{q}_2 = \frac{\underline{q}^{(k-1)} - \nu_1^2 \underline{q}^{(k)}}{\frac{1}{\nu_2^2}(1 - \frac{\nu_1^2}{\nu_2^2})} \quad .$$

If we now equate the two expressions for $b_1 \underline{q}_1$ or those for $b_2 \underline{q}_2$, we then obtain in every case the same equation, i.e.

$$\underline{q}^{(k-2)} - (\nu_1^2 + \nu_2^2) \underline{q}^{(k-1)} + \nu_1^2 \nu_2^2 \underline{q}^{(k)} = 0 \quad . \qquad (3.5)$$

This is a vector equation which is valid for every element of the vectors. If q_ℓ and q_m represent different elements, we therefore have,

$$q_\ell^{(k-2)} - (\nu_1^2 + \nu_2^2)\, q_\ell^{(k-1)} + \nu_1^2\, \nu_2^2\, q_\ell^{(k)} = 0 \quad ,$$

$$q_m^{(k-2)} - (\nu_1^2 + \nu_2^2)\, q_m^{(k-1)} + \nu_1^2\, \nu_2^2\, q_m^{(k)} = 0 \quad .$$

It follows from this that

$$\nu_1^2 + \nu_2^2 = \frac{q_\ell^{(k-2)}\, q_m^{(k)} - q_m^{(k-2)}\, q_\ell^{(k)}}{q_\ell^{(k-1)}\, q_m^{(k)} - q_m^{(k-1)}\, q_\ell^{(k)}} \quad \text{and} \quad \nu_1^2\, \nu_2^2 = \frac{q_\ell^{(k-2)}\, q_m^{(k-1)} - q_m^{(k-2)} q_\ell^{(k-1)}}{q_\ell^{(k-1)}\, q_m^{(k)} - q_m^{(k-1)}\, q_\ell^{(k)}} \, .$$

This means that ν_1^2 and ν_2^2 are the roots of the following quadratic equation:

$$\left\{ q_\ell^{(k-1)} q_m^{(k)} - q_m^{(k-1)} q_\ell^{(k)} \right\} \nu^4 - \left\{ q_\ell^{(k-2)} q_m^{(k)} - q_m^{(k-2)} q_\ell^{(k)} \right\} \nu^2 +$$

$$+ \left\{ q_\ell^{(k-2)} q_m^{(k-1)} - q_m^{(k-2)} q_\ell^{(k-1)} \right\} = 0 \quad . \qquad (3.6)$$

Generally, we will introduce a normalization by equating the m^{th} element with 1. If we indicate these normalized vectors with $\overset{o}{\underline{q}}$, then

$$\underline{q}^{(k-2)} = \overset{o}{\underline{q}}{}^{(k-2)}, \quad N^{(k-1)}\, \underline{q}^{(k-1)} = \overset{o}{\underline{q}}{}^{(k-1)}, \quad N^{(k)}\, N^{(k-1)}\, \underline{q}^{(k)} = \overset{o}{\underline{q}}{}^{(k)}$$

and

$$\overset{o}{q}{}_m^{(k-2)} = \overset{o}{q}{}_m^{(k-1)} = \overset{o}{q}{}_m^{(k)} = 1 \quad .$$

With the normalized vectors, the quadratic equation 3.6 is transformed into

$$\frac{\overset{o}{q}{}_\ell^{(k-1)} - \overset{o}{q}{}_\ell^{(k)}}{N^{(k)} \left\{ N^{(k-1)} \right\}^2} \nu^4 - \frac{\overset{o}{q}{}_\ell^{(k-2)} - \overset{o}{q}{}_\ell^{(k)}}{N^{(k)}\, N^{(k-1)}} \nu^2 + \frac{\overset{o}{q}{}_\ell^{(k-2)} - \overset{o}{q}{}_\ell^{(k-1)}}{N^{(k-1)}} = 0$$

or

$$\nu^4 - N^{(k-1)} \left\{ 1 + \frac{q_\ell^{(k-2)} - q_\ell^{(k-1)}}{q_\ell^{(k-1)} - q_\ell^{(k)}} \right\} \nu^2 + N^{(k)} N^{(k-1)} \frac{q_\ell^{(k-2)} - q_\ell^{(k-1)}}{q_\ell^{(k-1)} - q_\ell^{(k)}} = 0 \,. \quad (3.7)$$

This equation is very important and we recommend including it in programming if the calculations are carried out with an electronic computer. As roots of equation 3.7, we obtain values for ν_1^2 and ν_2^2. Although we can take in principle any element for the ℓ^{th} element, it is recommended to select ℓ so that the accuracy of the coefficients in the equation becomes as high as possible.

If we employ the quadratic equation, we need only continue with iteration until the component $\underline{q}_3$ has disappeared. When $\underline{q}_3$ has disappeared after k-2 steps of iteration, within the degree of accuracy employed in calculation, then the calculation indicated above is exact. We then obtain for ν_1^2 a result which is as exact in as many numbers /digits?/ as that in which iteration was carried out. We therefore have inversely the criterion that $\underline{q}_3$ has disappeared when the calculated value for ν_1^2 no longer changes. The accuracy of the value for ν_2^2 is dependent on the number of digits with which $\underline{q}_2$ is still represented in the iterated vector when $\underline{q}_3$ disappears. With further steps, the accuracy of ν_2^2 becomes smaller and smaller. More steps therefore offer no advantage.

The end result for $\underline{q}_1$ is obtained from equation 3.4 as

$$\underline{q}_1 = \underline{q}^{(k-2)} - \nu_2^2 \, \underline{q}^{(k-1)} \,.$$

The result for $\underline{q}_2$, i.e.

$$\underline{q}_2 = \underline{q}^{(k-2)} - \nu_1^2 \, \underline{q}^{(k-1)} \,,$$

can be used as starting vector for iteration with the transformed matrix $\underline{D}^{(2)}$.

If we also calculate the natural vectors $\underline{s}_i$ of the transposed matrix $\underline{C}'$, we need to determine the natural vectors $\underline{q}_i$ and $\underline{s}_i$ only to half the number of the exact figures desired for the natural values. We then utilize the formula

$$\nu_i^2 = \frac{\underline{s}_i' \, \underline{q}_i}{\underline{s}_i' \, \underline{C} \, \underline{q}_i} \,. \quad (3.8)$$

If there are three natural frequencies whose absolute amounts are only slightly different, we can then derive, in principle, an equation of the third degree in the same manner. In practice, however, this is of little use because the method then becomes relatively complicated.

3.3 Calculation of Interference

It may be very important to be able to follow in simple manner the influence of small changes in the mechanical system. It would be extremely cumbersome to repeat the entire computations. It will probably be always possible to utilize the static-vibration forms of the original system again as prescribed changes of form for the flutter vibrations. This means in essence that the new flutter-vibrations forms are developed from the static-vibration forms of the original system in accordance with equation 3.1. The new system will then also not have been brought into normal form for the static vibration. We must then form for the new system the matrix $\underline{C} = \underline{G}' \underline{D} \underline{F}$ and could determine the natural values and the natural vectors from this matrix as previously.

In general, this method will also still require much time. An appreciably faster method is furnished by the calculation of interference. The calculation of interference can be employed when the changes are sufficiently small. It is then not necessary to again determine the natural values of the changed matrix through iteration but we can utilize immediately the formula

$$\nu_i^2 = \frac{\underline{s}_i' \underline{q}_i}{\underline{s}_i' (\underline{C}+\Delta\underline{C}) \underline{q}_i} \tag{3.9}$$

Here $\Delta\underline{C}$ is the change in the matrix $\underline{C}$ whereas $\underline{q}_i$ and $\underline{s}_i$ represent the natural vectors of the original matrix $\underline{C}$ and of the transposed $\underline{C}'$. It is evident that this formula for the original matrix $\underline{C}$, i.e. with $\Delta\underline{C} = 0$, furnishes the exact natural values (cf. equation 3.8). The fact that it also gives a logical approximation for $\Delta\underline{C} \neq 0$, is a consequence of the bi-orthogonality relation. A change $\Delta\underline{C}$ which is small of the first order, will also change the natural vectors by magnitudes which will be small of the first order. By reason of the bi-orthogonality relation, the error produced when equation 3.9 is employed with the natural vectors of the original matrix, will be only small of the second order.

If we had introduced an arbitrary vector in equation 3.8 instead of the vector $\underline{s}_i$, it would still be possible to determine the natural value for the original system but only with the same number of digits which we have available also in $\underline{q}_i$. However, there would be no point in employing equation 3.9 with an arbitrary vector in place of $\underline{s}_i$ because the error would then be small of the first order and therefore of the same order as the correction found.

If the system has adjoining natural values and a close linkage exists between the corresponding vibration forms, it is necessary to exercise care in the utilization of this method. The changes made, although apparently small, may still be too great for furnishing good results by the method described above. It may be stated in general that the change found in a natural value in the complex plane should remain small in comparison to adjoining natural values.

Although it is possible in principle to find, with the aid of calculation of interference, the change in the natural vectors and subsequently also the change in the natural values up to a higher order, these methods are not employed in practice because they are relatively cumbersome. If the accuracy of equation 3.9 is inadequate, it is better to again determine the natural values by iteration.

4. COMPARISON BETWEEN CALCULATED AND MEASURED STATIC-VIBRATION FORMS

An endeavor will be made to complete the calculations of flutter indicated above before undertaking the first flight. This means that the results of the static-vibration test can be employed only as a subsequent control. The measured natural frequencies and static-vibrations forms will be compared with those calculated. If appreciable differences are disclosed, it may become necessary to improve or complement the calculation of flutter.

In general, it is very difficult to solve the problem of changing the mechanical system so that an exact concordance between measured and calculated natural frequencies and static-vibration forms is obtained. One source of error is when the mechanical attenuation is neglected in the calculations of static vibration by which all motion in a vibration form is either in phase or in phase opposition. Occasionally other phase differences also occur during measurement.

Another cause of the differences between measured and theoretical results may be that certain deformations have not been included in the theory but reveal themselves as important during the test. For example, this was shown in earlier calculations of the deformation between wing and fuselage in the horizontal plane under anti-symmetrical vibrations. Such a neglected degree of freedom may induce a new natural frequency, may change the existing ones and may extensively influence the vibration forms occurring in this. In the example given here, it may be necessary to compensate the aileron also vertically because this might otherwise produce a mass linkage. Horizontal wing motions then have aileron deflections as consequence which may essentially affect flutter characteristics by the aerodynamic forces so induced.

If it becomes necessary subsequently to add one degree of freedom in the calculation of flutter, this is done best by introducing a further coordinate q_{p+1} in equation 3.1 and by adding one line and one column to the matrix $\underline{F}$ in which all elements are equal to zero, with exception of the common element which is equated with one. The

coordinates q_i ($i = 1, 2, \ldots, p+1$) are then no longer normal coordinates for static vibration because the matrix in the right member of equation 3.2 contains one line and one column with elements not equal to zero.

In conclusion, let us consider the case in which all degrees of freedom have been included in calculation but in which the calculated natural frequencies do not agree with those measured. In principle, this can be caused both by deviations in the magnitudes of mass as well as in those of rigidity. The magnitudes of mass are normally much better known so that we will generally attempt to obtain better agreement by correcting rigidity. The problem then is that of changing the matrix $\underline{K}$ so that the natural values of equation 3.2 or of

$$\underline{q} = \nu^2 \underline{G}' \underline{K} \underline{m}^* \underline{F} \underline{q}$$

assume predetermined (i.e. the measured) values. Most of the time an attempt will be made to solve this problem, not by changing the distribution of deflective or torsional rigidity over wing or fuselage but merely by introducing general correction factors which change these rigidities in each cross-section at the same percentage. The matrix $\underline{K}$ is then changed in $\underline{\tilde{K}}$ and the equation

$$\underline{q} = \nu^2 \underline{G}' \underline{K} \underline{G} \underline{q} \quad (\underline{m}^* \underline{F} = \underline{G})$$

will have the predetermined natural values. The natural vectors are then no longer normal coordinates for static vibration.

If now

$$\underline{L} = \underline{G}' \underline{K} \underline{G}$$

we then necessarily obtain the condition that

$$\left| \nu^2 \underline{L} - \underline{I} \right| = 0 \qquad (4.1)$$

for given values of ν^2. The elements of $\underline{L}$ are lineary combinations of the correction factors introduced for rigidity. However, the difficulty in this is that the equations 4.1 do not become linear in these correction factors. It is therefore preferable not to examine the entire system simultaneously but to subdivide the system as far as possible in partial systems which are either not or only slightly linked to each other. For a partial system of m degrees of freedom, $m!$ solutions may be expected. We must obviously select that solution for which the natural vector also agrees as far as possible with the measured one, in order to prevent that, for instance, a torsional vibration occurs at a measured natural frequency of deflection. In order to find the correct solution, we may frequently still have to have recourse to the trial and error method. A direct solution of this problem does not yet exist as far as the author knows.

LITERATURE REFERENCES

1. A. I. van de Vooren, Theory and Practice of Flutter Calculations for Systems with Many Degrees of Freedom. Thesis Delft, NLL Report F. 100, Vol. XVII, Rep. and Transactions NLL, 1952.
2. I.C.A.O. Airworthiness of Aircraft, Standards and Recommended Practices. Annex 8, Third Edition, 1952. Montreal, Canada.
3. R. A. Frazer, W. J. Duncan, A. R. Collar, Elementary Matrices. Cambridge University Press, 1938.
4. E. G. Broadbent, Research on Wing and Control Surface Flutter with Particular Reference to the Choice of Coordinates. R.A.E. Techn. Note Structures 168 (1955).

APPENDIX: The Elimination of Fuselage Motion

For a bending and twisting wing, the deformations $z_d(y)$ and $\varphi_d(y)$ are determined by the equations

$$\left.\begin{aligned} z_d(y) &= \nu^2 \int_0^b K_{11}(y,\eta)\,\left[m_{11}(\eta)\; z(\eta) + m_{12}(\eta)\;\varphi(\eta)\right]\,d\eta\,, \\ \varphi_d(y) &= \nu^2 \int_0^b K_{22}(y,\eta)\,\left[m_{12}(\eta)\; z(\eta) + m_{22}(\eta)\;\varphi(\eta)\right]\,d\eta\,. \end{aligned}\right\} \qquad (A.1)$$

The functions $z(\eta)$ and $\varphi(\eta)$ describe the absolute vibration amplitudes and can therefore be replaced by

$$z_d(\eta) + z(o) \quad \text{and} \quad \varphi_d(\eta) + \varphi(o) \quad .$$

The equations A.1 can be regarded as integral equations for the loadings $m_{11}z+m_{12}\varphi$ and $m_{12}z+m_{22}\varphi$. These loadings are then determined by the deformations $z_d(y)$ and $\varphi_d(y)$ and follow from them by employing a certain operation. We can therefore write

$$\left.\begin{aligned} m_{11}(\eta)\,\left[z_d(\eta)+z(o)\right] + m_{12}(\eta)\,\left[\varphi_d(\eta)+\varphi(o)\right] &= 0_1(\eta,y)\;z_d(y)\quad, \\ m_{12}(\eta)\,\left[z_d(\eta)+z(o)\right] + m_{22}(\eta)\,\left[\varphi_d(\eta)+\varphi(o)\right] &= 0_2(\eta,y)\;\varphi_d(y)\quad. \end{aligned}\right\} \qquad (A.2)$$

For a straight wing, $0_1(\eta,y)$ is the same as $\frac{d^2}{dy^2}(B\,\frac{d^2}{dy^2})$ and $0_2(\eta,y)$ is $\frac{d}{dy}(T\,\frac{d}{dy})$ where $B(y)$ and $T(y)$ represent the deflective and torsional stiffness of the wing in the cross-section y.

We now employ the equations A.2 for those cross-sections $\eta_i(i = 1, 2, \ldots, k)$ for which we desire to calculate the deformation. The left member of equation A.2 can then be brought into the following matrix form:

$$\begin{Vmatrix} m_{11}(\eta_1) & 0 & 0 \ldots. & m_{12}(\eta_1) & 0 & 0 \ldots. & m_{11}(\eta_1) & m_{12}(\eta_1) \\ 0 & m_{11}(\eta_2) & 0 \ldots. & 0 & m_{12}(\eta_2) & 0 \ldots. & m_{11}(\eta_2) & m_{12}(\eta_2) \\ \vdots & & & \vdots & & & & \\ m_{12}(\eta_1) & 0 & 0 \ldots. & m_{22}(\eta_1) & 0 & 0 \ldots. & m_{12}(\eta_1) & m_{22}(\eta_1) \\ 0 & m_{12}(\eta_2) & 0 \ldots. & 0 & m_{22}(\eta_2) & 0 \ldots. & m_{12}(\eta_2) & m_{22}(\eta_2) \\ \vdots & & & \vdots & & & & \end{Vmatrix} \cdot \begin{Vmatrix} z_d(\eta_1) \\ z_d(\eta_2) \\ \vdots \\ \varphi_d(\eta_1) \\ \varphi_d(\eta_2) \\ \vdots \\ z(o) \\ \varphi(o) \end{Vmatrix}$$

(A. 3)

The rectangular matrix has $2k$ rows and $2k + 2$ columns.

The first two integrals with whose aid the fuselage motions can be eliminated, are equations 2.5:

$$\begin{aligned} \int \left[m_{11}(\eta) \left\{ z_d(\eta) + z(o) \right\} + m_{12}(\eta) \left\{ \varphi_d(\eta) + \varphi(o) \right\} \right] d\eta = 0 \quad , \\ \int \left[m_{12}(\eta) \left\{ z_d(\eta) + z(o) \right\} + m_{22}(\eta) \left\{ \varphi_d(\eta) + \varphi(o) \right\} \right] d\eta = 0 \quad , \end{aligned} \tag{A.4}$$

or in matrix form

$$\begin{Vmatrix} a_1 m_{11}(\eta_1) & a_2 m_{11}(\eta_2) \ldots. a_1 m_{12}(\eta_1) & a_2 m_{12}(\eta_2) \ldots. \\ a_1 m_{12}(\eta_1) & a_2 m_{12}(\eta_2) \ldots. a_1 m_{22}(\eta_1) & a_2 m_{22}(\eta_2) \ldots. \end{Vmatrix}$$

$$\ldots. \int m_{11}(\eta)\, d\eta \quad \int m_{12}(\eta)\, d\eta$$

$$\ldots. \int m_{12}(\eta)\, d\eta \quad \int m_{22}(\eta)\, d\eta$$

$$\cdot \begin{Vmatrix} z_d(\eta_1) \\ z_d(\eta_2) \\ \vdots \\ \varphi_d(\eta_1) \\ \varphi_d(\eta_2) \\ \vdots \\ z(o) \\ \varphi(o) \end{Vmatrix} = 0 \quad .$$

(A. 5)

The rectangular matrix appearing here gives us two rows needed to transform the rectangular matrix in A.3 into a square matrix. The coefficients a_1 are found by utilizing the integration rule. If we also multiply the rows of the matrix in A.3 with respectively a_1, $a_2 \ldots\ldots a_1$, $a_2 \ldots\ldots$, then the resulting square matrix becomes symmetric. We know that the elimination of unknowns in a symmetric system of linear equations can always be carried out so that symmetry is maintained. This is therefore also true for the system which is formed by A.3 and A.5. Since the right member of A.5 is equal to zero, the right member of A.2 is not changed through elimination. If we finally also invert the operations $O_1(y,\eta)$ and $O_2(y,\eta)$, the influence functions $K_{11}(y,\eta)$ and $K_{22}(y,\eta)$ are recreated and we have then obtained a system which can be written in the form

$$\underline{f}_d(y) = \nu^2 \, \underline{K} \cdot \underline{m}^* \cdot \underline{f}_d$$

in which $\underline{m}^*$ is also symmetric.

DISCUSSION

Küssner: To me the method of using the reflected matrix appears to be especially welcome because we can greatly reduce errors in this manner. The method is moreover very important for the calculation of contiguous natural values. One of my collaborators sometime ago investigated a case in which the natural values were closely contiguous by chance. He developed an experimental method in order to be able to still treat this problem without requiring 200 steps of iteration and was still able to handle it relatively well with a manual calculator. However, certain tricks must be employed to derive useful results in case of contiguous natural frequencies.

I should like to make a remark concerning the observations made in your lecture: in practice, it is a very important question how well the actual aircraft can be represented through the constants in the matrices. However, how well are the natural-vibration forms developed in this? If I understood you correctly, you first carry out calculations for aircraft of which you have only the design. You test subsequently whether the static-vibration test is satisfactory and agrees with the theoretical calculations.

Van de Vooren: These calculations are so time-consuming that we cannot wait this long to carry out the static-vibration test.

Küssner: Should this test be regarded as an independent control? I should like to stress particularly that the execution of accurate static-vibration tests on aircraft is not too simple and that the responsibility should not always be sought in the theory. In order to determine the natural-vibration forms correctly, we need undoubtedly, at the higher natural frequencies, more exciters than are customarily employed. We have now tried this out in the Aerodynamic Experimentation Institute and Dr. Schoen will discuss this in detail. A strict resonance condition is the one that the phase angle must amount everywhere to $\frac{\pi}{2}$ or $\frac{3\pi}{2}$ as against the force of excitation; otherwise we do not obtain any clear natural-vibration form and actually should not compare it with the theory. We attempt, by changes in the number of exciters, excitation forces and points of action on the aircraft, to comply with this phase condition as well as possible experimentally.

De Vries: I am interested in knowing how close was conformance between calculations and the static-vibration test?

Van de Vooren: Dr. Greidanus may be able to better answer this question because the methods described by me have been employed by him in the calculation of flutter for the Fokker F-27 and their results were compared with those of the static-vibration test.

Greidanus: In order to give a detailed answer to this question, I should like first to make some remarks on the computer employed for flutter calculation.

This is a full-automatic electronic instrument with a rotating drum (3,000 rpm) as magnetic memory. The machine has no separate "fast memory" and the speed of calculation is therefore in essence determined by the speed with which the binary numbers (30 bits) can be written in or read from the memory.

Because each channel in the memory carries 32 numbers, the reading of one number or of one "instruction" lasts about $1/32 \times 20 \approx 0.6$ milliseconds. Because any elementary step requires at least the reading of one instruction and the transport of one digit and because short "switching intervals" must be added to the "reading intervals," the execution of a "fast" instruction, e.g. addition or subtraction, lasts about 3 milliseconds. The multiplication of two binary numbers with 30 digits, approximately the most complicated task that can be programmed directly, requires about 20 milliseconds.

Because these reading and writing operations in the memory represent the most critical physical processes in the machine, an automatic control with the aid of a "check bit" has been added. The machine stops automatically as soon as the "check bit" control, carried out for any reading operation from the memory, indicates a simple binary error during the preceding write-in or during the actual reading. This automatic control has proved to be extremely valuable.

All vibration and flutter calculations of greater extent are carried out primarily with the aid of the iteration method. For the static-vibration calculations, this is a real, symmetric method in which iteration of the natural vector and "deflation" of the basic matrix alternate with each other. In flutter calculation, there is created for each nominal reduced frequency a complex, no longer symmetric matrix from which are now calculated successively, by the customary iteration but generalized to complex numbers, the natural vector and its conjugate with basically the same accuracy. The deflation takes place exclusively by elimination of the direct and conjugated natural vector from the basic matrix and is again a calculation carried out in complex form.

It is always somewhat difficult, in this calculation by iteration, to determine how long iteration should be continued. We must always expect that the errors in rounding off may prevent an exact reproduction of the natural vector. Occasionally we observe that iteration leads to a relatively short cycle of several iterations which is reproduced accurately on the whole and which subsequently, when continued, leads to periodicity. In practice, the repetition of the calculation is controlled by the digit switch at the control desk. The reading instruction for iteration calculation established in the machine program for this switch interprets the binary number inserted as "number of iterations to be automatically executed with subsequent single print-out of the results and stopping." The print-out of each single-step result of iteration requires far too much printing time.

Both for calculation of static vibration and, to an even higher degree, for calculation of flutter, it has been shown to be absolutely necessary to include in the iteration program a special program that can be cut in when normal iteration converges too slowly, i.e. when two natural values have almost the same modulus. In a real case, this means that the iteration vector becomes "slowly variable" in a complex case, the situation cannot be made clear quickly unless the complex numbers of an intermediate result are not occasionally brought in polar representation. If such a special program is not available, we will experience difficulties in almost any calculation of aircraft vibration with many degrees of freedom. The respective calculation utilizes in customary manner the results of three successive, poorly converging basic steps of calculation.

If it is intended in particular to control theoretical results through vibration tests with the actual aircraft, it then becomes preferable, when a computer is available, not to divide the calculation of vibration into calculation of "wing" and "tail" surfaces as before. The components of the aircraft are in reality always so closely linked that any separation causes an appreciable falsification which makes it only more difficult to recognize the theoretical result in the experimental result or even completely prevents this.

The detailed calculations carried out for the Fokker F-27 contained 14 degrees of freedom, including the 3 cyclical ones, in the basic, asymmetrical static-vibration case. In this, the continuous freedom of deformation, e.g. of the wing, was represented through predetermined form-change functions which were taken from preliminary calculations. In the final calculation, the wing was represented as isolated by 12 "stations" with one each displacement and torsion (distortion) co-ordinate.

The cyclic degrees of freedom were eliminated in the machine in the normal algebraic manner which led to a vibration matrix of the 11th order. For all calculations, the inertia constants of the system were determined by a careful analysis of mass on the basis of construction drawings and weighing during assembly. For stiffness, there were available in general estimates considered in part as quite accurate but in part also as only very approximate.

The first calculation led to completely unacceptable deviations from the experimental result. It proved to be extremely difficult to bring about concordance. 25 very carefully selected variations were necessary in which computations were always made with the same masses (because accurately known) but each time with another stiffness, in order first to clear up a gap in the experimental result (an overlooked resonance of which subsequently traces were found in the experimental data) and, second, in order to achieve complete concordance of "signs." "Sign correspondence" here means that all coordinates agree in all natural vibrations with the signs found in the test which leads to a qualitative concordance in the representation of the vibration form

(specifically of the positions of the nodal lines). In this, the natural frequencies resulted throughout with only very small deviations (less than 5%) as against the experimental findings.

It is partly due to the high number of 25 calculated variations that, after extensive concordance had already been reached, further tempting proposals for further improvement could be worked out which were then always again completely exploited.

The lowest natural vibration of the system has a frequency of about 3 c/s and the 8th, the highest calculated, lies at about 18 c/s.

The model system of the aircraft so developed was subsequently utilized for an asymmetrical flutter calculation by adding, for all degrees of freedom, appropriate representations of aerodynamic forces.

It should be pointed out that the case of symmetric vibrations is appreciably simpler than the asymmetrical case. This is due to the fact that certain fixation-deformations are eliminated in the symmetric case and the corresponding degrees of freedom consequently can be left out. It should further be considered that the respective aircraft permitted us to obtain very accurate and highly satisfactory experimental results because the internal damping was relatively small in a wide range of frequency (probably as a consequence of the extensive use of the metal and adhesive-assembly method). This led to very marked resonances in the experiment.

Thielemann: I have a question on experimental technique. How many exciters did you use in your static-vibration test?

Greidanus: This was a very simple test in which we used one exciter.

Thielemann: In consideration of the internal damping, can we still expect in this case that theory and experiment will concord?

Greidanus: This may differ from case to case. Here a concordance between theory and experiment may well be expected. The F-27 has a glued construction (metal and adhesive-assembly method). Due to this, damping is relatively low which is a considerable advantage in the static-vibration test. We obtain clear resonances. In an unfavorable case in which the evaluation of the static-vibration test is interfered with by non-clear resonances, calculations and experiment will never concord as well because the test itself does not have adequate accuracy.

Sorg: In the comparison of the results of theoretical and experimental static vibration, I have had the experience that very satisfactory results can be achieved by carefully carrying out calculation of stiffness. The calculation methods for this are rather complicated and extensive. I have observed that the normal worker in static aerodynamics can carry out such calculations only when he has lost the habit of regarding as object of his calculation the determination of maximum stresses. The calculation of stiffness for the purpose of flutter calculation demands a different point of view and/or basic attitude of such a worker to the object of his calculations.

Greidanus: Only few results of stiffness calculation are introduced in these computations. On the other hand, mass distribution is analyzed very accurately. It is assumed that the mass matrix is sufficiently accurate. Then a first calculation is performed and we may find that the natural frequencies are not sufficiently clearly defined. We then do not correct the mass matrix but simply the stiffness. We might say that the stiffness is determined implicitly by the calculation of static vibration.

Von Gorup: I have one question for Dr. van de Vooren. You treated in your lecture the example of a symmetrical wing vibration. In this, you grouped the deformations into a four-dimensional vector. Is this possible also for another type of vibration, e.g. an asymmetric or a torsional vibration?

van de Vooren: The deformations are characterized through a multi-dimensional vector. The number of vector elements is dependent on how many values of y are required in order to sufficiently accurately establish the deflective and torsional functions $z(y)$ and $\varphi(y)$. For symmetric or asymmetrical vibrations, this is the same in principle.

von Gorup: Is it possible to then use matrix algebra in exactly the same way?

van de Vooren: Yes, there is no difference in principle.

von Gorup: In the flutter problem, you have assumed in principle p as appreciably smaller than n, e.g. p about in the magnitude 6 to 8 and n at a magnitude of 20 to 24. Is this done only to keep the effort of calculation within tolerable limits?

van de Vooren: Yes. In the example mentioned by Dr. Greidanus, $p = 10$. There is no point in considering more vibration forms. Although we work for the static vibrations, for example, with a vector of 24 elements, we calculate here also not more than for example, 10 vibration forms. We calculate only as many as are needed for calculation of flutter.

RATIONAL USE FOR FLUTTER CALCULATION OF VALUES FOUND BY STATIC-VIBRATION TEST

by G. de Vries

SUMMARY

The report demonstrates that in cases in which the number of natural-vibration forms introduced into flutter calculation is restricted, these forms must first be simplified by neglecting the deformations of certain structural elements in the calculation of the aerodynamic forces. The appropriate physical considerations involved are explained. A method of experimentation is indicated which facilitates the selection of the structural elements used in calculation. Further development of this procedure may make it possible to obtain also numerical data for certain structural values.

ARRANGEMENT:

		Page
1.	Introduction.	79
2.	Introduction of Natural-Vibration Forms into Flutter Calculation	79
3.	Observations on Aerodynamic Forces to be Considered in Flutter Calculations.	81
4.	Estimation of Coupling Values in Static-Vibration Tests	81
5.	Literature References	85
	Illustrations	86
	Discussion.	95

1. INTRODUCTION

If we measure all natural-vibration forms together with the respective generalized masses in a static vibration test, we can then calculate the critical speed from the natural values of that matrix which is obtained from the diagonal matrix of the natural-vibration forms without aerodynamic forces by addition of the general, non-symmetric matrix of the aerodynamic forces. This procedure is utilized exclusively by O.N.E.R.A. However, since we have not as yet available the computers required for introducing all forms simultaneously into calculation, we are compelled to make a suitable selection among the forms. Such selection is facilitated by considerations of energy on the basis of results of computation with one or two degrees of freedom (1). These calculations but also quite generally any calculations with a restricted number of degrees of freedom, raise the question which values should be introduced in the calculation. It turns out that these are not always the measured natural-vibration forms.

2. INTRODUCTION OF NATURAL-VIBRATION FORMS INTO FLUTTER CALCULATIONS

A simple example will best show the tasks resulting when the number of the natural-vibration forms used in calculation is largely restricted, e.g., to two. In a wing, let us select the basic deflection and torsion which will have the amplitude distribution in the reference section shown in Fig. 1. A simple physical consideration will show that it would be erroneous to use the measured natural-vibration forms unchanged in the calculation. This would mean that we assume the relation between control-surface and wing amplitudes as fixed or as a kinematic linkage which obviously does not exist. The results of such a calculation scarcely have any physical meaning because they belong to a substitute system which may be very different from the wing.

We need apparently to "correct" the natural-vibration forms before using them in the calculation. The manner of effecting this correction is shown when we start from a more complete equation system, i.e. add the natural-vibration form of the control-surface, in the present case. After introducing the aerodynamic forces λ_{ik}, we obtain the determinant

$$D = \begin{vmatrix} \varphi_{11} - \mu_{11} \cdot \omega^2 + \lambda_{11} & \lambda_{12} & \lambda_{13} \\ \lambda_{21} & \varphi_{22} - \mu_{22} \cdot \omega^2 + \lambda_{22} & \lambda_{23} \\ \lambda_{31} & \lambda_{32} & \varphi_{33} - \mu_{33} \cdot \omega^2 + \lambda_{33} \end{vmatrix} \quad (1)$$

in which

φ_{11} , φ_{22} , φ_{33} = generalized stiffness,

μ_{11} , μ_{22} , μ_{33} = generalized mass,

λ_{ik} = generalized aerodynamic forces,

ω = angular velocity (real for critical speed).

It is meaningful only to equate a subdeterminant with zero instead of the determinant D when the elements of a row or a column, except for one, become infinitely small. This can be accomplished if we assume added masses for the control-surface so that the latter remains, for the wing forms, in the wing plane. With this, the determinant D_s of the static-vibration forms changes. We first obtain the new determinant

$$D_s' = \begin{vmatrix} \varphi_{11}-\mu_{11}\cdot\omega^2-m_{11}\cdot\omega^2 & -m_{12}\cdot\omega^2 & -m_{13}\cdot\omega^2 \\ -m_{21}\cdot\omega^2 & \varphi_{22}-\mu_{22}\cdot\omega^2-m_{22}\cdot\omega^2 & -m_{23}\cdot\omega^2 \\ -m_{31}\cdot\omega^2 & -m_{32}\cdot\omega^2 & \varphi_{33}-\mu_{33}\cdot\omega^2-m_{33}\cdot\omega^2 \end{vmatrix} \quad (2)$$

and can calculate the new natural-vibration forms in which deflection and torsion of the wing no longer have any control-surface motion. This makes it possible to carry out calculation for the wing. The result is then valid for a system contiguous to the basic system, i.e. a wing with a dynamically compensated control-surface.

Since in general a difference exists in the magnitude of the values μ of the generalized masses of control-surface and wing forms, the μ-values of the wing will change, due to the small added masses on the control-surface, only within the range of the accuracy of measurement of the basic values so that calculation of the new natural-vibration forms becomes unnecessary. It is sufficient to suppress the control-surface amplitudes.

We should therefore remember that in some cases the natural-vibration forms must be changed before introducing them into calculation. However, it is not always possible to base ourselves on the difference in magnitude of the μ-values in order to simplify them. In the general case, another logical approach is a better way to arrive at useable guide lines.

3. OBSERVATIONS ON AERODYNAMIC FORCES TO BE CONSIDERED IN FLUTTER CALCULATIONS

There is no doubt that many calculations of flutter carried out with a wing or empennage alone have shown satisfactory conformity with the results in the wind tunnel or in flight. If we consider the natural-vibration forms of an aircraft, we will note that the amplitudes of the empennage can be paralled, for example, by equally large amplitudes of the wing. This raises again the question whether the aerodynamic forces acting on the wing should or should not be introduced in the calculations of the empennage. Here the same is again true which has already been said in regard to the ailerons. If the amplitude relation of the elements considered, i.e. wing and empennage in this case, does not change under the influence of the aerodynamic forces, then the wing must also be taken into account in calculation of the empennage. This corresponds to a case of strong coupling between wing and empennage. In a weak coupling, there is no firm relation between the amplitudes and we are safe in neglecting the amplitudes of the wing.

The concept of the natural-vibration forms of the complete aircraft is momentarily abandoned with this and the system is assumed to be subdivided into a series of partial systems such as elevator, rudder and wing with their own natural-vibration forms which become linked into the natural-vibration forms of the complete aircraft.

It is therefore the coupling which is of interest in the cases discussed and in many others. We can, as in the example of the aileron, state the static-vibration determinant for many natural-vibration forms and draw conclusions from it by introducing added masses or stiffness in a structural part and observing the change of amplitude relations after solving the determinant. However, it is simpler to gain a clear insight into this already during the static-vibration test, especially since this is possible without appreciable additional effort /expense?/ as will be shown.

4. EVALUATION OF COUPLING VALUES IN STATIC-VIBRATION TESTS

The following investigations are carried out on the system represented in Fig. 2 which consists of two simple vibrators with a coupling spring. The vibrators shall here correspond to the structural elements wing and empennage. Let m_1 and m_2 be the masses of the vibrators and c_1, c_2 and c the spring constants. Without coupling, the vibrators have the natural frequencies $\omega_1^* = \sqrt{c_1/m_1}$ and/or $\omega_2^* = \sqrt{c_2/m_2}$. The vibration equations for the system with coupling read

$$m_1 \ddot{y}_1 + c_1 y_1 - c (y_2 - y_1) = o \quad ,$$

$$m_2 \ddot{y}_2 + c_2 y_2 + c (y_2 - y_1) = o \quad . \tag{3}$$

With the basic formulation

$$y_1 = A_1 e^{i\omega t} \quad , \quad y_2 = A_2 e^{i\omega t}$$

there results for the two natural frequencies ω_1 and ω_2 of the system the equation

$$\omega^4 - m_1 m_2 - \omega^2 \left\{ m_1 (c_2 + c) + m_2 (c_1 + c) \right\} + c_1 c_2 + (c_1 + c_2) = o \quad . \tag{4}$$

For each of the two amplitudes belonging to each of the two natural frequencies, the equation then reads

$$\frac{A_1(\omega_k)}{A_2(\omega_k)} = 1 + \frac{c_2 - m_2 \omega_k^2}{c} \quad , \quad k = 1 \, , \, 2 \quad . \tag{5}$$

The spring constant c of the coupling spring was changed and m_1 and m_2 as well as ω_1 and ω_2 were kept constant. The corresponding values c_1 and c_2 were selected in correspondence with this. More detailed indications can be found in Fig. 2. We now identify the two vibrating masses with the mass of the wing and/or the mass of the empennage and assume them to be connected by a mass-less beam (fuselage). In Fig. 2, there are further entered, for each of the two natural frequencies ω_1 and ω_2 in each case for three values of c, the amplitudes of the points of this mass-less beam as a function of the distance x of the respective point from m_1 (longitudinal coordinate of the fuselage). In the case considered here, the vibrations of the masses m_1 and m_2 belonging to the natural frequency ω_1 show a phase difference of π whereas they oscillate in the same phase for the natural frequency ω_2.

The calculations were carried out so as if they concerned an experiment; only such values appear as could be determined in an experiment. (The structural values were utilized for the calculation of amplitude changes and frequency displacements resulting from the fixation of the added masses.)

We know that we can determine the mass m of a vibrator when we measure the displacement of the natural frequency by the added mass Δm.

If ω designates the original frequency and $\bar{\omega}$ the new frequency (2.3), we obtain

$$m = \Delta m \frac{\bar{\omega}^2}{\omega^2 - \bar{\omega}^2} \tag{6}$$

These relations are, in expanded form, also valid for natural vibration forms of systems with arbitrary mass and stiffness distribution if the added masses are proportional to the existing masses (adapted added masses). For sufficiently small added masses, adaptation is not required, e.g. one added mass is sufficient. A prerequisite herein is that the natural vibration form does not noticeably change by fixation of this added mass.

For a natural-vibration form assumed as non-variable, mass and stiffness can be grouped in one reference point so that nothing is changed concerning the energy regime of the system in regard to the natural-vibration form considered. With this, the system is replaced, for the respective natural-vibration form, by a simple vibrator which imparts to the system (assumed to be mass-less) the deformation prescribed by the natural-vibration form. The properties of the vibrator obviously change with the reference point (4). We call the value m obtained by equation 6 for the reference point "the mass reduced to the reference point" of the system for the natural-vibration form under consideration. By normalizing the amplitude in the reference point to 1 (m), we obtain the generalized mass μ. The numerical values of m and μ are equal in this so that equation 6 may also be written in the form

$$\mu = \Delta m \frac{\bar{\omega}^2}{\omega^2 - \bar{\omega}^2} \tag{6a}$$

Whereas the value $\frac{\omega^2 - \bar{\omega}^2}{\bar{\omega}^2}$ changes proportionally to Δm for the simple vibrator so that, first, the value obtained from equation 6 becomes independent of Δm and, second, the function $\frac{\omega^2 - \bar{\omega}^2}{\bar{\omega}^2}(\Delta m)$ results in a straight line, this linear relation for the natural-vibration form of an arbitrary system is obtained only then when the added masses have been adapted. For non-adapted added masses, the natural-vibration form changes and the "theoretical straight line" becomes a curve whose starting tangent for $\Delta m = 0$ coincides with this

straight line. The value $m = \Delta m \frac{\varpi^2}{\omega^2 - \varpi^2}$ also does not remain constant and we obtain $m = f(\Delta m)$.

It has been shown in practice that a very restricted number of small and appropriately distributed added masses is sufficient to determine the μ-values in the experiment. (Hereafter, μ will be written in place of m where natural-vibration forms are concerned.) The criterion for this is constituted by the fact that, within the range of accuracy of measurement, μ becomes independent of Δm and/or $\frac{\omega^2 - \varpi^2}{\varpi^2} (\Delta m)$ becomes a straight line.

This now constitutes an inducement to utilize the deviations from these conditions observed with arbitrarily arranged added masses for drawing conclusions as to the internal structure of the system. Among the possible information, we are here interested in the coupling between the individual structural elements. We here proceed in the following manner:

We assume that the natural-vibration forms of the system in Fig. 2 are known from tests. By affixing added masses at two arbitrarily selected points of the system, we follow the deviations from the theoretical value μ = const. (Fig. 3-6) and, in the other representation (Fig. 7-8), from the theoretical straight line for adapted added masses. Because computation is here intended to replace a test, the theoretical values for μ as well as for the straight line are assumed as unknown and were not drawn in.

In the system represented in Fig. 2, we first affix added masses at m_1 and then at m_2 and determine the μ-values for different values of the added masses. For adapted added masses, the value of μ calculated from equation 6 is independent of the value of the added mass affixed. The poorer the adaptation is, the more do the deviations from the theoretical value increase with increasing Δm. Figs. 3 and 4 show the results for the natural frequency ω_1. The masses were affixed in m_1 (Fig. 3) and in m_2 (Fig. 4) and selected so that the frequency changes in both cases became about the same because these are the only base for the selection of the magnitude of the added masses in a test. In addition to the curves $\mu(\Delta m)$, the curves $\mu \cdot \beta$ were drawn in with

$$\beta = \left(\frac{A_r}{A_s}\right)^2_{\Delta m = 0} \cdot \left(\frac{A_s}{A_r}\right)^2_{(\Delta m)} , \qquad (7)$$

r = 1; s = 2 for μ in relation to m_1 (Figs. 3,4),
r = 2; s = 1 for μ in relation to m_2 (Figs. 5,6,7,8).

In this manner, we enclose the real μ-values between two curves. We see from Fig. 3 that the uncertainty range so defined becomes very small for the frequency changes (less than 5%) of practical interest. However, in Fig. 4, it becomes very great and strongly dependent on the coupling.

From this we can draw the following conclusion: in a test, if the added masses are affixed successively at the structural elements to be investigated concerning their coupling and if in both cases, at the same magnitude of frequency displacements, a small range of uncertainty results, we are in the presence of firm coupling. If, in one case, a small and, and in another case, a large range of uncertainty results, we are in the presence of weak coupling; obviously, the measured μ-value is determined in essence through the element which produces the smaller range of uncertainty.

Corresponding results are obtained for the natural frequency ω_2 (Figs. 5 and 6).

It should be noted further that the representation in Figs. 3-6, selected because of its clear arrangement, is not the one customary in the test. Because of the scatter of the experimental results, there is no point in calculating the μ-values from equation 6 as was done in Fig. 3-6. On the contrary, $\frac{\Delta\omega^2}{\omega^2}$ is entered in dependence on Δm and the gradient of the theoretical straight line produces $1/\mu$. In Figs. 7 and 8, the results of Figs. 5 and 6 are recorded in this form utilized in the test. The theoretical straight line coincides with the starting tangent of the curve (with non-adapted added masses). The enclosing of this straight line by two curves is here especially advantageous.

5. LITERATURE REFERENCES

1. G. de Vries, Sondage des systemes vibrants par masses additionelles. La Rech. Aeron. No. 30, 1952.
2. C. Beatrix, Methode energetique pour la detection des modes de vibration responsables du risque de flottement. La Rech. Aeron. No. 58, 1957.
3. R. Mazet, Quelques aspects des essais de vibration au sol et en vol. Note Technique No. 34 der O.N.E.R.A., 1956.
4. G. de Vries, Eigenschwingungsformen von mechanischen Schwingungsgebilden. VDI Berichte Band 4, 1955, Seite 53 ff.

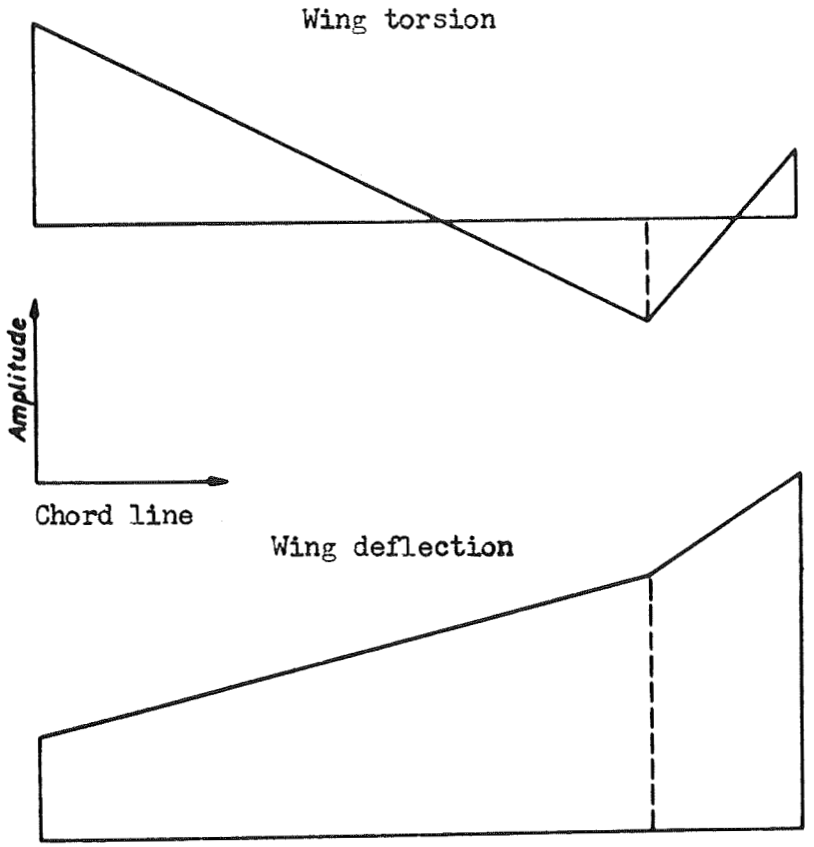

Fig. 1. Deformations for two modes of natural vibration in a reference section of a wing with control surface.

Part I of Fig. 2:

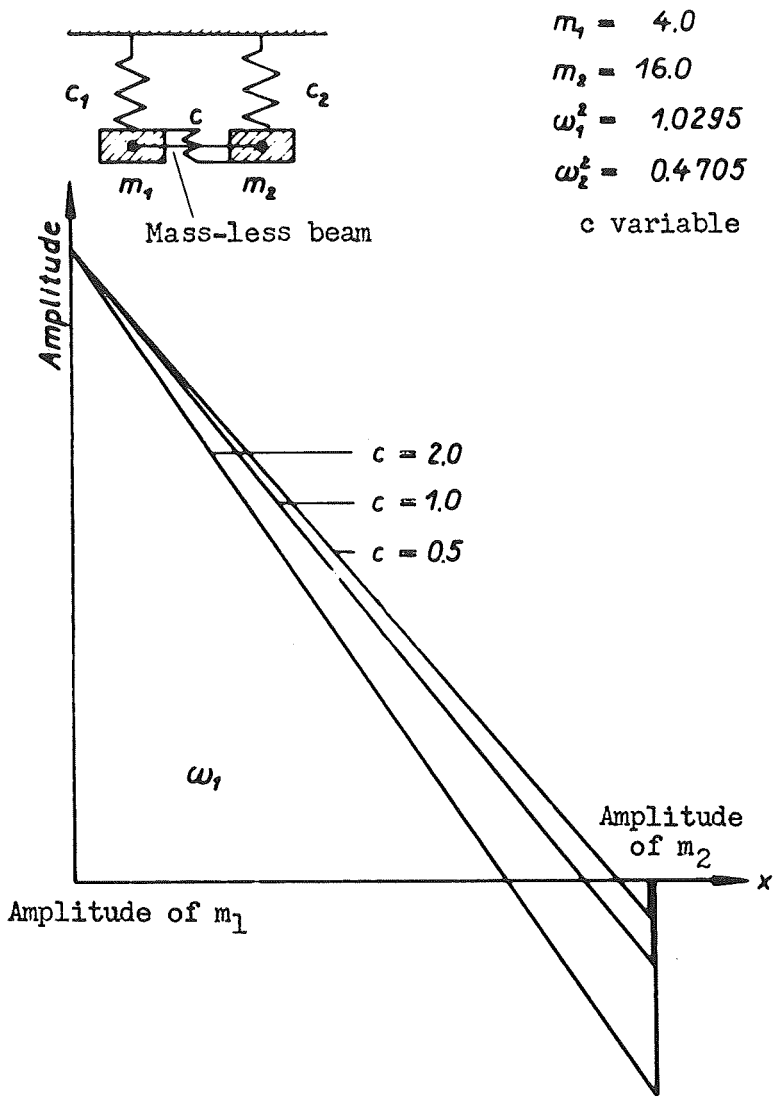

Fig. 2. Amplitudes for the natural vibration modes for different values of c.

Part II of Fig. 2:

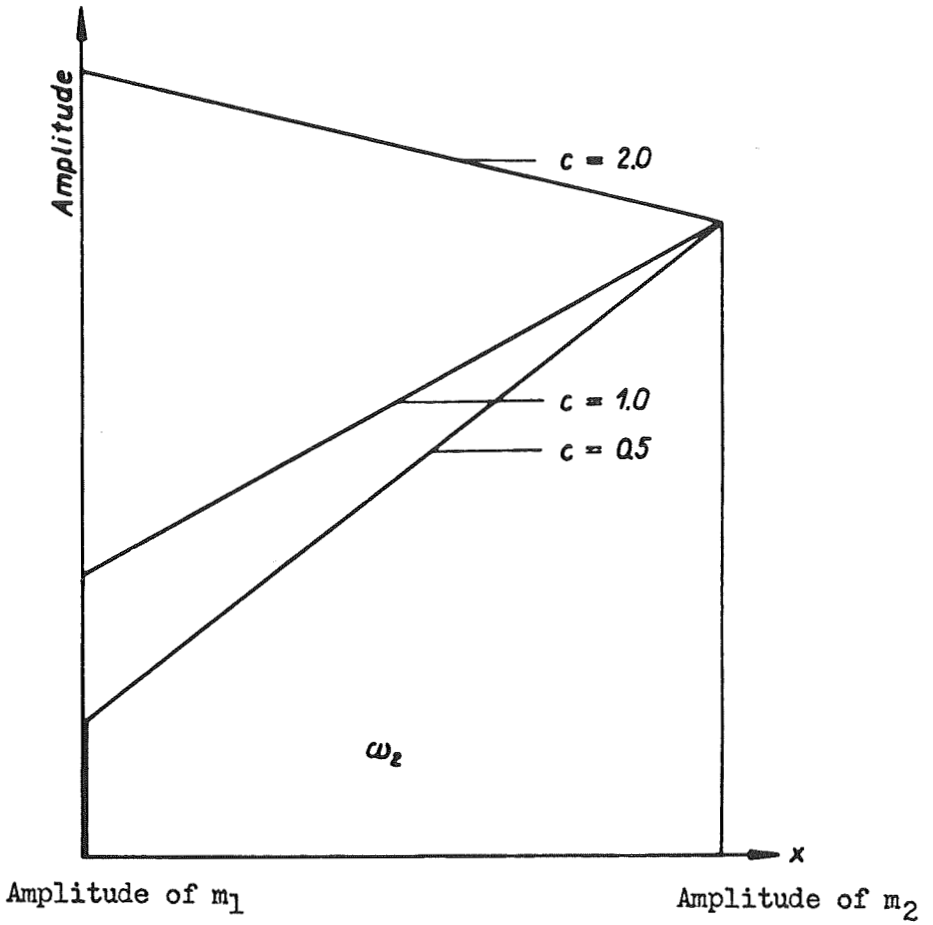

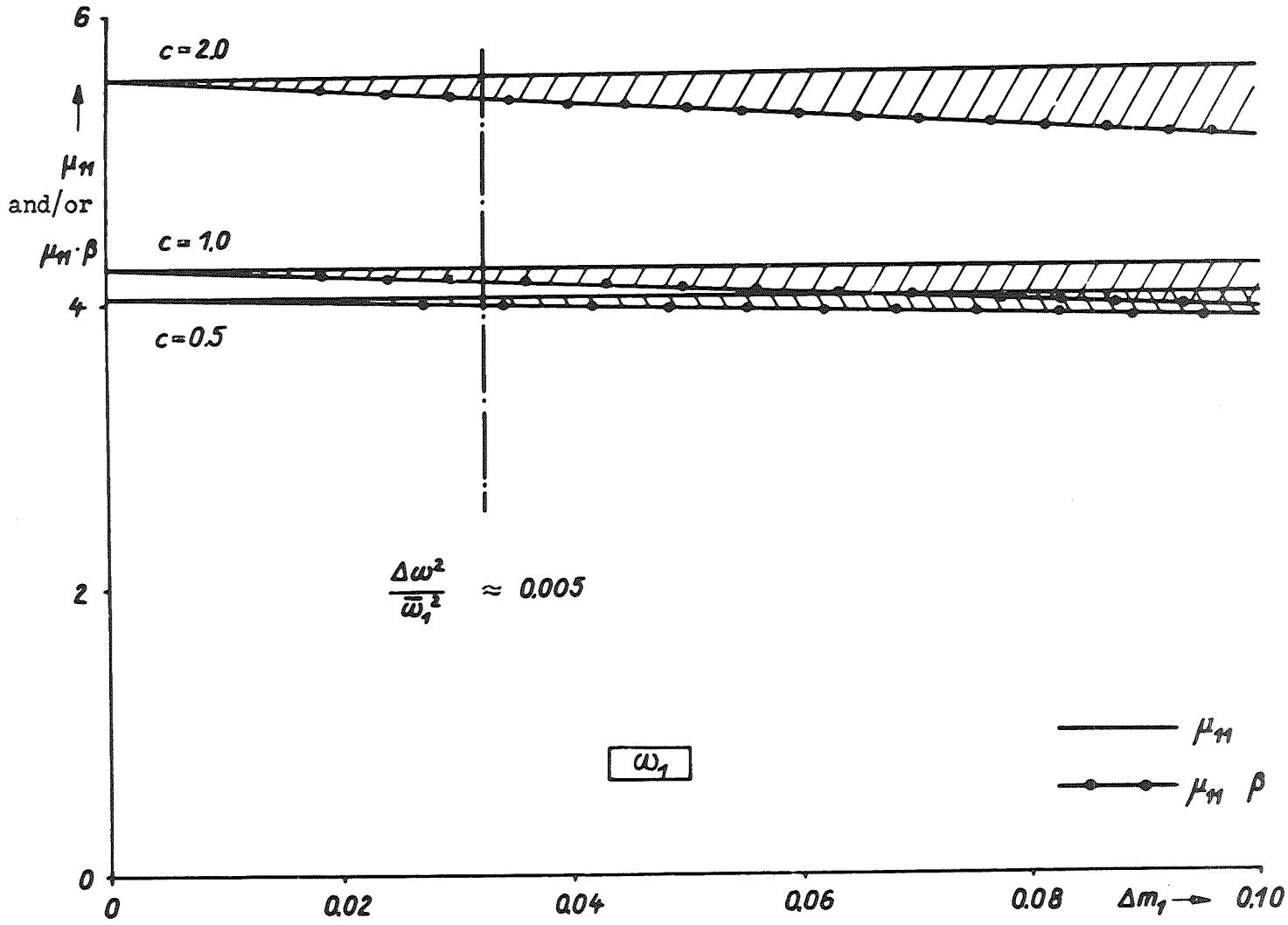

Fig. 3. Values of μ_{11} in dependence on Δm_1 for different values of c.

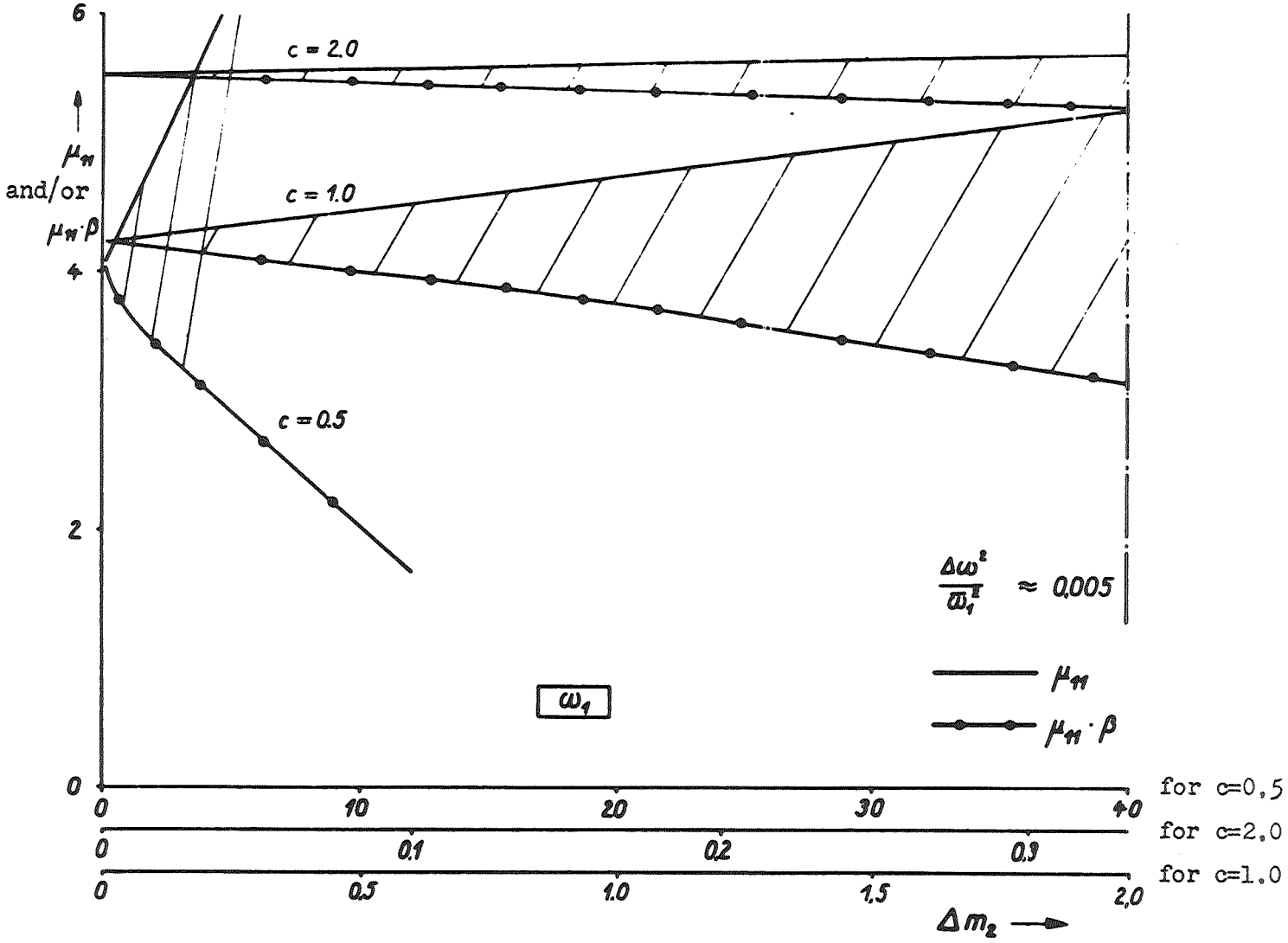

Fig. 4. Values of μ_{11} in dependence on Δm_2 for different values of c.

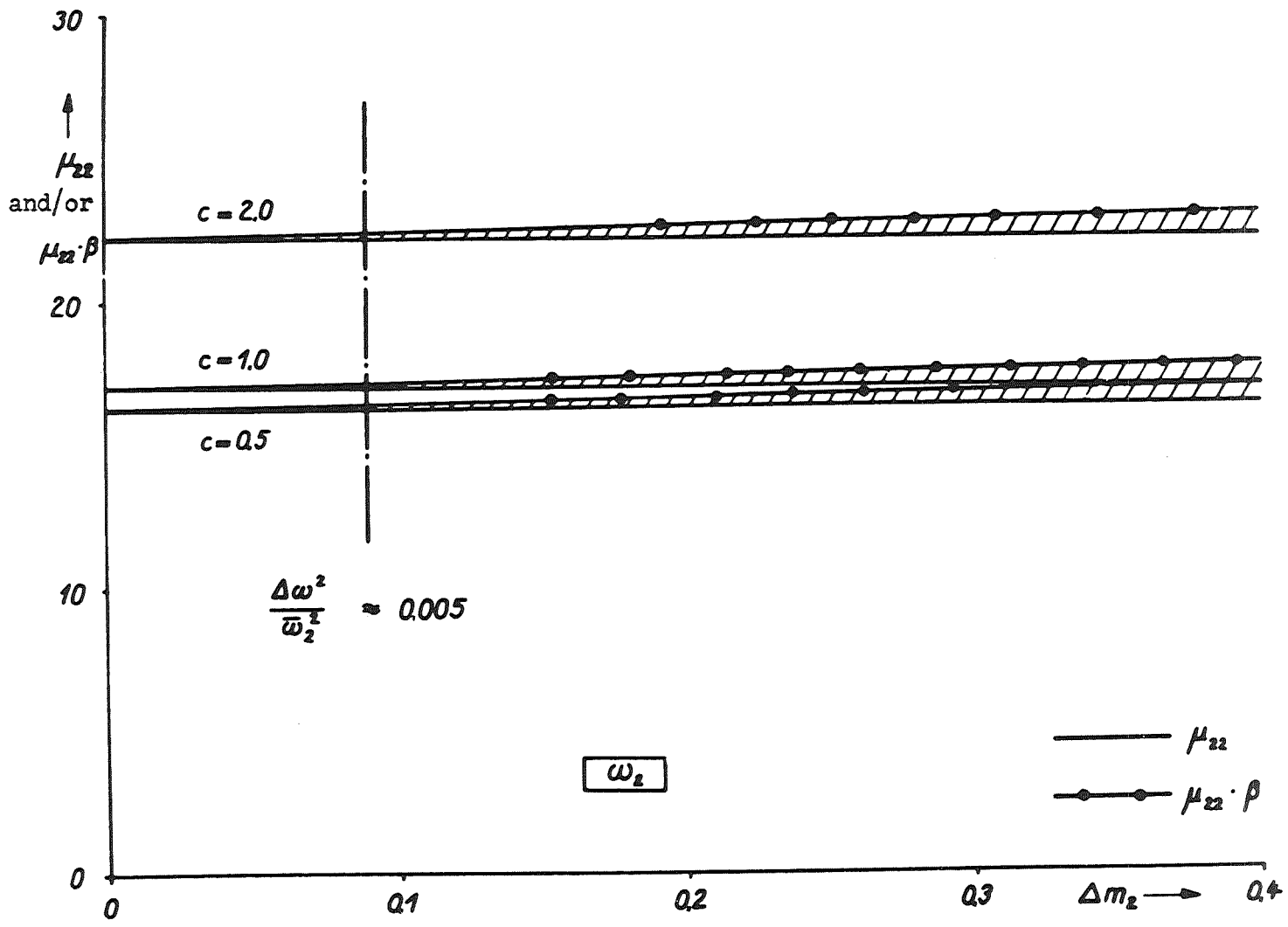

Fig. 5. Values of μ_{22} in dependence on Δm_2 for different values of c.

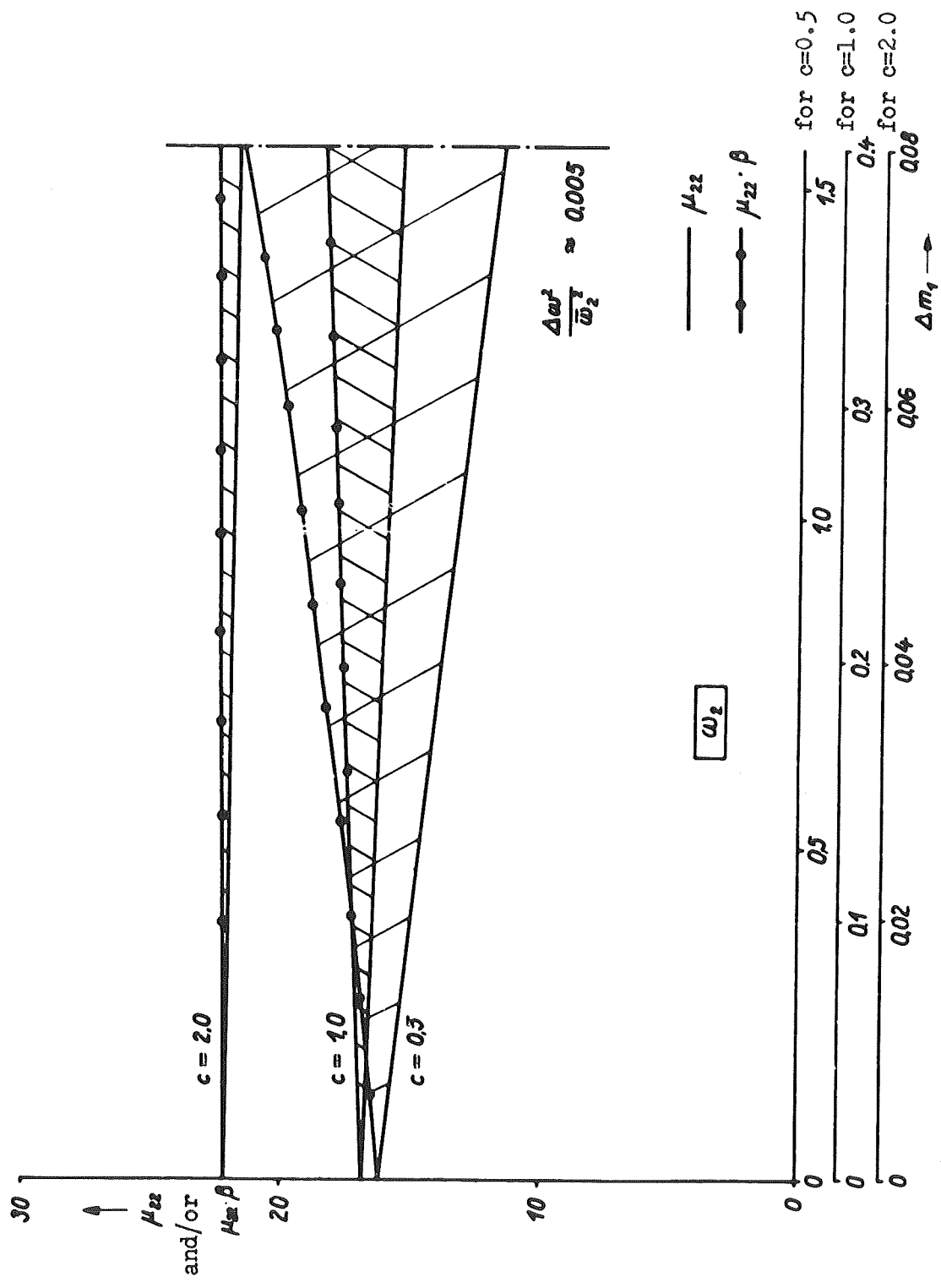

Fig. 6. Values of μ_{22} in dependence on Δm_1 for different values of c.

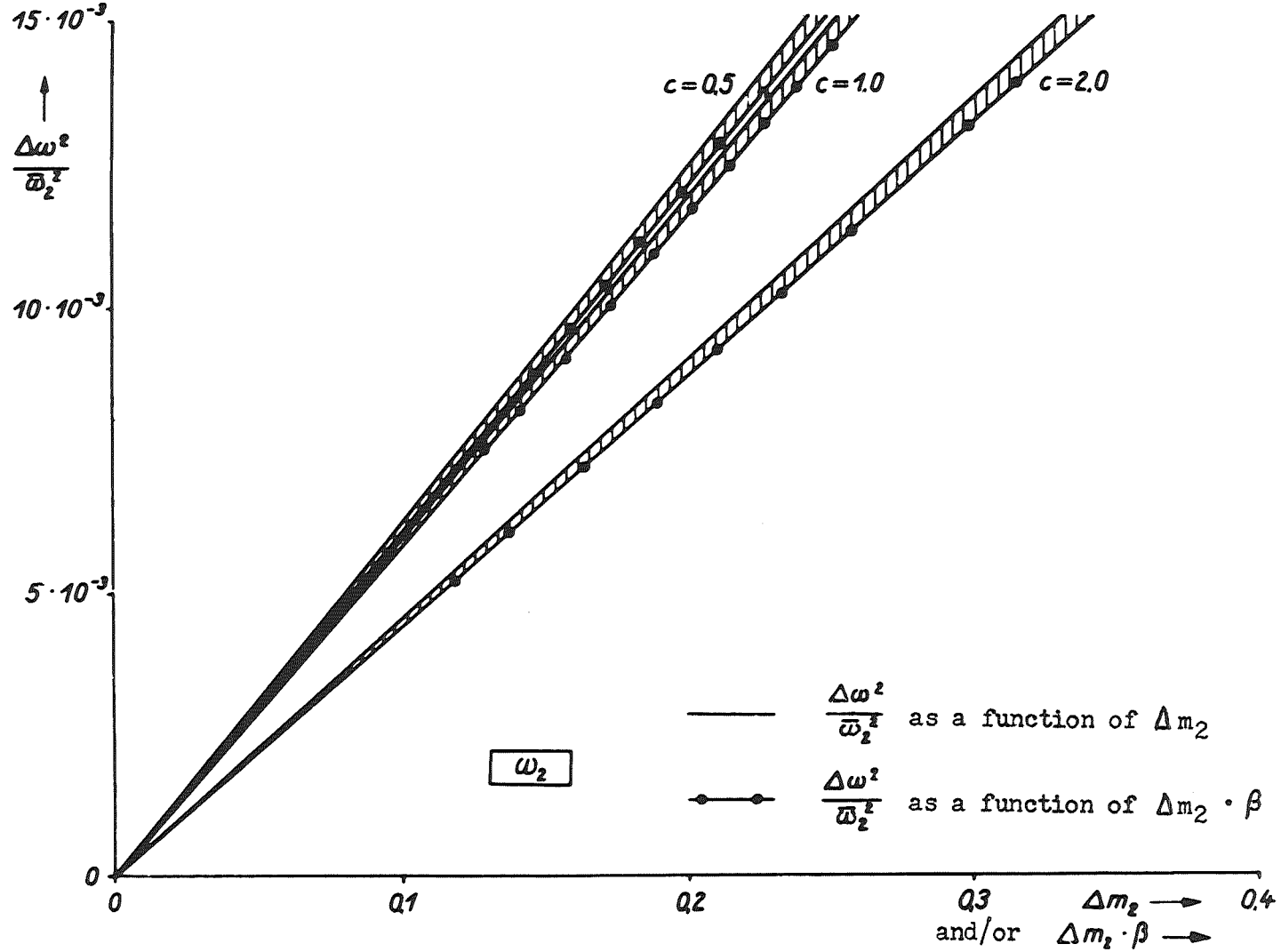

Fig. 7. Customary representation of the results in Fig. 5.

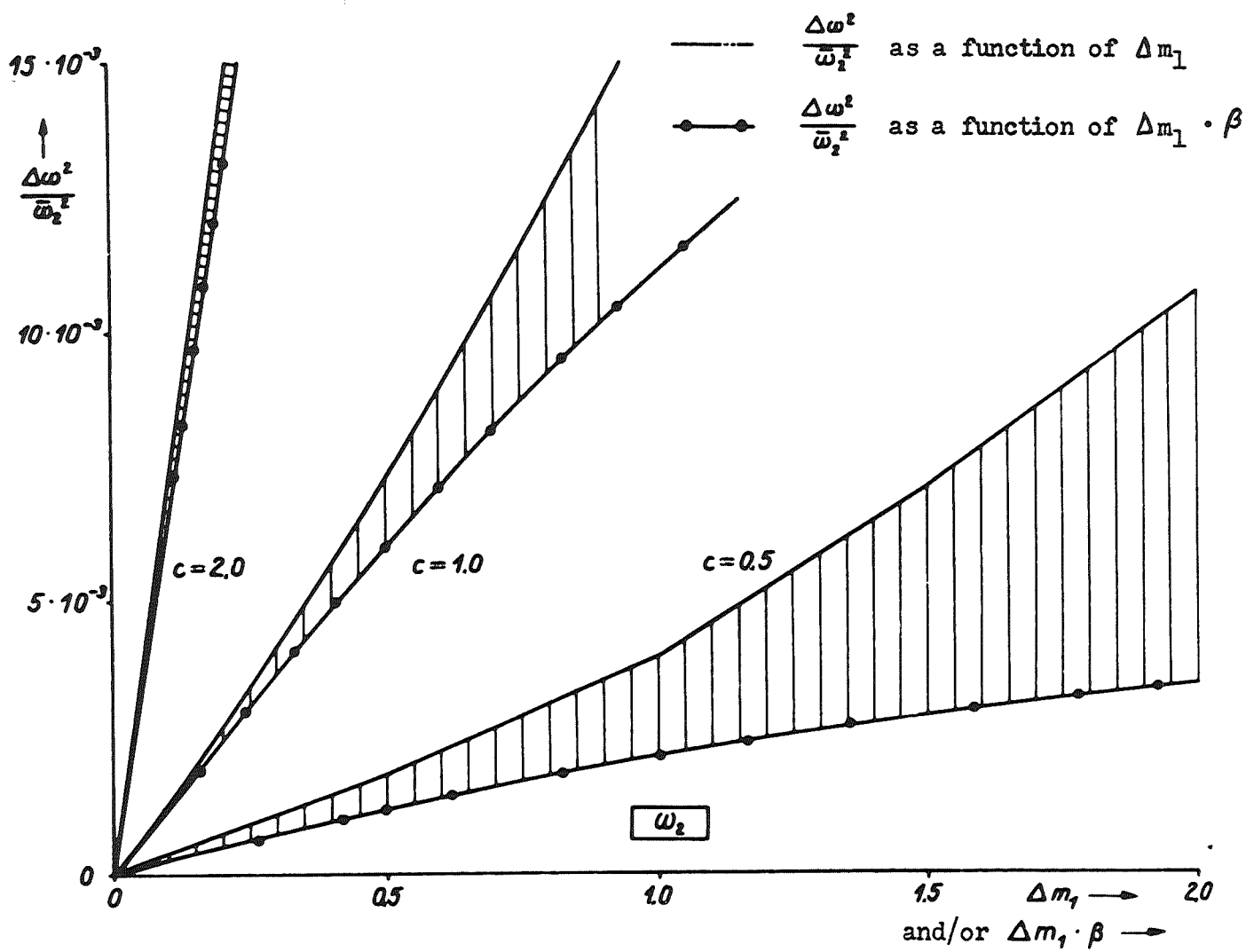

Fig. 8. Customary representation of the results in Fig. 6.

DISCUSSION

Küssner: Especially recently, we have occupied ourselves intensively with the determination of the generalized mass which is fundamental in the calculation of flutter. The investigations of Mr. de Vries now show indirectly the existence of possibilities of error which concern the resonance situation in a totally unexpected manner. It is not sufficient to comply with the phase conditions for two points of the aircraft but we must pose even stricter conditions. One of the means for this is that of introducing artificial errors into the distribution of the added masses, i.e., to affix them in the reverse sense from that corresponding to a proportional distribution. This affords us indirectly an insight into the overlapping of natural-vibration forms. It is important for us to realize that we have not yet reached our final goal but must employ much stricter criteria in order to obtain the higher natural-vibration forms. Otherwise we will measure some arbitrary natural-vibration forms, continue our calculations and then be surprised at the large deviations when their cause actually lies in the measurements.

One more point: can, shall or must we carry our calculation of flutter with a small number of natural-vibration forms? I should be more inclined to agree with the Dutch point of view of considering seven or eight forms in this but then also adding the degrees of freedom of rigid-body motion, i.e., the degrees of freedom of the complete aircraft, and obviously also the motions of the control surfaces as rigid body.

Greidanus: I have been aware for several years that Mr. de Vries occupies himself with generalized masses. I have wondered occasionally at the purpose of determining generalized masses by a new static-vibration test whereas an analysis of direct mass distribution is not really so very difficult. We have never found it necessary to carry out such measurements because we had to determine the mass distribution in the aircraft for many purposes and the former can be determined adequately, accurately without any great difficulties. We have always obtained the Lagrange equation as well as the flutter equation, without being forced to perform special tests for the determination of generalized mass.

de Vries: The answer to this is simple: in the static-vibration test, in general only the exterior of an aircraft is accessible to measurement. However, for example, jet engines, fuel tanks, etc. represent large masses which may have motion relative to fuselage and wing. We are therefore not justified, in integral formation, to multiply the masses with the amplitudes measured on the exterior of the aircraft. Since these masses are large, the error may also be very large. The same is true for the vibration forms of control surfaces and control mechanisms. It is easy to determine the inertial moment of a control surface. However, in order to indicate the generalized mass of

a vibration form, e.g., control stick against control surface, we would have to know the amplitude distribution along the control mechanism which obviously can hardly be measured.

For these reasons, appreciable errors (30% and more) can result in the calculation of generalized mass from amplitude and mass distribution. In a satisfactory result of measurement in which the results of both methods of measurement (energy method and added masses) agree, uncertainty is scarcely larger than $\pm$ 5%. Moreover, experimental determination can be carried out much faster than the respective calculation.

Küssner: You are right from one point of view, Dr. Greidanus. To you as aircraft builder, parameters are much more easily available. I endeavored, during the war, with my Flutter Team to calculate cases of flutter observed in flight. It was nearly impossible to collect the parameters. For someone on the outside, it is very difficult to procure the mass values. (Mountains of construction drawings). As an experimental institute, we are very pleased to have experimental procedures for the determination of generalized masses. We would prefer to avoid the calculation of stiffness because this requires numerous additional simplifying assumptions. Just as you do, Mr. de Vries, we also attempt to determine everything experimentally as far as possible. I should like to begin the calculation of flutter only after I have a static vibration test as good as possible. In industry, the situation is different (trained personnel for the determination of mass values, etc. from construction drawings).

Sorg: A remark on the question of the number of degrees of freedom in flutter calculation: during my activities with O.N.E.R.A., I found that quite satisfactory results can be achieved for aircraft with straight, i.e., not swept-back, wings and without heavy assemblies such as engines, wing tanks, etc. already with three degrees of freedom. I was able to observe that, in general, by the addition of more degrees of freedom such as top deflection, top torsion and the degrees of freedom of the rigid body of oscillation and torsion, the result of the flutter calculation for the wing was very little changed. The degrees of freedom always taken into account were basic wing deflection, basic wing torsion and control-surface torsion. In strongly swept-back wings or those with heavy assemblies as well as for empennages, however, conditions were different.

While re-calculating the factors of a crash due to flutter (rupture of the wing of a freight glider, equipped with engines subsequent to construction), we even calculated, with two degrees of freedom, a critical speed which, if memory serves me, agreed within 5% with the speed at the moment of crash. This concerned deflective and torsional wing flutter. The ailerons were not involved.

Ebner: Broadbent demonstrated in a report that a number of crashes due to flutter occurred because of not taking into consideration higher natural-vibration modes.

Küssner: The question of the number of degrees of freedom to be considered can probably not be decided in a general manner. In an earlier (heroic) time, we did carry out calculations with very few degrees of freedom which agreed quite well with the observed critical speeds. To me, it seems to be a safer method to introduce many degrees of freedom. Even if they have no effect on the vibration form, at least they do not introduce any additional errors into calculation. This may be a superfluous effort of computation, but it presents less of a risk.

de Vries: At O.N.E.R.A., we proceed in the following manner: we first establish considerations of energy through preliminary calculations (cf. C. Beatrix, "The Energy Method for the Detection of Vibration Modes Responsible for Flutter," Recherche Aeronautique, No. 59, 1957) by investigating, among about five degrees of freedom, in each case combinations of 2 and 2 degrees of freedom in regard to which mode imparts energy to other modes and how much energy is transmitted in the process. From these calculations, we are already able to note which, if any, of the modes enter into the conditions of flutter and which modes must be taken into account. Variations may be made in these calculations with two degrees of freedom by varying, for example, mass and by investigating whether and how the exchange of energy among the modes is influenced by this. We do not by any means want to restrict the number of natural-vibration forms in the calculation. We measure as many as 24 modes but can obviously not introduce all modes simultaneously into the calculation. These simple calculations therefore afford us a method of selection. After the preliminary calculations have been completed, the major calculation is carried out with the 5, 6 or 8 modes which are of particular interest. This final calculation then becomes controlling on the designer. It has been shown so far that not more than 5 degrees of freedom are of influence in any calculation. Normally, 3 to 4 degrees of freedom are the maximum. This would also seem to explain why we obtained good results in the past from calculation with very few degrees of freedom.

Thielemann: I would like to add one remark concerning the report of Broadbent mentioned by Prof. Ebner. Broadbent reported that he knew of two cases in which flutter occurred due to a controlling mode of oscillation which was not found during the vibration test. Theoretical determination of the natural vibration modes had not been made concurrently with the vibration test and there were utilized, in the calculation of flutter, only those modes found in the vibration test which produced sufficiently high critical speeds. After flutter occurred in the aircraft, mathematical determination of the vibration forms was made and it was noted that there must have existed two very closely contiguous natural frequencies, one of which was overlooked in the test and the natural vibration form of the latter was essentially responsible for the flutter in the two cases mentioned. In control tests carried out subsequently with great care, the existence of two

very closely contiguous natural vibration modes was actually established. In order to exclude such cases of flutter as far as possible, it would seem necessary to always carry out mathematical determination of the natural mode of the complete aircraft, in addition to the static vibration tests, in order to uncover any possible very close contiguity of frequency.

VARIOUS CALCULATIONS OF FLUTTER FOR AILERONS WITH HYDRAULIC SERVO-CONTROL MECHANISM

by E. Gruschwitz

The aerodynamic forces on ailerons have such a variable behavior close to Mach 1 that a satisfactory aerodynamic compensation is hardly possible. Aircraft flying within this range are therefore equipped as a rule with power-steering (servo-controls) and preferably of a type which is irreversible and consequently does not retransmit any energy from the control surface to the control mechanism. Disregarding elastic deformations of the control surface and the linkage between the control surface and the servo-mechanism, such an irreversible servo-control does not permit any motion of the control surface by forces of mass or aerodynamic forces. This might tempt us to neglect compensation of mass. The elastic deformations mentioned would then obviously have to be eliminated to the largest possible extent. This is in general the case only when the servo-control is installed in close vicinity to the control surface and if it acts at about the middle of the control surface. These servo-controls are, as a rule, designed for hydraulic operation and we need then only consider the possibility of failure of pressure in the hydraulic installation. Provision is made generally for the possibility of deflecting the control surfaces manually, at least to a small extent. Since considerable damping remains present in the servo-control, there is the possibility that the control surfaces will remain free of induced oscillation even without compensation of mass.

We therefore calculated, for a wing with ailerons and without compensation of mass, the flutter speeds, with and without damping proportional to speed, of the ailerons. The flutter equations were based on the formulation of the station-function method proposed by Rauscher* and we calculated with four station functions and therefore with five degrees of freedom, including the ailerons. The damping due to this

---

* M. Rauscher, Station-Functions and Air Density Variations in Flutter Analysis. J. Aer. Sc. Vol. 16, (1949), p. 345-353.
cf. Urs Hochstrasser, Flutter Calculation with the Aid of Program-Controlled Computers. Journal for Applied Mathematics and Physics, Vol. VI, 1955, page 300.

servo-control was formulated herein as rudder damping moment = $k \left|\frac{d\beta}{dt}\right|$ (β = rudder angle, t = time, k = damping constant). Because of the rudder friction proportional to speed, there occurs in the flutter determinants not only the square of the natural frequency but also the latter itself. The characteristic equation therefore is not of the fifth but of the tenth degree. In order to avoid calculation of all 10 roots of this equation, we proceeded in the following manner:

We first solved the flutter equations for the system without rudder damping (i.e. a characteristic equation of the 5th order). The flutter solutions of the latter were considered as approximate solutions for the system with low damping and then improved according to the Newton method. From the solutions so obtained, we were then able in the same way to arrive at solutions for the system with greater damping, etc.

In case of symmetrical wing flutter, we calculated with different natural frequencies of the aileron. In Fig. 1, the flutter speed v_k is entered, in relation to $\nu_o l_o$ (ν_o = lowest natural frequency of wing, l_o = one-half of reference wing chord), above the natural frequency of the aileron. The actual flutter speed of the wings lies at $v_k/\nu_o l_o = 32.4$ and is independent of the natural frequency of the aileron. In addition to this flutter speed, there results, at relatively low values of $v_k/\nu_o l_o$, a range of induced oscillation whose extent depends on the magnitude of the damping constants k.

For $k > 2$, this range of induced oscillation disappears. In a case of asymmetrical wing flutter, only the non-elastic aileron can be considered. In Fig. 2, the value $v_k/\nu_o l_o$ is entered over k for this case. Here a minor difference between the actual flutter speed of the wing with a locked and that with a free rudder was shown. With a free rudder, it is somewhat lower. In addition, there occur here also ranges of induced oscillation, i.e. one with predominating wing deflection and aileron torsion and one with predominant wing torsion and aileron torsion. Here also, the ranges of induced oscillation for $k > 2$ disappear. The servo-control mechanism installed in the respective aircraft has a damping value $k > 35$ mkg/sec, or far more than is needed for the disappearance of the ranges of induced oscillation.

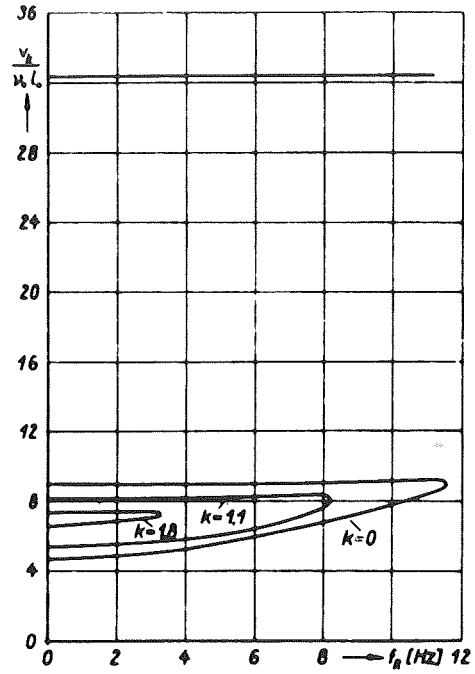

Fig. 1. Symmetric flutter.

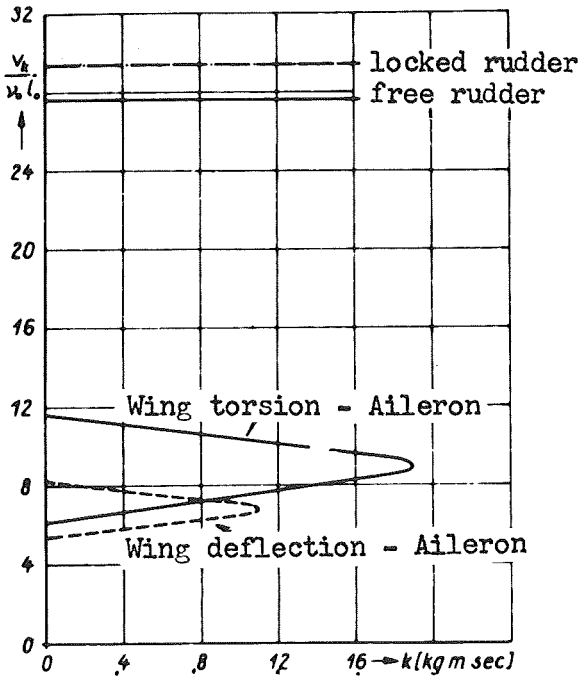

Fig. 2. Asymmetric flutter.

DISCUSSION

Sorg: Between 1947 and 1949, I carried out flutter calculations at O.N.E.R.A. according to an iteration method developed by R. Mazet (Scientific Director of O.N.E.R.A.). In this, we calculated complex natural values ω for different values of the reduced frequency ω^* occurring in the aerodynamic coefficients. The real magnitude $\mathrm{Im}\,\omega/\mathrm{Re}\,\omega$ was then entered above the flutter speed,

$$V = \frac{l \cdot \mathrm{Re}\,\omega}{|\omega^*|}$$

First carried out by the Aerodynamic Experimentation Institute during the war, this type of plotting permits a satisfactory comparison of the results obtained for different aircraft. In general, the curves obtained from calculations with two and/or three degrees of freedom show the trace indicated by the following curves

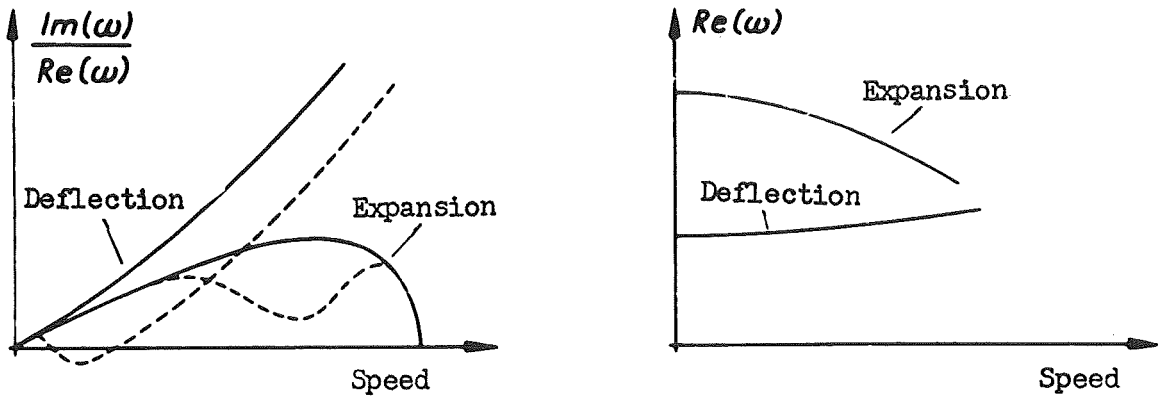

The solid curves shown in the figure on the left were found in all calculations with two degrees of freedom as also the curves of the figure on the right. If the degree of freedom of aileron torsion was taken into account additionally in the flutter calculation for the wing, the curves received invaginations such as are entered in the left picture in the form of broken lines. Depending on the selection of the aileron parameters, these invaginations did not transgress the abscissae further to the left or to the right and/or not at all. Through qualitative considerations similar to those of Quessel (illustrative interpretation of flutter with rudder participation?), direction and approximate magnitude of displacement of these invaginations could be determined.

After we constantly derived the same experiences, I then drew the practical conclusion that rudder flutter can always be eliminated by simple and tested means and that we can omit the introduction of the

degrees of freedom of the rudder into calculation, both during designing as well as in the control of resistance to flutter of completed aircraft. The degree of freedom saved in this manner brings about an appreciable simplification of calculation. If the wing or the empennage for blocked rudders is in order, then it is possible, by a suitable estimate of the relation of rudder frequency to the torsion and deflection frequency of the wing and empennage and by taking into consideration the magnitude of aerodynamic compensation, to judge the necessity for affixing mass compensation. The numerical calculation with degrees of freedom of the rudder does not produce any suitable quantitative results because of the uncertainty of the non-steady aerodynamic coefficients.

de Vries: I should like to mention an observation made by me during the tests. If a static vibration test is carried out on a rudder with servo-control mechanism and the pressure is released, this does not change anything in the oscillation behavior during the first minute. The natural frequency remains exactly the same and we observe only after about one minute (this varies for individual aircraft) that the oil is forced out of the control cylinder through the oscillations. Under certain circumstances, this presents a certain danger in flight because at this moment the piston acts against an air cushion and the frequency drops but the damping does not become larger. Actually, as already stated by Mr. Gruschwitz, the damping is so great in the working cylinder that it is still supercritical, i.e., the damping acts like an elastic fixation. The oil no longer follows the motion of the aileron. When the pressure drops, we have a new frequency which is lower as soon as an air cushion forms in the cylinder. For this reason, we have so far recommended in principle not to eliminate mass compensation from rudders with hydraulic control. If an aircraft in which the hydraulic control fails, is to be regarded as lost because the pilot has no expectation of landing it in this condition, we can obviously permit elimination of mass compensation. However, if manual activation is anticipated, i.e. when possibility of continued flight is provided, I should like to strongly caution against too great a reliance on damping because such damping may act merely like an elastic fixation because it is too high.

A classical example for the fact that a force of friction, i.e., damping, not only does not prevent flutter but may even induce it, was observed for normal rudder controls. During flight and by reason of the aerodynamic forces acting on the rudder, the friction in the linkage becomes so high that the linkage is at one point simply fixed. The rudder then begins to flutter at a frequency which also cannot be found in the static vibration test. It can be disclosed during static vibration tests by loading the rudder linkages artificially. In this way, we can observe all frequencies from zero up to a certain frequency. This also is one of the cases which must be taken into consideration in the calculations and explains my earlier remarks that it is absolutely necessary to carry out a variation of the rudder frequency.

One more remark on the significance of rudder flutter. Mr. Schwarzmann has collected statistics on flutter accidents which indicate that it is almost exclusively rudders which lead to flutter. I might even say that I know of no case of flutter in which participation of the rudder was definitely excluded. In my opinion, further research on flutter should first be devoted to the rudders which cause new difficulties in today's fast aircraft. (Cf. G. de Vries, "Particular Problems of Flutter Concerning Rudders and Ailerons," La Rech. Aeron. No. 58, 1957).

Addition During Composition of Text for Printing.

Kussner: We know that free-swinging rudders are one of the main causes of the cases of flutter in aircraft observed so far. As shown by the lecture and the discussions, this cause can be completely eliminated by a self-locking control mechanism and a correspondingly rigid construction method. This has so far been done very infrequently and it is even questionable whether an adequately stiff construction method is always possible in practice.

The unfavorable influence of free-swinging rudders on flutter behavior can in most cases be reduced to a tolerable limit if the rudders are compensated dynamically around their hinge axis in which one of the three main axes of the inertial ellipsoid of the rudder coincides with its hinge axis and if we moreover avoid contiguity of the natural frequency of the system "rudder-control mechanism" with the natural frequencies of vibration modes of the aircraft capable of inducing oscillation.

Subsequent carrying out of these rules has eliminated in many cases aircraft flutter occurring in the operational range. It is obviously best if these rules are followed already in the construction of an aircraft. Professor Tank told me recently that his aircraft model "Pulqui" with the customary free-swinging rudders was built according to these rules, tested in the static vibration test and then flown, without further investigation, up to supersonic speeds.

If we desire in such cases to carry out previous calculation of flutter for greater safety, we are confronted by the question whether rudders corresponding to the rules listed always increase or decrease the flutter speed as against a comparable model with blocked rudders. If they would always increase the flutter speed, we could then content ourselves with the calculation of the simpler comparable model with blocked rudders for the estimation of a lower limit. Many comparative calculations on spatial wings in the Aerodynamic Experimentation Institute and at Focke-Wulf have shown, however, that a compensated, free-swinging rudder or one flexible through the elasticity of the control mechanism can both increase and decrease the flutter speed as against the comparison model with blocked rudders. The results of these calculations can be made more reliable by improving either the aerodynamic

theory of swinging rudders or introducing experimentally determined aerodynamic forces. However, it is not possible to eliminate a priori the degree of freedom "rudder torsion" without interlock unless all results are to become illusory.

EXPERIMENTAL DETERMINATION OF AERODYNAMIC COEFFICIENTS OF VIBRATING WINGS*

by H. Bergh

ARRANGEMENT:

		Page
1.	Introduction	106
2.	Some Experimental Methods for a Simple Wing	107
3.	Experimental Method for Wing with Aileron	109
4.	Execution of Measurements	110
5.	Experimental Findings for a Simple Wing	111
6.	Experimental Findings for a Wing with Aileron	111
7.	Measurements in Steady Air	113
8.	Influence on the Results of Flutter Calculation	113
9.	Conclusion	114
10.	Literature References	114
	Illustrations	115
	Discussion	130

1. INTRODUCTION

99

The conformity between calculated and actual flutter speed would certainly be better if the flutter engineer had available not only theoretically determined aerodynamic forces but also non-steady aerodynamic forces obtained by measurement. Unfortunately, so far only a very small number of experimental investigations have been carried out and the results are generally not adequate in order to determine all of the aerodynamic coefficients needed for flutter calculation. The lack of experimental findings is caused by the difficulties in making such measurements. In addition to the difficulties with instrumentation even the question for the most suitable experimental procedure is made difficult by the fact that, when we want to measure the total aerodynamic forces, we also always obtain the very high inertial forces at the same time. For this reason, the various experimental methods are generally oriented in the sense of devising suitable installations to compensate

* The lecture was published as report MP 147 of the Dutch National Aviation Laboratory in March 1957.

for the forces of inertia. Only when we measure not the entire aerodynamic forces but the pressure distribution, then the difficulties caused by inertia disappear but additional problems of instrumentation are introduced. Progress in electronics, however, has made today possible quantitative measurement of pressure. We might here point out that H. Drescher was successful, by employing water as the flow medium, in carrying out measurement of pressure on a wing with vibrating rudder by means of a special multiple pressure gauge (1). Recently, several institutes have developed small pressure indicators which are suitable for the measurement of non-steady pressure. Here in the Dutch National Aviation Laboratory, we have also built several pressure indicators for the measurement of pressure on a two-dimensional wing with vibrating rudder.

2. SOME EXPERIMENTAL METHODS FOR A SIMPLE WING

As already mentioned, various arrangements are possible for measurement of the total aerodynamic forces. Fig. 1 shows an experimental method developed in England (2). A bilateral vibration exciter has been built into a rigid frame and the exciter activates one wing in the wind tunnel and a similar system outside of the wind tunnel. The complete frame is suspended from two dynamometers. If the masses are so adjusted without air flow in the tunnel, that no exchange forces are indicated by the dynamometers, there will be measured only the aerodynamic forces under air flow. Although the principle is perfectly sound, difficulties occur in practical execution due to the high weight of the complete frame which makes extremely high demands on the dynamometers.

In the U.S., the Aeroelastic Division of MIT has developed a special exciter which imparts an enforced motion to one wing (3). The principle is shown in Fig. 2. The reactive forces in the suspension point which also contain the forces of inertia, are measured with two dynamometers. It is therefore possible to determine the aerodynamic forces when we initially, in the operative wind tunnel, make the deflections of several built-in acceleration meters equal to the deflections of the dynamometers and when we then compare the deflections of the dynamometers and the acceleration meters by electrical means during the experiments with the wind tunnel in operation. Because the total experimental arrangement possesses rather high mass, the maximum attainable frequency is not very high. For this reason, the accuracy of the acceleration meters must be very high because an error of 1% in the forces of inertia has as consequence a much greater error in the aerodynamic forces.

In the Dutch National Aviation Laboratory, we undertook an extensive series of experiments with the objective of submitting the non-steady, two-dimensional theory of sustentation surfaces to an intensive examination and of making available to the flutter engineer

aerodynamic coefficients obtained by measurements. The method utilized for these experiments as well as the findings for a simple wing and a wing with rudder and a chord ratio $\tau = 0.4$ (by chord ratio is understood the ratio of rudder chord to the chord of the total wing) will be treated in detail in this report.

The experimental arrangement shown in Fig. 3 was utilized for an individual wing (4). A rectangular wing model is located in the wind tunnel along an axis parallel to the span and so that it can be rotated (Fig. 3). The model is connected by a spring with an oscillator. Other springs are needed in order to adjust the median angle of incidence to a given value. If the oscillator creates a harmonic excitation, then the wing will resonate harmonically. The amplitude of this oscillation and its phase difference with the oscillator vibration are entirely determined by the moments around the axis of rotation.

Let us consider first the case without air flow. The moments around the axis of rotation acting on the wing can be divided into:

1) The moment of the forces of inertia T. In the vector representation, the corresponding vector and the oscillation vector have directions opposite to each other (Fig. 4).

2) The retarding moment of the spring R whose vector has the direction of the oscillation vector.

3) The moment of damping D whose corresponding vector has a 90° advance over the vector of the retarding moment R under damping proportional to speed and hysteresis.

4) The oscillator moment E. Its vector and the sum of the vectors of the three moments listed above have the same length but directions opposite to each other because the condition for the equilibrium of the moments must be fulfilled.

The oscillator moment E is determined by the amplitude of the oscillator vibration, the spring constant, the leverage of the force of excitation and the phase angle between the oscillator and the wing vibrations.

If the tunnel air is made to flow over the wing with the velocity V, the original wing amplitude can be retained only if we, by suitable variation of the oscillator moment, compensate the moment of aerodynamic force L. The oscillator moment changed in this manner shall be designated as E_V. Because the wing motion has not changed, the moments T, R and D remain equally large. The vector representation is again shown in Fig. 4. Because the oscillator moment E_V must be equal and opposite to the sum of the vectors of L, T, R, and D, the desired moment of aerodynamic force L can only be determined by measurement of the vectors E and E_V.

The moment of the inertial forces is very much larger than the desired moment of aerodynamic force, and, in general, the vector E will then also be large. This has as consequence that the vector L is constituted by the difference of two large vectors E_V and E which form only a small angle with each other. The accuracy of such a measurement

is not very great because small errors in amplitude and phase of the vectors E_v and E are transmitted in the moment of aerodynamic force with a large increase. Considerable improvement is achieved if, by suitable adjustment of the springs, the vector R is made equally as large as the vector T so that the oscillator moment at $V = 0$ has to overcome only the minor moment of damping. This means that the natural frequency of the system not subjected to air flow is adjusted to the oscillator frequency. The correct adjustment at $V = 0$ is effected by changing the leverage of the springs until the phase angle between wing and oscillator vibrations is exactly 90°. The forces of inertia are therefore compensated in this method by spring tension.

The relation between the moment of aerodynamic force around an arbitrary axis of rotation and the aerodynamic coefficients is shown in Fig. 5. The coefficients k_a, k_b+m_a, m_b (a definition of the coefficients will be found in literature reference 5) can be determined after the moment of aerodynamic force has been measured for at least three positions of the axis. However, it is not possible to determine the magnitudes k_b and m_a individually by means of this experimental arrangement.

Fig. 6 shows a modified experimental installation which makes it possible to measure the coefficient m_a also separately. In this installation, the axis of rotation oscillates so that the wing carries out an oscillatory and torsional vibration which are not connected with each other by a simple geometric term. Through consideration of the equilibrium around the oscillating axis of rotation, it is again possible to find a relation between the moment of aerodynamic force, the vibration of the wing and the oscillator vibration.

3. EXPERIMENTAL METHOD FOR A WING WITH RUDDER

The experimental arrangement shown in Fig. 7 is very suitable for determination of the aerodynamic coefficients for an oscillating wing with rudder (6). The equation of motion of the oscillating system is very similar to that for the simple wing and the moment of aerodynamic force L around the forward axis of rotation is again equal to the vector differential of the oscillator moments E_v and E. For the moment of aerodynamic force, we now obtain an expression which makes possible, in the case of an aerodynamically non-compensated rudder, the determination of $k_c + n_a$, $m_c + n_b$ and n_c when the positions of the axes are varied. If we also measure the moment of aerodynamic force for a rudder with aerodynamic compensation through moving back of the rudder axis, then we can also determine $k_d + r_a$, $m_d + r_b$, $n_d + r_c$ and r_d (7). A special case of the installation illustrated is obtained when we oscillate only the rudder around the rudder axis. By measuring the moment for at least three positions of the rudder axis, we can then determine n_c, $n_d + r_c$ and r_d.

The values of n_b and r_b can then also be measured with the aid of the experimental arrangement shown in Fig. 8. It would be possible in principle to also determine n_a and r_a with this arrangement if we do not let the axis of rotation pass through quarter chord. However, in this case, the influence of n_a and r_a on oscillation is too small to furnish any useful results.

4. EXECUTION OF MEASUREMENTS

The experiments were carried out in an enclosed test section with a height of 1.10 m and a width of 0.80 m. The span of the rectangular model was equal to the width of the test section so that the flow can be regarded as two-dimensional. The symmetric profile had a chord of 0.30 m and was a NACA-0012 profile, scaled down to 7.3% of greatest thickness for the experiments with the simple wing because the wing with rudder also had a NACA-0012 profile.

Fig. 9 shows the three arrangements of the wing and aileron utilized.

The oscillations from the wing and from the oscillator are transformed, by means of electrodynamic oscillation meters, into two alternating tensions whose magnitudes can be determined by a vacuum tube voltmeter. Measurement of phase is carried out as follows. The two alternating tensions first create an ellipse on the screen of an Oscillograph. By means of a special circuit, the phase of the two tensions is changed until the ellipse has been degenerated into a straight line. As soon as this has been accomplished, the activated phase shift is equal to the original phase differential between wing and oscillator vibrations.

In order to obtain the desired values of the reduced frequency ω, the velocity V is changed at constant oscillator frequency so that the Reynold number also changes. In order to examine the influence of the Reynold number, measurements for two values of the oscillator frequency, i.e. 4.17 and 8.33 c/s were then carried out. For each reduced frequency ω, we thereby obtain measurement points which are different by a factor of two in the Reynold number.

Since it is necessary for the accuracy of measurement that the adjusted condition $R = T$ is strictly complied with during the experiments, the oscillator frequency must be kept very accurately to a constant value. For this purpose, the frequency of the oscillator vibration is calibrated against a standard 50-c/s frequency.

During the experiments, the wing amplitudes were kept to a constant value of 1% and the rudder deflection to 1.5%.

Preliminary measurements have shown that it is absolutely necessary to determine the point of transition of the boundary layer because the experimental findings otherwise change appreciably due to the oscillation of the transition point during one period.

5. EXPERIMENTAL FINDINGS FOR A SIMPLE WING

Because the moments of aerodynamic force measured were determined as difference between measurement with and without tunnel air flow, the aerodynamic coefficients obtained no longer contain the constituents effective in steady air. Moreover, the influence of the walls of the wind tunnel was taken into account by means of a theoretically calculated correction.

The theoretically assumed linearity between aerodynamic forces and wing oscillation was confirmed by the experiments. The influence of the Reynold number can be neglected when the point of transition of the boundary layer is established.

The measured values of k_a, k_b, m_a and m_b for 8.33 c/s are represented in Figs. 10, 11, 12, 13 in dependence on the reduced frequency ω. As comparison, the theoretical findings of Kussner have also been plotted. In general, the variations from theory are not very large. The steady values of k_b and m_b plotted agree well with the non-steady values measured.

6. EXPERIMENTAL FINDINGS FOR WING AND AILERON

One difficulty in measurements on a wing with rudder is the problem of the position of the rudder axis in the case of an aerodynamically non-compensated rudder. If we have a plate, we can then, as in theory, let the axis coincide with the rudder nose but this is not as simple for a rudder with finite thickness. In the case where the trailing edge of the fin and the nose of the rudder are formed as two concentric circles, it would seem preferable to locate the reference axis in the center of the circle because the motion of the rudder points located ahead of the center does not influence the flow (burble flow excepted). If the trailing edge of the fin is straight but the nose of the rudder round, experiments have shown that the moment of aerodynamic force around the rudder axis conforms well to the case mentioned above. The reference axis for a rudder with round nose is therefore located in the center of the nose and the chord of the rudder is equated with the distance between reference axis and trailing edge of the rudder.

For a rudder with medium-sharp nose, the reference axis is located in the center of a circle which passes itself through the leading edge of the rudder and touches the profile of the complete wing (Fig. 14), i.e. the assumption here being that the rudder has a round nose.

In order to test these assumptions, the aerodynamic coefficients n_c, $n_d + r_c$ and r_d have been determined from measurements of the moment of aerodynamic force for various rudder arrangements and different positions of the rudder axis. Fig. 15 shows that the three different

values of n_c agree well. However, a comparison with the theoretically calculated values shows that the experimentally determined values are appreciably smaller than the former.

The results of $n_d + r_c$ for two rudder shapes are represented in Fig. 16. The accuracy of measurement is not as good as for n_c but this is not particularly important in flutter calculation because in such a calculation the sum $n_d + r_c$ is multiplied with the small number ε_b, i.e. the ratio between the distance of rudder axis and reference axis and of the half chord. In general, the shape of the rudder results in a relatively constant difference only for the real constituent which points to the fact that the cause lies in the difference of the steady values. The variation between the imaginary constituents for higher values of ω is very probably the result of the small Reynold numbers. Conformity with the theoretical values is not as good.

Fig. 17 shows the coefficient r_d. Here we can also say that the real constituents are different only because of the difference of the steady values (except for the higher values of ω). However, the damping constituents are also different for this coefficient. The comparison with the theory presents another difficulty because, in the theoretical expression for r_d', the slot width $2\tau_{SR}\ell$ occurs, the value of which for a rudder with thickness is not sharply defined. For physical reasons, we therefore selected $2\tau_{SR}\ell$ equal to the distance of the trailing edge of the fin from the point where the actual contour of the rudder touches the profile. In this case, the stationary theoretical values conform relatively well to the measured values extrapolated from $\omega = 0$. However, the behavior of the non-steady measuring points is quite different than the behavior in theory.

Briefly resuming, we can say that the findings listed above have shown that the non-steady behavior of the coefficients n_c, $n_d + r_c$ and r_d is relatively independent of the rudder shape when the reference axis is selected in the manner indicated above.

The other experimentally determined coefficients k_c, n_b, r_b and $k_d + r_a$ are represented together with the corresponding theoretical curves in Figs. 18, 19, 20, 21, and 22.

A few supplementary remarks can be added. The coefficient n_a could not be measured because of its small size. Theoretically, n_a is about 2 to 4% of k_c. The coefficient m_d is not indicated. It could not be determined with sufficient accuracy because the difference of $m_c - \varepsilon_b m_d$ and m_c lay within the order of magnitude of the inaccuracy of measurement. For the flutter calculation, we need only $m_c - \varepsilon_b m_d$ and this expression can then be selected equal to m_c.

The results for a rudder which is equipped with a so-called "pressure seal" (Fig. 9c) for purposes of aerodynamic compensation, have shown that the influence of an extension of the fin can be neglected in comparison with a non-extended arrangement (7).

7. MEASUREMENTS IN STEADY AIR

In order also to compare the theoretical constituents for $V = 0$ with measured values, similar experiments were carried out in a vacuum chamber on a very light wing model with aerodynamically non-compensated rudder (6). The experimental arrangement with two fixed axes of rotation was utilized for the measurements and the experiments were carried out in the following manner:

The natural frequency of the system is first attuned to the oscillator frequency at atmospheric pressure so that a phase differential of 90° exists between the oscillator and model vibrations. We then affix a known mass to the wing which destroys the state of resonance. If then so much air is pumped out that the phase differential is again 90°, we know that the moment of air inertia is equal to the moment of inertia of the mass around the axis. The damping of the air can then be determined from the amplitude ratio between model and oscillator vibrations at the two different pressures. The aerodynamic coefficients were calculated from experiments with different positions of the axes. In order to calculate the individual summands from the sums $k_b + m_a$, $k_c + n_a$ and $m_c + n_b$, it is assumed that the summands occurring in one sum are each time equal to each other.

The values of the inertia constituents shown in Fig. 23 agree well with the theory. Since the theory is valid only for potential flow, there are no theoretical damping constituents for $V = 0$.

On the basis of these results, it would appear permissible to derive the inertia constituent of the different coefficients for a compensated rudder from the theory.

8. INFLUENCE ON THE RESULTS OF FLUTTER CALCULATION

Before I answer this question, I shall mention here the results of some flutter experiments. We calculated already before the start of the measurements that the experimental arrangement with two axes of rotation shown in Fig. 7 would produce flutter under the influence of the theoretical aerodynamic forces for some special positions of the axes. This result was confirmed through the experiment on the wing with aerodynamically non-compensated rudder (6). The experimental findings were compared with calculations based either on theoretically calculated or on measured coefficients. Fig. 24 shows the flutter speed in dependence on the position of the rudder axis. The measured points agreed very well with the calculations utilizing the measured

coefficients. The transition from flutter to divergence are also indicated accurately. These results reinforce confidence in the reliability of the measured aerodynamic coefficients.

Some flutter calculations with the degrees of freedom of deflection and torsion have been carried out for a simple wing (8). It resulted from this that the flutter speed calculated on the basis of the measured coefficients may lie either higher or lower than the theoretical value, depending on the particular case. It will never lie lower than a maximum of 15% (Fig. 25).

For a wing with rudder, we have not yet made any systematic calculations. In one particular case of an aircraft, calculations have shown that the measured coefficients produced intensive flutter whereas almost no flutter was to be expected when utilizing the theoretical coefficients (Fig. 26).

9. CONCLUSION

The results of the experiments can be summarized in the following manner:

1) The assumption of linearity was confirmed by experiment.

2) The Reynold number has an influence which may be neglected when the transition point of the boundary layer has been established.

3) The shape of the rudder has only a very minor influence on the non-steady behavior of the coefficients.

4) The inertia constituents conform very well to the theory.

10. LITERATURE REFERENCES

1. H. Drescher, Eine experimentelle Bestimmung der aerodynamischen Reaktionen auf einen Flugel mit schwingendem Ruder. Oesterreich. Ingenieur-Archiv IV (1950), p. 270-290.
2. W. G. Molyneux, Measurements of the aerodynamic forces on oscillating aerofoils. AGARD Report 35 (1956).
3. R. L. Halfman, Experimental aerodynamic derivatives of a sinusoidally oscillating airfoil in two-dimensional flow. NACA TN 2465 (1951).
4. J. H. Greidanus, A. I. van de Vooren, H. Bergh, Experimental determination of the aerodynamic coefficients of an oscillating wing in incompressible, two-dimensional flow. Nat. Aero. Res. Inst. (NLL) Rep. F 101, 102, 103, 104 (1952).
5. H. G. Küssner, L. Schwarz, Der schwingende Flugel mit aerodynamisch ausgeglichenem Ruder. Luftfahrtforschung 17 (1940), p. 337-354.
6. H. Bergh, Experimental determination of the aerodynamic forces on an oscillating wing with control surface in incompressible, two-dimensional flow. Nat. Aero. Res. Inst. (NLL), Rep. F 175 (1955).
7. H. Bergh, Experimental determination of the aerodynamic forces on an oscillating wing with an aerodynamically balanced flap in incompressible, two-dimensional flow. Nat. Aero. Res. Inst. (NLL), Rep. F 205 (1957).

8. H. Bergh, J. Ijff, Applications of experimental aerodynamic coefficients to flutter calculations. Nat. Aero. Res. Inst. (NLL), Rep. F 122 (1952).

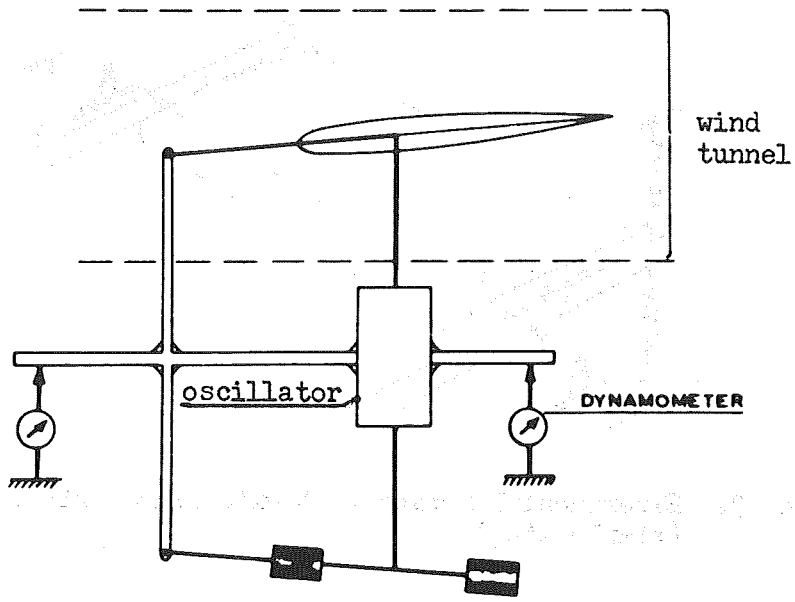

Fig. 1. Example of experimental arrangement developed in England.

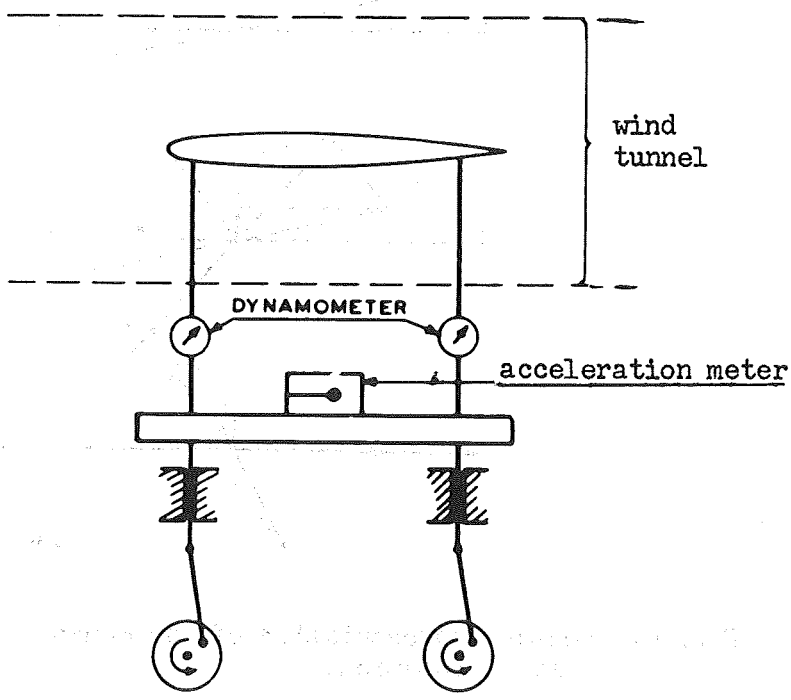

Fig. 2. Diagram of experimental arrangement developed at MIT.

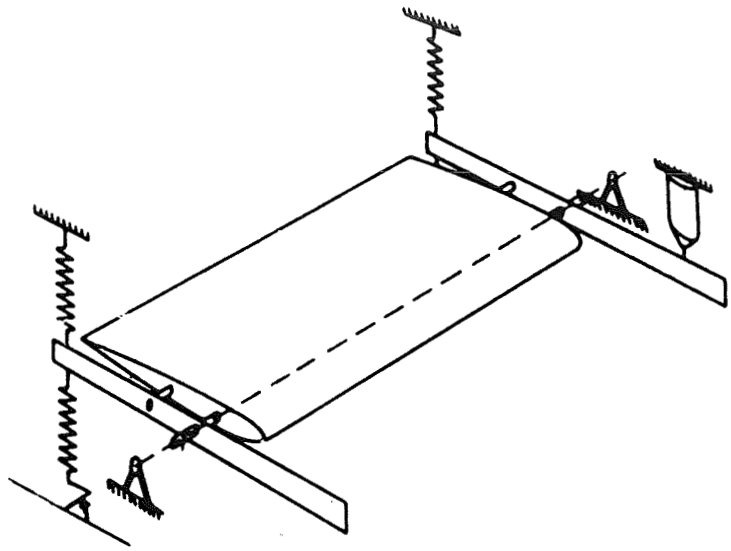

Fig. 3. Experimental arrangement with fixed axis of rotation (simple wing).

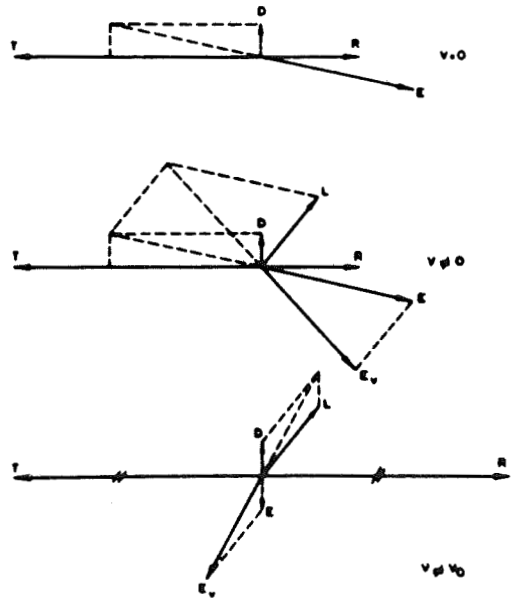

Fig. 4. Vector representation of the moments around the axis of rotation.

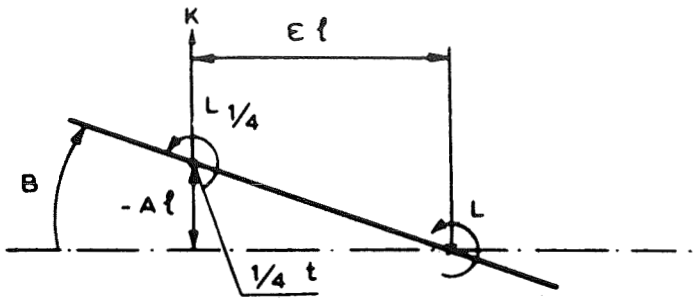

$$L = L_{1/4} - K.\varepsilon.\ell$$

$$\cdot \pi \rho v^2 \ell^2 b \left\{ \varepsilon^2 k_a - \varepsilon(k_b + m_a) + m_b \right\} e^{ivt}$$

Because $A = -\varepsilon B$

Fig. 5. Expression for the moment of aerodynamic force around an arbitrary axis of rotation.

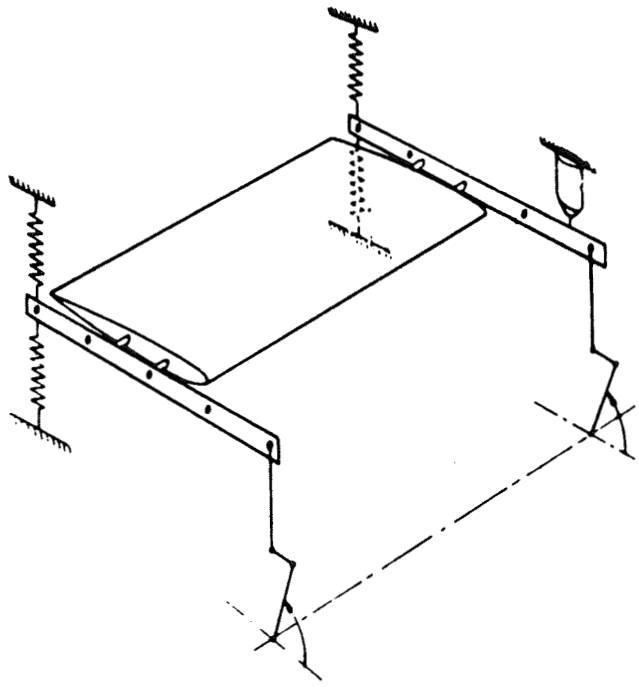

Fig. 6. Experimental arrangement with oscillating axis of rotation (simple wing).

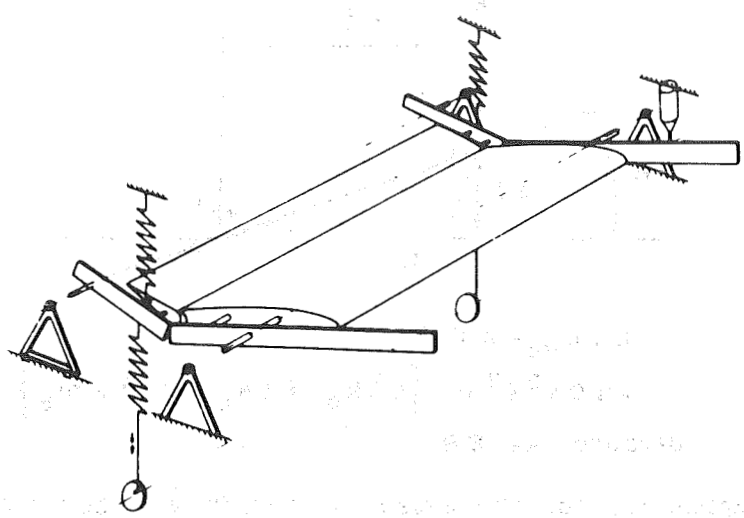

Fig. 7. Experimental arrangement with two fixed axes of rotation (wing with rudder).

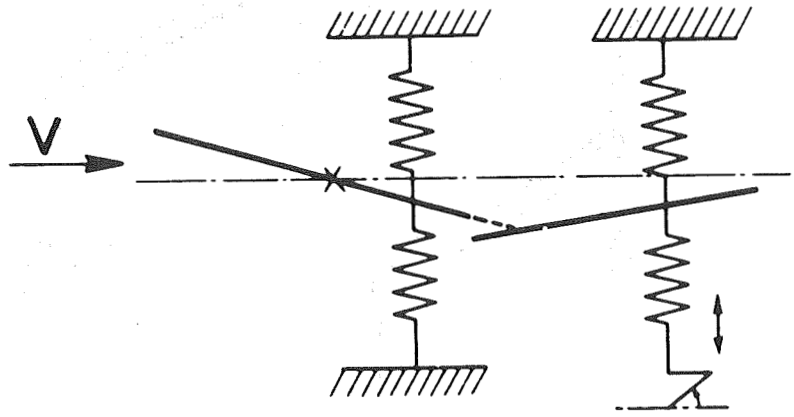

Fig. 8. Basic experimental arrangement for the determination of the coefficient n_b and r_b.

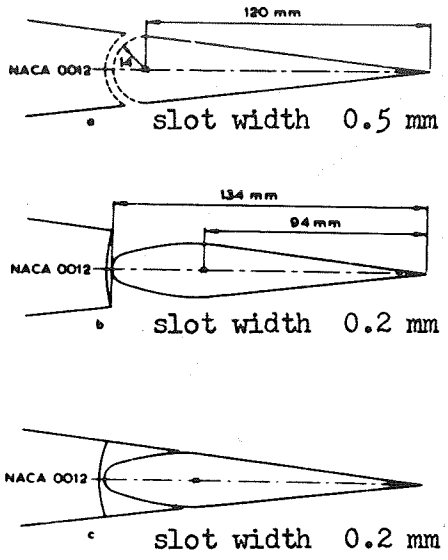

Fig. 9. Wing and rudder arrangements employed.

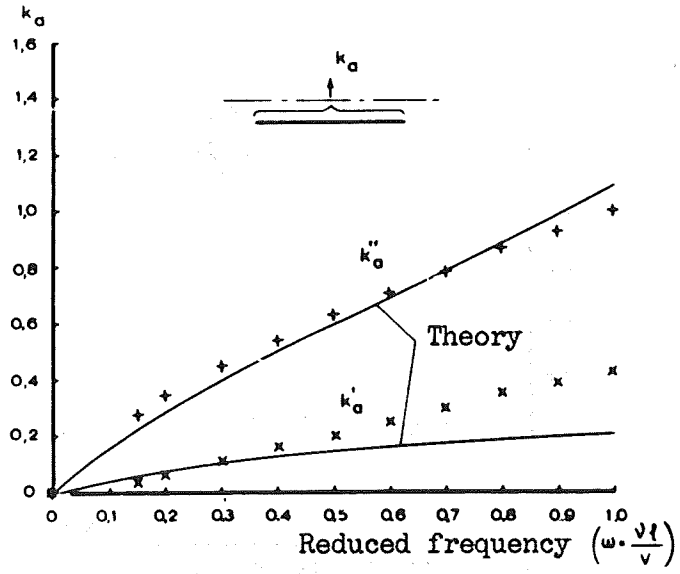

Fig. 10. Coefficient k_a in dependence on reduced frequency ω.

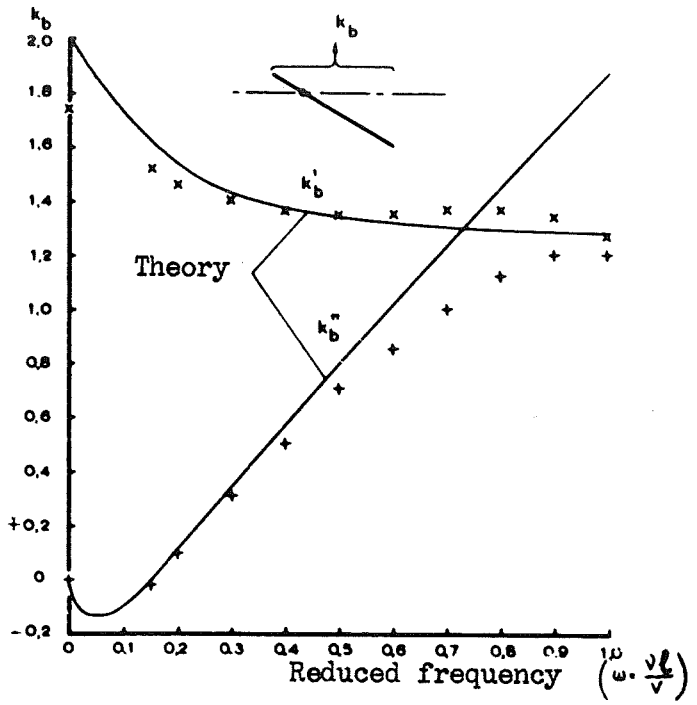

Fig. 11. Coefficient k_b in dependence on reduced frequency ω.

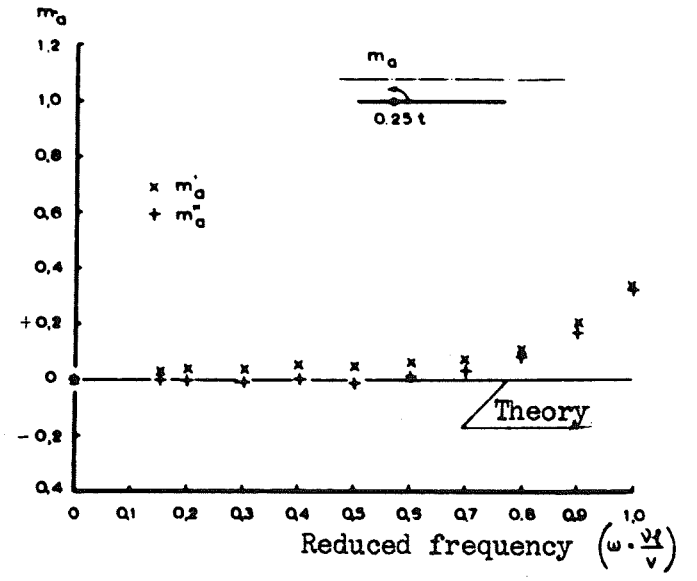

Fig. 12. Coefficient m_a in dependence on reduced frequency ω.

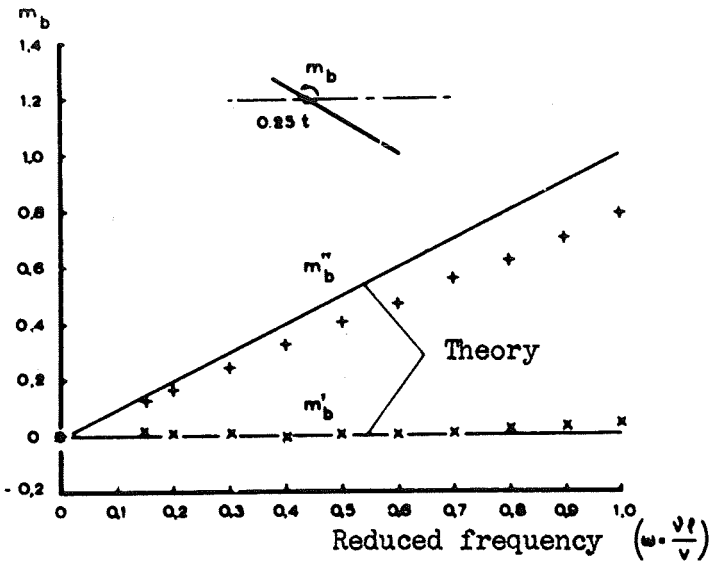

Fig. 13. Coefficient m_b in dependence on reduced frequency ω.

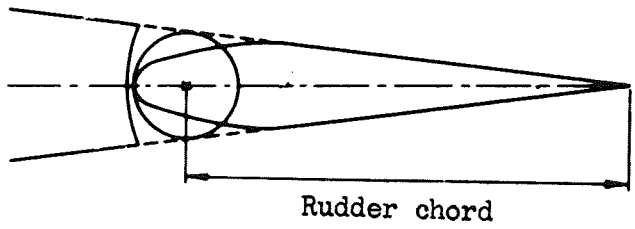

Fig. 14. Position of rudder axis of an aerodynamically non-compensated rudder.

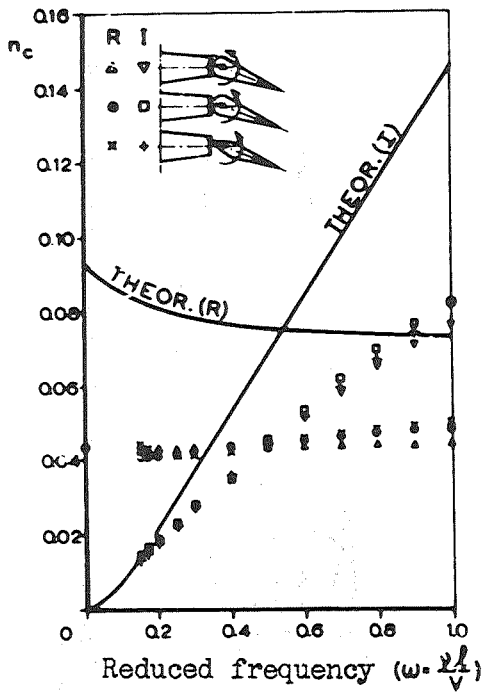

Fig. 15. Coefficient n_c determined by measurements of three different rudder arrangements.

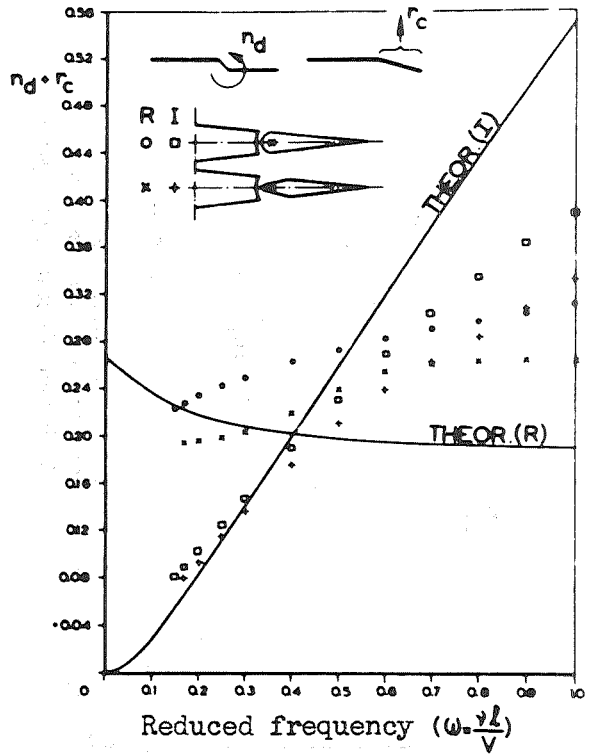

Fig. 16. Coefficients $n_d + r_c$ in dependence on reduced frequency ω for two rudder shapes.

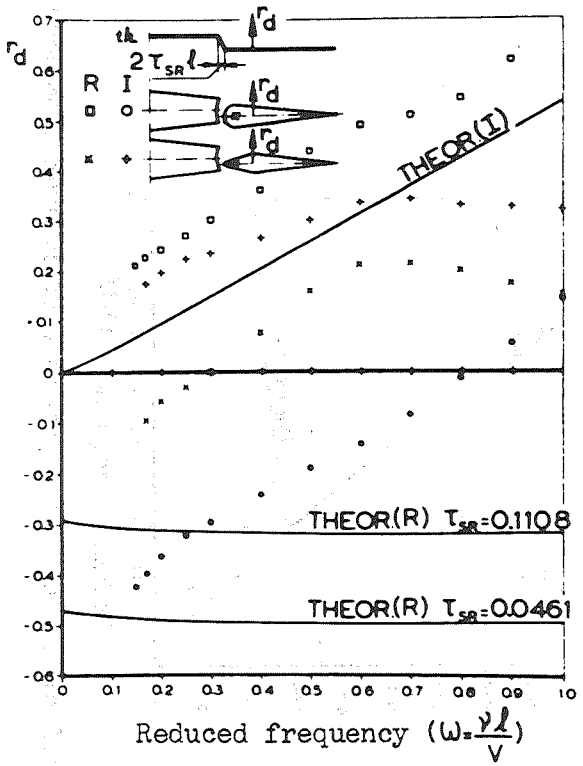

Fig. 17. Coefficient r_d in dependence on reduced frequency ω for two rudder shapes.

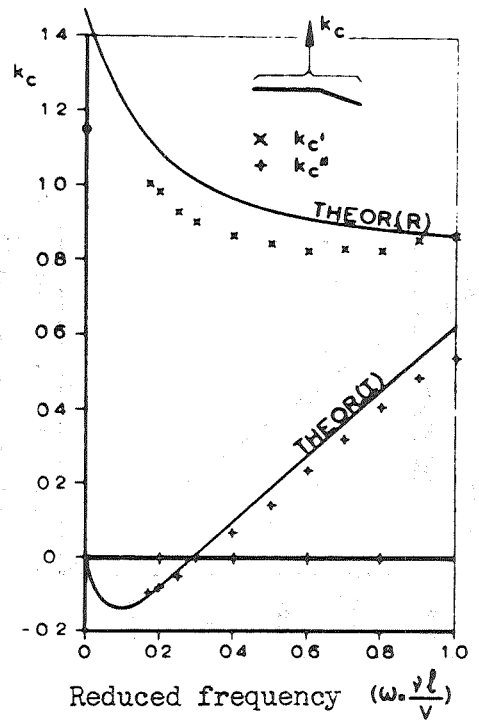

Fig. 18. Coefficient k_c in dependence on reduced frequency ω.

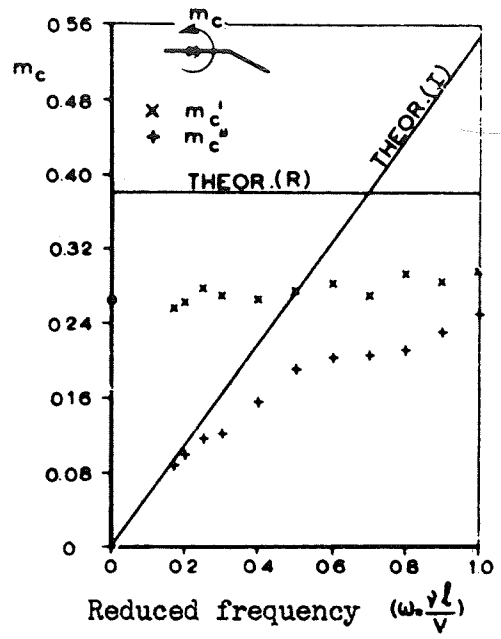

Fig. 19. Coefficient m_c in dependence on reduced frequency ω.

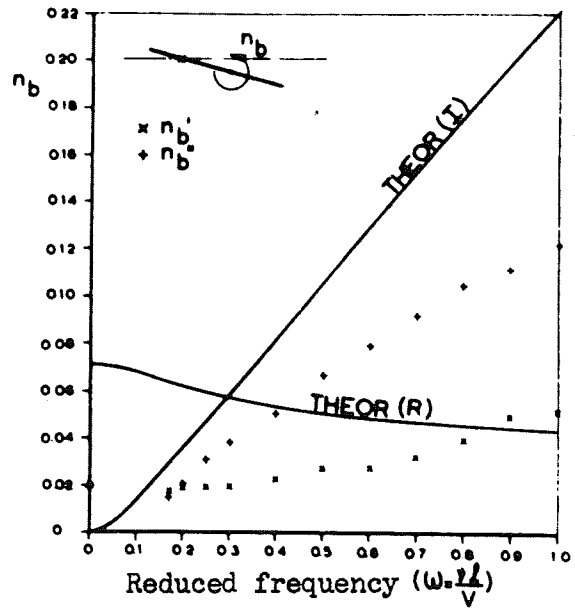

Fig. 20. Coefficient n_b in dependence on reduced frequency ω.

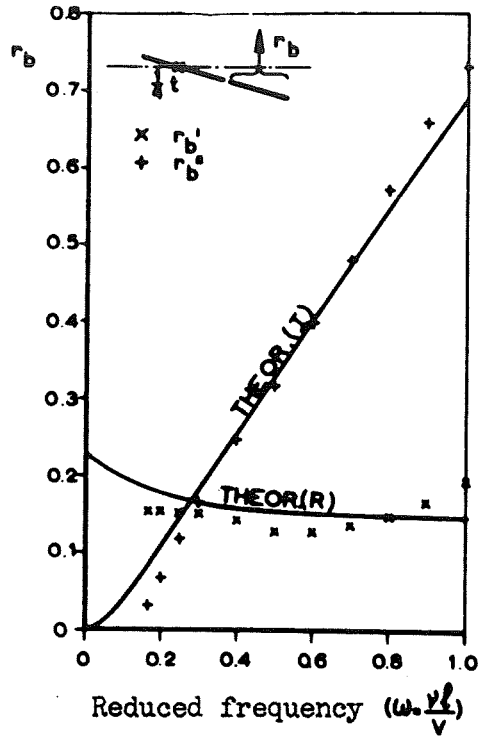

Fig. 21. Coefficient r_b in dependence on reduced frequency ω.

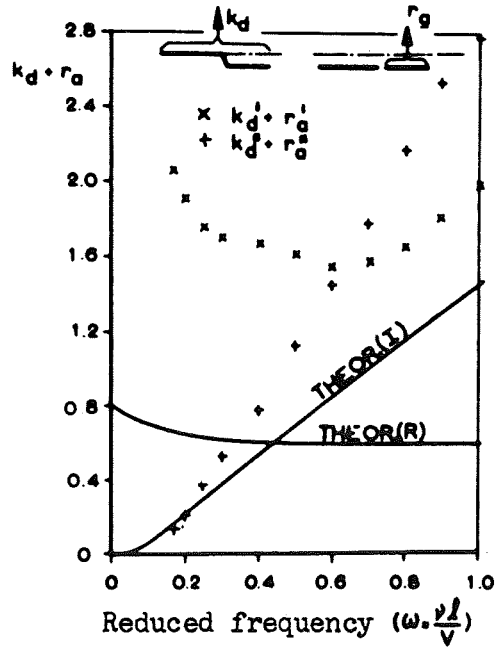

Fig. 22. Coefficient $k_d + r_a$ in dependence on reduced frequency ω.

Coefficients for V = 0		
Coefficient	Measured value	Theoretical value
$\frac{k_a}{\omega^2}$	-0.997 + 0.087 i	-1.0
$\frac{k_a}{\omega^2} = \frac{m_a}{\omega^2}$	-0.479 + 0.069 i	-0.5
$\frac{m_b}{\omega^2}$	-0.368 + 0.063 i	-0.375
$\frac{k_c}{\omega^2} = \frac{n_a}{\omega^2}$	-0.138 + 0.016 i	-0.125
$\frac{m_c}{\omega^2} = \frac{n_b}{\omega^2}$	-0.0993 + 0.020 i	-0.104
$\frac{n_c}{\omega^2}$	-0.0362 +0.0033 i	-0.0343

Fig. 23. Coefficients for V = 0

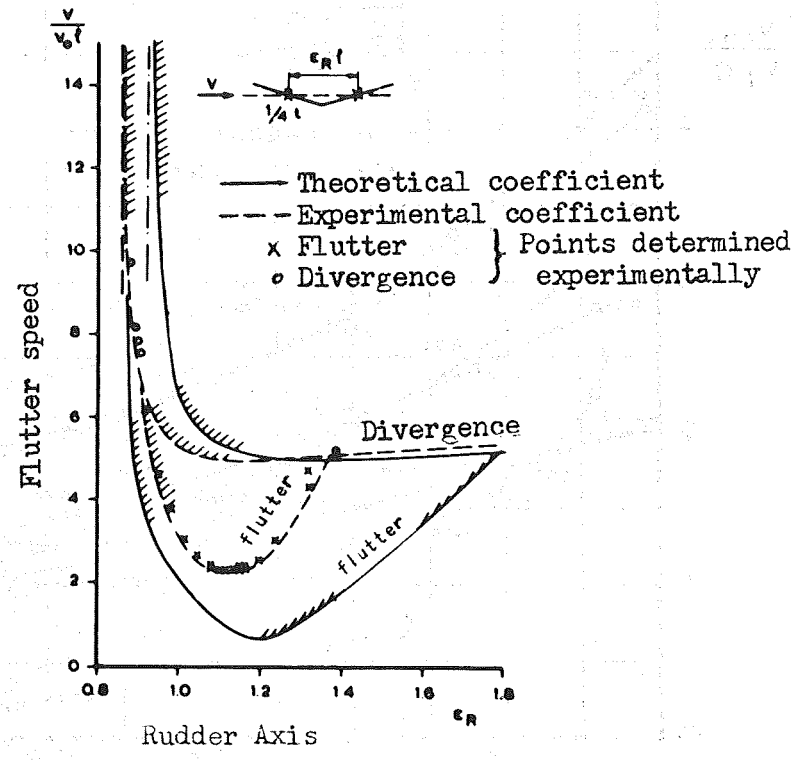

Fig. 24. Results of flutter experiments on wing with rudder.

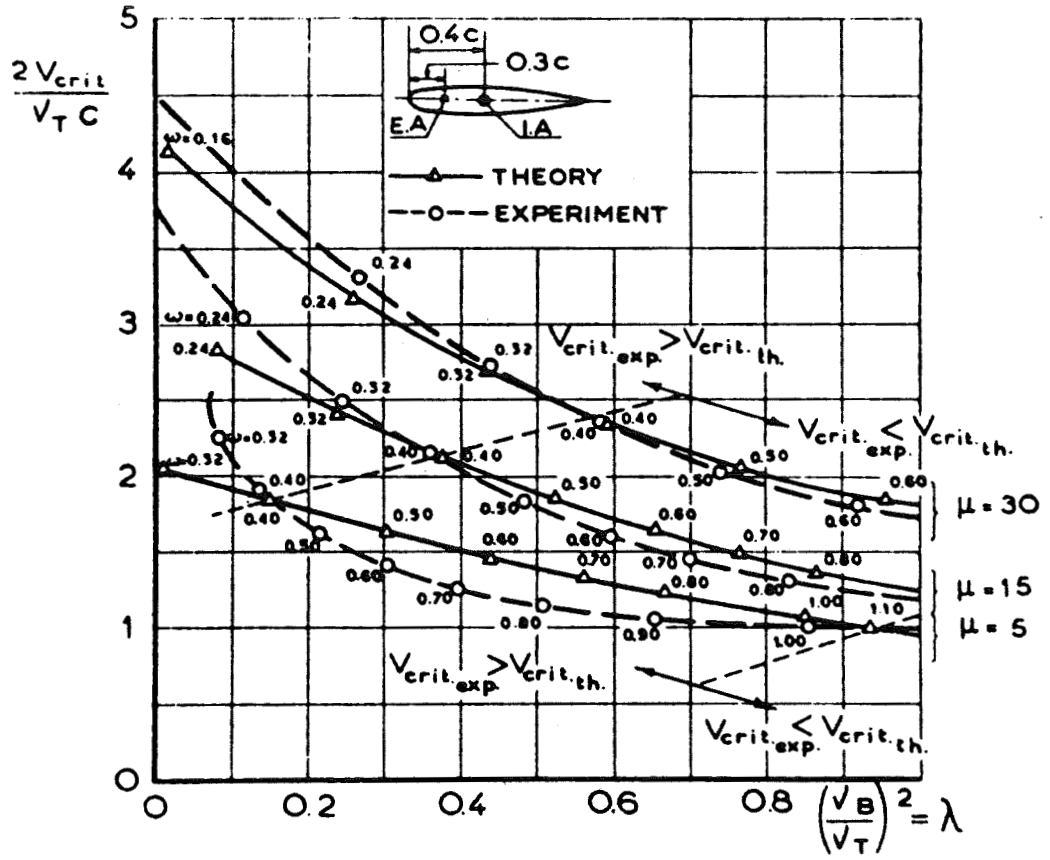

Fig. 25. Flutter speed calculated with theoretical and with measured aerodynamic coefficients.

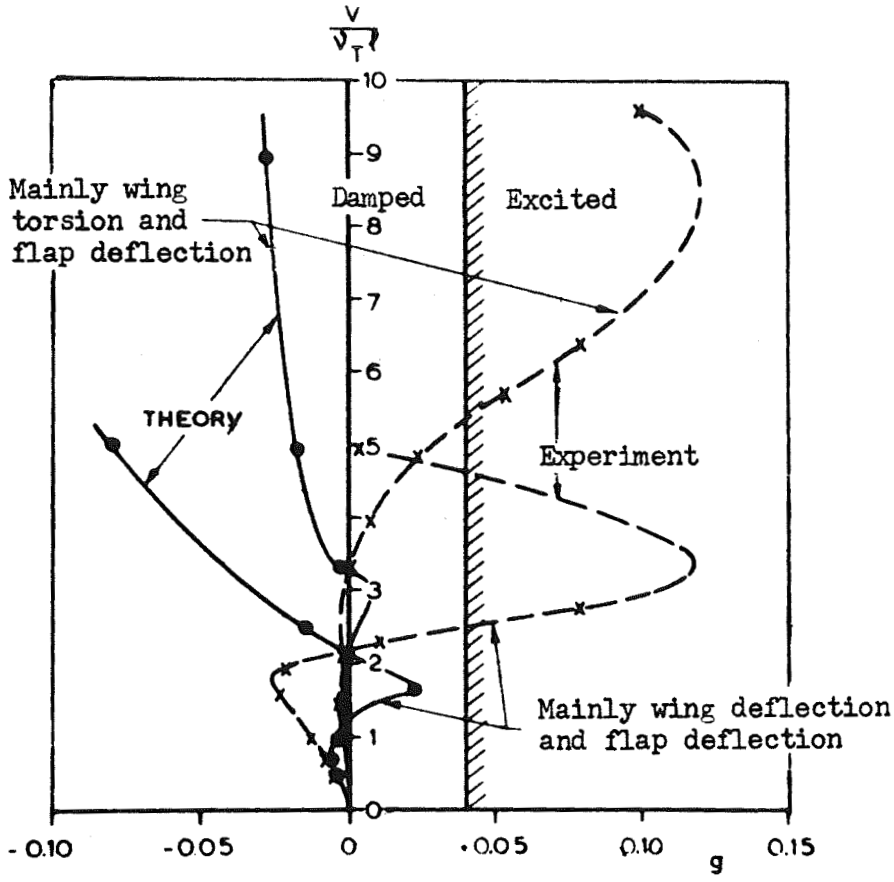

Fig. 26. Results of flutter calculation for a specific aircraft.

DISCUSSION

Küssner: Your measurements may well be characterized as the best ones existing of their kind. I do have the following question: How did you take into account the frictional boundary layer on the walls? We do need a steady /level?/ flow. Did you place the wall in a wedge /acute?/ angle so that the friction layers at the wing ends will not interfere?

Bergh: The friction layer at the measuring point is very thin and has only a very small influence. However, we did effect a small correction by replacing the actual span of the wing model of 0.800 m by an effective span of 0.795 m.

Küssner: In the theory, the down-flowing /down-wash?/ vortical layer has an infinite length but it dissolves rapidly in the diffusor of the wind tunnel. This produces differences as compared to a wing in the open atmosphere.

Bergh: We utilize a diffusor so that the distribution of velocity is very well maintained two-dimensionally and only the velocity itself is reduced. Calculations have been made in which the drop in velocity behind the wing was introduced. The result shows only a slight deviation (about 2%) from the usual theoretical results. The circumstance that the vortical layer does not have an infinite length produces appreciable deviations only when the vortical layer has a length of only a few wing chords. In our case, the dissolution of the vortical layer took place after more than 50 wing chords.

Küssner: How has the influence of the walls been considered? Perhaps by a calculation according to R. Timman?

Bergh: We corrected the measurements with the aid of the Timman theory.

van de Vooren: Corrections are necessary especially at reduced frequencies in the vicinity of 1/4.

Küssner: These are corrections which somewhat improve the comparison between theory and measurements. In the theory, so far calculations have been carried out unfortunately only for the infinitely thin plate. We should endeavor to consider the finite wing thickness. Such investigations are under way in the Aerodynamic Experimentation Institute (Dr. von Gorup). The boundary layer should also be taken into consideration. What explanation do you have for the deviations between the result of the measurements and the results of the theory of the infinitely thin plate?

Bergh: The influence of the boundary layer is here especially important. If we consider only the wing thickness in calculations, this will by itself probably bring about no great improvement.

Küssner: This is also our opinion. The consideration 122
of plate thickness is only a first step. With the infinitely thin plate, we enter into certain difficulties when calculating the boundary layer at the leading edge. Have you tried any calculations of the boundary layer?

Bergh: No, we have not carried out non-steady boundary-layer calculations.

Küssner: This will be rather difficult for the infinitely thin plate.

van de Vooren: In general, the deviations on the wing are about 10%. Greater deviations occur at the rudder. Experimental determination of the rudder coefficients is very important. This will make it possible to increase the accuracy of the flutter calculations appreciably.

Küssner: One picture did show that the non-stable range reaches much further to the right when considering the experimental coefficients.

van de Vooren: The determination of the theoretical rudder coefficients is also very difficult. Because of the hypothesis of the wing as an infinitely thin plate, the rudder chord, the dimension of the rudder ahead of the axis as well as the slot width, for example, are not definitely established.

Merbt: There is an additional effect. The condition of Kutta is no longer fulfilled. At rapid oscillations, the stagnation point at the trailing edge oscillates in phase-shift around the trailing edge. An indication of this effect can be found already in the measurements by Drescher in the water channel of the Aerodynamic Experimentation Institute. We have made corresponding observations in the smoke channel.

Bergh: Yes, this is correct. In general, in the actual oscillating wing, two effects occur which are not considered in the potential theory. The first of these is the influence of the boundary layer and the second is the circumstance that the condition of Kutta is not fulfilled at all times. If we include the thickness of the non-symmetric boundary layer in the calculations, then the mean camber line will change. This effect is approximately covered in a semi-empirical theory by W. P. Jones. N. Rott has pointed out this second effect and also devised a semi-empirical theory in which the condition of Kutta is replaced by a certain ratio between the singularities at the leading and at the trailing edges of the wing. In the Dutch National Aviation Laboratory, Bosschaart combined the two theories so that we can include simultaneously in the calculations both of the effects referred to above. His work is not yet entirely completed.

Merbt: Are the values in the table of Fig. 23 independent of the frequency?

Bergh: Yes. Experiments in a vacuum channel at 4 and 8 c/s show scarcely any deviation.

de Vries: These measurements produce a very valuable confirmation of the practical methods employed by us. We enter into flutter calculation with corrected non-steady aerodynamic forces and such correction is made from the existing wind tunnel or flight measurements of the steady coefficients for the corresponding construction model.

DETERMINATION OF NON-STEADY AERODYNAMIC FORCES AT M = 0 THROUGH ELECTRIC ANALOGY (POTENTIAL TANK)

by H. Merbt and S. Hansson

SUMMARY

For several years, the Institute of Flight Technics of the Royal Institute of Technology at Stockholm has available an electric-potential tank for the determination of non-steady aerodynamic forces at M = 0. A description of the method of utilization is given by Landahl and Stark (5). This report is discussed in the first part of the lecture. In the second part, the practical execution of the measurements in a three-dimensional tank is explained (example: rectangular wing; acknowledgement is here made for permission by the SAAB Company in Linkoping to use a number of illustrations from KTH Aero Rapport FI 158 in this lecture).

ARRANGEMENT:

		Page
	Part I.	133
1.	Basic Theory and Method of Solution for Two-Dimensional Cases (H. Merbt).	133
	1.1 Formulation of Problem	133
	1.2 Arrangement of Problem for Solution by Analogy	133
	1.3 Potential-Tank Analogy for Two-Dimensional Wings	136
	1.4 Extension to M > 0	137
	Part II	138
2.	Execution of Measurements in Three-Dimensional Potential Tank and Findings for Rectangular Wings (S. Hansson).	138
	2.1 Construction of Potential Tank; General Remarks on Measuring Apparatus.	138
	2.2 Relation Between Electric and Aerodynamic Values	139
	2.3 Determination of the Preliminary Integral.	140
	2.4 Calibration of Potential Tank.	142
	2.5 Method for Solution.	143
	2.6 Example of Rectangular Wing.	144
	2.7 Suggestions for Further Development of Potential Tank. . .	146
3.	Literature References	147
	Illustrations	148
	Discussion.	165

PART I

1. BASIC THEORY AND METHOD OF SOLUTION FOR TWO-DIMENSIONAL CASES (H. MERBT)

1.1 Formulation of Problem

For the ideal incompressible fluid, the wave equation of non-steady aerodynamics is reduced both for the velocity potential Φ as well as for the acceleration potential φ to the Laplace equation

$$\phi_{xx} + \phi_{yy} + \phi_{zz} = 0 \quad , \tag{1}$$

which must be solved for the predetermined boundary conditions (cf. 1). The difficulties in the solution of this problem in the case of an arbitrary shape of wing with an arbitrary mode of oscillation and frequency are well known.

For the corresponding steady wing problem, solutions by analogy have been indicated by Legras, Malavard, Duquenne and Campbell (2, 3, 4) during the years after the war. A corresponding solution for the non-steady wing problem was developed by M. Landahl in collaboration with D. Stark in Stockholm during 1951 and 1952. Their paper, published in 1953 (5), contains the results of measurements in a two-dimensional potential tank, in addition to a description of the theoretical principles. This report is discussed in the first part of the lecture.

The second part contains a discussion of the practical utilization of the method by analogy in three-dimensional cases as well as the results of measurements on a rectangular wing (taken in part from 6).

1.2 Arrangement of Problem for Solution by Analogy

The development of a method of solution by analogy for the non-steady case produces some additional difficulties by comparison with the steady problem. We know that the non-steady potential is a complex function so that it is always necessary to solve two inter-related problems instead of only one, in order to determine the phase angle of the aerodynamic forces as against the wing motion. On the other hand, compliance with the boundary conditions in the wake makes it necessary for the velocity potential to be here a harmonic function (in the direction of the basic flow). This difficulty can be eliminated by utilization of the acceleration potential but then acquires a disagreeable singularity at the leading edge.

It is possible to overcome these difficulties through the introduction of a special pressure potential ψ , in accordance with

$$\Psi = \int_{-\infty}^{x} \bar{\varphi}\, d\xi \quad , \tag{2}$$

in which

$$\varphi = \bar{\varphi} \cdot e^{i\nu t} \tag{3}$$

and correspondingly

$$\phi = \bar{\phi} \cdot e^{i\nu t} \tag{4}$$

is applied. The potential Ψ also satisfies the (Laplace) equation 1.

Between velocity potential ϕ and acceleration potential φ, there exists the following connection:

$$\phi(x, y, z, t) = \frac{1}{U} \int_{-\infty}^{x} \varphi(\xi, y, z, t - \frac{x-\xi}{U})\, d\xi \quad , \tag{5}$$

or, with the aid of equations 3 and 4 and the designation

$$\omega = \frac{\nu \cdot \ell}{U} \quad , \tag{6}$$

$$\bar{\phi}(x, y, z) = \frac{1}{U} \int_{-\infty}^{x} \bar{\varphi}(\xi, y, z)\, e^{-\frac{i\omega(x-\xi)}{\ell}}\, d\xi \quad . \tag{7}$$

In this, U = the velocity of the incident flow and ℓ = appropriate reference length. $0, \varphi$ and consequently also Ψ are odd functions in z and it is therefore sufficient to consider the half-space $z \geq 0$. Outside of wing and wake, $\Psi = 0$ in the plane $z = 0$.

Ψ_x is proportional to pressure and must therefore vanish in the wake. This produces, with $x_{\text{trailing edge}} = x_{T.E.}$:

$$\Psi(x, y, +0) = \Psi(x_{T.E.}, y, +0) \quad \text{for} \quad x \geq x_{T.E.} \quad \text{in wake.} \tag{8}$$

The condition of Kutta at the trailing edge is fulfilled by the requirement that Ψ and Ψ_x must be steady here. This produces, for the analogy, the equivalent requirement that

$$\Psi_z(x_{T.E.} - 0, y, z) = \Psi_z(x_{T.E.} + 0, y, z) \tag{9}$$

must be valid. At a large distance from wing and wake, Ψ and all its deviations should vanish.

The boundary condition on the wing itself is obtained in the following manner: if we partially integrate equation 7 in regard to x and partially differentiate subsequently after z, we then obtain for $z = o$

$$\overline{\phi}_z = \overline{W}(x, y, 0) = \frac{1}{U}\left[\Psi_z - \frac{i\omega}{\ell}\int_{-\infty}^{x} \Psi_z(\xi)\, e^{-i\omega\frac{x-\xi}{\ell}}\, d\xi\right] . \tag{10}$$

The velocity amplitude $\overline{W}$ at the location of the wing is determined from the (predetermined) wing motion

$$z = f(x, y)\, e^{i\nu t} \tag{11}$$

as

$$\overline{\phi}_z = \overline{W}(x, y, 0) = i\nu f + U f_x . \tag{12}$$

Correspondingly,

$$\overline{\varphi}_z = i\nu \overline{W} + U \overline{W}_x . \tag{13}$$

If we apply $x = x_{L.E.}$ (L.E. = leading edge) in equation 10 and combine the equation obtained with equation 13, integrated between $x_{L.E.}$ and x, there then follows

$$\Psi_z(x, y) = U\overline{W}(x, y) + i\nu \int_{x_{L.E.}}^{x} \overline{W}\, d\xi + \frac{i\omega}{\ell} I(y) , \tag{14}$$

in which

$$I(y) = \int_{-\infty}^{x_{L.E.}} \Psi_z\, e^{-i\omega\frac{(x-\xi)}{\ell}}\, d\xi . \tag{15}$$

The normal derivation of our potential Ψ on the wing surface consequently consists of a known constituent which contains only $\overline{W}$ and an unknown constituent $I(y)$.

Because of the linearity of the problem, we can write this

$$\Psi = \Psi_1 + \Psi_2 \quad , \tag{16}$$

so that

$$\Psi_{1_z} = U\overline{W} + i\nu \int_{x_{L.E.}}^{x} \overline{W}\, d\xi \tag{17}$$

and

$$\Psi_{2_z} = \frac{i\omega}{\ell} I(y) = \frac{i\omega}{\ell} I_1(y) + \frac{i\omega}{\ell} I_2(y) \quad , \tag{18}$$

if we correspondingly define

$$I_1(y) = \int_{-\infty}^{x_{L.E.}} \Psi_{1_z}(\xi, y)\, e^{-\frac{i\omega(x-\xi)}{\ell}}\, d\xi \quad , \tag{19}$$

$$I_2(y) = \int_{-\infty}^{x_{L.E.}} \Psi_{2_z}(\xi, y)\, e^{-\frac{i\omega(x-\xi)}{\ell}}\, d\xi \quad . \tag{20}$$

For the constituent Ψ_1, we therefore obtain a boundary-value problem entirely analogous to the steady problem. The normal derivation of the potential Ψ_1 is predetermined everywhere on the wing and Ψ_1 as well as $I_1(y)$ can be determined in the potential tank. However, in the normal derivative for Ψ_2, only the constituent $I_1(y)$ is known but not $I_2(y)$ which must be determined.

1.3 Potential-Tank Analogy for Two-Dimensional Wings

In the two-dimensional case, the determination of $I_2(y)$ is possible accurately because the function here is not dependent on y so that we can apply

$$\Psi_{2_z} = a_o \qquad \text{(on the wing)} \quad . \tag{21}$$

From equation 18, there then follows

$$a_o = \frac{i\omega}{\ell} I_1 + \frac{i\omega}{\ell} a_o G_o \tag{22}$$

or

$$a_o = \frac{\frac{i\omega}{l} I_1}{1 - \frac{i\omega}{l} G_o} \quad , \tag{23}$$

in which G_o must be determined, according to equation 15, as the I belonging to the Ψ_z distribution $\Psi_z = 1$.

For further treatment, the above equations must be separated into real and imaginary constituents before the coefficients of aerodynamic forces can be written in the customary manner. These calculations have been carried out in (5) where information is given also on the results of two-dimensional control measurements. The results obtained by measurements in the potential tank agree well with known theoretical results (Fig. 1 shows the two-dimensional potential tank of the Royal Institute of Technology of Stockholm). The same satisfactory conformity between theory and findings by analogy is later shown also in the case of three-dimensional measurements on a rectangular wing and is discussed in detail in Part II (cf. 6). We here want to point out merely the possibility of deriving results for $M > 0$ from the results obtained for $M = 0$.

1.4 Extension for $M > 0$

The results obtained for $M = 0$ can be used in principle to prepare solutions for other subsonic Mach numbers. For example, we can proceed as follows:

The linearized fundamental gas-dynamic equation on which the calculations of non-steady aerodynamics are based, can be converted, through simple transformations, in a simpler "acoustic" wave equation

$$\Delta \underline{\Phi} + k^2 \underline{\Phi} = 0 \tag{24}$$

in which $k = \frac{\omega M}{1-M^2}$.

Equation 24 is solved by the integral equation

$$\underline{\Phi}_Z = -\frac{1}{4\pi} \iint_S \gamma \frac{\partial^2}{\partial Z^2} \left(\frac{e^{-ik\bar{r}}}{\bar{r}}\right) d\xi \, d\eta \quad , \tag{25}$$

in which S designates the wing surface and $\bar{r} = \sqrt{(X-\xi)^2 + (Y-\eta)^2 + Z^2}$.
If we write equation 25 in the form

$$\Phi_Z + K = -\frac{1}{4\pi} \iint_S \gamma \frac{\partial^2}{\partial Z^2} \left(\frac{1}{\bar{r}}\right) d\xi \, d\eta \quad , \tag{26}$$

with

$$K = \frac{1}{4\pi} \iint_S \gamma \frac{\partial^2}{\partial Z^2} \left(\frac{e^{-ik\bar{r}} - 1}{\bar{r}}\right) d\xi \, d\eta \quad , \tag{27}$$

equation 26 can then be regarded as the integral equation of an equivalent incompressible problem with $(\Phi_Z + K)$ as predetermined function of downwash at the location of the wing surface. With this, equation 26 can be solved in the tank. According to a suggestion by W. P. Jones (Arc 15, 642, 1953), equation 26 can be solved approximately when we apply $\gamma = \sum a_n \gamma_n$ and determine the coefficients a_n through appropriate assumptions for the distribution functions γ_n. The distribution functions γ_n are here selected by approximation to known results, e.g. corresponding to the distribution functions in the incompressible case for the respective form of wing and mode of oscillation.

Calculations similar to this suggestion were carried out successfully for the two-dimensional problem at Stockholm in 1952 with the purpose of investigating the influence of compressibility at high frequency parameters close to $M = 0$.

We can therefore proceed so that equation 26 is first solved for $M = 0$ $(K = 0)$ in the potential tank and then, starting from this solution, treat the actual problem for $M \neq 0$ either purely numerically or, again by using equation 26 iteratively, in the potential tank.

PART II

2. EXECUTION OF MEASUREMENTS IN THE THREE-DIMENSIONAL POTENTIAL TANK AND FINDINGS FOR RECTANGULAR WINGS (S. HANSSON)

The method by analogy described in Part I was developed and further improved by the Royal Institute of Technology in Stockholm for the three-dimensional wing (cf. V. J. E. Stark; M. T. Landahl: Bestamning av instationara luftkrafter pa rektangular vinge med hjalp av potentialtanks-analogi. KTH AERO RAPPORT FI 158 (1954) (unpublished).

2.1 Construction of Potential Tank; General Remarks on Instrumentation

The three-dimensional tank consists of a glass tank (inside dimensions 1390 x 800 x 800 mm) and supported on a vibration-free base (Fig. 2). Ordinary tap water is used as electrolyte. The electrode

model consists of silver foil glued to a plexiglass plate. The plate is located so in the water that the electrodes are just covered by the water.

The electrode model is separated into the following parts:

Wing and wake area;

Advance electrodes (in the direction of flow ahead of the wing electrodes);

Remainder area of the x,y-plane (Fig. 3).

The desired potential Ψ is represented in the analogy by the electric potential E in the electrolyte. Compliance with the boundary conditions is accomplished as follows: the electrodes representing the area exterior to wing and wake receive potential zero (i.e. they are grounded).

The wing electrode on which the z-derivation (current density) is to assume specified values, is divided into a number of sections insulated from each other. In each section, the total currents through the surface must be equal to the integral value of the specified current density above the corresponding wing section.

The wake area is represented by small electrodes parallel to the direction of flow. In order to comply with the Kutta condition at the trailing edge of the wing, these electrodes receive the same potential as the last wing electrode in the same section.

In order to make the apparatus as simple as possible, half-models are utilized. In case of symmetric modes of oscillation, one lateral (glass) wall is utilized as plane of reflection for this. In cases of assymmetric modes of oscillation, we obtain reflection plus inversion through a metal electrode along the lateral wall (zero potential in the center plane).

Adjustment and measurement of current density is made by means of a bridge circuit (Fig. 4). For each electrode, this consists of a potentiometer for adjustments of the predetermined current density through the wing electrodes by measurement of the voltage drop through an interposed resistance. Measurement in the bridge circuit affords independence from tension as well as greater accuracy (utilization of a zero-indicator oscillograph).

Because of interaction between the individual electrodes, adjustment must be corrected until the specified values have been reached.

Measurement of current density in the advance electrodes is made by interposition of a variable resistance and equilibration so that the potential assumes the value zero in accordance with the boundary condition. The current through the variable resistance then corresponds to the desired z-derivation of the potential.

2.2 Relation Between Electric and Aerodynamic Values

$$j_z = -\sigma \frac{\partial E}{\partial z} \quad , \tag{1}$$

is generally valid (first law of Ohm) in which

j_z = vector of current density perpendicular to wing plane;

σ = conductivity of electrolyte;

E = electric potential.

In the analogy, j_z is measured by the voltage drop across an interposed resistance R so that

$$j_z = \frac{\alpha E_o}{R \Delta A} \tag{2}$$

in which

E_o = measuring tension;

αE_o = voltage drop;

ΔA = size of electrode surface.

If we apply

$$\Psi_z = C_1 \alpha \ , \tag{3}$$

in which Ψ_z is the normal derivation of the desired potential in the wing surface, this becomes, with $\frac{E}{E_o} = \mu$,

$$-\sigma \frac{\partial E}{\partial z} = \frac{E_o}{R \Delta A} \frac{\Psi_z}{C_1}$$

or

$$\Psi_z = -C_1 \cdot \sigma R \Delta A \cdot \frac{\partial \left(\frac{E}{E_o}\right)}{\partial z} = -C_2 \frac{\partial \mu}{\partial z} \ . \tag{4}$$

From this follows, for the relation between electric and aerodynamic potential, except for one free constant:

$$\Psi = -C_2 \mu \ . \tag{5}$$

2.3 Determination of Preliminary Integrals

The so-called preliminary integrals enter into the integral equation for the potential Ψ and are defined as follows:

$$G_n(\omega, y) = i\omega \int_{-\infty}^{x_o(y)} \Psi_{nz}(\xi, y, 0)\, e^{i\omega \left[\xi \cdot x_o(y)\right]}\, d\xi \ . \tag{6}$$

These integrals must be calculated numerically with the aid of the z-derivations measured at the advance electrodes. This has shown that it is sufficient generally to subdivide the advance electrode for each section y = const. into five partial electrodes of suitable size.

For the execution of integration, the integration interval $-\infty < x \leq x_0(y)$ was subdivided, for the rectangular wing, into the following partial intervals

1. $-\infty < x \leq -2$,
2. $-2 < x \leq -0,5$,
3. $-0.5 < x \leq -0,1$,
4. $-0.1 < x \leq 0$.

The subdivision of the advance electrode was made so that the center points of the partial electrodes lay at the following values of x:

$$x_1 = -0.050 ,$$
$$x_2 = -0.1845 ,$$
$$x_3 = -0.4155 ,$$
$$x_4 = -0.817 ,$$
$$x_5 = -1.680 .$$

In the individual intervals, the additives to the preliminary integral were calculated with the aid of the following formulations.

<u>In Interval 1</u>:

$$\Psi_z(x,y,0) = \bar{\Psi}_z(x_5,y,0)\left(\frac{x_5}{x}\right)^2 , \quad -\infty < x \leq -2 , \qquad (7)$$

where $\bar{\Psi}_z(x_5,y,0)$ is measured at the fifth electrode at the distance $x = x_5$ from the leading edge. The bars above Ψ indicate that the values measured at the individual electrodes are to be considered as mean values over a part of the x-interval.

<u>In Interval 2 and 3</u>:

The utilization of the Gauss integration formula for two values of the function in the interval produces as additives to this interval

$$i\omega\, 0.75 \left[\bar{\psi}_{z_5} e^{i\omega x_5} + \bar{\psi}_{z_4} e^{i\omega x_4} \right] \tag{8}$$

and

$$i\omega\, 0.75 \left[\bar{\psi}_{z_3} e^{i\omega x_3} + \bar{\psi}_{z_2} e^{i\omega x_2} \right] \quad .^{1)} \tag{9}$$

In the Interval 4:

Formulation in approximation of the results in the two-dimensional case

$$\psi_z = A(1 - 2\sqrt{-x}) + \frac{B}{2\sqrt{-x}} \quad , \quad -0.1 < x \leq 0 \quad , \tag{10}$$

Where A and B are determined so that the mean values $\bar{\psi}_{z_2}$ and $\bar{\psi}_{z_1}$ over the first two electrodes calculated by means of this formula correspond to the values measured here.

We can then write, for the preliminary integral $G(\omega, y)$,

$$G(\omega, y) = \sum_i p_i(\omega)\ \bar{\psi}_{z_i}(y) \quad , \quad i = 1, 2, 3, 4, 5 \quad , \tag{11}$$

in which $p_i(\omega)$ is determined by the formulas above.

In practice, the calculation of $G(\omega, y)$ is made with the help of a built-in "summator" which saves a relatively considerable amount of time in determining ω for a number of values in a given case of oscillation $G(\omega, y)$.

2.4 "Calibration" of Potential Tank

Because of the influence of the walls as well as of the finite gap between the individual electrodes for wing and wake on the distribution of the potential as well as its normal derivation ahead of the wing, it is necessary to calibrate the potential tank. For this purpose, the normal derivation calculated for a wing with elliptical distribution of potential in the direction of span as well as with "two-dimensional" distribution of potential in the direction of the chord line was adjusted in the tank. The respective distribution of potential was measured and compared with the known theoretical values. Subsequently, the width of the gap between the electrodes was corrected until no further deviations occurred (Fig. 5 and 6).

---

1) In order to abbreviate, this is written $\bar{\psi}_{z_i} = \bar{\psi}_z(x_i, y, o)$, $i = 1, 2, .., 5$.

The normal derivation was measured on the electrodes in the same way. Conformity with the theoretical values was satisfactory, except in the immediate vicinity of the leading edge (error about 5%) (Fig. 7 and 8).

All observed deviations of the result of measurements are likely to be errors of systematics. We may consequently expect errors of the same relative magnitude also for any other given distributions of normal derivation on the wing.

In all of the following measurements, the φ_z-distributions measured in the area of the advance electrodes have been corrected correspondingly.

2.5 Method of Solution

The integral equation to be solved is

$$\varphi_z(x,y,0) = W(x,y) + i\omega \int_{x_o(y)}^{x} W(\xi,y)\,d\xi + i\omega \int_{-\infty}^{x_o(y)} \varphi_z(\xi,y,0)\, e^{i\omega\left[\xi - x_o(y)\right]}\, d\xi \tag{12}$$

or

$$\varphi_z(x,y,0) = H(\omega,x,y) + J(\omega,y) \quad , \tag{13}$$

with

$$H(\omega,x,y) = W(x,y) + i\omega \int_{x_o(y)}^{x} W(\xi,y)\,d\xi \quad , \tag{14}$$

$$J(\omega,y) = i\omega \int_{-\infty}^{x_o(y)} \varphi_z(\xi,y,0)\, e^{i\omega\left[\xi - x_o(y)\right]}\, d\xi \quad . \tag{15}$$

Solution A:

For $J(\omega,y)$, a series formula $J(\omega,y) = \sum a_n(\omega) F_n(y)$ is introduced in which the real functions $F_n(y)$ must be selected suitably. The constants $a_n(\omega)$ are determined numerically.

The integral equation can then be broken down into the partial boundary-value problems:

$$\varphi^H \quad \text{according to} \quad \varphi_z^H(x,y,0) = H(x,y) \quad , \tag{16}$$

$$\varphi_n^F \qquad\qquad \varphi_{nz}^F(x,y,o) = F_n(y) \quad . \tag{17}$$

The respective preliminary integrals are calculated from

$$J^H(\omega, y) = i\omega \int_{-\infty}^{x_o(y)} \Psi_z{}^H(\xi, y, o)\, e^{i\omega \left[\xi - x_o(y)\right]}\, d\xi \quad , \tag{18}$$

$$G_n^F(\omega, y) = i\omega \int_{-\infty}^{x_o(y)} \Psi_{nz}{}^F(\xi, y, o)\, e^{i\omega \left[\xi - x_o(y)\right]}\, d\xi \quad . \tag{19}$$

Because of the linearity of the problems, we obtain the following determinant equations for the coefficients a_n:

$$\sum_{n=1}^{m} a_n(\omega) \left[F_n(y) - G_n^F(\omega, y) \right] = J^H(\omega, y) \quad . \tag{20}$$

$a_n(\omega)$, $G_n^F(\omega,y)$ and $J^H(\omega,y)$ are complex functions. It is obvious that the effort necessary greatly increases with the number m of the distribution functions F_n. Very careful selection of these functions is therefore necessary.

Solution B:

The equation system 12 to 15 can also be solved iteratively in the potential tank.

To start with, $\Psi_z = H(\omega,x,y)$ is set up in the tank from which follows a corresponding additive $J_1(\omega,y)$ of the preliminary integral.

As the second step, $\Psi_z = H(\omega,x,y) + J_1(\omega,y)$ is set up in the tank, etc.

This method has converged for all of the wing forms and modes of oscillation measured so far in the tank. The convergence speed is very low, however, for certain combinations of wing shape, frequency, and mode of oscillation so that it is better, during iteration, to start from a distribution $J_1(\omega,y)$ determined or estimated in some manner.

2.6 Example of Rectangular Wing

A rectangular wing with a side ratio $A = 3$ was measured according to solution A in subsection 2.5. The following functions were selected for $F_n(y)$:

$$F_1(y) = 1 \quad ,$$
$$F_2(y) = y^2 \quad ,$$
$$F_3(y) = y^6 \quad .$$

This formula proved itself as suitable for all modes of oscillation investigated

$$z(x,y,t) = h(x,y)\, e^{i\nu t} \tag{21}$$

(z and h measured with the wing chord as unit).

The following modes of oscillation were investigated:

Oscillatory:	$h(x,y) = 1$,
Rotational:	$h(x,y) = x - \frac{1}{4}$,
Buckling:	$h(x,y) = \lvert y \rvert$,
Bending:	$h(x,y) = y^2$,
Torsional:	$h(x,y) = (x - \frac{1}{4}) \lvert y \rvert$,
Rotational of Aileron:	$h(x,y) = \frac{x-\tau}{1-\tau}\, T(x-\tau)$,
Torsional of Aileron:	$h(x,y) = \frac{x-\tau}{1-\tau} \lvert y \rvert\, T(x-\tau)$,

in which $T(x-\tau) = \begin{Bmatrix} 0 \\ 1 \end{Bmatrix}$ for $\begin{cases} x < \tau , \\ x \geq \tau . \end{cases}$

$(1-\tau)$ is the chord of the aileron.

The given part of the normal derivation $H(\omega,x,y)$ can be represented with this as lineary combination of the following basic functions $f_n(x,y)$:

$$H(\omega, x, y) = \sum_n C_n(\omega)\, f_n(x,y) . \tag{22}$$

n	$f_n(x,y)$	n	$f_n(x,y)$
1	1	9	$x^2 \lvert y \rvert$
2	y^2	10	$T(x-\tau)$
3	y^6	11	$\frac{x-\tau}{1-\tau}\, T(x-\tau)$
4	x	12	$(\frac{x-\tau}{1-\tau})^2\, T(x-\tau)$
5	x^2	13	$\lvert y \rvert T(x-\tau)$
6	$\lvert y \rvert$	14	$\frac{x-\tau}{1-\tau} \lvert y \rvert T(x-\tau)$
7	$x \lvert y \rvert$	15	$(\frac{x-\tau}{1-\tau})^2 \lvert y \rvert T(x-\tau)$
8	xy^2		

cf. Fig. 9 to 20.

For all of the 15 basic functions the corresponding preliminary integrals

$$G_n^f(\omega, y) = i\omega \int_{-\infty}^{x_o(y)} \varphi_{nz}^f(\xi, y, 0)\, e^{i\omega [\xi - x_o(y)]}\, d\xi \qquad (23)$$

were measured and calculated. By the superposition of suitable $G_n^f(\omega,y)$ we obtain the preliminary integral $J^H(\omega,y)$ corresponding to the function $H(\omega,x,y)$ as well as the distribution of potential belonging to $H(\omega,x,y)$:

$$\varphi^H = \sum C_n(\omega)\ \varphi_n^f(x, y) \qquad (24)$$

and, according to the formula 16 to 17, the desired distribution of potential as

$$\varphi(x, y, 0) = \sum C_n\ \varphi_n^f + \sum a_n\ \varphi_n^F \quad . \qquad (25)$$

In the figures, normal force and moment coefficients are calculated for the basic functions $f_n(y)$ defined above with the aid of the following definitions:

$$\text{Normal Force} \quad K(y) = \frac{1}{2}\varrho V^2\, S\, e^{i\nu t}\, k(y) \quad , \qquad (26)$$

$$\text{Moment} \quad M(y) = \frac{1}{2}\varrho V^2\, S\, c\, e^{i\nu t}\, m(y) \quad . \qquad (27)$$

According to the definition of φ in TN 34, we obtain:

$$k(y) = 4\varphi(1, y, +0) \quad , \qquad (28)$$

$$m(y) = 3\varphi(1, y, +0) - 4 \int_0^1 \varphi(\xi, y, +0)\, d\xi \quad . \qquad (29)$$

(M(y): moment around 25%-point, positively nose-heavy).
cf. Fig. 21 to 25.

2.7 Suggestions for Further Development of Potential Tank

Further development of the analogy described above is being considered in the direction of complete automation. The solution can then be procured faster and with greater accuracy. In order to do so, the additive member $J(\omega,y)$ in equation 13 for φ_z is to be summated

automatically to $H(\omega,x,y)$ by a feed-back arrangement. This requires additional electrical apparatus but saves on the other hand determination and measurement of the functions $F_n(y)$ as well as numerical calculation of the coefficients a_n. The desired potential is obtained directly without superposition. The non-steady aerodynamic force at $M = 0$ can be simply determined from this for any given mode of oscillation of the wing, e.g. determined from static vibration tests. For $M \neq 0$, an approximate solution can be derived iteratively by means of the solution found for $M = 0$, as stated in Part I of the lecture.

3. LITERATURE REFERENCES

1. H. G. Küssner, Allgemeine Tragflugeltheorie. Lufo, Bd. 17 (1940), Heft 11/12, p. 370-378.
2. J. Legras, L. Malavard, Etude au bassin electrique du probleme de la surface portante. VIth Int. Congress Appl. Mech., Paris 1946.
3. L. Malavard, L. Duquenne, Etude des surfaces portantes par analogies rheoelectriques. Rech. Aeronautique No. 23, 1951.
4. W. F. Campbell, Two electrical analogies for the pressure distribution on a lifting surface. N.R.C.C. Rep. No. MA-219, 1949.
5. M. T. Landahl, V. J. E. Stark, An electrical analogy for solving the oscillating-surface problem for incompressible nonviscid flow. KTH AERO TN 34, 1953.
6. V. J. E. Stark, M. T. Landahl, Bestamning av instationara luftkrafter pa rektangular vinge med hjalp av potential-tanksanalogi. KTH AERO RAPPORT FL 158, 1954.
7. H. R. Lawrence, E. H. Gerber, The aerodynamic forces on low aspect ratio wings oscillating in an incompressible flow. Journ. Aeron. Sci., Vol. 19 (11) (1952), p. 769-781.

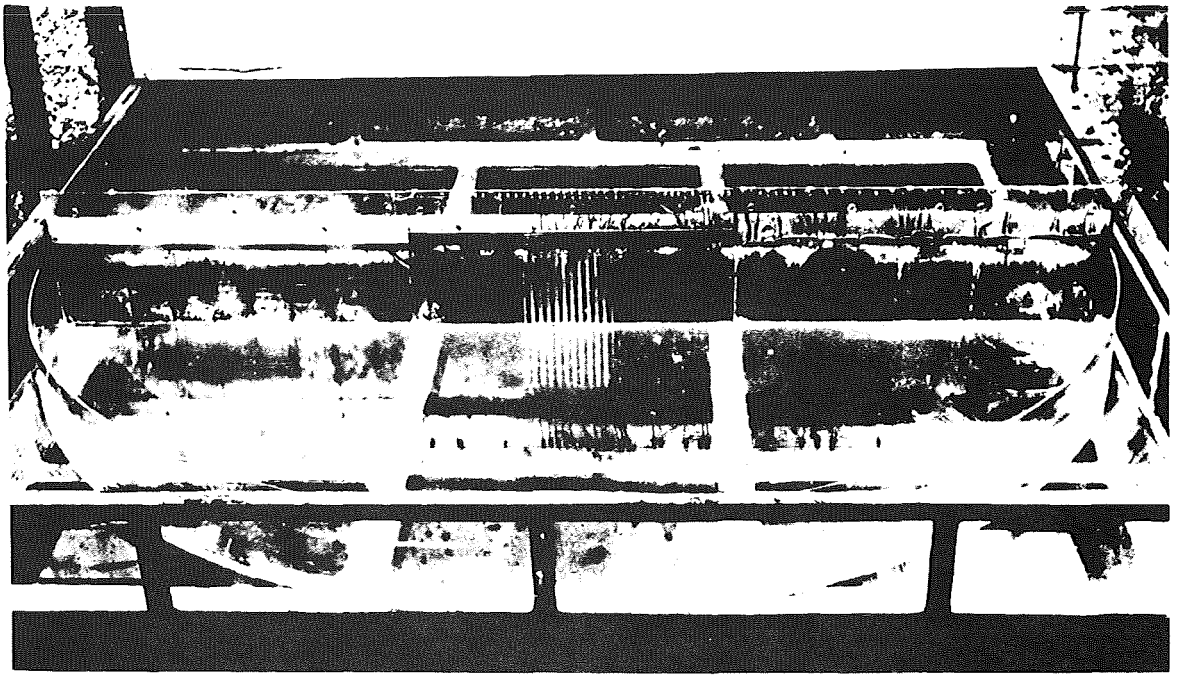

Fig. 1. The two-dimensional potential tank of the Institute of Flight Technics of the Royal Institute of Technology at Stockholm with electrode model.

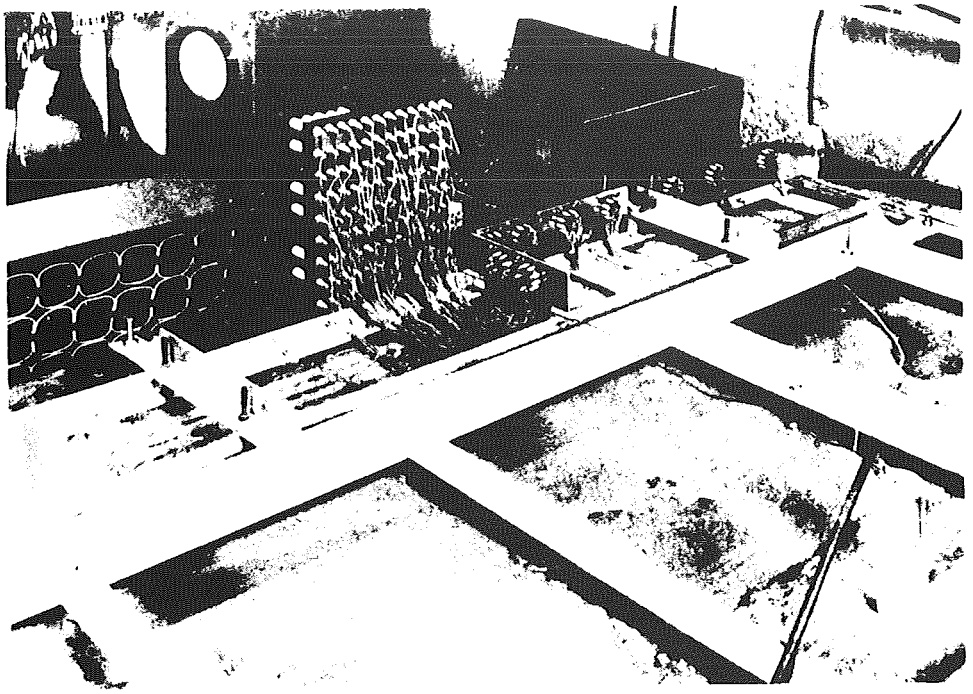

Fig. 2. The three-dimensional potential tank at Stockholm from an oblique top view.

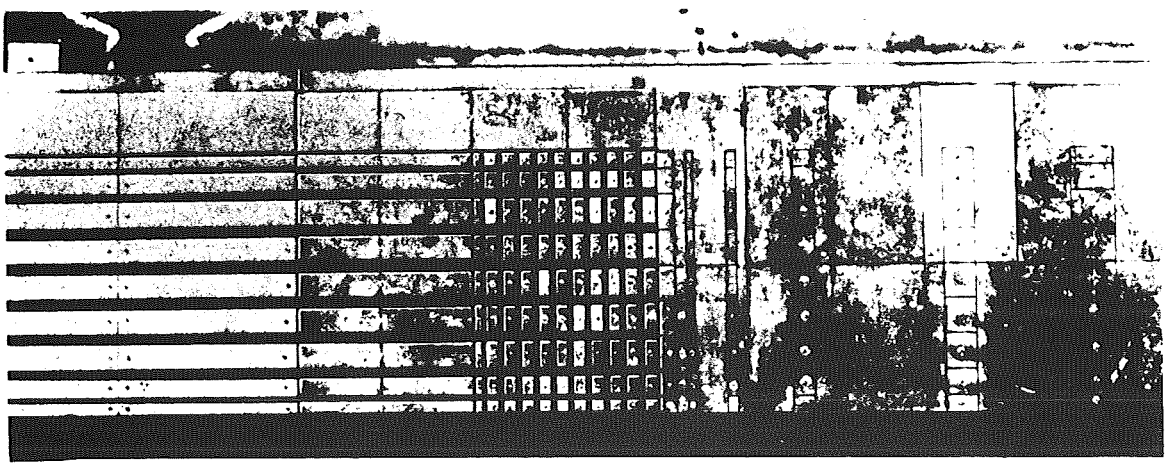

Fig. 3. The electrode model for the rectangular wing.

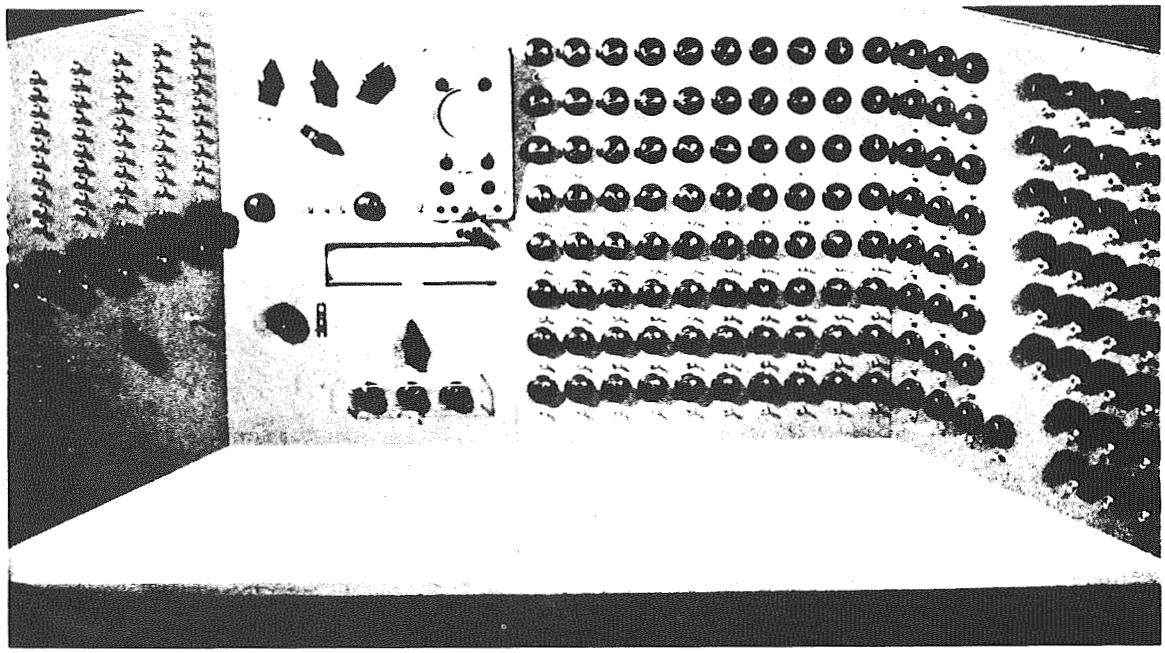

Fig. 4. The measuring bridge for the three-dimensional tank.

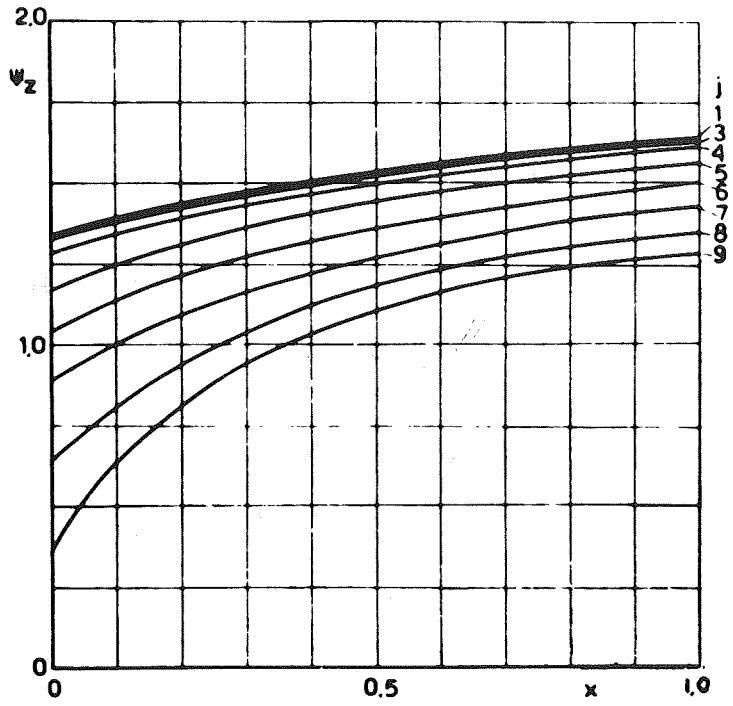

Fig. 5. Theoretically calculated z-derivation on the rectangular wing (cf. 2.4).
x = 0: Leading edge; x = 1: Trailing edge.

j =	1	2	3	4	5	6	7	8	9
y_j =	.0317	.1127	.2300	.3650	.5000	.6350	.7700	.8873	.9683

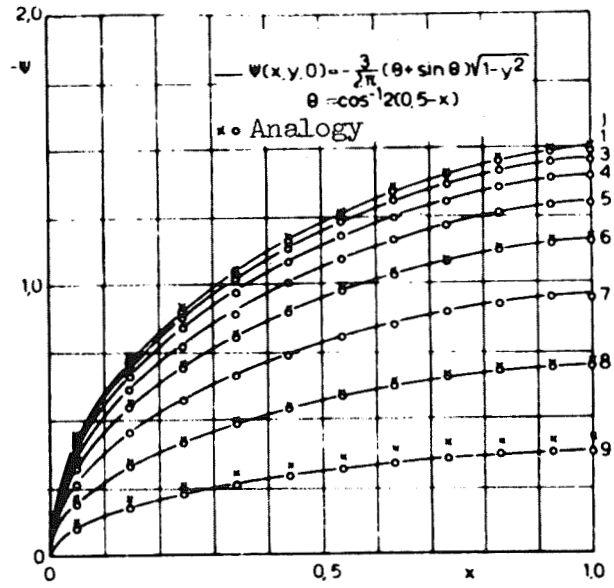

Fig. 6. Calibration of potential tank.
The theoretical potential function belonging to the z-derivations of Fig. 5 as well as measurement results with the original electrode model (x) and also after variation of the gap width (o). (j: cf. Fig. 5)

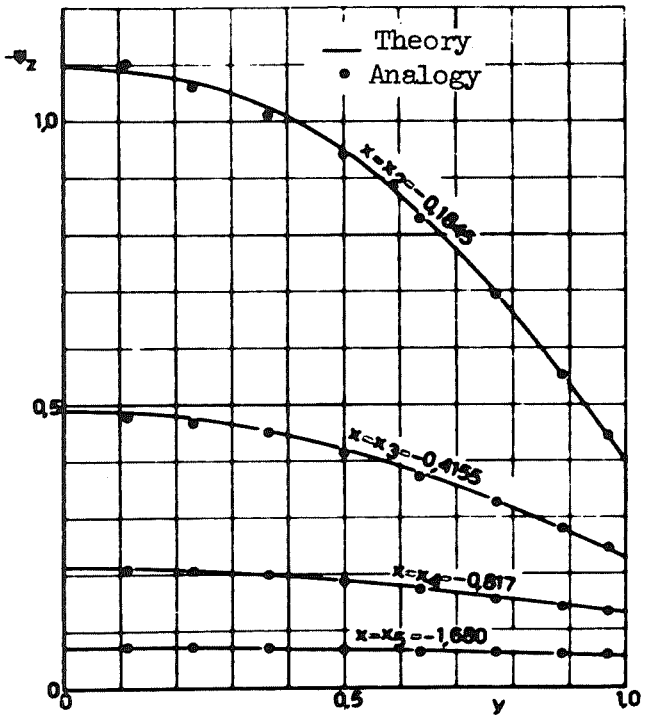

Fig. 7. The z-derivation of potential Ψ ahead of the wing for the example in Fig. 5 and 6 (2nd to 4th advance electrode).

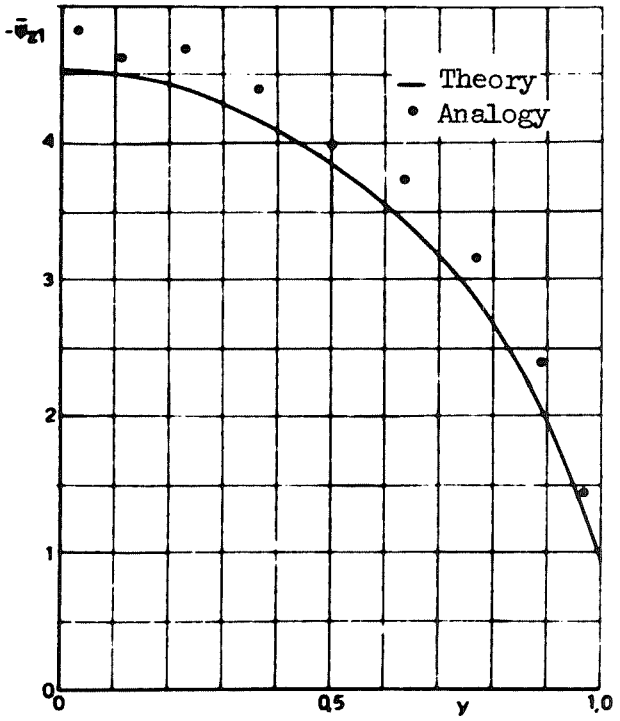

Fig. 8. Mean values of the z-derivation in the interval $-0.1 < x \leq 0$ (1st advance electrode) for the example in Fig. 5 and 6.

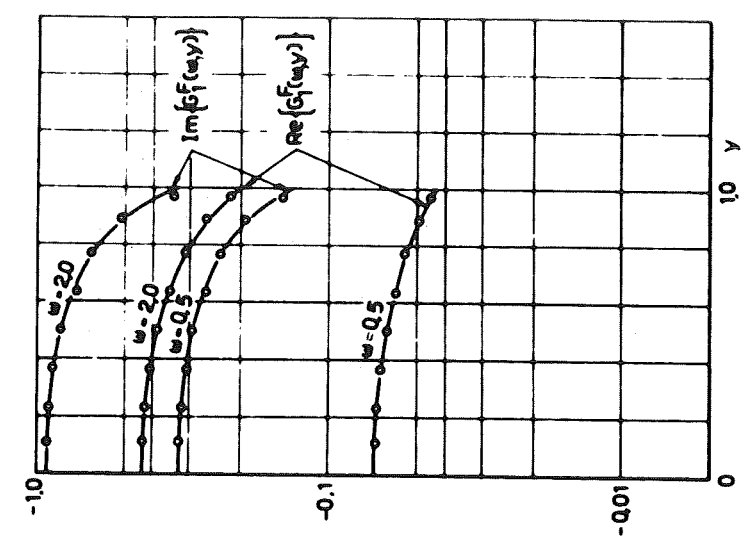

Fig. 10. Preliminary integral for $\Psi_z = 1$ for two values for the frequency parameter.

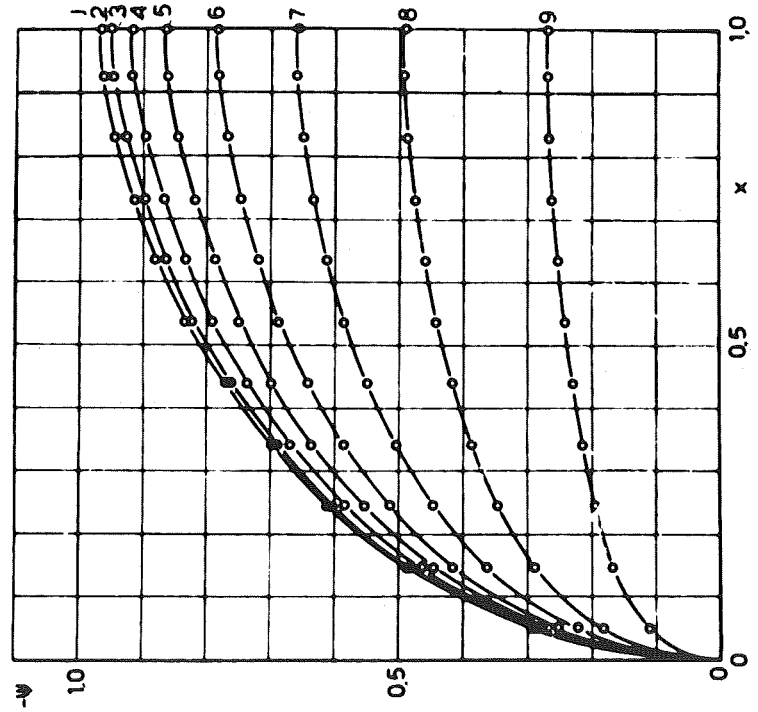

Fig. 9. Measured distribution of potential for $\Psi_z = 1$. (j: cf. Fig. 5)

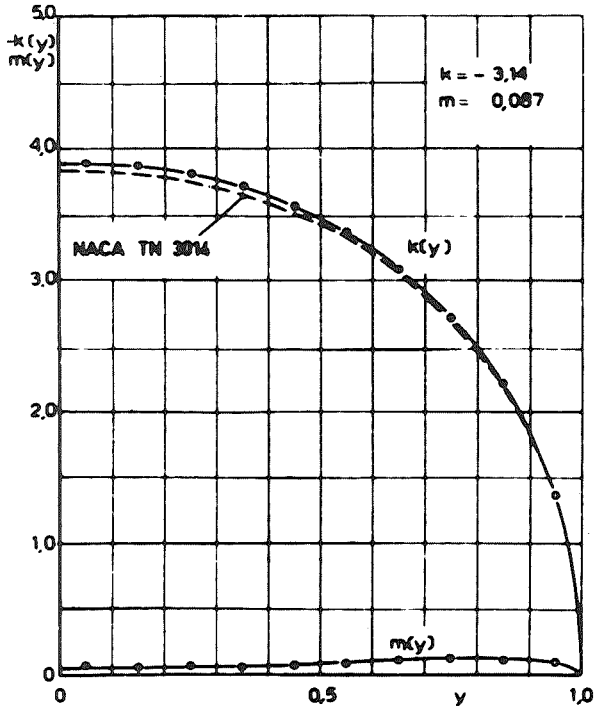

Fig. 11. Lift and moment coefficients for $\Psi_z = 1$.

$$k = \int_0^1 k(y)\,dy \quad ; \quad m = \int_0^1 m(y)\,dy \ .$$

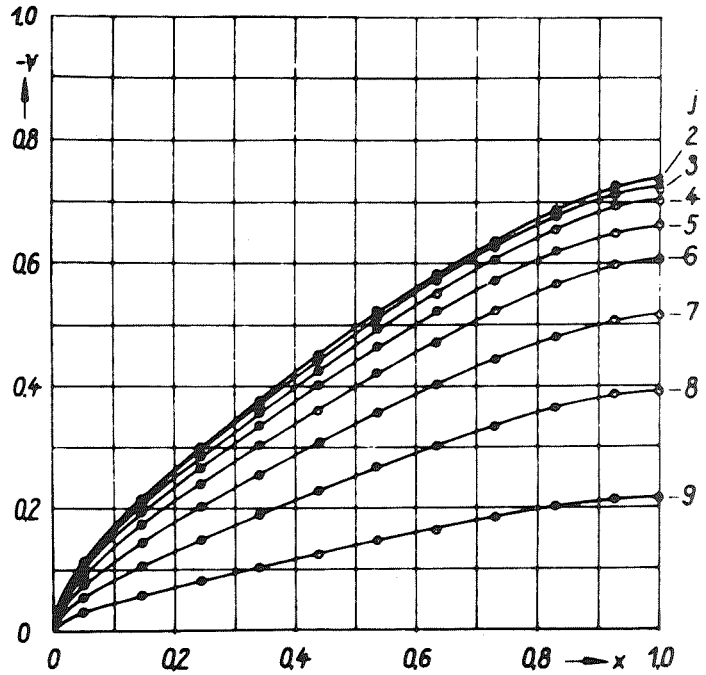

Fig. 12. Measured potential distribution for $\Psi_z = x$. (j: cf. Fig. 5)

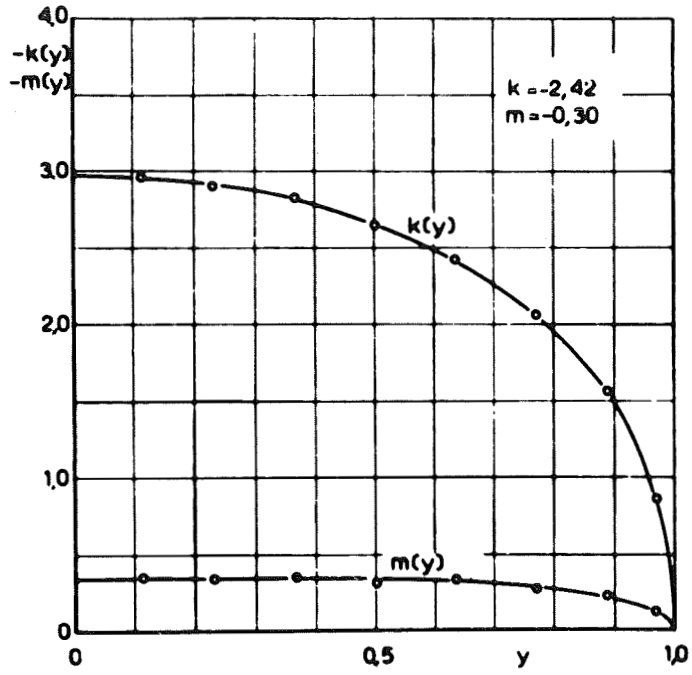

Fig. 13. Lift and moment coefficients for $\Psi_z = x$.

$$k = \int_0^1 k(y)\,dy \quad ; \qquad m = \int_0^1 m(y)\,dy \ .$$

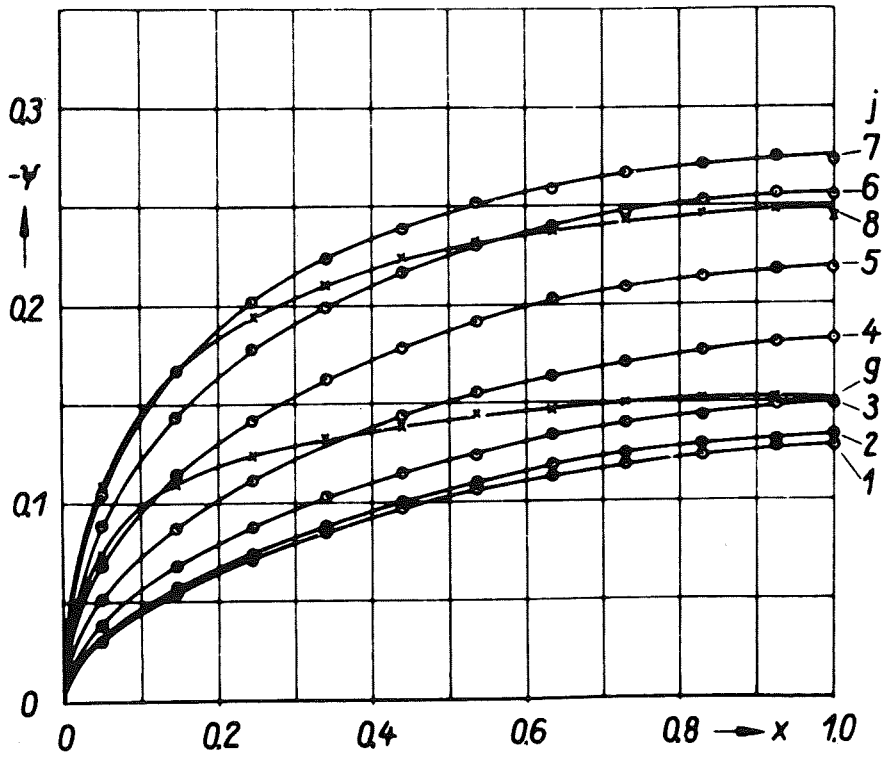

Fig. 14. Measured potential distribution for $\Psi_z = y^2$.
(j: cf. Fig. 5)

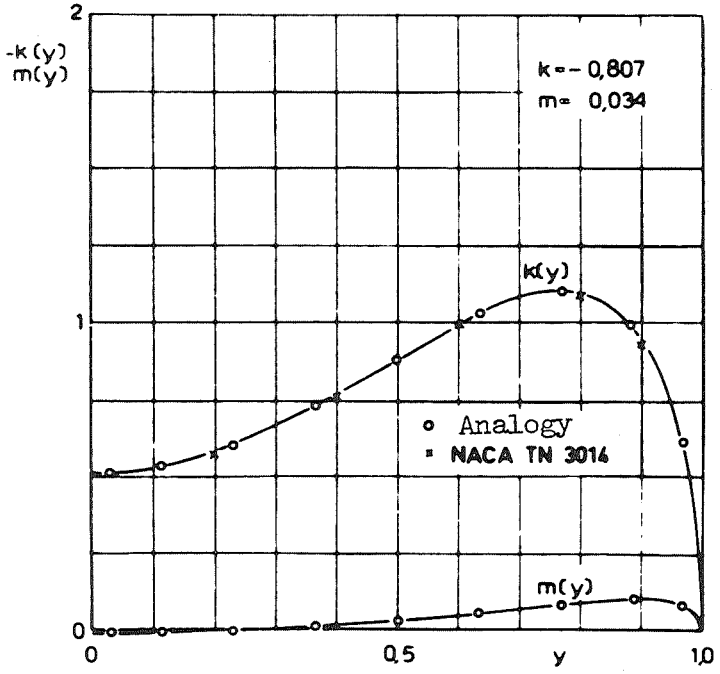

Fig. 15. Lift and moment coefficients for $\Psi_z = y^2$.

$$k = \int_0^1 k(y)\,dy \quad ; \quad m = \int_0^1 m(y)\,dy \,.$$

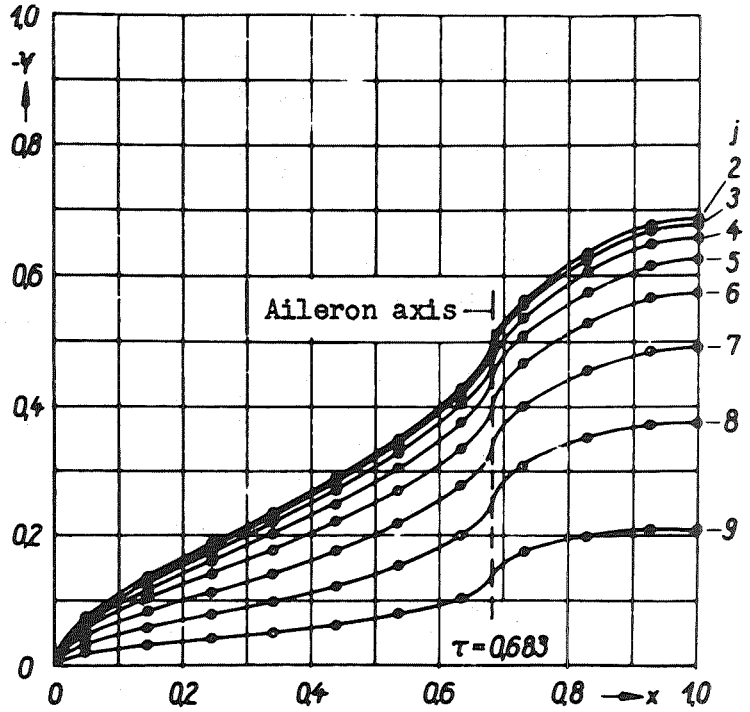

Fig. 16. Measured distribution for $\Psi_z = T(x - \tau)$.
(j: cf. Fig. 5)

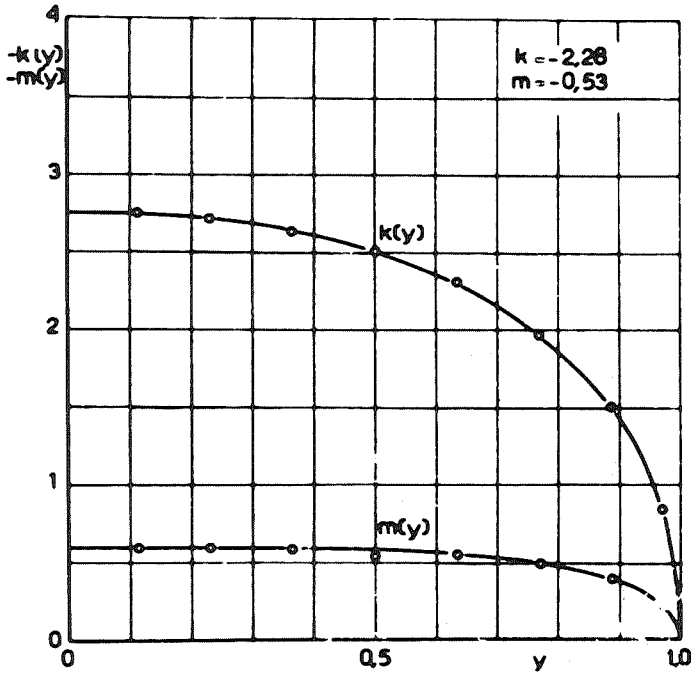

Fig. 17. Lift and moment coefficients for $\psi_z = T(x - \tau)$.

$$k = \int_0^1 k(y)\,dy \quad ; \quad m = \int_0^1 m(y)\,dy .$$

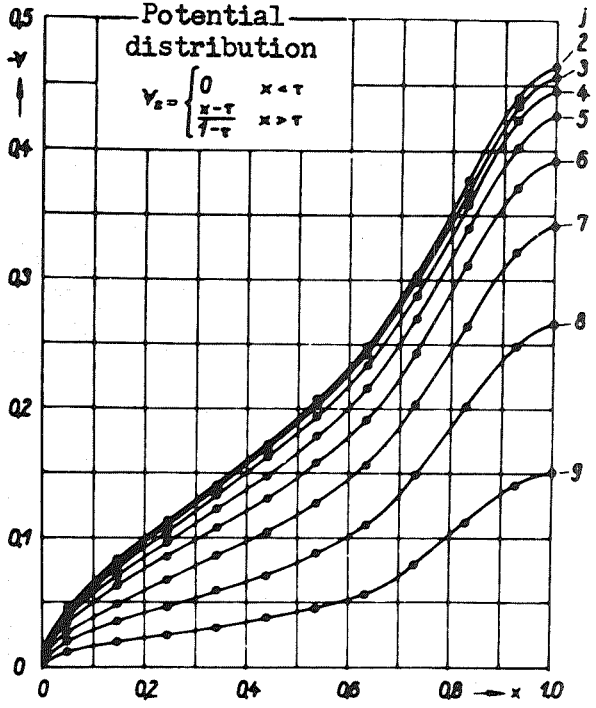

Fig. 18. Measured distribution of potential for $\psi_z = \frac{x - \tau}{1 - \tau}\, T(x - \tau)$.
(j: cf. Fig. 5)

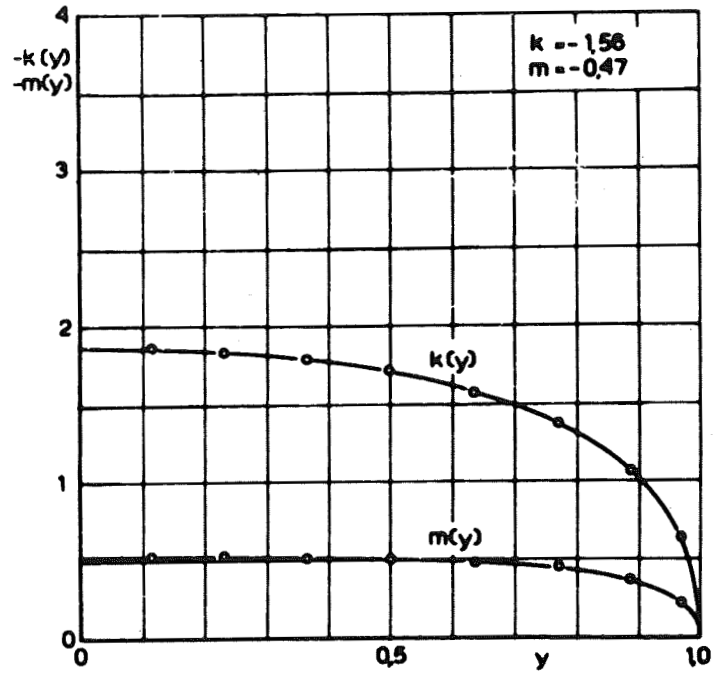

Fig. 19. Lift and moment coefficients for

$$\psi_z = \frac{x-\tau}{1-\tau}\, T(x-\tau)\,.$$

$$k = \int_0^1 k(y)\,dy \quad ; \qquad m = \int_0^1 m(y)\,dy\,.$$

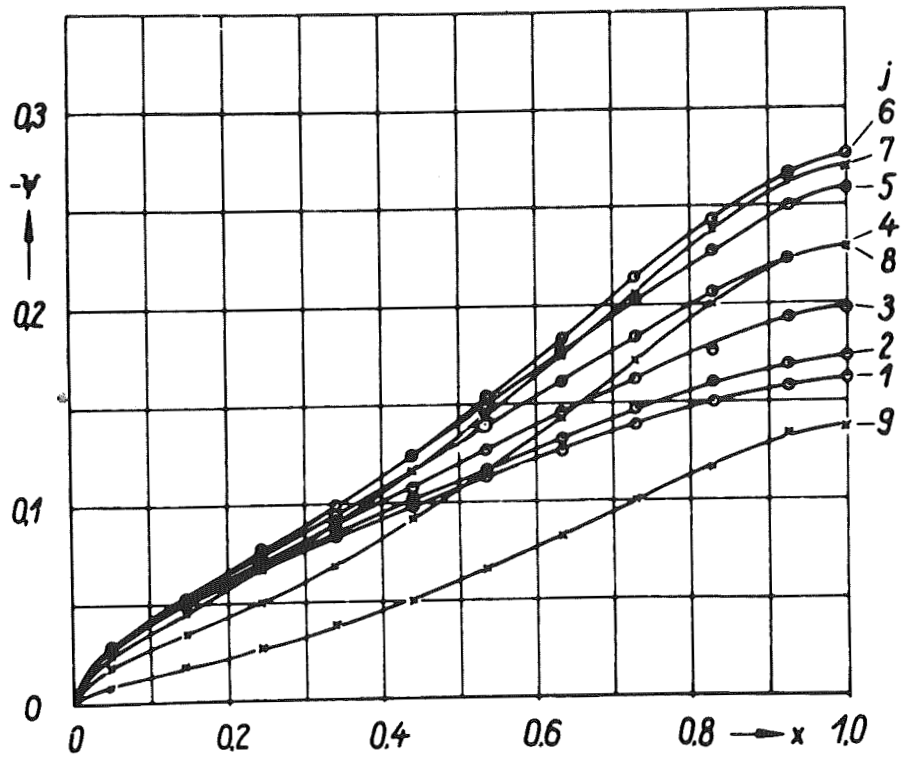

Fig. 20. Measured distribution of potential for $\psi_z = x^2 |y|$.
(j: cf. Fig. 5)

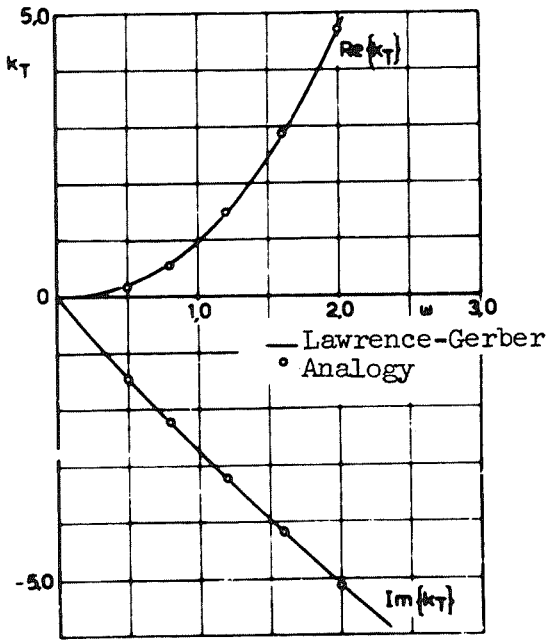

Fig. 21. Lift coefficients for oscillatory vibration of a rectangular wing, A = 3, and comparison with theoretical values (7). (CAL - Rep. AF - 781 - A - 1).

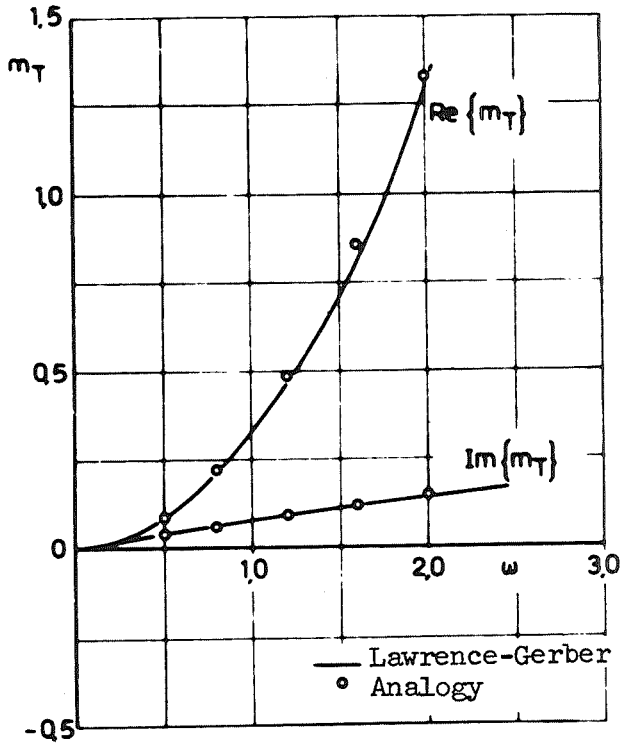

Fig. 22. Moment coefficients for oscillatory vibration of a rectangular wing, A = 3, and comparison with theoretical values (7). (cf. Fig. 21).

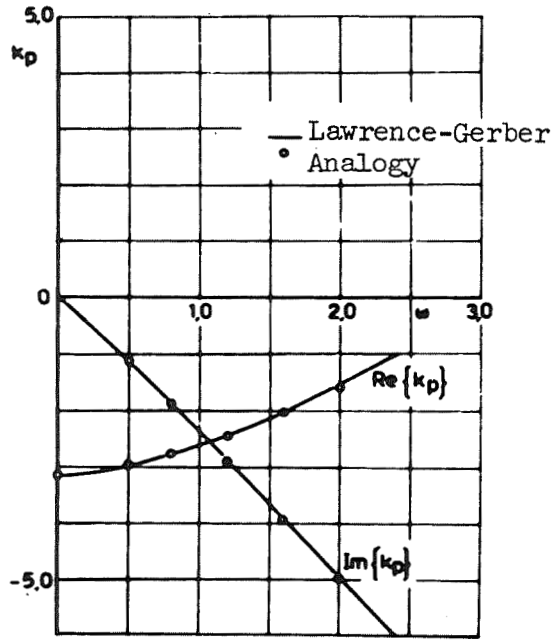

Fig. 23. Lift coefficients for rotational vibration around the 25%-point of a rectangular wing, A = 3, and comparison with theoretical values (7). (cf. Fig. 21).

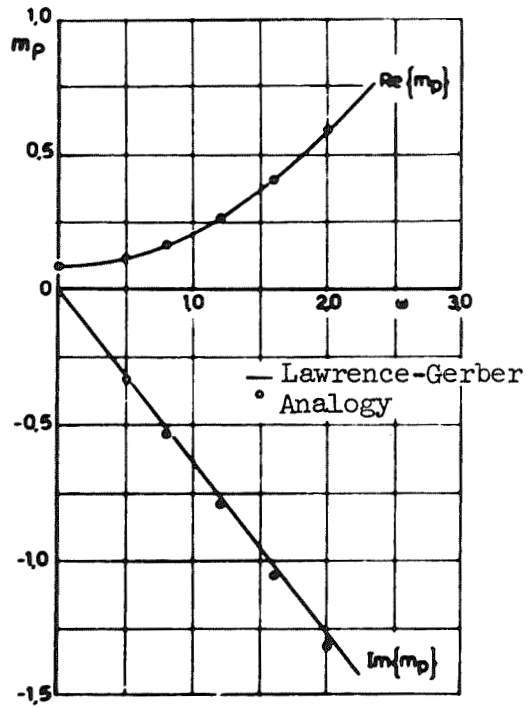

Fig. 24. Moment coefficients for rotational vibration around the 25%-point of a rectangular wing, A = 3, and comparison with theoretical values (7). (cf. Fig. 21).

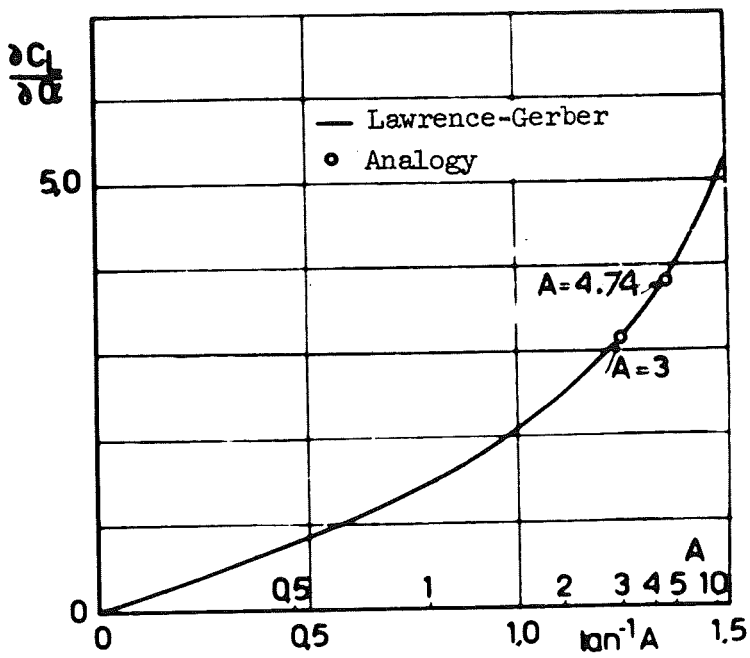

Fig. 25. Lift gradient $\frac{\partial C_L}{\partial \alpha}$ as function of the side ratio A for a rectangular wing and comparison with theoretical values (7). (cf. Fig. 21).

DISCUSSION

Küssner: The iteration method for $M > 0$ here employed by you corresponds exactly to the method of Dietze which has been carried out numerically. However, the method here is, without a doubt, more accurate and can be performed quicker. The potential-tank method appears to be much more accurate than the station method with the rectangular tables which I discussed yesterday and which gave a very oscillating pressure distribution. How about your pressure distribution, does it also oscillate as strongly or is it more uniform? Let us assume you have oscillatory vibrations.

Merbt: Among the modes of oscillation which we have investigated so far, oscillating forms did not occur.

Küssner: The rheometric method therefore does converge better than the numerical collocation method which has been utilized by P. T. Hsu, J. R. Martucelli and H. Ashley, among others.

Merbt: We still used our box method (collocation method) in 1951 but were not particularly well satisfied. The difficulties at the leading edge and at the sides are too great.

van de Vooren: The method of Hsu, Martucelli and Ashley can also be used in the compressible range; however, the method here is one of iteration which converges for Mach numbers which are not too high, as does the method of Dietze.

Küssner: The method here explained appears to be more promising. It is a type of analog computer. Basic assumptions: wing infinitely thin, pure potential flow, boundary layer neglected. After such simplifying assumptions have been made, one would like to complete calculation at least properly mathematically. This seems to be possible to a large extent with the potential method. The compressibility of the fluid can be taken into account by an additional iteration process which Mr. Merbt has described.

de Vries: Can the method also be utilized for swept-back wings or is it absolutely necessary to have a straight wing?

Merbt: The question whether the trailing edge must absolutely be straight, has not been completely clarified.

de Vries: Don't you have any difficulties with the capacities? You do work with a frequency of 1,000 c/s, you do measure the phase displacements?

Merbt: No, we do not measure phase displacement. The determination of the complex potential Ψ (independent of time) is made separately for real and imaginary constituents in which these are linked by way of the preliminary integral. In the analogy, we work only with real magnitudes.

de Vries: Here the distribution of potential was assumed as a steady distribution also over the span of the wing. In the preceding lecture, we were shown that the non-steady aerodynamic forces are greatly dependent on the stationary values. In flutter calculations

by the strip method, is the variable distribution of potential along the wing now taken into account? Or is it always left at the assumption of the distribution in all strips as uniform?

Merbt: We determine pressure distribution over the entire wing so that the variations of potential distribution in the direction of the span are fully taken into account.

Küssner: Knowledge of pressure distribution at any point of the wing is desired.

de Vries: I was thinking of the practical flutter calculation with the strip method. Are the coefficients for each strip assumed as uniform, or are the strips lying closer to the wing ends reduced in accordance with the theory?

Küssner: This depends on whether an assumption of steady flow is made or not. If we assume steady flow, it is possible to calculate two-dimensionally in each strip and take the solution from known tables.

Sorg: In the example cited by you, were the oscillatory and the rotational amplitude constant over the entire wing span?

Merbt: The amplitudes of the fundamental functions from which given modes of oscillation can be composed, can be represented by double-polynomials in x and y. With this, any given mode of wing oscillation can be approximated.

STATIC VIBRATION TESTS OF SAILPLANE WITH ELECTRONIC MEASURING INSTRUMENTS

by J. Schoen

SUMMARY

A static vibration test installation with electronic instrumentation was developed for aircraft up to about 1,000 kg flying weight and utilized for static vibration tests of a sailplane. Excitation was induced by electrodynamic means. The recording of the natural modes and of the damping coefficient was made by a stroboscopic process with "measuring wedges" /test keys?/. The generalized mass was also determined.

ARRANGEMENT

		Page
1.	Introduction.	168
2.	Suspension of Aircraft for Test	168
3.	Excitation of Natural Modes	168
4.	Measurement Methods for Amplitude and Phase for Recording Natural Modes and Damping Coefficients.	170
5.	The Recorded Natural Modes of the Sailplane	171
6.	The Determination of the Generalized Mass	172
7.	Further Development of Equipment.	174
	Illustrations	175
	Discussion.	182

1. INTRODUCTION

After revocation of the prohibition against aircraft construction, static vibration tests became again a necessity in the design of new aircraft in Western Germany. The aeroelastic division of the Aerodynamic Experimentation Institute at Gottingen therefore received the task of developing apparatus for static vibration tests.

It was not possible to procure a complete measuring installation from abroad and even the purchase of individual measuring instruments encountered great difficulties. We therefore needed to restrict ourselves to smaller equipment obtainable here. On the other hand, it was also more appropriate to first gather experience with a less expensive installation before starting on the design and construction of a large and expensive measuring apparatus. Without development costs, the expense for such a large and modern installation is estimated at about DM 75,000 to 100,000.

Accordingly, we first developed a small electronic measuring installation for static vibration tests and tested it by performing a static vibration test of a sailplane. The latter was made available to us by the Group for Aviation Science at Gottingen.

2. SUSPENSION OF AIRCRAFT FOR TEST

The static vibration test of an aircraft serves for the determination of its natural modes of vibration, natural frequencies and of the damping and mass coefficients at an incident-flow velocity $v = 0$. These magnitudes then become the basis for flutter calculation in order to compute the critical flying speed. For this, the aircraft is suspended elastically, when possible, in the nodes of the natural mode just investigated and/or set on elastic supports. The natural frequency of the elasticity/mass system should not amount to more than one-third of the basic bending frequency of the wing so that the aircraft will react approximately as a free-floating body.

Fig. 1 shows the suspension of the sailplane. The wing is suspended in its center by a rubber rope attached to a block and tackle. The rubber rope can be adapted easily to the required elastic constant and tensile strength required. In order to prevent interference by oscillation, spring-equipped tripods are used which are raised against the wing from below in the respective vibration nodes.

3. THE EXCITATION OF NATURAL MODES

The inducement of enforced vibrations in a test is today generally effected electrodynamically. The force of excitation is produced by an alternating-current plunger coil which swings in an annular and constant magnetic field. The oscillators are hooked into suitable elastic tripods and the force of excitation from the plunger coil is transmitted by means

of an articulated pressure rod to the respective locations in the wing. Fig. 2 shows a section through such an oscillator and a suspension tripod.

At this point, we should like to thank Mr. de Vries and O.N.E.R.A. for their valuable suggestions.

Fig. 1 further shows the point of action of the oscillators. Electrodynamic exciters have great advantages in comparison with formerly used rotating compensators and/or eccenters. This makes it possible to regulate frequencies, amplitude and phase independently of each other and to keep them constant. However, with these oscillators, we have the possibility of applying forces of excitation to the aircraft at several points in a desired direction and magnitude by utilizing several small oscillators which can be controlled independently of each other. Only this has made it possible to produce a pure natural mode. If the aircraft is excited only at one point as was formerly of necessity the case by excitation through compensators, the enforced vibration can only be maintained by transmitting energy from this point to other locations. Due to the continuously distributed internal damping, phase shift and a gradual change of vibration amplitude occur at the individual points of the aircraft with increasing distance from the source of energy so that the deformation function deviates appreciably from the pure natural mode when damping is not negligibly small. The deformation function of the complete aircraft so created can be represented by a lineary combination of all of the natural modes. Theoretically, the inducement of a pure natural mode would be possible only through a continuous application of energy adapted to the natural mode. In practice, however, a finite number of oscillators is sufficient. It depends essentially on the highest order of the natural modes which we desire to obtain pure (undistorted).

Theoretical consideration will show that it is possible to eliminate natural modes with n oscillators (n-1) (E. Schultze, ZAMP, 1955, p. 126). The number of exciters can be further reduced when the points of excitation for the desired natural modes are placed as far as possible in the nodes of the non-desired contiguous modes. If we therefore appropriately vary the points of attack of the exciters and moreover adjust the forces of excitation approximately proportional to the mass and amplitude at the point of excitation, we are able to obtain, with a lesser number of exciters, pure natural forms up to the desired order. Depending on requirements, 4 to 12 exciters are adequate for one aircraft. The production of energy of the individual exciters does not need to be very large. Because in a case of resonance only the damping losses need to be covered, a total energy of only 5 to 10 kp is needed per 1,000 kg of flying weight, depending on the type of aircraft. As criterion for a pure natural mode, all points of the oscillating system must have a phase difference of 0° and/or 180° to each other and must be displaced, in relation to the force of excitation, by 90°. The phases of the sinusoidal forces of excitation need

therefore only be capable of being rotated by 180°, depending on the point of activation, which consequently eliminates continuous phase shifters.

4. METHODS OF MEASURING AMPLITUDE AND PHASE FOR RECORDING NATURAL MODES AND DAMPING COEFFICIENTS

Measurements of amplitude at the individual points of the aircraft can be made more or less easily with various types of recorders ("Pick-ups"). Since we are here concerned only with the magnitudes of the individual measurements relative to each other, the indicated values of the path, velocity, or acceleration amplitudes can be proportional. Electric acceleration recorders can be built smallest and easiest with barium-titanate crystals. However, the relatively greatest measuring efficiency at high sensitivity is furnished by electrodynamic velocity recorders which generally do not need amplifiers. For the recording of the path amplitude, mechanically operating instruments such as a direct vibration recorders are used principally. In a very simple and inexpensive manner, path amplitudes can be read with the aid of measuring wedges of paper illuminated stroboscopically. This procedure was developed by us and utilized for recording natural modes in the sailplane. However, reading of the individual measurements is more or less painstaking. However, the procedure is very simple, does not require calibration before or during testing and is therefore very suitable. It is also possible to carry out accurate phase measurements with this method. Because of its light dimensions, the measuring wedge does not interfere with the vibrations of even such light aggregates as rudder and aileron.

The procedure can be explained with the aid of Fig. 3. The measuring wedges pasted to the aircraft are limited logarithmically and are illuminated by a stroboscope with high luminous intensity whose flashes are synchronized with the exciter frequency. The synchronization tension passes through an instrument in which frequency is doubled and in which the phase position of the flash impulses can be changed as against the vibrations of the measuring wedges. If the flashes are activated exactly at the maxima of the vibrations of the measuring wedges, the latter then present the following picture: at frequencies over 3 c/s, we see two measuring wedges which intersect in the center (cf. Fig. 3, top left). From the point of intersection, the amplitude can be read off by geometric enlargement. By using optical means, we can measure amplitudes as low as 0.05 mm with an accuracy of ± 3%. If the flashes are activated in the zero passages of the vibration, then the measuring wedges appear to stand still. This allows us to establish the zero point. If the flashes are then captured by a photocell and these impulses, together with the sinusoidal exciter current, are made to impinge on a double-ray oscillograph, we can then read off the displacement of phase between a measuring point and the exciter current (cf. Fig. 3). This gives us the possibility to record the phase-

resonance curve of a measuring point and to so determine the exact resonance frequency which should have a phase displacement of 90° from the force of excitation. Moreover, the criterion for the pureness of a natural mode -- i.e., the condition that all points of the aircraft must show a phase displacement $\varphi = 0°$ and/or 180° to each other -- can be controlled at several measuring points. For this purpose, we need only to check that all measuring wedges appear to stand still when several measurement points of the aircraft are illuminated by a flash sequence adjusted to the zero passages of one measuring wedge. In order to decide whether the phase angle is 0° or 180°, each second flash can be suppressed and we then see the illuminated measuring wedge stand either at the top or at the bottom. Fig. 4 shows a phase-resonance curve recorded in this manner and next to it an amplitude resonance curve. Both curves can be utilized for the determination of the damping degree; for the amplitude curve from the half-power width and for the phase curve from the slope of the curve at point $\varphi = 90°$. The damping coefficients can also be determined from the deflection curves of a measuring point when switching the excitation on or off. The internal damping of the aircraft can always then be described by expressions which were actually developed for damping linear to velocity, when it is independent of frequency and possesses an elliptic hysteresis loop. This is approximately the case for aircraft. Damping can then be represented by a loss angle β of which the tangent is equal to twice the damping degree.

5. THE RECORDED NATURAL MODES OF THE SAILPLANE

For our sailplane, we used four converted Phillips exciters which produce together a maximum force of 5 to 6 kp. With them, we recorded on the sailplane four natural modes with predominant bending constituent and two natural modes with predominant torsion constituent of the wing. In order to induce the natural bending mode, the points of action of the exciters were located each time below the spar of the single-spar wing and, for inducing the torsion modes, at a heavy rib in the center of both wing halves.

Fig. 5 shows the bending lines of the wing spar obtained from our sailplane for 4 natural modes. In addition, the points of attack and the direction of phase of the forces of excitation have been plotted on them.

The points of attack of the exciters were located mainly below the wing because the wing requires the largest share of excitation energy as compared to the fuselage because of the large span of the wings of the sailplane. When inducing the third top vibration, however, it was shown that the phase condition stated above was then no longer complied with for the fuselage and especially for the empennage. The empennage was then no longer excited at its pure natural mode. The individual measuring points described instead small ellipses. In this case, it

would be necessary to place two additional exciters at the elevator. Fig. 6 shows the amplitude distribution along the complete aircraft for the second top vibration under symmetric excitation. Fig. 7 illustrates two natural modes of the wing with predominant torsion, one under symmetric and the other under asymmetric excitation. The torsion frequencies lay close together at 26.2 c/s. Fig. 8 represents the frequency mode of the aileron together with the control linkage. For this purpose, the aircraft was placed on the ground and the wings were held by tripodes at the tips. Symmetric excitations was produced by two exciters in the center of the ailerons. The recording of the frequency mode is used here for detecting hazardous contiguity of natural frequencies of the aileron and of the wing.

6. THE DETERMINATION OF GENERALIZED MASS

In order to fully characterize the elastomechanical properties of the aircraft, we also need information on its mass distribution $\varrho(P)$. This might be determined from the construction drawings of the craft but this procedure is complicated and inaccurate. We therefore endeavored to establish mass distribution through an experimental method during the static vibration test. Experimental determination is very much simplified by the circumstance that, for flutter calculation, the mass distribution of the aircraft does not need to be known in detail because it always occurs in the form of an integral value over the complete aircraft, the so-called "generalized mass." For the r^{th} natural mode, this is

$$M_r = \iiint u_r^2(P) \cdot \varrho(P) \cdot dP \quad .$$

In this, $u_r(P)$ designates the absolute amount of the vibration amplitude in space and $\varrho(P)$ designates the density of mass at point P of the aircraft.

For the determination of this integral value, several methods are available from vibration technics. If we know the internal damping, the generalized mass M_r can be calculated from the effort of excitation. For the r^{th} natural mode, the damping force at point P is proportional to the force of inertia:

$$dR = g_r \cdot \omega_r^2 \cdot u_r(P) \cdot \varrho(P) \quad .$$

The energy consumed by damping at point P then is:

$$dE(P) = g_r \cdot \omega_r^2 \cdot u_r^2(P) \cdot \varrho(P) \quad .$$

The total energy consumption for the complete aircraft then is:

$$E = g_r \cdot \omega_r^2 \cdot \iiint u_r^2(P) \cdot \varrho(P) \cdot dP = g_r \cdot \omega_r^2 \, M_r \quad .$$

This energy must be equal to the total effort of excitation:

$$g_r \cdot \omega_r^2 \cdot M_r = \sum_{\ell=1}^{n} K_\ell \cdot u_r(P_\ell) \quad .$$

Since $g_r = tg\beta = 2D$ is the degree of damping, there follows for the generalized mass M_r :

$$M_r = \frac{\sum_{\ell=1}^{n} K_\ell \cdot u_r(P_\ell)}{\omega_r^2 \cdot g_r} \quad .$$

The forces of excitation can be determined from the excitation current. However, this method is not very accurate because, at low internal damping of the aircraft, the additional damping effects in the transmission of energy distort the measurement. By direct measurement of force by means of a suitable small dynamometer at the point of action of the exciter on the aircraft, these errors could be greatly reduced. It is, of course, necessary to substract the mass forces of the vibration coil and of the push rod with their 90° shift of phase.

Another method also utilized by us employs the displacement of the natural frequency by affixing added masses on the aircraft. The detuning $\Delta\omega$ of the original natural frequency is determined by a count of the vibrations which originate through addition of the detuned natural frequency f_n to the original natural frequency f_o maintained by a special frequency generator. The distribution of the added masses Δm_ℓ over the aircraft must, however, correspond, in a rough approximation, to its real mass distribution $\varrho(P)$. This determines in principle the accuracy of the method. All added masses are then enlarged in several steps at the same ratio and the respective detuning is measured each time. The values so obtained are plotted in the form shown in Fig. 9 and, from this, the value of $\Delta m_\ell / \Delta\omega$ extrapolated to zero can be read off. The value of the generalized mass results from the following relation:

$$M_r = -\frac{\omega_r}{2} \sum_{\ell=1}^{n} u_r^2(P_\ell) \cdot \frac{\Delta m_\ell}{\Delta\omega} \quad .$$

In this, ω_r designates the natural frequency of the r^{th} natural mode and $u_r(P_\ell)$ the amount of the amplitude at point P_ℓ at which the added mass Δm_ℓ is affixed. The product $u_r^2(P_\ell) \cdot \Delta m_\ell$ is formed and summated for all the added masses of the aircraft. The expression for M_r was obtained from the integral representation of the r^{th} natural mode, on the assumption that the natural mode was not changed in its shape through the detuning of the natural frequency due to the added masses. Because the experiments are carried out in atmospheric air and therefore mass forces of the resonating air also are effective which depend in turn on the mode of oscillation, this assumption will be fulfilled so much better as the distribution of the added masses is accurately proportional to the real mass distribution of the aircraft.

7. FURTHER DEVELOPMENT OF EQUIPMENT

The installation for static vibration tests developed by us can be utilized for small aircraft up to 1,000 kg flying weight. It is to be gradually enlarged and improved on the basis of experience gathered. We contemplate primarily the utilization of a greater number of stronger exciters, in order to be able to induce, also in larger aircraft, still higher pure natural modes. In addition, the system of measuring wedges which, although complicated, is very reliable and clear in operation, is to be complemented by a purely electrical procedure. In order to be suitable for simple transportation without risk, the apparatus is to be designed, through a system of unit-construction, for transport in a motorized vehicle. Considering the high cost for such an installation and the somewhat complicated execution of a static vibration test, it would not seem profitable for an individual aircraft-construction plant to purchase such an installation for itself. Similar to France and other countries, it would seem more efficient to create a central mobile installation which is able to travel, together with the required skilled personnel, to the particular plant in which an aircraft design is to be tested. Such a central installation could be developed much larger and more modern and produce greater accuracy of measurement than if the tests were left to the individual plant which would be forced to be more or less improvised in order to save expenses. Such greater accuracy of measurement would undoubtedly have a favorable effect on the accuracy of determining critical flying speeds and in general on the overall reliability of flutter calculation.

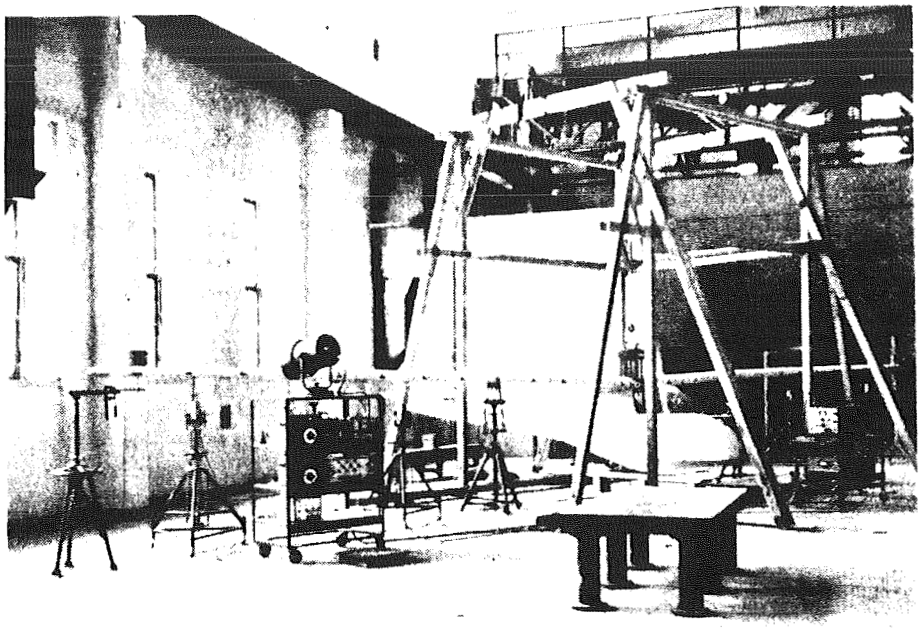

Fig. 1. Static vibration test on sailplane (L-Spatz-55).

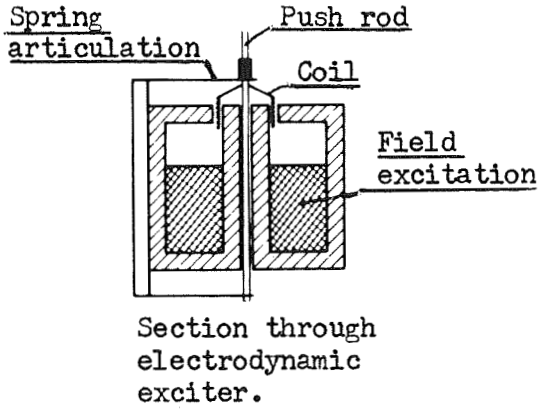

Section through electrodynamic exciter.

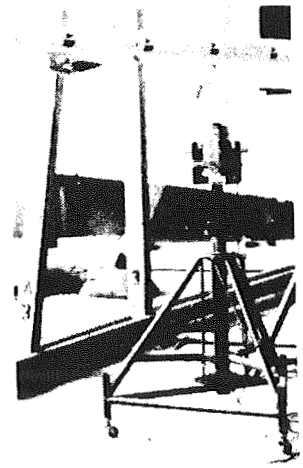

Fig. 2. Electrodynamic oscillator with tripod.

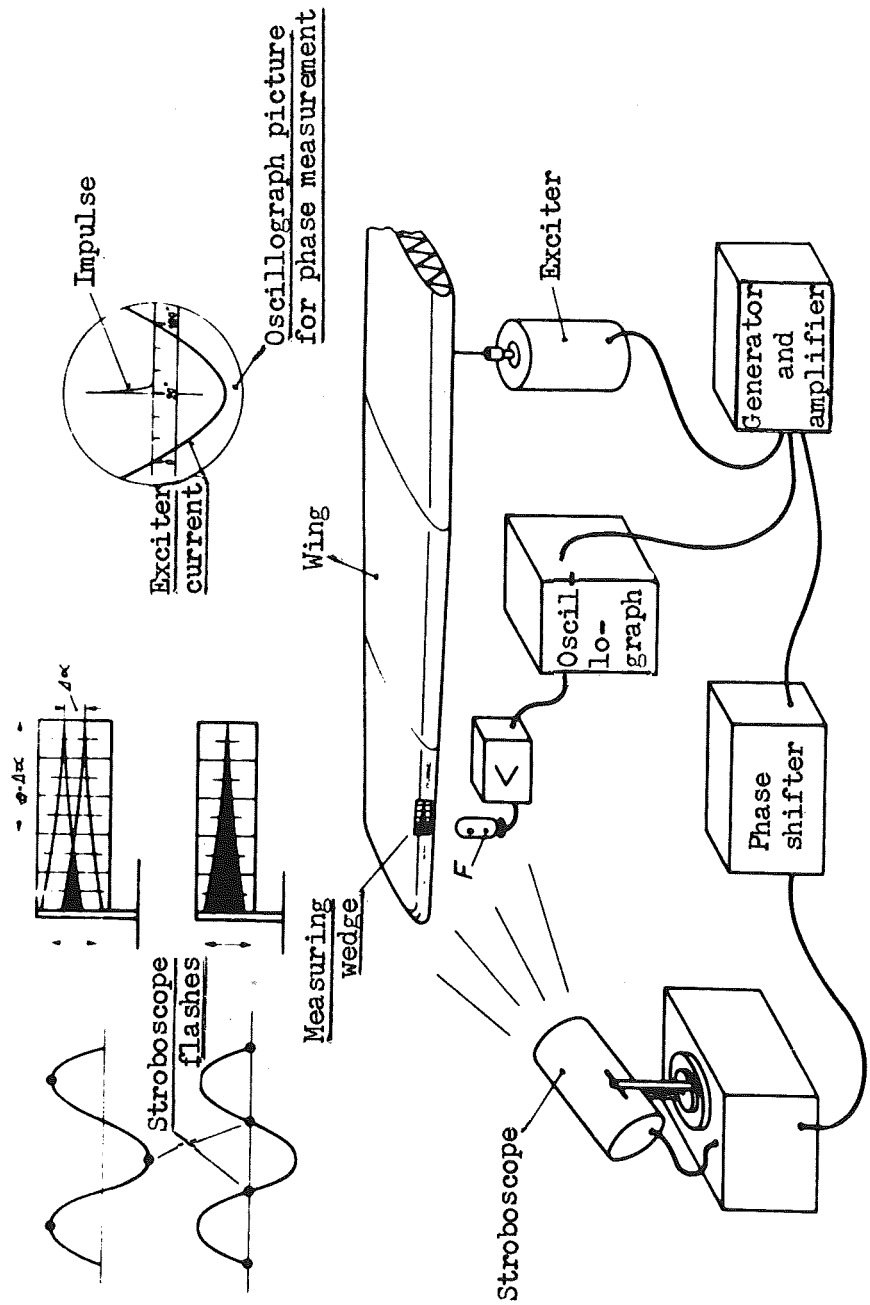

Fig. 3. Stroboscopic method of measuring amplitude and phase.

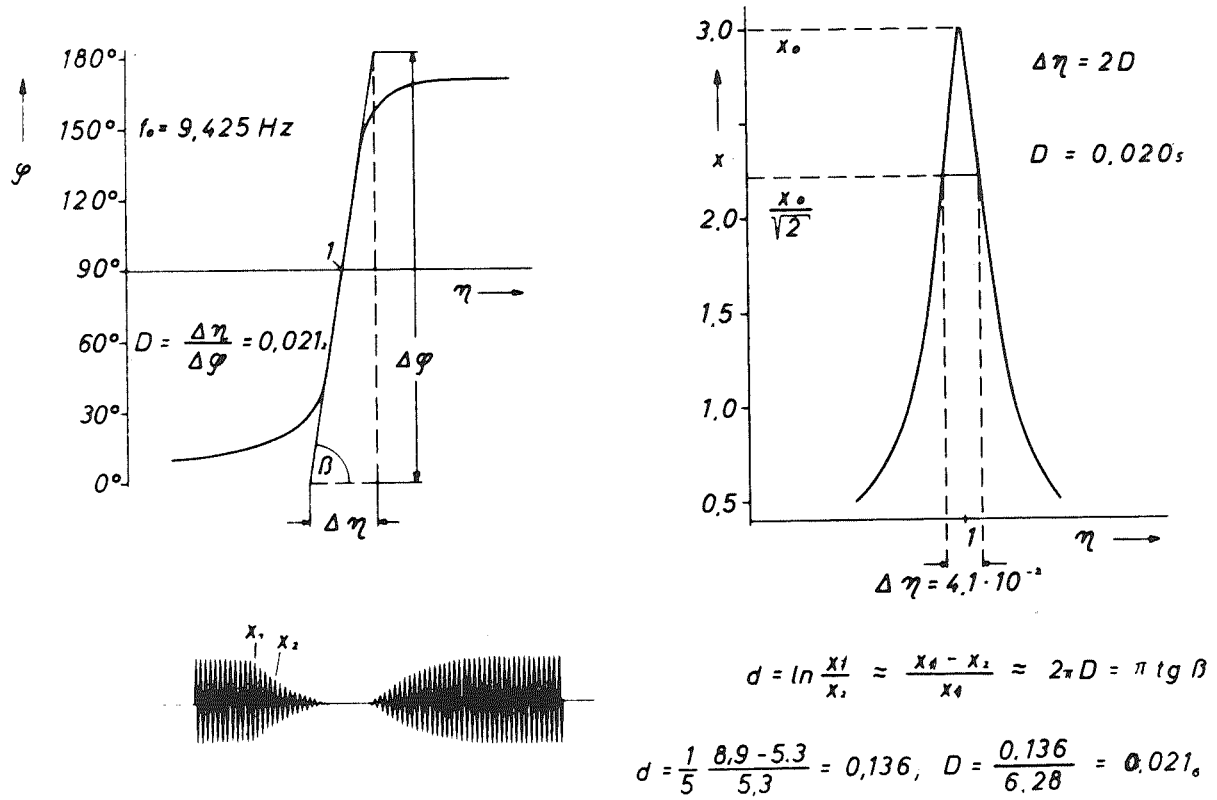

Fig. 4. Determination of damping.

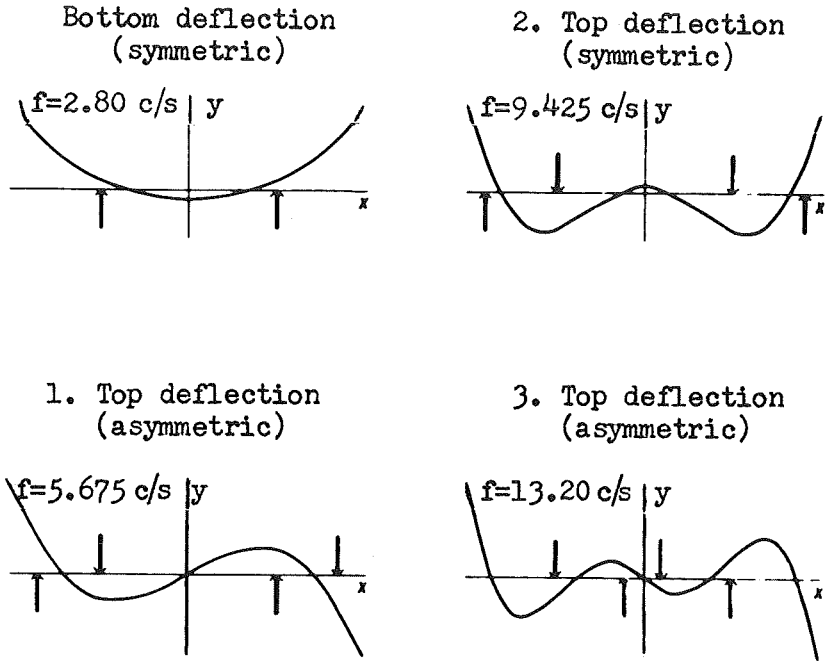

Fig. 5. Bending lines of spar in single-spar sailplane (L-Spatz-55).

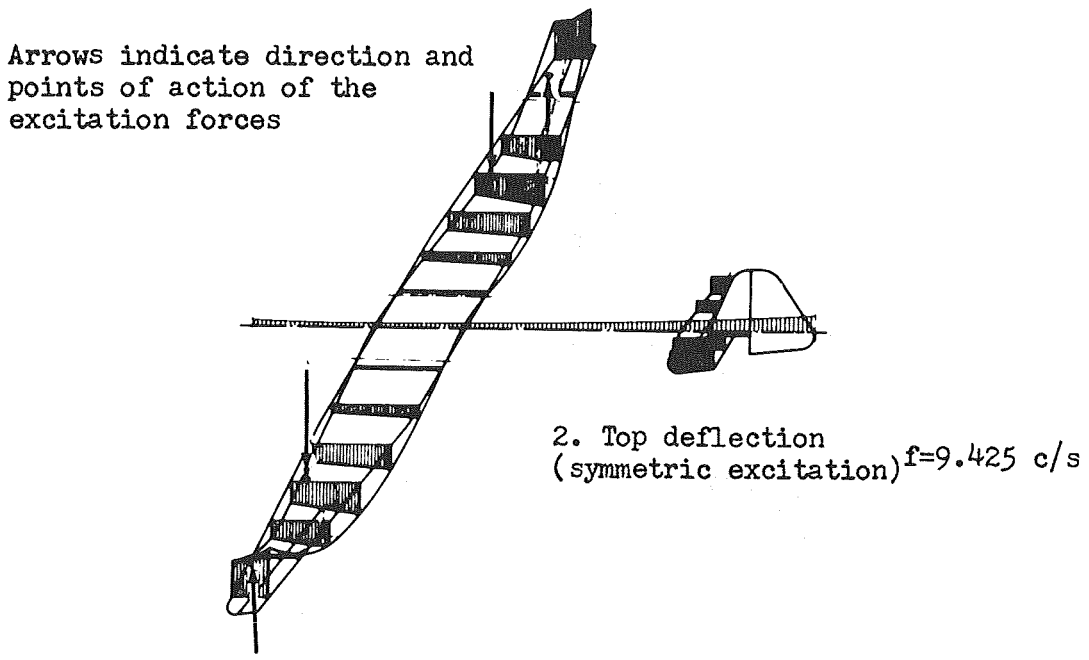
Arrows indicate direction and points of action of the excitation forces
2. Top deflection (symmetric excitation)
f=9.425 c/s

Fig. 6. Symmetric natural mode (bending vibration) of sailplane (L-Spatz-55).

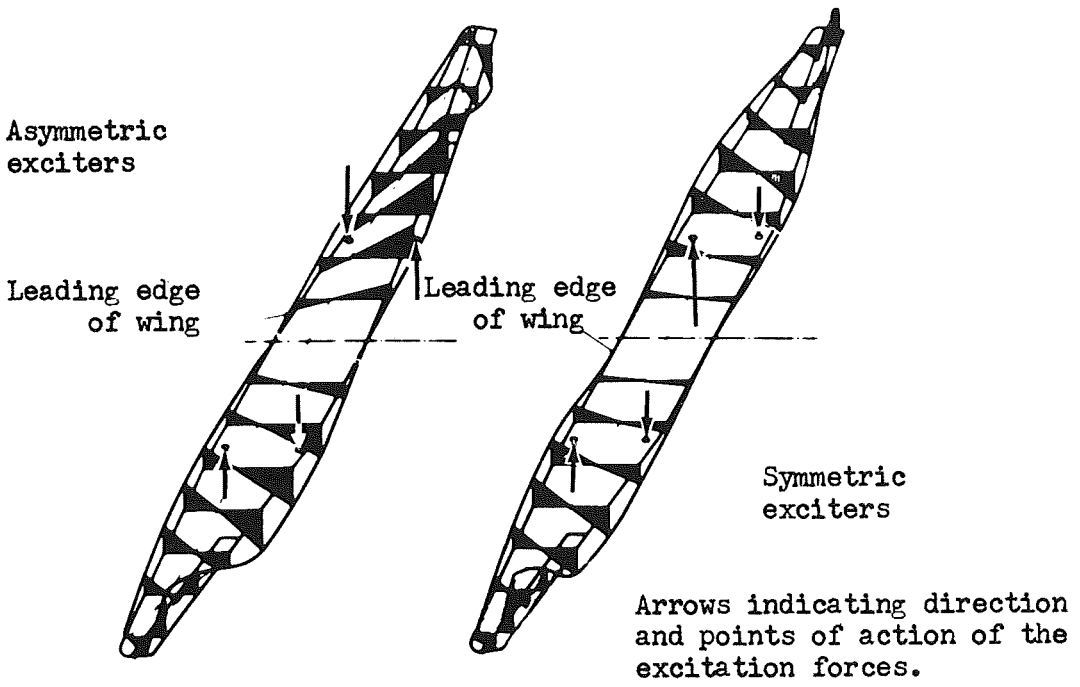

Fig. 7. Symmetric and asymmetric natural mode of torsion of sailplane wing (L-Spatz-55).

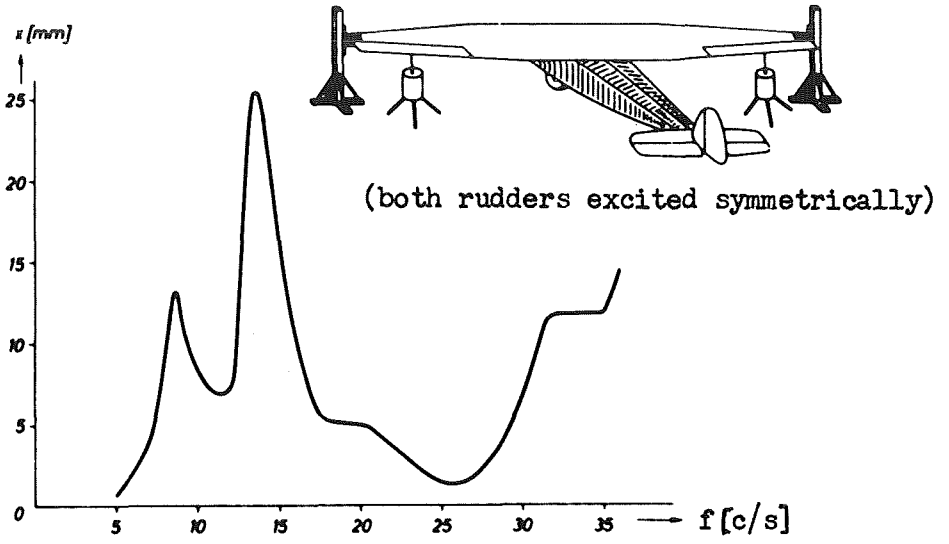

Fig. 8. Frequency mode of aileron with control linkage.

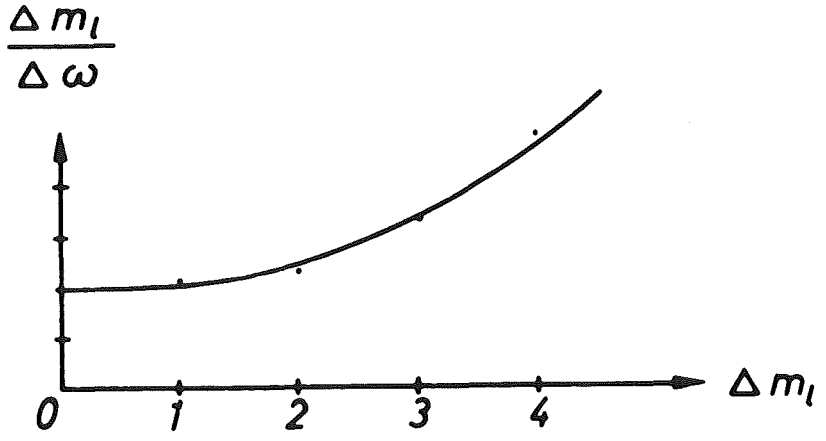

Fig. 9. Determination of generalized mass.

DISCUSSION

de Vries: Mr. Schoen has reported on some very interesting new information and I feel he is much too modest in saying that he wanted to abandon the method employed in favor of a more elegant one. The stroboscope method doubtless has the advantage that it includes light measurement elements so that the aircraft is not influenced by the measuring instruments. This may be extremely important, under certain circumstances, in the case of control surfaces.

Krumhaar: I have one question: Mr. Schoen did describe a method for the determination of damping in the wing. This is done by recording a declining wing vibration which is caused by shutting off the electric current flowing through the exciters. My question now is: Has provision been made that the inducers or exciters are shut off from the wing in the same instant? Because otherwise the damping due to the exciters will also be in the measurement.

Schoen: The mechanical damping is very low. Obviously, the inducers must be shut off so that electric damping does not occur.

Küssner: I should like to point out one detail. In one of the slides, Dr. Schoen shows a schematic curve for the determination of the quotient $\Delta m_1/\Delta \omega$ in the generalized mass. However, for the measurements made, the added masses were so small that all points lay nearly on a horizontal straight line. The determination of the boundary value $\Delta m_1/\Delta \omega$ was therefore completely definitive in this case.

Schoen: This depends on the size of the added masses. If we continue to enlarge the added masses, then the curve shown in Fig. 9 begins to rise with the greater added masses.

Küssner: We utilize only small added masses. In the first case, we affixed added masses at certain points on the wing. This gave us a generalized mass of 14. In the second case, we slightly shifted the added masses as compared to the first case. We then obtained 12.7 for the generalized mass. A relatively small shift of mass therefore already changes by about 10% the generalized masses calculated with the approximation formula mentioned. It is possible that the measurement may have been erroneous. We would naturally welcome it if this procedure could be more accurate.

de Vries: This is probably due to one of the difficulties which I already mentioned yesterday, that of accurately determining resonance. Quite generally, we carry the determination of the generalized mass out so that we affix only 2 or at the most 4 small masses and accuracy is satisfactory with that. However, we do select a somewhat different form of representation which I described in my lecture. This form has the advantage that the measured points must lie on a straight line and are therefore easier to interpolate.

Ebner: I have one question for Dr. Schoen. Did you ever compare both procedures, the energy method and the method of the added masses? Such a comparison would certainly be very interesting.

Schoen: No. There is also the following difficulty which I already indicated. In a given instant, the determination of the energy transmitted is not too simple because friction still occurs in its transmission agents, i.e., in the push rods and in the contacts on the aircraft. We will have to find a method of eliminating this friction.

Küssner: This difficulty will probably best be eliminated by affixing extension-measuring strips at the push rods.

de Vries: No, this should not be done for the following reasons: with extension-measuring strips, we would measure the difference between force of excitation and force of mass of the vibration coil. We simply have to accept that the oscillation system of the aircraft is slightly changed by the additional masses of the vibration coils and must determine all the coefficients for this new system. In special cases, the values for the aircraft separately can be obtained later by calculation. For the changed system, however, the force between vibration coil and aircraft represents an internal force which is of no interest.

This is also the answer to the question of Mr. Krumhaar as to how the friction of the (non-current carrying) exciters can be taken into account.

For the calculation of critical speed, the exact value of the damping of the aircraft has little interest because this changes immediately in flight, e.g.,with temperature. For experimental determination of the generalized mass (cf. G. de Vries "Determination experimentale des masses generalisees," La Rech. Aeron. No. 18, 1950), we must know the exact value of damping. In this, we consider the system with the exciters and the damping of the latter must therefore be contained in it. I should like to briefly recapitulate the programme. We first record the resonance curve. We then determine a natural frequency in some manner. The next thing is the so-called impedance curve. This term has been borrowed from electrics. The measured amplitudes at various points of the aircraft are plotted as a function of force. In the case of a linear system, we obtain a series of straight lines which intersect in one point on the axis of the forces. This amount is dry friction. According to a report by Rost (cf. "Determination de la masse generalisee a l'aide du procede par impedance," La Rech. Aeron. No. 28, 1952), dry and velocity-dependent damping can be separated with these measured values. The next step is measurement of the oscillation-decay curve from which damping can be determined in known manner. We can obviously use the oscillation-start curve equally well for the determination of damping. It has certain advantages because in this case the force acts in the exciter. For example, if the exciter is not perfectly centered and has a small lateral component, then the component may change, depending on whether current is flowing through the coil or not. Consequently, measurement of the oscillation-start curve is a valuable control of the measurement of the oscillation-decay curve. Theoretically, the damping values so determined should agree. However, the difficulty with the oscillation-start curve is the fact that we must

form the difference between the maximum value of the amplitude and the characteristic amplitude value which is variable in time (cf. G. de Vries "Determination experimentale des masses generalisees," La Rech. Aeron. No. 18, 1950).

Thielemann: As far as I am able to understand this, excitation of the aircraft with the four exciters was made only on the wing. It may be suspected that the amplitudes of the empennage measured in the resonance do not correspond to those of the natural vibration mode of the aircraft because of the damping forces occurring in the structure. Under these conditions, is it possible to determine the generalized mass accurately?

de Vries: Unfortunately, I was not able yesterday to project the slides in my lecture. But I can say this: when the masses are small enough, they can be affixed wherever desired and here I should stress that a suitable excitation is not at all necessary for the determination of the generalized mass. I could, of course, affix an added mass to a system and then investigate the latter again as a new system. If I am successful in determining the new resonance in some manner, it is then immaterial whether the measurement obtained by me is a linear superposition of different natural vibration forms or not. The added mass does have an effect on every load and changes each mode. Consequently, in every superposition of the modes, each new mode is contained separately. Only metrological reasons make it necessary to have a suitable excitation in order to determine the resonance and/or the shift in resonance of the desired mode. This is always the same difficulty and only for this reason do we need suitable excitation which is otherwise not needed at all.

The whole matter can be easily demonstrated by an example. Let us assume that we have a wing. We measure two modes with different nodal lines for the wing. We are then asked to determine the generalized mass for mode 1. We may have poor excitation. In that case, it is sufficient to locate the measuring (reference) point for the resonance into a nodal point of mode 2. Then mode 2 may be superposed on mode 1, without having any effect at all on the determination of the resonance.

This may be the answer to your objection. Even if the empennage is not excited, there is no difficulty then when we are certain that the point of determination of resonance is in perfect phase.

Schoen: We must also remember that the vibration character of the sailplane investigated, in contrast to an engine-powered aircraft, is determined by the wing which is long in relation to the fuselage. For the lower modes of vibration, excitation at the wing is sufficient so that the empennage will also vibrate approximately in perfect phase.

Ebner: My question concerns the number of the exciters necessary. I have the impression that the Netherlands operate with a substantially smaller number of exciters.

Greidanus: This was a somewhat older installation with excitation by imbalance.

Ebner: Do Dr. de Vries and Dr. Schoen agree that the number of five exciters is sufficient in general also for large aircraft? Does this number depend on the order of the natural oscillation modes?

de Vries: This is understood but we should not forget this: if you have more than five exciters, the difficulties of adjusting the exciters become so great that there is no longer any benefit in the greater number of exciters. The Americans have developed a method for the adjustment of the exciters. This method has been developed from an erroneous physical basis. It functions even so. It was mentioned in the report of Mr. Schultze (Ernst Schultze: "Die Erregung einer Eigenschwingung von Flugzeugflugeln. - Eine Anwendung der Theorie der Intergralgleichungen," ZAMP, Band 6, 1955). If you have an aircraft and then assume some arbitrary distribution of mass over the wing, it is of course very convenient for calculation to assume that the distribution of damping (absolute damping!) over the complete aircraft is proportional to the distribution of mass and amplitude. However, in actuality, the aircraft is in the air and I cannot very well see how a force of absolute damping can here act on the system. Because from the assumption that the forces of damping are proportional to the masses and because the mass forces are absolute forces, it would follow that the forces of damping must also be absolute forces; but this is actually not so. In order to have natural-vibration modes, the damping forces must be either proportional to the matrix of the masses M or else proportional to the matrix of stiffness. Actually, they can never be proportional to M because they concern internal, i.e., relative, damping forces. However, the assumption of Schultze concerns absolute forces. The Americans also have utilized this (erroneous) formulation that damping is proportional to M -- which I incidentally also indicated in my first reports on the determination of μ by small added masses -- in order to simplify this problem.

With this method, American engineers first locate over the system arbitrarily distributed excitation forces, then carry out a first measurement and correct the formulation with estimated distributions of amplitude and mass and with the measured amplitude. This is more or less an experimental iteration which obviously is not physically founded. It is possible that the method itself may be operable. In O.N.E.R.A., we have tried to find a strict solution of the problem for the adaptation of the excitation forces to a natural-vibration mode but have not been successful so far.

Thielemann: Would it not be possible to have an automatic control which adjusts the excitation forces in the desired manner by measurement of the amplitudes and their phase position?

de Vries: This is not very simple because in that case we would have to know first clearly, before starting experimentation, what we

actually do desire to know and I feel that even the definition of that which is desired, actually is not simple.

Thielemann: The excitation force should be adjusted proportional to amplitude and phase.

de Vries: No! It does not need to be proportional to amplitude. If we had damping proportional to velocity and proportional to distribution of mass, then the excitation forces would need to be proportional to the product of mass and amplitude in which the mass distribution is obviously unknown. As already stated, because we do not have absolute but relative damping and the latter is moreover not distributed according to a known law, we can initially make no statement on the required distribution of the excitation forces.

Küssner: If we wanted to construct exciters furnishing a physically approximately correct excitation proportional to the damping in each structural element, then these exciters would have to be located and constructed from entirely different physical viewpoints. They would then have to work proportional to distortion and not proportional to the bending amplitudes. Anything of this kind does not exist and I cannot even imagine a physical principle with whose aid this might be achieved.

de Vries: That is right. For example, we are already confronted by the following difficulty: let us assume we have some arbitrary bending mode and some other arbitrary mode is superposed to this wing-bending mode. Obviously, this component is in phase shift as against the original mode. How are we now to arrive at the criterion for the best excitation? Obviously, it would be ideal if we could say: "let us eliminate the contiguous mode." This would be Utopia. We must therefore formulate a minimum condition which may take quite different forms. For example, we can say, for the structural units of greatest interest, e.g. with the highest amplitudes, we want to have the lowest phase shift. However, we may also require that the scattering of the phase angles in each measuring point shall be smaller than 5°. It might also be required that we have a summation of the phase errors over the whole in which we include the amplitudes and the wing chord, as is done later in flutter calculation. There is consequently quite a number of possible criteria before we even start.

We did try to do the following: instead of the amplitudes and the phase, the two components of the vibration vector are plotted. This gives us two curves:

$$A \cdot \sin\varphi \qquad \text{and} \qquad A \cdot \cos\varphi$$

$A \cdot \sin\varphi$ has its maximum value in the resonance, $A \cdot \cos\varphi$ then becomes zero. We locate a number of inducers along the wing and these inducers furnish the deviation $A \cdot \cos\varphi$ from zero which consequently corresponds to the phase shift. We now form $\frac{A \cdot \cos\varphi}{A \cdot \sin\varphi}$ and have the relative phase

shift at all points with this. We might now require that

$$\sum \frac{\cos\varphi}{\sin\varphi}$$

becomes the minimum. This is a possible condition. We did not insist on further investigating the question of the best criterion because we have enough other difficulties, e.g. non-linearities. Even if we do establish the criterion and were able to realize a corresponding experimental arrangement, we would probably have difficulties of convergence because of the non-linearities (cf. G. de Vries "Influence de l'amortissement interne sur les caracteristiques des avions," La Rech. Aeron. No. 38, 1954).

Thielemann: May I return again to my question? When employing several exciters, how do you write the criterion indicating that you have found a natural-vibration mode?

de Vries: In principle, it is the criterion of the phase or, if you prefer, $A \cdot \cos\varphi = 0$, that all points are in phase, i.e., that all galvanometers indicate zero.

Thielemann: In practice and at least for the fundamental natural frequencies -- even if the physical foundation of the method is not exact -- could this not be achieved by an automatic control and eventually by suitable correction?

de Vries: This is entirely possible but produces another difficulty. After all, two magnitudes enter into this, first the location of excitation and then the force of excitation. The force of excitation can be easily changed. The location of excitation cannot be changed as easily. I believe the most efficient procedure for accurate measurement is still the following: we first carry out a measurement with an apparently appropriate excitation so that we become familiar with the approximate nodal line of all modes. From this, we naturally also know the relation of the frequencies to each other and since we know that a frequency removed by more than 10 or 20% from the desired natural frequency, cannot have any great influence and if we then do not make very great errors in excitation, we can restrict the number of interfering contiguous modes to one or two. If we now enter into the nodal line of this interfering contiguous mode, not only with the measuring instruments, as stated earlier, but also with the excitation, we should then be likely to obtain good modes. In general, this is the manner in which we proceed.

Ebner: If the wing is made to vibrate by impact in some manner, we then obtain some sort of combination of all vibration modes. In that case, is there no possibility of separating the latter so that all natural vibration modes and all natural frequencies can be determined by an impact test?

de Vries: Yes, this is possible. I do have to say that this is one of the things which were an extraordinary surprise to me. For this

vibration test, one of our teams developed an impact test with rockets. In the response of the aircraft to such an impact, the entire vibration characteristics of the aircraft are actually contained more or less, unless we have the mischance to be in a nodal line with the measuring instrument and with the excitation. This was confirmed when the response of the aircraft to impact excitation was recorded through an acceleration meter on a magnetic tape and later analyzed by electric filter. In this manner, we can obtain frequency, damping and starting amplitude of the respective vibration. It is possible to read out of such a measurement up to 10 natural frequencies, i.e., the frequencies and damping values, but obviously not the modes because the phases cannot be determined in this manner. For aircraft wings, this is obviously of considerable interest because we can excite practically all modes with one impact (cf. G. Coupry, R. Valid and G. Piazzoli "Etude de l'amortissement des vibrations en vol par percussions sur les surfaces portantes," La Rech. Aeron. Nr. 47, 1955, and R. Mazet "Quelques aspects des essais de vibration au sol et en vol," Note Technique Nr. 34, 1956, O.N.E.R.A.).

Küssner: Such a recording should be made simultaneously at many, perhaps at 20 points.

de Vries: This method does not permit us to determine the phase so that we cannot record the mode even with many measuring points.

Thielemann: I have one more question, the question of the orthogonalization of the vibration modes. Do you make an attempt to orthogonalize the vibration modes found in the vibration tests?

de Vries: Not any more. Before we started to determine the generalized masses, we carried out parallel experiments, first on a simple beam and then on the aircraft. That is, we determined the generalized mass from this experimental procedure and simultaneously also with the aid of the distributions of amplitude and mass. These values were compared and the orthogonality examined at the same time.

Nor should we forget the following. When we draw an aircraft on the blackboard, it is then very satisfactorily flat. But a fuselage is relatively short. For example, it may have a height of 2 m. We would then be very bold in assuming that the amplitudes measured along the bottom of the fuselage are the same as those at the top and in the center the situation is completely hopeless. Disregarding this, the determination of rotational amplitudes of the fuselage, of the engines, etc. which in general have no significance in flutter because they do not introduce any aerodynamic forces, is metrologically very difficult. However, in order to test orthogonality, this would have to be taken into account. We repeatedly noted that the high and narrow fuselages become deformed within themselves. It would appreciably increase the required effort if we would also measure all this.

Schoen: I have one more question. How has the arrangement of a central static-vibration test installation worked out for you? I mentioned this at the end of my lecture.

de Vries: We succeeded in developing an installation which can be purchased by individual aircraft builders who can then carry out the simpler tests themselves. One obvious disadvantage is the fact that the aircraft engineers of the companies often are not adequately familiar with vibration problems. I do believe that your idea is sound and this is also the form into which this has crystallized with us, i.e., a large central installation as up-to-date as possible and several smaller installations which are suitable for basic tests. In any aircraft-construction plant, an engineer is charged with carrying out smaller measurements such as, for instance, the aileron frequency. If the entire installation were needed only for the determination of aileron frequency, this would be too cumbersome. In France the situation now is that almost all companies have begun or are beginning to acquire more or less modest test equipment. For more difficult problems, the mobile test equipment of O.N.E.R.A. is sent out.

MOTION PICTURES SHOWN

Following the lectures of the first day of the meeting, two flutter films were shown. The first one of these, entitled

"Aircraft Flutter in the Wind Tunnel"

was made in the Aerodynamic Experimentation Institute in the year 1943. It shows several forms of flutter in a large, dynamically analogous model of an He-219 aircraft where several parameters are changed.

The second film with the title

"Investigation of the Flutter Characteristics of a Flying Wing"

was produced in Stockholm after the war. It shows several forms of flutter on the model of half of a swept-back wing at several parameters.

Subsequent to the lectures of the second day of the meeting, a film of Scandinavian Airlines (SAS)

"Ready to Start"

was shown. The film presents an informative picture of the maintenance and general overhaul of SAS planes and of the training of the crews.

LIST OF PARTICIPANTS AT SYMPOSIUM

Adams, Ernst, Dr.-Ing., Deutsche Forschungsanstalt fur Luftfahrt, Institut fur Aerodynamik, Braunschweig.
Baiter, Hans-Jurgen, cand. phys., Flugwissenschaftliche Fachgruppe Gottingen.
Becker, Ernst, Dr., Aerodynamische Versuchsanstalt Göttingen.
Bergh, Henk, Ir., Nationaal Luchtvaartlaboratorium, Amsterdam.
Betz, Albert, Prof. Dr., Dr.-Ing. E.h., Aerodynamische Versuchsanstalt Gottingen.
Braun, Winfried, Dr., Deutsche Versuchsanstalt fur Luftfahrt, Prufstelle fur Luftfahrtgerat, Essen.
Bruning, Gerhard, Dipl.-Math., Deutsche Forschungsanstalt fur Luftfahrt, Institut fur Flugmechanik, Braunschweig.
Drescher, Hans, Dr.-Ing., Max-Planck-Institut fur Stromungsforschung, Abteilung Reibungsforschung, Göttingen.
Ebner, Hans, Prof. Dr.-Ing., Deutsche Versuchsanstalt fur Luftfahrt, Mulheim/Ruhr.
Falkenheiner, Helmut, Ernst Heinkel Fahrzeugbau GmbH, Speyer/Rhein.
Geisler, Ernst, Dr., Messerschmitt AG, Munchen.
Giencke, Gustav, Dipl.-Ing., Technische Hochschule, Lehrstuhl fur Luftfahrttechnik, Darmstadt.
von Gorup, Guntram, Dr., Aerodynamische Versuchsanstalt Göttingen.
Greidanus, Johan H., Dr., Koninklijke Nederlandse Vliegtuigenfabriek Fokker, Amsterdam.
Gruschwitz, Eugen, Dr., Flug- und Fahrzeugwerke Altenrhein, Rorschach (Schweiz).
Hansson, Sven, Ingenieur, Kungl. Tekniska Hogskolan Fl, Stockholm.
Heins, Wilfried, Mathematiker, Deutsche Forschungsanstalt fur Luftfahrt, Institut fur Flugmechanik, Braunschweig.
Herbeck, Margot, Dr., Max-Planck-Institut fur Stromungsforschung, Göttingen.
Kehl, Albin, Dr., Aerodynamische Versuchsanstalt Göttingen.
Krauss, Julius, Prof. Dipl.-Ing., Technische Hochschule, Darmstadt.
Krumhaar, Hans, Dr., Aerodynamische Versuchsanstalt Göttingen.
Küssner, Hans Georg, Prof. Dr.-Ing., Aerodynamische Versuchsanstalt Göttingen.
Lehnigk, Siegfried, Mathematiker, Deutsche Forschungsanstalt fur Luftfahrt, Institut fur Flugmechanik, Braunschweig.
Liebing, Oskar, Dipl.-Ing., Ingenieurburo Prof. Blume, Duisburg-Ruhrort.
Ludwieg, Hubert, Dr., Aerodynamische Versuchsanstalt Göttingen.
Ludwig, Rudolf, Dr., Deutsche Forschungsanstalt fur Luftfahrt, Institut fur Flugmechanik, Braunschweig.
Merbt, Horst, Dr., Kungl. Tekniska Hogskolan, Stockholm.
Piepers, Gijsbrecht G., Ir., Koninklijke Nederlandse Vliegtuigenfabriek Fokker, Amsterdam.

Riegels, Friedrich-Wilhelm, Dr., Aerodynamische Versuchsanstalt Gottingen.
Rotta, Julius, Ingenieur, Aerodynamische Versuchsanstalt Gottingen.
Schoen, Josef, Dr., Aerodynamische Versuchsanstalt Gottingen.
Schwarzmann, Karl, Studienrat, Amberg, Moritzstr. 1.
Sorg, Fridolin, Ingenieur, Dornier GmbH, Friedrichshafen/Bodensee.
Tesarik, Hans, Dipl.-Ing., Ernst Heinkel Fahrzeugbau GmbH, Speyer/Rhein.
Thielemann, Wilhelm, Dr.-Ing., Deutsche Versuchsanstalt fur Luftfahrt, Institut fur Festigkeit, Mulheim/Ruhr.
van de Vooren, Adriaan I., Prof. Dr.-Ing., Nationaal Luchtvaart-laboratorium, Amsterdam.
de Vries, Gerhard, Dr.-Ing., O.N.E.R.A., Paris.
Weib, Siegfried, Dr.-Ing., Bolkow-Entwicklungen KG, Stuttgart.
Wiekhorst, Friedrich, Dipl.-Phys., III. Physikalisches Institut, Gottingen.
Winter, Hans, Prof. Dr.-Ing., Technische Hochschule, Graz.
Wuest, Walter, Dr., Aerodynamische Versuchsanstalt Gottingen.

For sale by Office of Technical Services, Department of Commerce,
Washington, D.C. Price $3.00